2006

Novel nanostructured conducting polymer systems based on sulfonated polyaniline

Fatemeh Masdarolomoor
University of Wollongong

Novel Nanostructured Conducting Polymer Systems based on Sulfonated Polyaniline

Fatemeh Masdarolomoor

B.Sc., MSc. Chemistry

A thesis presented for the degree of

Doctor of Philosophy

Department of Chemistry

University of Wollongong

Australia

March 2007

In the name of Allah the Beneficent the Merciful

Dedicated to

My family for their love, support and encouragement

And

All my teachers for leadership and inspiration

Abstract

The fully sulfonated polyaniline, Poly(2-methoxyaniline-5-sulfonic acid) (PMAS), is a watersoluble and electroactive conducting polymer. Its high water solubility makes it a potentially very attractive material for a range of applications. However, to date problems with its synthesis from MAS monomer and the impure nature of the PMAS product have hindered its exploitation. This thesis successfully addresses these problems and then subsequently exploits the pure high molecular weight PMAS obtained as a novel electroactive dopant in composite materials with other conducting polymers.

The initial focus of this thesis was the development of a rapid purification technique capable of fractionating in gram scale quantities the crude mixture of PMAS and low molecular weight oligomers formed in established syntheses of PMAS. A new method was successfully established using cross flow tangential filtration to obtain, for the first time, the high purity, high molecular weight (HMWt) and low molecular weight (LMWt) PMAS fractions. Gel permeation chromatography, UV-visible spectroscopy and four point probe conductivity were used for characterisation of these fractions. The new separation technique was found to be a more efficient, rapid and scalable method for purification of PMAS than the conventional dialysis previously employed. Results have shown that the presence of the LMWt PMAS has an unexpected influence upon the electronic properties of the HMWt PMAS such that conductivity increases by two fold after its effective removal.

Detailed optimisation studies were then performed on the synthesis of PMAS via the chemical polymerisation of 2-methoxyaniline-5-sulfonic acid (MAS) monomer, using ammonium persulfate as oxidant. These demonstrated that experimental variables such as time, temperature, monomer concentration, pH, and the rate of addition of oxidant influence the yield, molecular weight and conductivity of the resultant PMAS. Employing the optimal synthetic conditions resulted in a HMWt PMAS product with enhanced conductivity of 1.74 ± 0.09 S/cm, M_p 16,900 and recovered yield (after tangential cross flow filtration) of 50 % w/w.

The pure HMWt and LMWt PMAS fractions obtained following the above purification were fully characterised using techniques such as cyclic voltammetry (CV), electron spin resonance (ESR), photoluminescence (PL) spectroscopy and transmission electron microscopy. The HMWt PMAS fraction (M_n 13,400 kDa, M_w 33,600 kDa, M_p 16,900 kDa and PDI 2.5) was found to be paramagnetic due to the presence of radical cations (polarons). In contrast, the LMWt PMAS fraction (M_n 2,400 kDa, M_w ,700 kDa, M_p 2,800 kDa and PDI 1.1) was non-electroactive and non-conducting with no paramagnetic properties. Both HMWt and LMWt PMAS fractions exhibited nanodimensional morphology. The recently reported photoluminescence properties of PMAS have been reassessed in this thesis, revealing that the LMWt PMAS fraction in the presence of HMWt PMAS was the source of the unexpected photoemission reported for aqueous PMAS. In contrast, pure HMWt PMAS was found to statically quench the photoluminescence of LMWt PMAS.

These optimisation and purification studies provided an opportunity to study, for the first time, the incorporation of pure HMWt PMAS as a conducting polyelectrolyte dopant without the complication of oligomeric impurities, which were shown above to dramatically influence the properties of PMAS. Pure HMWt PMAS was incorporated as a dopant during chemical and electrochemical polymerisation of unsubstituted polyaniline (PAn). PAn/PMAS materials were prepared as water-insoluble films using electrochemical polymerisation, and as highly dispersed nanomaterials via chemical polymerisation of aniline in the presence of HMWt PMAS. The incorporation of PMAS into the polyaniline was confirmed by elemental analysis, UV-vis spectroscopy and CV studies. The conductivity of the PAn/PMAS nanomaterial was found to be 3.0 ± 0.18 S/cm, approximately two orders of magnitude higher than that reported for polyaniline in the presence of non-conducting polyelectrolytes, such as poly(styrenesulfonate). Signifcantly, this new class of material exhibited conductivity at neutral pH values where polyaniline itself is de-doped to give a non-conducting material.

The enhanced PAn/PMAS stability was exploited in this thesis in the area of electrochromics, giving an enhanced electrochromic contrast (57.0 %ΔT at 770 nm). Its

extended pH stability will also permit future studies into the utility of these materials in biological environments, which to date have been unavailable in unsubstituted PAn due to its lack of conductivity and electroactivity.

Certification

I, Fatemeh Masdarolomoor, declare that this thesis, submitted in fulfilment of the requirements for the award of Doctor of Philosophy, in the Department of Chemistry, University of Wollongong, is wholly my own work unless otherwise referenced or acknowledged. The document has not been submitted for qualifications at any other academic institution.

Fatemeh Masdarolomoor
March 2007

Acknowledgments

First of all, I would like to express my deep sense of gratitude to my supervisors Professor Gordon G. Wallace, Associate Professor Peter C. Innis, and Dr. Syed Ashraf for encouragement, inspiration, continued support, advice and critical review of several aspects of this study.

I especially express my sincere thank to Associate Professor Peter C. Innis for technical collaboration throughout the course of research and proof reading of my thesis.

I would like to express my gratitude to Professor Leon.A.P. Kane-Maguire for helpful suggestions and proof reading of some chapters and to Dr. Mark Imisides, Briana Tompson, Dr. Philip Whitten, Shannon Little and Dr. Toni Campbell for proof reading of my final thesis chapters.

I also deeply appreciate Dr. Violeta Misoska, Dr. Carol Lynam and Yong Liu for performing electron microscopy, Prof Robert Forster and Dr Tia Keyes from Dublin City University for assistance in photoluminscence lifetime measurements, Dr. Jun Chen for assistance in cyclic voltammetry experiments, Dr. Vahid Mottaghitalab for useful discussions and technical help, and Phil Smugreski and A/Prof Chee O. Too for administrative support.

I express my gratitude to my friends in IPRI especially Yingpit, Jenny, Orawan, Dr. Jian Wu and Dr. Caiyun Wang for the useful discussions, help and the friendly times they shared with me.

I would like to express my gratitude to the Ministry of Science, Research and Technology of Islamic Republic of Iran for the Scholarship awarded and the financial supports.

Most importantly I would like to express my deepest sense of gratitude to my parents,

family, and my husband's family for the continued help, support and encouragement they always provide me. I especially must restate my sincere appreciations to my dear husband, Saeid, for unconditional love, continued support and help over the years.

Finally, I dedicate my thesis to the most patient, innocent heart of my little pretty angel Mahya whose inspiring brief note of "I love you Mum" was always standing like the Goddess of Revelation before my eyes, motivating me hopefully to write. Unlimited thanks to her great sense of realization I always adore**.**

List of Publications

1. Masdarolomoor, F., Innis, P.C., Ashraf, S., and Wallace, G.G., *Purification and characterisation of poly(2-methoxyaniline-5-sulfonic acid).* Synthetic Metals, 2005, 153(1-3): p. 181-184.

2. Masdarolomoor, F., Innis, P.C., Ashraf, S., Kaner, R., and Wallace, G.G., *Nanocomposite of polyaniline/poly(2-methoxyaniline-5-sulfonic acid).* Macromolecular Rapid Communications, 2006, 27(23): p. 1995-2000.

3. Innis, P.C., Masdarolomoor, F, Kane-Maguire L.A.P., Forster R.J, Keyes T.E, and Wallace, G.G., Chemical and photoluminescence properties of purified *poly(2-methoxyaniline-5-sulfonic acid) and oligomer.* , submitted Macromolecules.

4. F. Masdarolomoor, P.C. Innis, S.A. Ashraf, and G.G. Walace., *Synthesis of Water Soluble Conducting Polymer, Poly(2-methoxy-aniline-5-sulfonic acid): an Optimization Study* in The International seminar on Polymer Science and Technology. 2005. Tehran, Iran.

5. F. Masdarolomoor, P.C. Innis, S.A. Ashraf, and G.G. Walace., *Effect of Addition rate of Oxidant on Synthesis of Poly(2-methoxy-aniline-5-sulfonic acid) studied by conductivity and ESR Spectroscopy* in The International seminar on Polymer Science and Technology. 2005. Tehran, Iran.

6. P.C. Innis, F. Masdarolomoor, S. Ashraf and G.G. Wallace., *ESR, Raman and Conductivity and Studies on Fractionated Poly(2-methoxy-aniline-5-sulfonic acid), ICSM 2006 Dublin Ireland*

Abbreviations

A	ampere
A^-	anion
ACN	Acetonitrile
Ag/AgCl	silver/silver chloride reference electrode
An	aniline
APS	Ammonium persulfate
C	Coulomb
ClO_4^-	perchlorate anion
cm	centimeter
CV	Cyclic voltammetry/voltammogram
Da	Dalton
DMSO	Dimethyl sulfoxide
DPMAS	dialysed PMAS (purified using conventional dialysis membrane)
DSC	differential scanning calorimetry
E	Potential (volts)
EB	emeraldine base
Echem/ESR	Electrochemical/Electron Spin Resonance
ES	emeraldine salt
ESR	Electron Spin Resonance
g	gram
GC	glassy carbon
GPC	gel permeation chromatography
h	hour
HA	protonic acid
HCSA	10-camphorsulfonic acid
HMWt	High molecular weight
Hz	Hertz
I	current
ICP	Inherently conducting polymer
ITO	Indium-tin oxide
kDa	Kilo Dalton
LB	leucoemeraldine base
LMWt	Low molecular weight
LS	leucoemeraldine salt
M	molar
mA	milliampere
mg/mL	milligram/milliliter
min	minute
mm	millimeter
mM	millimolar
mV	millivolt

MWCO	molecular weight cut off
nm	nanometer
NMP	1-methyl-2-pyrrolidinone
PAn	polyaniline
PB	pernigraniline base
PL	Photoluminescence
PLL	poly-L-lysine
PMAS	poly(2-methoxyaniline-5-sulfonic acid)
PPy	polypyrrole
PS	pernigraniline salt
PSS	poly(styrenesulfonate)
Pt	platinium
PVP	poly (4-vinylpyridine)
S/cm	siemens per centimeter
sec	second
SEM	Scanning Electron Microscopy
SPAN	sulfonated polyaniline
TEM	Transmission Electron Microscopy
TGA	Thermogravimetric analysis
UV-vis	ultraviolet-visible
UV-vis-NIR	Ultraviolet-visible-near infrared
V	volt
ºC	degree Celsius
ε	molar extinction coefficient
λ	wavelength
μ	micro
μm	Micro meter
μg/mL	microgram/milliliter

Table of Contents

Chapter 1

Introduction

Chapter 2

Introduction to experimental techniques used

Chapter 3

Synthesis and Purification of PMAS

Chapter 4

Chemical Synthesis of PMAS, an Optimisation Study

Chapter 5

Characterisation of PMAS fractions

Chapter 6

Synthesis and characterisation of PAn/PMAS

Chapter 7

Electrochemical synthesis of PAn/PMAS

List of Figures

List of Tables

Chapter 1

Introduction

1.1 Inherently Conducting Polymers (ICPs)

Conducting polymers are polymers that inherently conduct electricity. They are conjugated polymers with substantial π electron delocalisation along their backbones giving rise to interesting optical and electrical properties. These properties make these materials suitable for applications such as information storage and optical signal processing, energy storage and energy conversion [1].

Well known organic conducting polymers are the trans-polyacetylene, polypyrrole, polythiophene and polyaniline classes of materials, although polyacetylene (possessing a nearly ideal conjugated structure required for an ICP) has found limited utility due to its environmental instability and complex synthesis.

1.2 History of ICPs

Many organic ICPs have been reported since the first synthesis of doped polyacetylene in 1977 [2] by Shirakawa and coworkers, who reported high conductivity in oxidised, iodine-"doped" polyacetylene. This discovery, along with the extensive research in this area, eventually culminated with the award of the 2000 Nobel Prize in Chemistry to MacDiarmid, Heeger, and Shirakawa for *"The discovery and development of conductive polymers"*.

Conducting polymers have received great attention over the last decade, with an apparent explosion of publications from 1996, Figure 1.1. The research in this area has provided the fundamental understanding of the chemistry, physics and material science of these materials and has supported the industrial development of conducting polymer products [1, 3-8]. The most widely studied ICPs are polypyrrole, polyaniline and polythiophene.

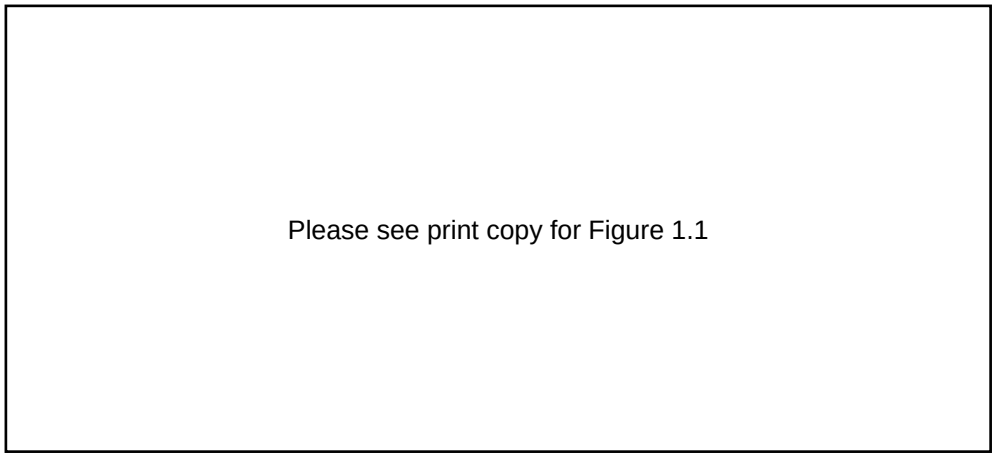

Figure 1.1. Plot showing publications in the area of conducting polymer since 1977 (Source - Scifinder Scholar).

At present it is possible to create conducting polymers with a diverse range of chemical, electrical and mechanical properties [1]. Due to this collection of dynamic properties conducting polymers have found uses in a range of different application in areas such as within mechanical actuators, corrosion protection, anti-static coatings, sensors, membranes, energy storage and conversion devices, polymer photovoltaics, light emitting diodes and display technologies [1, 9-13].

1.3 Synthesis of ICPs

ICPs can be produced using either chemical or electrochemical oxidation of the monomers [14, 15]. Polymerisation involves formation of low molecular weight oligomers that are further oxidised at lower potentials than the initial monomer to form a polymer that eventually precipitates, or is electrodeposited onto the electrode surface. Common chemical oxidants employed are ferric chloride ($FeCl_3$) and ammonium persulfate [$(NH_4)_2S_2O_8$]. The resultant ICPs produced by these routes are considered to be in an oxidised (p-type) state, subsequently containing cationic sites resulting from the formation of stable radical cations (also referred to as polarons) upon its conjugated backbone. A counterion (A^-) is incorporated during synthesis to balance the charge upon the polymer backbone, subsequently doping the polymer in the relatively stable conducting form. The dopant anion can itself be provided by the oxidant employed

during chemical polymerisation or the electrolyte ions used during electrochemical polymerisation. Electrochemical oxidation can provide a greater degree of flexibility over the doping process in terms of the range of dopant anions that can be incorporated from the electrolyte (MA salt or HA acid). However, larger quantities of polymer can be obtained through chemical polymerisation methods as it is not limited by the heterogeneous interfacial nature of electrochemical processes.

Of the ICP's, polypyrroles can be readily synthesised from neutral aqueous solutions, while acidic conditions are required for the successful synthesis of polyaniline. Acidification of the aniline monomer, forming the anilinium cation, is critical for the synthesis of polyaniline. Polyaniline is also unique in that the degree of polymer protonation plays a critical role in the conductivity of the polymer. Both polypyrrole and polyaniline can be synthesised in aqueous environments, whereas, polymerisation of thiophene is usually carried out in organic solvents such as acetonitrile due to poor thiophene monomer solubility in aqueous electrolytes.

It should be noted that oxidative polymerisation is one of a number of methods that can be used for production of ICPs. Other methods such as condensation methods or organometallic aryl-aryl coupling [4, 16] are also used; however oxidative polymerisation is the only method that results in the production of "doped" or oxidised material. In the other cases, the neutral material is produced that can be doped/oxidised in a second step.

1.4 Polyaniline

Polyaniline (PAn) was discovered in 1934 and referred to as "aniline black". Interestingly, polyaniline like structures are known to exist as part of a mixed copolymer with polyacetylene and polypyrrole in some biologically sourced melanins. Due to the unique electrical, chemical and mechanical properties associated with polyaniline it has to date become one of the most investigated polymers. Many reviews have been published on synthesis, processing, properties, theory and applications of polyaniline [17-27].

Unlike polypyrrole and polythiophene, polyaniline can be found in three distinct oxidation states [1] (Scheme 1.1). Leucoemeraldine with y = 1, is the fully reduced state. Pernigraniline is the fully oxidised state (y = 0) with imine links. The emeraldine (y = 0.5) form of polyaniline is referred to as emeraldine base (EB). Emeraldine base is regarded as the most useful form of polyaniline due to its high stability at room temperature. In comparison, the leucoemeraldine is easily oxidised while the pernigraniline is easily degraded.

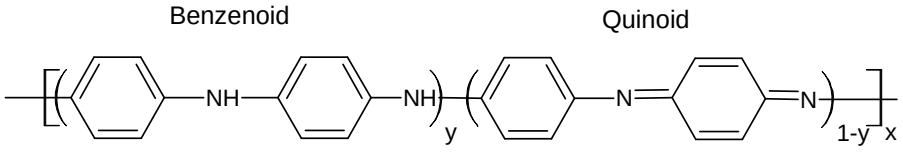

Scheme 1.1. Different oxidation states of polyaniline as base forms. y = 1 (leucoemeraldine), 0.5 (emeraldine) and 0 (pernigraniline).

1.4.1 Synthesis of polyaniline

Polyanilines are prepared by chemical or electrochemical oxidative polymerisation of the respective aniline monomers in acidic solution. Other polymerisation techniques that have also been used to prepare polyaniline include photochemically initiated polymerisation, and enzyme-catalyzed polymerization [1, 28].

Electrochemical polymerisation is carried out by employing either a constant current, a constant potential or potentiodynamic techniques in an aqueous solution of aniline. The electrolyte used is normally an acid (HA), which provides a sufficiently low pH as well as the dopant A^- to solubilise the monomer and to generate polyaniline in the doped emeraldine salt (ES) form. Polymerisation can occur on a variety of substrates; such as glassy carbon, platinum or gold plates and the transparent indium-tin-oxide (ITO)-coated glass. Electrochemical synthesis is flexible in terms of the dopant that can be incorporated from the electrolyte and is a useful tool for the preparation and characterisation of small films or coated electrodes [10].

Chemical polymerisation of aniline is carried out under acidic conditions in the presence of a chemical oxidant that supplies the oxidising force. The type of the oxidant and the influence of the synthetic conditions on the polymerisation of aniline are discussed in section 1.4.1.4. Chemical synthesis is simple and capable of producing bulk quantities of polyaniline powders.

Pron *et al.* [29] reported that the competing degradation reactions of the polymer in chemical polymerisation was slower than in electrochemical polymerisation. This suggests that under proper reaction conditions the side reactions are negligible in chemical polymerisation as compared to electrochemical polymerisation.

1.4.1.1 Autoacceleration

Autoacceleration is a typical feature of aniline polymerisation that involves the oxidation of aniline by highly oxidised polyaniline with the incorporation of acid [30]. A typical plot of concentration versus time in a clean solution shows that aniline concentration decreases very slowly in the beginning. However, after an induction period has passed, aniline concentration decreases dramatically in a relatively short time (Figure 1.2) [30].

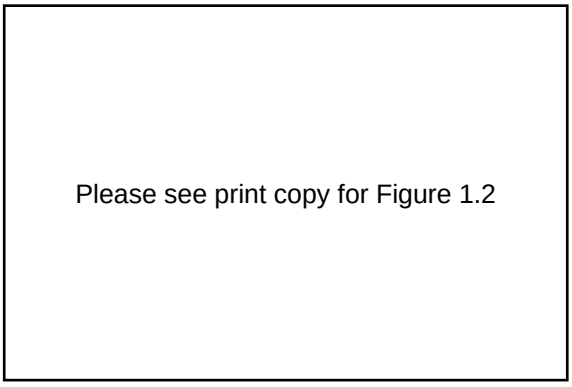

Figure 1.2. Aniline concentration vs. time for chemical polymerisation of 0.35 M aniline in 0.5 M HCl aqueous solution, aniline/APS 1:1 [30].

This mechanism proposes that aniline can be oxidised more easily (<0.7 V versus SCE) by the oxidised polyaniline than by the bare electrode or the oxidant employed.

Therefore, the reaction rate during polymersation increases as PAn is produced during both electrochemical [31] and chemical [30] oxidation.

1.4.1.2 Polymerisation mechanism

Both chemical and electrochemical polymerisation of aniline proceed via several steps as a radical propagation reaction (Figure 1.3). The steps are:

Step 1. Oxidation of aniline to a radical cation which exists in three resonance forms.

Step 2. Coupling of the radical cations, resulting in a dicationic dimer species. The coupling is predominantly "head to tail" or "para-coupling". This dimer then undergoes re-aromatisation to its neutral state, giving the intermediate *p*-aminodiphenylamine known as PADPA.

Step 3. Chain propagation via coupling the dimer radical cation (centred on the nitrogen atom) with an aniline radical cation centred in the para position.

Step 4. Oxidation of the growing polymer to a radical cation and doping with HA.

The chemical polymerisation mechanism has aspects of the electrochemical polymerisation mechanism but it also has subtle differences in that the initial product of step 3 in chemical polymersation is pernigraniline salt [32]. After consumption of all the oxidant, the pernigraniline salt is reduced by unreacted aniline to the green emeraldine salt [1] (Figure 1.4).

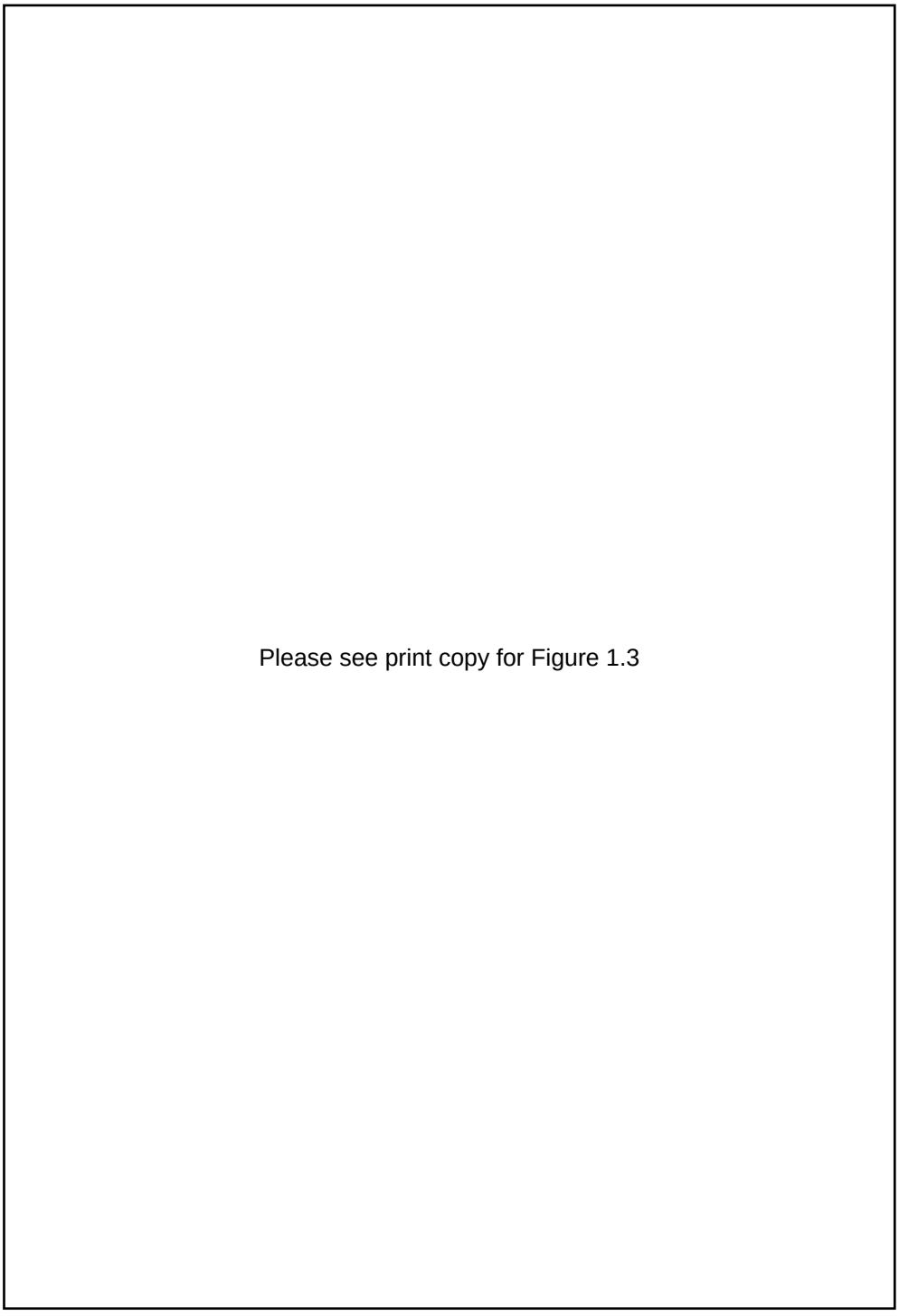

Figure 1.3. Mechanism for *electrochemical* polymerisation of aniline in aqueous HA acid, formation of polyaniline emeraldine salt [33].

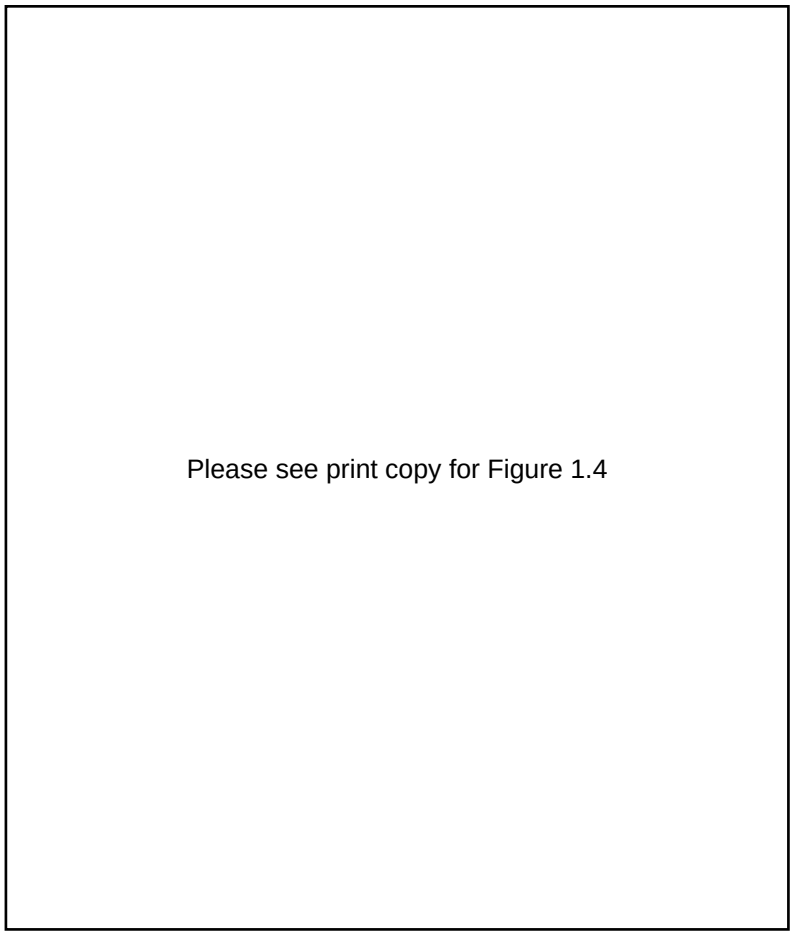

Figure 1.4. Chain propagation, and reduction of pernigraniline salt to emeraldine salt during *chemical* polymerisation of aniline in aqueous HA acid [33].

1.4.1.3 Monitoring the course of chemical polymerisation of aniline

Monitoring the evolution of the potential of the solution, pH, temperature and UV-visible spectra of the products obtained during the chemical synthesis of PAn are useful tools that have been used to determine the mechanism of polymerisation [34-36]. The hydrogen atoms displaced from aniline molecules during the polymerisation process are released as protons (see step 2 in Figure 1.3), increasing the acidity of the reaction medium. Moreover, the oxidation state of both the reactants and the products changes continuously during the redox reactions involved in polymerisation.

Typical changes in the pH and the open circuit potential during polymerisation of aniline involve the following steps (Figure 1.5):

Step 1. Oxidation of the aniline monomer to radical cations, which is associated with a decrease in potential.

Step 2. Dimers and oligomers are formed and the potential increases. Due to an autocatalytic polymerisation mechanism (see Section 1.4.1.1) the oxidation of aniline can be accelerated by the presence of oxidised oligomers during this step, resulting in a rapid increase in the reaction potential with a simultaneous rapid decrease in pH. The reduced oligomers can be oxidised again by remaining oxidant.

Step 3. In this step the potential reaches a plateau, a small decrease in pH is observed and the temperature increases sharply and eventually reaches a maximum. During this step polymerisation proceeds via chain propagation and polyaniline in the oxidised state of pernigraniline is formed.

Step 4. The potential and temperature drop rapidly and there is a further decrease in pH. During this step, the oxidant is assumed to be exhausted and the residual monomer slowly reduces the oxidised pernigraniline salt (PS) form to the emeraldine salt (ES) form of polyaniline.

Step 5. The reaction is completed with both the potential and pH leveling.

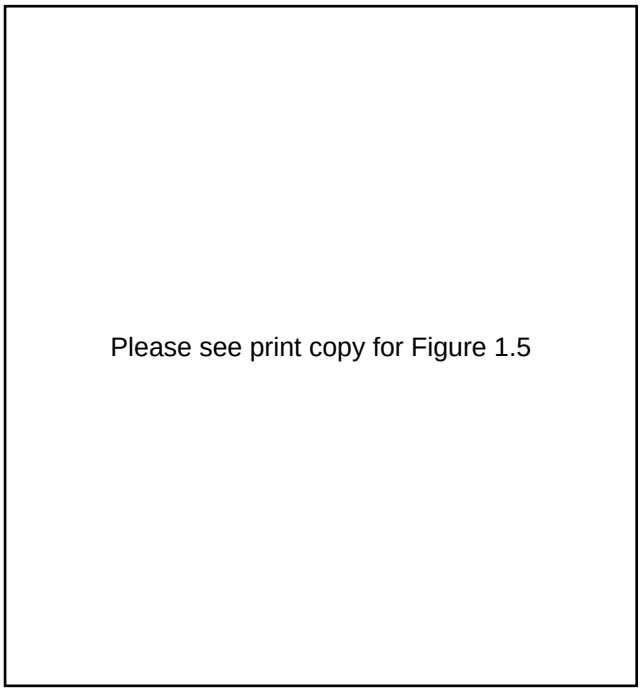

Figure 1.5. Potential and pH profiling during chemical synthesis of polyaniline at sub-zero temperatures [34].

1.4.1.4 Effect of synthetic conditions on chemical polymerisation of aniline

The properties of polyaniline are affected by polymerisation conditions, such as temperature, pH, time, monomer concentration, and oxidant/monomer molar ratio. The effect of different oxidising agents [29, 37, 38] and different protonic acids [37, 39] has also been widely studied.

Pron *et al.* [29] studied the chemical polymerisation of aniline in HCl solutions with four oxidising agents differing in redox potential; ammonium persulfate [$(NH_4)_2S_2O_8$], hydrogen peroxide (H_2O_2), potassium dichromate ($K_2Cr_2O_7$) and potassium iodate (KIO_3). Except hydrogen peroxide, the other three oxidising agents resulted in polyaniline products of similar conductivity. The conductivity of polyaniline synthesised with H_2O_2 was much lower.

The influence of synthesis temperature on yield and molecular weight has been reported for polyaniline [23, 40]. Generally, a decrease in polymerisation temperature results in higher yield and molecular weight. Adams *et al.* [41-44] found that the molecular weight (MWt) of PAn increased from 19,400 Da at 18ºC to 86,000 Da at 0ºC with further increases at sub-zero temperatures. Stejskal *et al.* [45] reported that the MWt and the conductivity of PAn increased as the reaction temperature was lowered.

It is generally accepted that acidic conditions are required for the polymerisation of aniline and substituted aniline to form a conjugated conducting polyaniline with higher yield and conductivity [18, 46, 47].

The first step in the polymerisation of aniline is formation of radical cations, which is not dependent on pH (the oxidation potential of APS is independent on pH) [48-50]. The radical cations are coupled differently in acidic and neutral media [18]. The head-to-tail (para-coupling) configuration predominates in acidic medium, while head-to-head coupling are observed for the products prepared under neutral conditions. The oxidising potential of aniline are decreased by increasing pH (50-60 mV/pH unit) [49, 50]. Thus initiation of oxidative polymerisation of aniline is more favorable in neutral or less acidic media than strongly acidic conditions.

The pH of the oxidative polymerisation of aniline by ammonium persulfate greatly affects the nature of the products. The formation of various organic products different from polyaniline have been recently reported by MacDiarmid [51] and Stejskal [52] when the oxidative polymerisation of aniline is carried out at mild acidic conditions (pH>3). Similar to the polymersation of aniline in strong acidic conditions (see Figure 1.5), the solution pH drops as the reaction proceeds due to production of protons in the course of aniline polymerisation.

When the conventional polymerisation solution was diluted (at a pH of 3-4) at the early stages to isolate the first product formed, or when the pH of polymerisation was held constant by a buffer solution, a brown product formed [51]. This brown product had different morphology (hollow microspheres) and different optical and magnetic

properties from those of polyaniline and was reported to be a member of the class of polyazanes, polymeric or oligomeric species containing a N-N backbone with three covalent single bonds for each nitrogen atom.

More recently Stejskal *et al.* have reported that polymerisation of aniline in 0.4 M acetic acid produces a mixture of para and ortho-coupled oligomers during the first phase of the reaction with low acidity (pH>4). Phenazine structures are subsequently produced by oxidation and intramolecular cyclization of these ortho-coupled oligomers (Figure 1.6). These needle-like oligomer crystallites are non-conducting [52]. As the solution pH falls during polymerisation, polyaniline in its conventional form [51] or polyaniline nanotubes (growing on the oligomeric crystallites) [52] are formed.

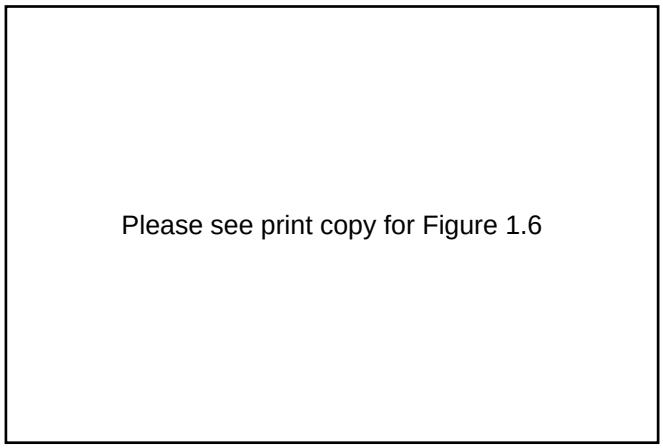

Figure 1.6. (A) Coupling of aniline molecules in both ortho- and para-positions during the oxidative polymerisation in mildly acidic media. (B) Formation of a phenazine unit by further oxidation of ortho-coupled units [52].

Chemical [53] and electrochemical [54] synthesis of polyaniline in alkaline solutions has also been reported. Morphologies such as hollow microspheres with low conductivity [53] and luminous materials [54] are produced using alkali-guided method.

The initial molar ratio of the reactants used has a significant influence on the properties of polyaniline. Armes and Miller [55] reported that the conductivity of polyaniline was independent on the APS/aniline ratio for oxidant/aniline molar ratios below 1; however

the yield of polyaniline increased linearly up to a ratio of 1. Both yield and conductivity were decreased via over-oxidation of the polymer at higher oxidant/monomer initial mole ratios. This study concluded that the most efficient ratio for polyaniline was about 1.15. Cao *et al.* [37] found that the aniline/oxidant used had a minor effect on the conductivity of the polyaniline produced but a major effect on the yield produced. The authors concluded that the high concentration of oxidant promoted the formation of soluble oligomers which resulted in a lower final yield. A maximum molecular weight was achieved at a oxidant/monomer ratio of 1.10-1.15 with a sharp drop in molecular weight observed above 1.15 reported by Adams *et al.* [41] for the polymerisation of polyaniline at low temperatures. Due to degradation of polymer at high concentration of oxidising agent several authors [56] have recommended the use of an oxidant/monomer ratio of 1.0 or less. In a study of chemical polymerisation of *o*-methoxyaniline by Gazotti and De Paoli [57], it was found that increasing the amount of oxidant reduced the conductivity and increased the yield of poly(*o*-methoxyaniline) due to facile oxidation of monomer and production of insoluble oligomers.

There have been a few studies on the effect of addition time or addition rate of oxidant in the chemical polymerisation of aniline. Adams *et al.* [41] reported a slight increase in molecular weight and yield of polyaniline synthesised at -26ºC by increasing the time of oxidant addition from instantaneous up to 36 h. Cao *et al.* [37] have reported the effect of addition rate of oxidant on the inherent viscosity of polyaniline and the powder morphology of the precipitated polyaniline. An extremely fine morphology was obtained when the oxidant was added rapidly, however coarse particles were produced at lower rates of oxidant addition. The presence of more structural irregularity, when the oxidant was added rapidly, in the polymer chain synthesised at low temperatures was elucidated by Adams and Monkman [42]. This was thought to be due to the higher extent of formation of pernigraniline intermediate in the polymerisation of aniline with rapid oxidant addition.

Rapidly mixing of a solution of aniline in acid and ammonium peroxydisulfate results in aqueous dispersion of polyaniline nanofibres [58]. The idea is to prevent the secondary growth by the even distribution of aniline and oxidant and consumption of

all the reactant. Slow addition of oxidant in conventional chemical synthesis results in agglomeration of polyaniline particles (produced at the early stage of polymerisation) that are exposed to aniline and oxidant.

Mechanical agitation can also control the shape and aggregation of the polyaniline particles [59]. Nanofibres of polyaniline can be simply prepared at an elevated temperature by not mechanically agitating the reaction.

1.4.2 Properties of polyaniline

Polyaniline has optical, chromic and electrochemical properties that distinguish it from other conducting polymers [1].

1.4.2.1 Redox activity

Polyaniline is unique among inherently conducting polymers in that it has three readily accessible oxidation states, the fully reduced leucoemeraldine, half-oxidised emeraldine, and fully oxidised pernigraniline [60, 61] (Figure 1.7). Only the emeraldine salt, which is the protonated form of emeraldine base, is electrically conductive. The basic sites (amine and imine groups) in the polymer backbone of emeraldine base can be protonated with adequately strong acids to produce emeraldine salt. Thus polyaniline is sensitive to pH changes. PAn is redox active at pH values lower than 4. At higher pH values, PAn deprotonates and loses its redox activity.

leucoemeraldine salt (LS)

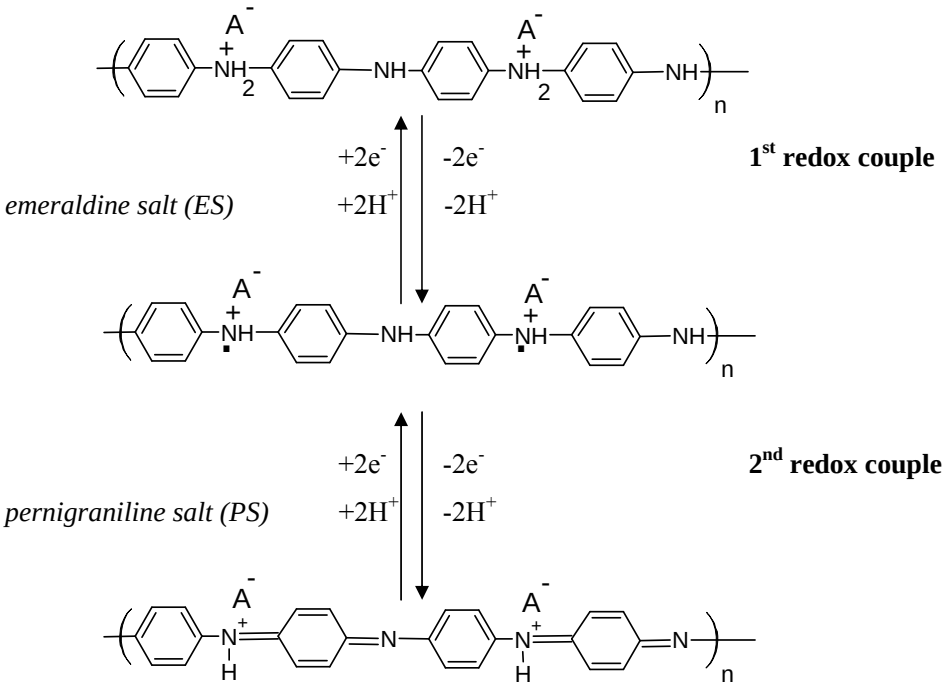

Figure 1.7**.** Redox reactions between the various forms of polyaniline.

1.4.2.2 Doping and conductivity

"Doping" in conducting polymers refers to the redox processes that transform polymers from an insulating form to their conducting form. A polymeric cation is formed by oxidative doping. The overall charge neutrality of the polymer chain is conserved by subsequent incorporation of a counter anion "dopant". The de-doping in turn is conversion of polymer from conducting form to insulating form. This generally results in expulsion of dopant counter anion except in the case of large dopants such as polyelectrolytes. Doping /de-doping in conducting polymers is a reversible process.

Unlike other conducting polymers, the conductivity of polyaniline is varied by the degree of oxidation (variation in the number of electrons) and the degree of protonation (variation in the number of protons) [62, 63]. Among the different oxidation states, only the emeraldine salt form of polyaniline is conducting. Polyaniline becomes conducting

when the moderately oxidised state, emeraldine base, is protonated and charge carriers are generated. This process is called "protonic acid doping" [63]. Polyaniline is unique in its doping process, since no electron is added to or removed from the insulating material to make it conducting [17], Scheme 1.2.

Please see print copy for Scheme 1.2

Scheme 1.2. Protonic acid doping in polyaniline [33]

The emeraldine base insulating form of polyaniline (conductivity 10^{-10} S/cm) can be converted to a metallic state (conductivity $4x10^{2}$ S/cm) upon protonation [64]. This is explained by a two-steps transition [62]. Addition of two protons at the –N= sites on either side of the quinoid rings in the emeraldine base form (Figure 1.8a) results in a spinless bipolaron defect as shown in Figure 1.8b. The first step is related to an internal redox reaction and formation of more stable two paramagnetic polarons (Figure 1.8c) on the polyemeraldine chain with respect to a bipolaron. The second step is separation of these two polarons, owing to their electrostatic repulsion, to yield a polaron lattice (Figure 1.8d).

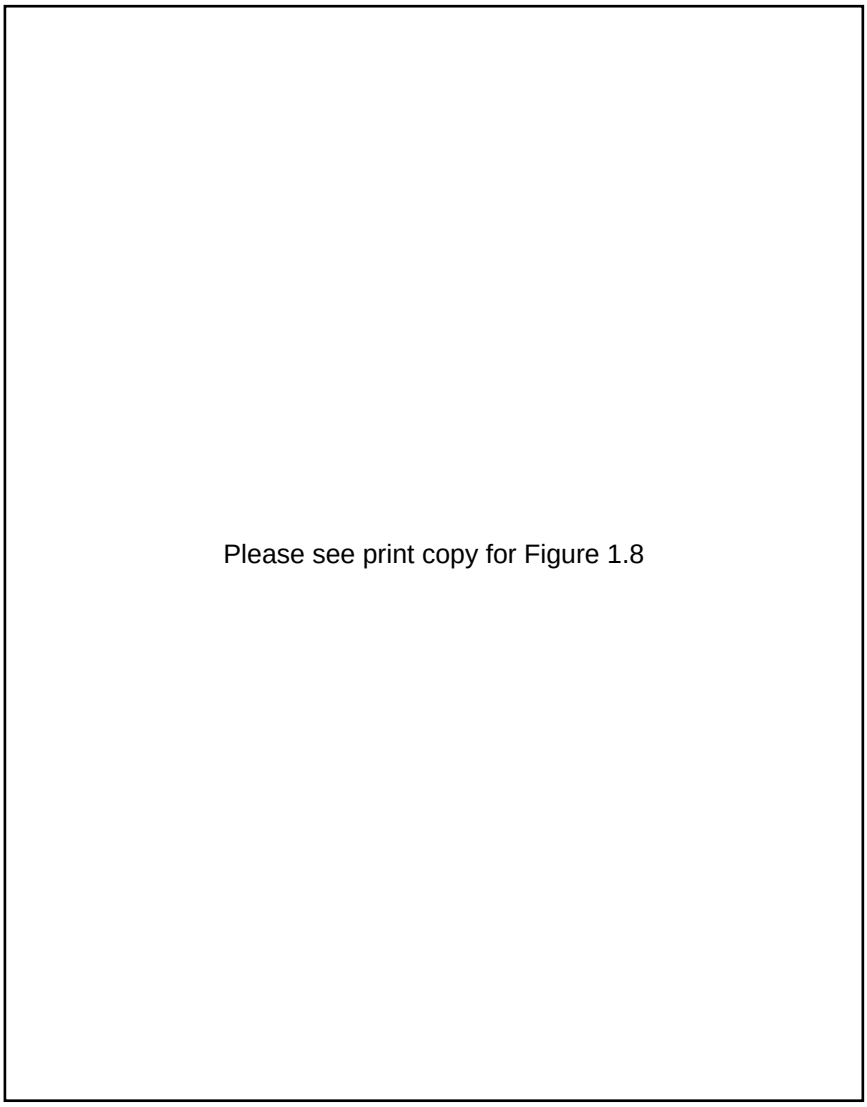

Figure 1.8. Sketch of the geometric structure of emeraldine form of polyaniline (a) before protonation and (b)-(d) after 50% protonation: Formation of (b) bipolarons, (c) polarons, and separation of polarons to form a polaron lattice (d) [62].

In the undoped state of a conjugated polymer, two types of π-bonding and π*-antibonding molecular orbitals form valance and conduction bands with a large band gap. A radical cation is formed by removal of one electron from the conjugated polymer. This is called a "polaron" and shows an electron spin resonance (ESR) signal

due to the unpaired electron. Removal of a second electron from the polymer forms additional polarons upon the polymer chain. It is then possible for these polaron structures to interact and pair, reversibly, resulting in the formation of a spinless bipolaron with no ESR signal.

Polarons and bipolarons are the charge carriers in conducting polymers. These charge carriers move along the polymer chain upon application of an electric field and are responsible for electrical conductivity. The concentration and mobility of these charge carriers determine the electrical conductivity. A number of mechanisms have been reported for conductivity of polyaniline including conduction via a polaronic (radical cation on nitrogen sites) lattice, formation of bipolarons [18, 65, 66], formation of metallic islands and conduction due to charge transport between the islands [67], and a three dimensional electron hopping model [64].

The conductivity is affected by the water content. Drying polyaniline samples lowers the conductivity by 5 times [17, 68, 69].

1.4.2.3 Optical properties

The UV-visible spectroscopy of polyaniline is sensitive to oxidation state, the solution pH and the conformation adopted by the polymer chains.

The emeraldine salt form of PAn in compact coil conformation exhibits three bands: a π-π^* band at ca. 330 nm and two bands in the visible region at ca. 440 nm and 780 nm assigned as π-polaron and polaron-π transitions, respectively (Figure 1.9). However, when an extended coil conformation is adopted, the localised polaron band at ~780 nm is replaced by a broad free carrier tail starting from ~1000 nm in the infrared region. PAn in this extended coil conformation has a much enhanced electrical conductivity as a result of delocalisation of the polaron band along the PAn chains [1, 70].

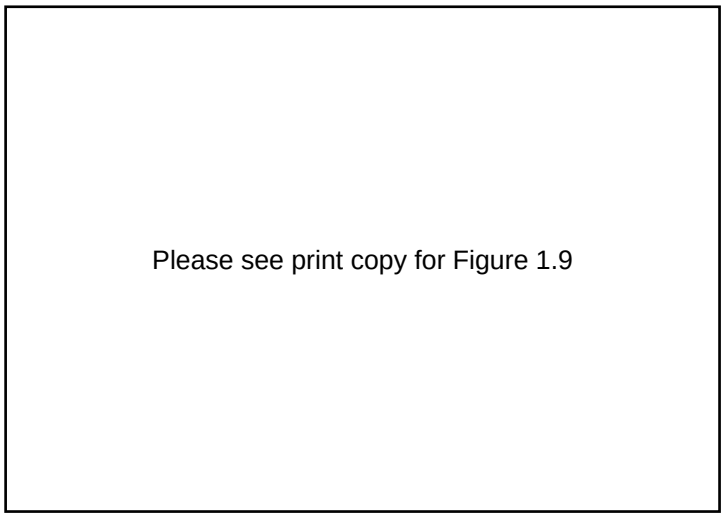

Figure 1.9. Schematic energy levels diagrams of fully protonated PAn/HCSA emeraldine salt with different conformations of PAn chains [70].

The emeraldine base form of PAn shows a low wavelength π-π* band and a strong absorption band at ca. 600 nm, attributed to a local charge transfer between a quinoid ring and the adjacent imine-phenyl-amine units (intramolecular charge transfer exciton) [1]. The reduced leucoemeraldine base (LB) form exhibits a band at ca. 320 nm attributed presumably to the π-π* electronic transition. Pernigraniline base (PB) shows two bands at ca. 320 nm (π-π* band) and at ca. 530 nm (Peierl gap transition) [1]. Protonation of PB results in the formation of PS form with the appearance of a strong PS peak at ca. 700 nm, instead.

Transitions of PAn between different oxidation states and upon protonation/deprotonation are associated with colour changes. ES and EB forms are green and blue, respectively. LB form is colourless to pale yellow. PB form is violet and turns to blue by protonation to PS form.

1.4.2.4 Solubility

The protonated emeraldine salt form of PAn is insoluble in aqueous solutions and most common organic solvents. It is soluble in concentrated sulfuric acid [71].

When the emeraldine salt is deprotonated to the insulating emeraldine base, it can be solubilised in a number of organic solvents [10, 17, 46] such as methyl pyrrolidinone (NMP), dimethyl formamide (DMF), dimethyl sulfoxide (DMSO), *m*-cresol, chloroform (CCl_3H) and tetrahydrofuran (THF). The process of deprotonation effectively removes the cationic charges upon the backbone, reducing the polymers ionic character making it more amenable to dissolution. Gelation of the polymer commonly occurs at high concentrations of the EB solutions, resulting in viscosity increases due to strong interchain hydrogen bonding between the amine hydrogens and the nearest neighbouring imine nitrogens. A more novel route to inducing solubility in the ES form is by the use of functionalised protonic acid dopants such as sulfonic acids {(10-champhor sulfonic acid (HCSA), and dodecyl-benzene sulfonic acid (DBSA)} [72], but similar to the EB route solubility is limited.

1.4.3 Self-doped polyanilines

Self-doped polyanilines are derivatives of polyaniline that have negatively charged functional groups which are covalently bounded to the polymer backbone. The acid groups on the polymer backbone replace the negative counterions which compensate for the positive charges present on the emeraldine salt form of polyaniline. Internal doping arises when the acid group is strong enough to sufficiently protonate the basic polymer backbone.

In 1990, the first syntheses of self-doped conducting polyaniline derivative was reported by Yue and Epstein [73] and Bergeron *et al.* [74] followed by the publishing of many papers about synthesis and the properties of self-doped conducting polymers [75]. The most important achievements dealing with the synthesis and properties of self-doped polyanilines have been recently reviewed by Malinauskas [75]. These polymers can be obtained either by chemical and electrochemical synthesis of appropriate substituted monomers or by the post synthesis chemical modification of polyaniline.

1.4.4 Processability

Processability has been one of the major issues in the synthesis and applications of conducting polymers. The possible applications of polyaniline are to some extent

limited by the lack of solubility and processability. A number of strategies aimed at improving the processability of polyaniline have been investigated.
To enhance the solubility of conducting polymers a great deal of research has been directed to functionalisation, copolymerisation, chemical modification and the use of suitable doping acids.

Alkyl or alkoxy substitution of the aniline monomer improves the solubility of the resultant polymer in organic solvents, but has a negative influence on the conductivity [76-78].

The first known examples of water-soluble conducting polymers reported in 1987, are the sodium salts and the 'proton salts' (acids) of poly-3-(2-ethanesulfonate)thiophene and of poly-3-(4-butanesulfonate)thiophene [79]. These polymers are self-doped polythiophenes. The electrochemical polymerisation of aniline carboxylic acid isomers has been recently reported [80] to result in short-chain conducting polymers with much lower electropolymerisation rates than aniline. Poly(o-aminobenzylphosphonic acid) is another type of self-doped conducting polyaniline synthesised by Tan *et al.* [81]. This polymer was soluble in dilute ammonia solution but insoluble in water. Electro-co-polymerisation of aniline and o-aminobenzesulfonic acid [82] resulted in sulfonated polyaniline which was soluble in neutral pH solutions.

The most successful approach to soluble polyaniline is to introduce a sulfonic acid group to the polyaniline chain to make self-doped sulfonated polyaniline (SPAN). Chemical and electrochemical polymerisation of methoxyaniline sulfonic acid [83-85] and also the post synthesis chemical modification of polyaniline [73, 86-88] have resulted in self-doped polyanilines with improved solubility and redox activity over a wide pH range. However, these polymers have low electrical conductivity due to the resulting chain torsion. Copolymers of aniline and ortho-alkoxy sulfonated polyaniline have also low conductivity (10^{-3} to 1 S/cm depending on the aniline fraction) and very low molecular weight (about 10 units) 1700-3000 g/mole [89].

A new subset in the field of conducting polymers is synthesis of nanodimensional materials. Polyanilines with nanoscale dimensions have been shown to have enhanced processability, surface area, conductivity and electrochemical switching processes. Some of the synthetic protocols for making these materials involve using stabilisers, physical templates and the use of preformed nanosized structures to make conducting polymer nanocomposites [14].

A route to solution processing and nonostructured materials is formation of colloidal dispersions with reasonable conductivity by using a range of steric stabilisers. These include surfactants and micelles such as dodecyl benzene sulfonic acid [90, 91], naphthalenesulfonic acid [92] polyethylene oxide [93, 94], water soluble polymers such as poly(N-vinyl-pyrrolidone) [95, 96], organic dopants [97], and silica colloids [98].

Water dispersable polyanilines can also be obtained by template guided polymerisation of aniline using polyelectrolytes such as poly(styrenesulfonic acid) [28], poly(acrilic acid) [99] and poly(2-acrylamido-2-methyl-1-propanesulfonic acid) [100] as template. The role of the anionic template is to align aniline monomers and promote head-to-tail coupling and minimise the parasitic branching. The polyacid template is thought to provide a localised low pH for growth of water soluble polyaniline and also the necessary counterions for doping polyaniline to the conducting form [28]. The reaction rate for polymerisation of templated aniline has been reported to be faster than ordinary chemical polymerisation owing to the high local concentration of aniline and hydrogen ions on the template matrix (polyamide) [100]. The use of these non-conducting polyelectrolytes however results in low conductivity of the resultant water dispersable polyanilines [101-103] .

Recently, polyaniline nanofibres were synthesised by using interfacial polymerisation at an aqueous/organic interface or rapid mixing of monomer and oxidant aqueous solutions in a controlled ratio[58, 104]. These methods have the advantage of facile stabiliser-template free polymerisation and ease of purification. The nanofibres have diameters between 30 and 50 nm and make relatively stable dispersions at pH around 2-3 [105].

PAn composites

The preparation of conducting polymer composites or blends with common polymers has been investigated [27] in order to improve the mechanical properties, and processability of ICPs. In general there are two main methods used to produce composites: 1) synthetic methods based on polymerisation of aniline in a matrix polymer, and 2) blending methods via mixing a previously synthesised polyaniline with a matrix polymer.

1.4.5 Sulfonated polyanilines

A study on the influence of different substituents on polymer self-doping capability of polypyrrole and polythiophene demonstrated that sulfonic acid substitution was more beneficial to the final conductivity than carboxyl acid substitution [106]. SPAN (Scheme 1.3, I), the first reported self-doped water soluble conducting polyaniline derivative, was synthesised by sulfonation of the emeraldine base of PAn using fuming sulfuric acid [73]. Elemental analysis of SPAN revealed a S/N atomic ratio of 0.48 and titration analysis established a doping level of 0.3 [107]. SPAN has lower conductivity than PAn (about 0.1 S/cm), but remains conductive until pH 7. SPAN is soluble in basic aqueous solutions (23 mg/ml). It has been shown that SPAN has better thermal stability than the parent polyaniline doped with HCl. These properties have resulted in the use of SPAN in rechargable batteries [108-110] with a high charge density and light emitting diodes [111]. Treatment of the reduced leucoemeraldine base form of PAn with fuming sulfuric acid leads to highly sulfonated (75%) SPAN [88], however fully sulfonated PAn can not be achieved in this way. Highly sulfonated PAn has increased solubility (38 mg/ml) and conductivity (1 S/cm) compared to 50% SPAN (mentioned above) and the former is conductive over the pH range of 0-14. Electrochemical preparation of fully sulfonated polyaniline in aqueous phase [87] has also been reported. Zhang *et al.* have recently (2006) synthesised a fully sulfonated polyaniline nano-network by electropolymerisation of orthanilic acid. This was achieved using a long three-step electrochemical deposition procedure in a mixed solvent of acetonitrile and water [112].

Other chemical modification agents have been used for preparation of water soluble N-substituted derivatives of PAn [74, 113]. Poly(aniline-co-N-propansulfonic acid)

(PAPSA) has been prepared by treatment of the polyaniline emeraldine base form with 1,3-propane sultone [113]. PAPSA has a S/N atomic ratio of 0.48, doping level of 0.33 and conductivity of 0.015 S/cm [114].

A distinct way of producing self-doped polyanilines is the chemical polymerisation of sulfonated anilines. Polymerisation of aniline sulfonic acid has not led to high molecular weight polymers because of the low reactivity of the monomer due to the presence of a strong electron-withdrawing sulfonate group [83]. Oligomers with molecular mass of 3000 are obtained by polymerisation of *m*-aniline sulfonic acid using ammonium persulfate as oxidant [83] with a low electrical conductivity ($3x10^{-6}$ S/cm). It is possible to polymerize metanillic acid by carrying out the reaction under high pressure, but the yield is only around 10% [115].

Substitution by an electron-donating group like methoxy [83] increases the electron density on the amino group and the reactivity of monomer. Chemical polymerisation of 2-methoxy aniline-5-sulfonic acid (MAS) under normal atmospheric pressure gives poly(2-methoxy aniline, 5-sulfonic acid) (PMAS, Scheme 1.3, II) with high molecular weight (10,000 Da) and conductivity of 0.04 S/cm. The monomer is soluble in basic solutions. PMAS has been synthesised under basic conditions using pyridine, whereas the polymer is not produced under acidic conditions. PMAS has also been prepared electrochemically by the use of electrohydrodynamic processing [84, 85].

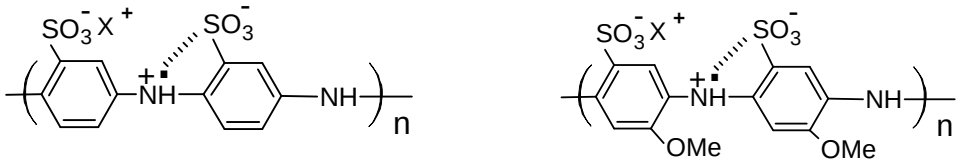

(I) (II)

X^+ = proton or monovalent cation

Scheme 1.3. Structures of (I) SPAn, and (II) PMAS.

Self-doped sulfonated polyanilines have many properties different from those of the parent polyaniline, particularly improved solubility, ease of processability and electroactivity over a broad range of pH. Additionally, similar to other self-doped polyanilines, sulfonated polyanilines have an inner dopant anion. Thus, unlike polyaniline no anion exchange takes place between sulfonated polyaniline and electrolyte during oxidation and reduction [75, 116]. Faster charge compensation instead is carried out by cation (usually a proton) exchange according to Eqn. 1 [75]:

$$(\mathrm{PANI \cdot H^+{-}SO_3^-})_n - n\mathrm{e}^- - n\mathrm{H}^+ \rightarrow (\mathrm{PANI^+{-}SO_3^-})_n \qquad \text{Eqn.1}$$

These features make them promising for some specific application fields such as rechargeable batteries, light emitting diodes, sensors and biosensors [75].

1.4.6 PMAS

Poly(2-methoxyaniline-5-sulfonic acid) (PMAS) is a self-doped fully-sulfonated polyaniline that can be synthesised by chemical or electrochemical oxidative polymerisation of the monomer (Scheme 1.4).

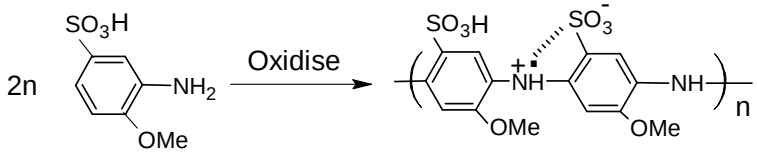

Scheme 1.4. Polymerisation of MAS to form PMAS.

PMAS properties

PMAS is highly water soluble (30% w/v). This self-doped polyaniline has two sulfonated groups in the dimer repeating unit. One sulfonate group is assumed to be involved in self-doping of the adjuscent radical cation in polyaniline backbone. The other sulfonate group is free and can interact electrostatically with cations such as H^+, Na^+ and NH_4^+ [117] or large positively charged molecules and polyelectrolytes (amines, amino acids, proteins and enzymes) such as phenylethylamine (PhEA) [118] , poly-L-lysine (PLL) [33] poly(4-vinylpyridine) [119] and poly(amidoamine) dendrimer [120].

It has also been used as a molecular dopant for preformed polyaniline [121]. PMAS has also been used as a molecular dopant for polypyrrole being incorporated during electrosynthesis [122].

The optical properties of PMAS in the emeraldine and leucoemeraldine states are different from SPAN and the parent polyaniline. A broad absorption band at 320-390 nm in the UV-vis spectrum of PMAS emeraldine salt (ES) is attributed to the π-π* transitions. The sharp peak at 473 nm and the free carrier tail in the near infrared region beginning at *ca.* 900 nm are assigned to the low wavelength polaron band and the high wavelength delocalised polaron transitions, respectively [123]. A film of PMAS emeraldine salt shows an intense near-infrared band at *ca.* 2,200 nm [117]. The presence of the latter peak suggests that unlike polyaniline emeraldine salt which exhibits the features of compact coil conformation, PMAS in aqueous solution exists in an extended coil conformation [123].

PMAS is resistant to alkaline dedoping, with no emeraldine base being formed even in 2.0 M NaOH [117, 124]. The spectroscopic changes observed in alkaline solutions are consistent with a conformational change to compact coil conformation.

The UV-vis spectrum observed for the leucoemeraldine base form of PMAS exhibits a sharp peak at 408 nm which is different from SPAN and the parent polyaniline [117]. The chemistry of the species with λ_{max} 480 nm was not clear, however thermochromism and salvatochromism studies by Pornputtkul *et al.* [33] showed that the intensity of the 408 nm peak was reversibly changed with temperature and solvent. These phenomena were presumably assigned to a rearrangement of the PMAS chains, possibly between two conformations [33].

PMAS is electroactive in solution and in the solid state when complexed with other materials. Two redox peaks are observed for PMAS complexes [120, 125]. These are similar to those observed for polyaniline corresponding to the interconversions between leucoemeraldine, emeraldine and pernigraniline salt forms, however the shape of the first peak is dramatically different (broad and weak). When the potential is scanned

above 0.8 V, an additional peak appears as with polyaniline and this is presumably due to degradation and hydrolysis of the imine to form benzoquinone [120].

A charge transport and magnetic study of PMAS by Lee *et al.* [126] shows that the addition of methoxy and sulfonate side groups leads to formation of bipolarons and a decreased density of states at the Fermi level as well as a lower room temperature conductivity. The conductivity of PMAS (0.02 S/cm) is less than SPAN (~0.1-1 S/cm) with the S/N ratios ~0.5 and 0.75.

1.5 Objectives of this project

Various studies have been presented here to investigate the optimum synthesis conditions for PMAS. The incorporation of this negatively charged conducting polymer into other conducting polymer systems, their properties, and their potential applications have also been investigated.

Following green chemistry principles in developing new ways to manufacture products that are not damaging or toxic to the environment, this study has adopted environmentally friendly solvents for synthesis of water soluble conducting PMAS. We have achieved this recently through the use of ammonia solution instead of pyridine to solubilise the MAS monomer.

In this work, PMAS has been produced by chemical polymerisation of MAS in NH_4OH solution using ammonium persulfate as an oxidant. This process leads to a mixture of high molecular weight (HMWt) polymer *ca.* 10 KDa and low molecular weight (LMWt) oligomers less than 2.5KDa, using either chemical or electrochemical synthesis methods [83, 84]. Due to the similar solubility characteristics of these two fractions, it has proven difficult to separate the oligomers from the polymer at the gram scale via conventional dialysis or chromatographic techniques such as GPC. The focus of the third Chapter described in this thesis was to develop a new method for purification and fractionation of chemically synthesised PMAS using a cross flow dialysis system.

To date, optimisation of the synthesis and influence of different variables on the chemical polymerisation of MAS have not been systematically studied. The effect of synthetic conditions was studied here and described in Chapter 4. The optimum conditions for polymerisation of MAS with respect to conductivity, molecular weight and yield have been established.

The studies on chemical and electrical properties of PMAS were mostly carried out on commercially available PMAS that contains oligomeric impurities. The aim of the work described in Chapter 5 was to explore more extensively the properties of the pure PMAS obtained in this work.

Another goal of this study was to incorporate PMAS as a conductive and electroactive polyelectrolyte dopant into other conducting polymer systems such as polyanilines. Chapters 6 and 7 explore the possibility of either chemical or electrochemical synthesis of novel PAn/PMAS materials. These novel materials could be produced as films and as nanodispertions.

1.6 References

1. Gordon G. Wallace, Geoffrey M. Spinks, Peter R. Teasdale, *Conductive electroactive polymers : intelligent materials systems*. Vol. 1. 2002: Boca Raton, FL : CRC Press.
2. Shirakawa H, L.E., MacDiarmid AG, Chiang CK, and Heeger AJ., *Synthesis of electrically conducting organic polymers: halogen derivatives of poly(acetylene), (CH)x.* J Chem Soc, Chem Commun, 1977. **16**: p. 578-579.
3. Jaiswal, M. and Menon, R., *Polymer electronic materials: a review of charge transport.* Polymer International, 2006. **55**(12): p. 1371-1384.
4. Weder, C., *Organometallic conjugated polymer networks.* Journal of Inorganic and Organometallic Polymers and Materials, 2006. **16**(2): p. 101-113.
5. Kirova, N., *Electronic correlations and excitons in conducting polymers.* Synthetic Metals, 2005. **152**(1-3): p. 313-316.
6. Prigodin, V.N., Hsu, F.C., Kim, Y.M., Park, J.H., Waldmann, O., and Epstein, A.J., *Electric field control of charge transport in doped polymers.* Synthetic Metals, 2005. **153**(1-3): p. 157-160.
7. Park, S.M. and Lee, H.J., *Recent advances in electrochemical studies of pi-conjugated polymers.* Bulletin of the Korean Chemical Society, 2005. **26**(5): p. 697-706.
8. Wallace, G.G., Too, C.O., Officer, D.L., and Dastoor, P., *Photoelectrochemical cells based on inherently conducting polymers.* Mrs Bulletin, 2005. **30**(1): p. 46-49.

9. Perepichka, I.F., Perepichka, D.F., Meng, H., and Wudl, F., *Light-emitting polythiophenes.* Advanced Materials, 2005. **17**(19): p. 1281-2305.
10. Spinks G.M., Innis P.C., Lewis T.W., Kane Maguire L.A.P. and Wallace G.G., *Current state and Future Directions of Research and Development in Conducting Polymers.* Materials Forum, 2000. **24**: p. 125-166.
11. Mortimer R.J., Dyer A.L., and Reynolds J.R., *Electrochromic organic and polymeric materials for display applications.* Displays, 2006. **27**(1): p. 2-18.
12. Ahuja T., Mir I.A., Kumar D., and Rajesh, *Biomolecular immobilization on conducting polymers for biosensing applications.* Biomaterials, 2007. **28**(5): p. 791-805.
13. James, D., Scott, S.M., Ali, Z., and O'Hare, W.T., *Chemical sensors for electronic nose systems.* Microchimica Acta, 2005. **149**(1-2): p. 1-17.
14. G.G. Wallace, S.E. Moulton, V.J. Misoska, L.A.P. Kane-Maguire and P.C. Innis, *Nanostructures Based on Inherently Conducting Polymers.* MATERIALS FORUM, 2002. **26**: p. 29-38.
15. Terje A. Skotheim, R.L.E., John R. Reynolds, *Handbook of conducting polymers*. 2nd ed. ed. 1998: New York : M. Dekker.
16. Cheng, Y.J. and Luh, T.Y., *Synthesizing optoelectronic heteroaromatic conjugated polymers by cross-coupling reactions.* Journal of Organometallic Chemistry, 2004. **689**(24): p. 4137-4148.
17. Feast, W.J., Tsibouklis, J., Pouwer, K.L., Groenendaal, L., and Meijer, E.W., *Synthesis, processing and material properties of conjugated polymers.* Polymer, 1996. **37**(22): p. 5017-5047.
18. Genies, E.M., Boyle, A., Lapkowski, M., and Tsintavis, C., *Polyaniline: A historical survey.* Synthetic Metals, 1990. **36**(2): p. 139-182.
19. Kang, E.T., Neoh, K.G., and Tan, K.L., *Polyaniline: A polymer with many interesting intrinsic redox states.* Progress in Polymer Science, 1998. **23**(2): p. 277-324.
20. Schrieffer, J.R., *theoretical concepts of conducting polymers.* Synthetic Metals, 1991. **43**(1-2): p. 3307-66.
21. Walton, D.J., *Electrically conducting polymers.* Materials & Design, 1990. **11**(3): p. 142-152.
22. Zhang, D. and Wang, Y., *Synthesis and applications of one-dimensional nano-structured polyaniline: An overview.* Materials Science and Engineering: B, 2006. **134**(1): p. 9-19.
23. Syed, A.A. and Dinesan, M.K., *Review: Polyaniline--A novel polymeric material.* Talanta, 1991. **38**(8): p. 815-837.
24. Adhikari, B. and Majumdar, S., *Polymers in sensor applications.* Progress in Polymer Science, 2004. **29**(7): p. 699-766.
25. Bhattacharya, A. and De, A., *Conducting composites of polypyrrole and polyaniline a review.* Progress in Solid State Chemistry, 1996. **24**(3): p. 141-181.
26. Gerard, M., Chaubey, A., and Malhotra, B.D., *Application of conducting polymers to biosensors.* Biosensors and Bioelectronics, 2002. **17**(5): p. 345-359.
27. Pud, A., Ogurtsov, N., Korzhenko, A., and Shapoval, G., *Some aspects of preparation methods and properties of polyaniline blends and composites with organic polymers.* Progress in Polymer Science, 2003. **28**(12): p. 1701-1753.

28. Liu, W., Cholli, A.L., Nagarajan, R., Kumar, J., Tripathy, S., Bruno, F.F., and Samuelson, L., *The Role of Template in the Enzymatic Synthesis of Conducting Polyaniline.* J. Am. Chem. Soc., 1999. **121**(49): p. 11345-11355.
29. Pron, A., Genoud, F., Menardo, C., and Nechtschein, M., *The effect of the oxidation conditions on the chemical polymerization of polyaniline.* Synthetic Metals, 1988. **24**(3): p. 193-201.
30. Tzou, K. and Gregory, R.V., *Kinetic study of the chemical polymerization of aniline in aqueous solutions.* Synthetic Metals, 1992. **47**(3): p. 267-277.
31. Shim, Y.-B. and Park, S.-M., *Electrochemistry of conductive polymers VII. Autocatalytic rate constant for polyaniline growth.* Synthetic Metals, 1989. **29**(1): p. 169-174.
32. Manohar, S.K., Macdiarmid, A.G., and Epstein, A.J., *Polyaniline: Pernigranile, an isolable intermediate in the conventional chemical synthesis of emeraldine.* Synthetic Metals, 1991. **41**(1-2): p. 711-714.
33. Pornputtkul, Y., *Development of Chiral Conducting Polymers for Asymmetric Electrosynthesis*, in University of Wollongong, 2005.
34. Beadle, P.M., Nicolau, Y.F., Banka, E., Rannou, P., and Djurado, D., *Controlled polymerization of aniline at sub-zero temperatures.* Synthetic Metals, 1998. **95**(1): p. 29-45.
35. Stejskal, J., Kratochvil, P., and Spirkova, M., *Accelerating effect of some cation radicals on the polymerization of aniline.* Polymer, 1995. **36**(21): p. 4135-4140.
36. Sbaite, P., Huerta-Vilca, D., Barbero, C., Miras, M.C., and Motheo, A.J., *Effect of electrolyte on the chemical polymerization of aniline.* European Polymer Journal, 2004. **40**(7): p. 1445-1450.
37. Cao, Y., Andreatta, A., Heeger, A.J., and Smith, P., *Influence of chemical polymerization conditions on the properties of polyaniline.* Polymer, 1989. **30**(12): p. 2305-2311.
38. Armes, S.P. and Aldissi, M., *Potassium iodate oxidation route to polyaniline: an optimization study.* Polymer, 1991. **32**(11): p. 2043-2048.
39. Kahol, P.K., Satheesh Kumar, K.K., Geetha, S., and Trivedi, D.C., *Effect of dopants on electron localization length in polyaniline.* Synthetic Metals, 2003. **139**(2): p. 191-200.
40. Mattoso, L.H.C., MacDiarmid, A.G., and Epstein, A.J., *Controlled synthesis of high molecular weight polyaniline and poly(o-methoxyaniline).* Synthetic Metals, 1994. **68**(1): p. 1-11.
41. Adams, P.N., Laughlin, P.J., and Monkman, A.P., *Synthesis of high molecular weight polyaniline at low temperatures.* Synthetic Metals, 1996. **76**(1-3): p. 157-160.
42. Adams, P.N. and Monkman, A.P., *Characterization of high molecular weight polyaniline synthesized at -40 [deg]C using a 0.25:1 mole ratio of persulfate oxidant to aniline.* Synthetic Metals, 1997. **87**(2): p. 165-169.
43. Adams, P.N., Laughlin, P.J., Monkman, A.P., and Kenwright, A.M., *Low temperature synthesis of high molecular weight polyaniline.* Polymer, 1996. **37**(15): p. 3411-3417.
44. Adams, P.M., Abell, L., Middleton, A., and Monkman, A.P., *Low temperature synthesis of high molecular weight polyaniline using dichromate oxidant.* Synthetic Metals, International Conference on Science and Technology of Synthetic Metals, 1997. **84**(1-3): p. 61-62.

45. Stejskal, J., Riede, A., Hlavata, D., Prokes, J., Helmstedt, M., and Holler, P., *The effect of polymerization temperature on molecular weight, crystallinity, and electrical conductivity of polyaniline.* Synthetic Metals, 1998. **96**(1): p. 55-61.
46. Shenglong, W., Fosong, W., and Xiaohui, G., *Polymerization of substituted aniline and characterization of the polymers obtained.* Synthetic Metals, 1986. **16**(1): p. 99-104.
47. Okamoto, H. and Kotaka, T., *Structure and properties of polyaniline films prepared via electrochemical polymerization. I: Effect of pH in electrochemical polymerization media on the primary structure and acid dissociation constant of product polyaniline films.* Polymer, 1998. **39**(18): p. 4349-4358.
48. Gospodinova, N., Terlemezyan, L., Mokreva, P., and Kossev, K., *On the mechanism of oxidative polymerization of aniline.* Polymer, 1993. **34**(11): p. 2434-2437.
49. Duic, L. and Mandic, Z., *Counter-ion and pH effect on the electrochemical synthesis of polyaniline.* Journal of Electroanalytical Chemistry, 1992. **335**(1-2): p. 207-221.
50. Gospodinova, N. and Terlemezyan, L., *Conducting polymers prepared by oxidative polymerization: polyaniline.* Progress in Polymer Science, 1998. **23**(8): p. 1443-1484.
51. Venancio, E.C., Wang, P.-C., and MacDiarmid, A.G., *The azanes: A class of material incorporating nano/micro self-assembled hollow spheres obtained by aqueous oxidative polymerization of aniline.* Synthetic Metals, 2006. **156**(5-6): p. 357-369.
52. Stejskal, J., Sapurina, I., Trchova, M., Konyushenko, E.N., and Holler, P., *The genesis of polyaniline nanotubes.* Polymer, 2006. **47**(25): p. 8253-8262.
53. Xing Wang, N.L., Xue Yan, Wanjin Zhang and Yen Wei, *Alkali-guided Synthesis of Polyaniline Hollow Microspheres.* Chemistry Letters, 2005. **34**: p. 42.
54. LI, N.B., *Polyaniline Formed in Alkaline Solution —A New Luminous Material.* Chinese Chemical Letters, 2000. **11**: p. 681.
55. Armes, S.P. and Miller, J.F., *Optimum reaction conditions for the polymerization of aniline in aqueous solution by ammonium persulphate.* Synthetic Metals, 1988. **22**(4): p. 385-393.
56. Ayad, M.M., Salahuddin, N., and Sheneshin, M.A., *Optimum reaction conditions for in situ polyaniline films.* Synthetic Metals, 2003. **132**(2): p. 185-190.
57. Gazotti, W.A.J. and De Paoli, M.-A., *High yield preparation of a soluble polyaniline derivative.* Synthetic Metals, 1996. **80**(3): p. 263-269.
58. Huang, J.X. and Kaner, R.B., *Nanofiber formation in the chemical polymerization of aniline: A mechanistic study.* Angewandte Chemie-International Edition, 2004. **43**(43): p. 5817-5821.
59. Li, D. and Kaner, R.B., *Shape and Aggregation Control of Nanoparticles: Not Shaken, Not Stirred.* J. Am. Chem. Soc., 2006. **128**(3): p. 968-975.
60. de Albuquerque, J.E., Mattoso, L.H.C., Faria, R.M., Masters, J.G., and MacDiarmid, A.G., *Study of the interconversion of polyaniline oxidation states by optical absorption spectroscopy.* Synthetic Metals, 2004. **146**(1): p. 1-10.

61. Albuquerque, J.E., Mattoso, L.H.C., Balogh, D.T., Faria, R.M., Masters, J.G., and MacDiarmid, A.G., *A simple method to estimate the oxidation state of polyanilines.* Synthetic Metals, 2000. **113**(1-2): p. 19-22.
62. Stafström, S., Brédas, J.L., Epstein, A.J., Woo, H.S., Tanner, D.B., Huang, W.S., and MacDiarmid, A.G., *Polaron lattice in highly conducting polyaniline: Theoretical and optical studies.* Physical Review Letters, 1987. **59**(13): p. 1464 LP - 1467.
63. Chiang, J.-C. and MacDiarmid, A.G., *`Polyaniline': Protonic acid doping of the emeraldine form to the metallic regime.* Synthetic Metals, 1986. **13**(1-3): p. 193-205.
64. Jr, M.C.a.B.B., *Mechanism of conduction in doped polyaniline.* J. Phys. D: Appl. Phys., 1997. **30**: p. 1531.
65. Monkman, A.P., Bloor, D., Stevens, G.C., Stevens, J.C.H., and Wilson, P., *Electronic structure and charge transport mechanisms in polyaniline.* Synthetic Metals, 1989. **29**(1): p. 277-284.
66. Luthra, V., Singh, R., Gupta, S.K., and Mansingh, A., *Mechanism of dc conduction in polyaniline doped with sulfuric acid.* Current Applied Physics, 2003. **3**(2-3): p. 219-222.
67. Javadi, H.H.S., Zuo, F., Cromack, K.R., Angelopoulos, M., MacDiarmid, A.G., and Epstein, A.J., *Charge transport in the "emeraldine" form of polyaniline.* Synthetic Metals, 1989. **29**(1): p. 409-416.
68. Scherr, E.M., MacDiarmid, A.G., Manohar, S.K., Masters, J.G., Sun, Y., Tang, X., Druy, M.A., Glatkowski, P.J., Cajipe, V.B., Fischer, J.E., Cromack, K.R., Jozefowicz, M.E., Ginder, J.M., McCall, R.P., and Epstein, A.J., *Polyaniline: Oriented films and fibers.* Synthetic Metals, 1991. **41**(1-2): p. 735-738.
69. Javadi, H.H.S., Angelopoulos, M., MacDiarmid, A.G., and Epstein, A.J., *Conduction mechanism of polyaniline: Effect of moisture.* Synthetic Metals, 1988. **26**(1): p. 1-8.
70. Xia, Y., Wiesinger, J.M., MacDiarmid, A.G., and Epstein, A.J., *Camphorsulfonic Acid Fully Doped Polyaniline Emeraldine Salt: Conformations in Different Solvents Studied by an Ultraviolet/Visible/Near-Infrared Spectroscopic Method.* Chem. Mater., 1995. **7**(3): p. 443-445.
71. Cho, H.S. and Park, Y.H., *Preparation and characterization of conducting poly(vinyl chloride)-g-poly(aniline) copolymer.* Synthetic Metals, 2004. **145**(2-3): p. 141-146.
72. Cao, Y., Smith, P., and Heeger, A.J., *Counter-ion induced processibility of conducting polyaniline and of conducting polyblends of polyaniline in bulk polymers.* Synthetic Metals, 1992. **48**(1): p. 91-97.
73. Jiang Yue, A.J.E., *Synthesis of self-doped conducting polyaniline.* J. Am. Chem. Soc., 1990. **112**(7): p. 2800-2801.
74. J.Y. Bergeron, J.-W.C., L.H. Dao,, J. Che. Soc. Chem. Commun., 1990. **112**: p. 180.
75. Malinauskas, A., *Self-doped polyanilines.* Journal of Power Sources, 2004. **126**(1-2): p. 214-220.
76. Macinnes, J., David and Funt, B.L., *Poly-o-methoxyaniline: A new soluble conducting polymer.* Synthetic Metals, 1988. **25**(3): p. 235-242.
77. Leclerc, M., Guay, J., and Dao, L.H., *Synthesis and characterization of poly(alkylanilines).* Macromolecules, 1989. **22**(2): p. 649-653.

78. Luiz H. C. Mattoso, R.M.F., Luis O. S. Bulhões, Alan G. MacDiarmid,, *Synthesis, doping, and processing of high molecular weight poly(o-methoxyaniline).* Journal of Polymer Science Part A: Polymer Chemistry, 1994. **32**(11): p. 2147-2153.
79. Patil, A.O., Ikenoue, Y., Basescu, N., Colaneri, N., Chen, J., Wudl, F., and Heeger, A.J., *Self-doped conducting polymers.* Synthetic Metals, 1987. **20**(2): p. 151-159.
80. Thiemann, C. and Brett, C.M.A., *Electropolymerisation and properties of conducting polymers derived from aminobenzenesulphonic acids and from mixtures with aniline.* Synthetic Metals, 2001. **125**(3): p. 445-451.
81. Chan, H.S.O., Ho, P.K.H., Ng, S.C., Tan, B.T.G., and Tan, K.L., *A New Water-Soluble, Self-Doping Conducting Polyaniline from Poly(o-aminobenzylphosphonic acid) and Its Sodium Salts: Synthesis and Characterization.* J. Am. Chem. Soc., 1995. **117**(33): p. 8517-8523.
82. Kilmartin, P.A. and Wright, G.A., *Photoelectrochemical and spectroscopic studies of sulfonated polyanilines Part I. Copolymers of orthanilic acid and aniline.* Synthetic Metals, 1997. **88**(2): p. 153-162.
83. Shimizu, S., Saitoh, T., Uzawa, M., Yuasa, M., Yano, K., Maruyama, T., and Watanabe, K., *Synthesis and applications of sulfonated polyaniline.* Synthetic Metals, 1997. **85**(1-3): p. 1337-1338.
84. Guo, R., Barisci, J.N., Innis, P.C., Too, C.O., Wallace, G.G., and Zhou, D., *Electrohydrodynamic polymerization of 2-methoxyaniline-5-sulfonic acid.* Synthetic Metals, 2000. **114**(3): p. 267-272.
85. Zhou, D., Innis, P.C., Wallace, G.G., Shimizu, S., and Maeda, S.-I., *Electrosynthesis and characterisation of poly(2-methoxyaniline-5-sulfonic acid)-effect of pH control.* Synthetic Metals, 2000. **114**(3): p. 287-293.
86. Wei, X.-L.W., Y. Z.; Long, S. M.; Bobeczko, C.; Epstein, A. J., *Synthesis and Physical Properties of Highly Sulfonated Polyaniline.* J. Am. Chem. Soc., 1996. **118**(11): p. 2545-2555.
87. Kitani, A., Satoguchi, K., Tang, H.-Q., Ito, S., and Sasaki, K., *Eletrosynthesis and properties of self-doped polyaniline.* Synthetic Metals, 1995. **69**(1-3): p. 129-130.
88. Wei, X. and Epstein, A.J., *Synthesis of highly sulfonated polyaniline.* Synthetic Metals, 1995. **74**(2): p. 123-125.
89. Prevost, V., Petit, A., and Pla, F., *Studies on chemical oxidative copolymerization of aniline and o-alkoxysulfonated anilines:: I. Synthesis and characterization of novel self-doped polyanilines.* Synthetic Metals, 1999. **104**(2): p. 79-87.
90. Han, M.G., Cho, S.K., Oh, S.G., and Im, S.S., *Preparation and characterization of polyaniline nanoparticles synthesized from DBSA micellar solution.* Synthetic Metals, 2002. **126**(1): p. 53-60.
91. Moulton, S.E., Innis, P.C., Kane-Maguire, L.A.P., Ngamna, O., and Wallace, G.G., *Polymerisation and characterisation of conducting polyaniline nanoparticle dispersions.* Current Applied Physics, 2004. **4**(2-4): p. 402-406.
92. Kinlen PJ, D.Y., Graham CR, Remsen EE, Macromolecules, 1998. **31**: p. 1735-44.
93. Kim, D., Choi, J., Kim, J.-Y., and Sohn, D., Macromolecules, 2002. **35**: p. 5314-6.

94. Barisci, J.N., Innis, P.C., Kane-Maguire, L.A.P., Norris, I.D., and Wallace, G.G., *Preparation of chiral conducting polymer colloids.* Synthetic Metals, 1997. **84**(1-3): p. 181-182.
95. Stejskal, J. and Sapurina, I., *On the origin of colloidal particles in the dispersion polymerization of aniline.* Journal of Colloid and Interface Science, 2004. **274**(2): p. 489-495.
96. Blinova, N.V., Sapurina, I., Klimovic, J., and Stejskal, J., *The chemical and colloidal stability of polyaniline dispersions.* Polymer Degradation and Stability, 2005. **88**(3): p. 428-434.
97. H. J. Qiu, M.X.W., b. Matthews, L. M. Dai, Macromolecules, 2001. **35**: p. 675.
98. Aboutanos, V., Barisci, J.N., Kane-Maguire, L.A.P., and Wallace, G.G., *Electrochemical preparation of chiral polyaniline nanocomposites.* Synthetic Metals, 1999. **106**(2): p. 89-95.
99. Yang*, J.-M.L.a.S.C., *Novel Colloidal Polyaniline Fibrils Made by Template Guided Chemical Polymerization.* J. CHEM. SOC., CHEM. COMMUN.,, 1991: p. 1529.
100. Ivanov, V.F., Gribkova, O.L., Cheberyako, K.V., Nekrasov, A.A., Tverskoi, V.A., and Vannikov, A.V., *Template Synthesis of Polyaniline in the Presence of Poly-(2-acrylamido-2-methyl-1-propanesulfonic Acid).* Russian Journal of Electrochemistry, 2004. **V40**(3): p. 299-304.
101. Stejskal, J., Omastova, M., Fedorova, S., Prokes, J., and Trchova, M., *Polyaniline and polypyrrole prepared in the presence of surfactants: a comparative conductivity study.* Polymer, 2003. **44**(5): p. 1353-1358.
102. Jayanty, S., Prasad, G.K., Sreedhar, B., and Radhakrishnan, T.P., *Polyelectrolyte templated polyaniline--film morphology and conductivity.* Polymer, 2003. **44**(24): p. 7265-7270.
103. Yuan, G.-L., Kuramoto, N., and Su, S.-J., *Template synthesis of polyaniline in the presence of phosphomannan.* Synthetic Metals, 2002. **129**(2): p. 173-178.
104. Huang, J.X. and Kaner, R.B., *A general chemical route to polyaniline nanofibers.* Journal of the American Chemical Society, 2004. **126**(3): p. 851-855.
105. Li, D. and Kaner, R.B., *Processable stabilizer-free polyaniline nanofiber aqueous colloids.* Chemical Communications, 2005(26): p. 3286-3288.
106. Wang, R.-S., Wang, L.-M., Fu, Y.-J., and Su, Z.-M., *The influence of different substituent on polymer self-doping conductive property.* Synthetic Metals, 1995. **69**(1-3): p. 713-714.
107. Hwang, S.-A.C.a.G.-W., *Structure Characterization of Self-Acid-Doped Sulfonic Acid Ring-Substituted Polyaniline in Its Aqueous Solutions and as Solid Film.* Macromolecules, 1996. **29**(11): p. 3950-355.
108. Barbero, C., Miras, M.C., Kotz, R., and Haas, O., *Sulphonated polyaniline (SPAN) films as cation insertion electrodes battery applications Part II: Exchange of mobile species in aqueous and non-aqueous solutions.* Journal of Electroanalytical Chemistry, 1997. **437**(1-2): p. 191-198.
109. Barbero, C., Miras, M.C., Kotz, R., and Haas, O., *Comparative study of the ion exchange and electrochemical properties of sulfonated polyaniline (SPAN) and polyaniline (PANI).* Synthetic Metals, 1993. **55**(2-3): p. 1539-1544.
110. Hwang, K.S., Lee, C.W., Yoon, T.H., and Son, Y.S., *Fabrication and characteristics of a composite cathode of sulfonated polyaniline and*

Ramsdellite-MnO2 for a new rechargeable lithium polymer battery. Journal of Power Sources, 1999. **79**(2): p. 225-230.

111. Rubner, M.F.a.M.F., *Molecular-Level Processing of Conjugated Polymers. 1. Layer-by-Layer Manipulation of Conjugated Polyions.* Macromolecules, 1995. **28**(21): p. 7107-7114.
112. Zhang, L., Jiang, X., Niu, L., and Dong, S., *Syntheses of fully sulfonated polyaniline nano-networks and its application to the direct electrochemistry of cytochrome c.* Biosensors and Bioelectronics, 2006. **21**(7): p. 1107-1115.
113. Hwang, S.-A.C.a.G.-W., *Synthesis of Water-Soluble Self- Acid-Doped Polyaniline.* J. Am. Chem. SOC., 1994. **116**(17): p. 7939-7940.
114. Hwang, S.-A.C.a.G.-W., *Water-Soluble Self-Acid-Doped Conducting Polyaniline: Structure and Properties.* J. Am. Chem. SOC., 1995. **117**(40): p. 10055-10062.
115. Chan, H.S.O., Neuendorf, A.J., Ng, S.C., Wong, P.M.L., and Young, D.J., *Synthesis of fully sulfonated polyaniline: a novel approach using oxidative polymerisation under high pressure in the liquid phase.* Chemical Communications, 1998(13): p. 1327-1328.
116. Mello, R.M.Q., Torresi, R.M., Cordoba de Torresi, S.I., and Ticianelli, E.A., *Ellipsometric, Electrogravimetric, and Spectroelectrochemical Studies of the Redox Process of Sulfonated Polyaniline.* Langmuir, 2000. **16**(20): p. 7835-7841.
117. Strounina, E.V., *Synthesis and Characterisation of Chiral Substituted Polyanilines*, in *Chemistry Department*. 2001, University of Wollongong.
118. Strounina, E.V., Kane-Maguire, L.A.P., and Wallace, G.G., *Optically active sulfonated polyanilines.* Synthetic Metals, 1999. **106**(2): p. 129-137.
119. Tallman, D.E. and Wallace, G.G., *Preparation and preliminary characterization of a poly (4-vinylpyridine) complex of a water-soluble polyaniline.* Synthetic Metals, 1997. **90**(1): p. 13-18.
120. Li, C., Mitamura, K., and Imae, T., *Electrostatic Layer-by-Layer Assembly of Poly(amido amine) Dendrimer/Conducting Sulfonated Polyaniline: Structure and Properties of Multilayer Films.* Macromolecules, 2003. **36**(26): p. 9957-9965.
121. Dominis, A.J., Spinks, G.M., Kane-Maguire, L.A.P., and Wallace, G.G., *A de-doping/re-doping study of organic soluble polyaniline.* Synthetic Metals, 2002. **129**(2): p. 165-172.
122. Zhao H., W.G.G., *Polypyrrole/poly(2-methoxy aniline, 5-sulfonic acid) polymer composite.* Polymer Gels nad Networks, 1998. **6**: p. 233-245.
123. Strounina, E.V., Shepherd, R., Kane-Maguire, L.A.P., and Wallace, G.G., *Conformational changes in sulfonated polyaniline caused by metal salts and OH.* Synthetic Metals, 2003. **135**(1-3): p. 289-290.
124. Strounina, E.V., Shepherd, R., Kane-Maguire, L.A.P., and Wallace, G.G., *Conformational Changes in Sulfonated Polyaniline Caused By Metal Salts and OH-.* Synthetic Metals, 2003. **135-136**: p. 289-290.
125. T. Tatsuma, T.O., R. Sato, and N. Oyama, J. Electroanal. Chem., 2001. **501**: p. 180-185.
126. Lee, W., Du, G., Long, S.M., Epstein, A.J., Shimizu, S., Saitoh, T., and Uzawa, M., *Charge transport properties of fully-sulfonated polyaniline.* Synthetic Metals, 1997. **84**(1-3): p. 807-808.

Chapter 2

Introduction to experimental techniques used

2.1. Introduction

The experimental techniques generally used in this research are briefly described. The details of procedures are presented in the experimental part of the corresponding Chapter.

2.2. Purification of polymer

(i) Dialysis

Dialysis is a routine method driven primarily by osmotic pressure forces, and used for desalting, concentrating and separating biomolecules and macromolecules differing substantially in molecular weight. Dialysis tubing is essentially a cylindrical membrane containing pores. The size of these pores determines the "molecular weight cut-off" (MWCO) of the tubing. The MWCO describes an indicative molecular weight at which a compound will be 90% retained following overnight dialysis. Generally, molecules smaller than the MWCO will pass freely through the membrane, driven by a concentration gradient between the high concentration dialate solution inside the dialysis tubing and the receiving solution which is essentially pure water (Figure 2.1).

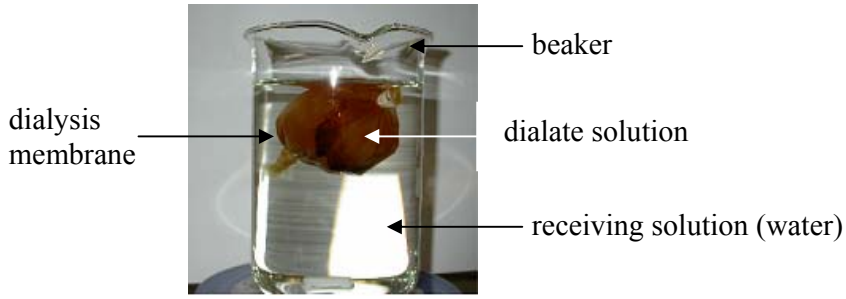

Figure 2.1. Dialysis of polymer solution by dialysis tubing.

(ii) Tangential flow filtration

Tangential flow filtration (also known as cross flow filtration) is a rapid and efficient separation technique for separation and purification of biomolecules. Membranes with pore sizes between 0.001 and 0.100 μm (ultrafiltration membranes), are used for concentrating and desalting dissolved molecules (proteins, peptides, nucleic acids, carbohydrates, and other biomolecules), exchanging buffers, and fractionation of large molecules from small molecules [1]. The use of tangential flow filtration has also been reported for purification of nanoparticle suspensions and drug-loaded nanoparticles [2]. These membranes are typically classified by their respective molecular weight cut-off rather than pore size.

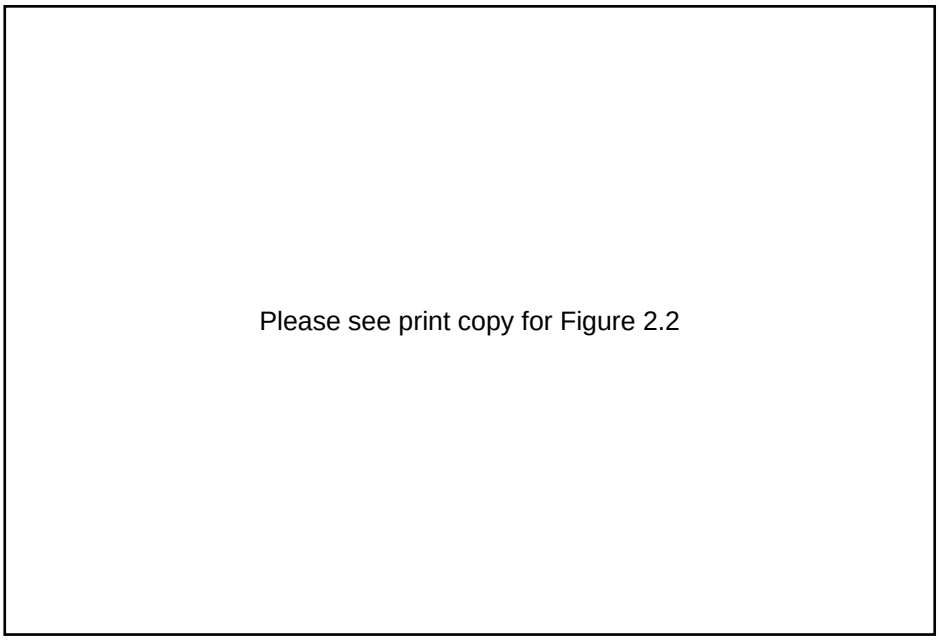

Figure 2.2. VivaFlow™ tangential flow dialysis system with Polyethersulfone membranes. (1) dilution reservoir, (2) sample reservoir, (3) peristaltic pump, (4) membranes, (5) filtrate collector, (6) recirculation line.

The solution to be concentrated or diafiltered is pumped across the face of a membrane filter of the desired molecular weight cut-off (Figure 2.2). A flow restrictor on the exit port supplies sufficient backpressure to force some of the solution through the membrane and into the filtrate container, the remainder is recirculated across the membrane. Recirculation prevents the formation of a restrictive layer on the membrane

and is allowed to continue until the desired degree of concentration or diafiltration has taken place. Tangential flow filtration can be used as continuous diafiltration, in which the diafiltration solution (water or buffer) is added to the sample feed reservoir at the same rate as the filtrate is generated. In this way the volume in the sample reservoir remains constant, but the small molecules that can freely permeate through the membrane are washed away.

In order to purify the PMAS polymer obtained after chemical synthesis and remove the residual monomer, oxidant and oligomers, two different membrane systems were used:
(a) Cellulose dialysis tubing with 12KDa molecular weight cut-off, purchased from Sigma. Dialysis was performed against Milli-Q water.
(b) VivaFlow tangential flow modules from VivaScience, Sartorius Group. Two types of polyethersulfone (PES) membranes with different active area and MWCO were used: VivaFlow™ 50 (active area 50 cm^2) and VivaFlow™ 200 (active area 200 cm^2).
The polymer sample was pumped across the face of the membrane at a rate of 400 mL/min using a Masterflex peristaltic pump (model 7518-00).

(iii) Centrifugation

Centrifugation techniques are commonly used for removal of solvents, electrolytes and free stabilisers in dispersion polymerisation. This technique was used for purification of PAn/PMAS dispersions obtained by chemical polymerisation of aniline in the presence of PMAS in Chapter 6. The polymer dispersion precipitated by spinning the solution at 4100 rpm using a Beckman (J2-MC, rotor JA10) centrifuge. The soluble unwanted products and unreacted materials were separated as the supernatant and decanted. The precipitate was redispersed in water and the centrifuging/washing process was repeated to obtain the pure PAn/PMAS material.

2.3. Gel permeation chromatography (GPC)

Gel permeation chromatography (GPC), so called “gel filtration chromatography”, is a chromatographic technique. The chromatographic bed consists of small grains as the stationary phase packed to a tube [3]. These particles consist of an uncharged gel with great affinity for the solvent being used. The space between the particles is occupied by

a liquid, or mobile phase, which is made to flow through the bed and carry the substances to be separated. Different substances are retarded by the stationary phase to a varying extent and pass through the chromatographic bed at different velocities. Substances are separated by GPC according to their molecular size. The high molecular weight species can not fit into the pores of the gel and will emerge first from the bed, while smaller molecules interact with the pores of the gel and their elution is consequently retarded (Figure 2.3).

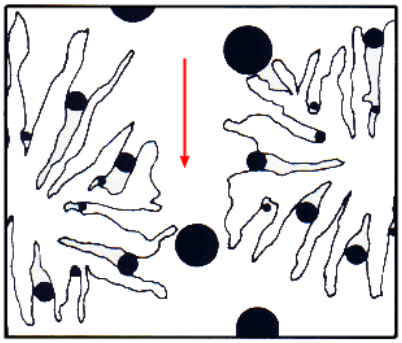

Figure 2.3. Separation of a mixture of molecules by GPC according to their molecular size.

Relative calibration is commonly used in GPC for determining the molecular weight of the polymer being analysed. In this case a range of monodisperse standards, most commonly polystyrene, are used to generate a calibration curve to determine the molecular weight of an unknown polymer. It is assumed that the standards employed have a similar molecular conformation defining a dynamic molecular volume as the unknowns in the GPC mobile phase. It is critical to define the relative standard type used, as a different standard will result in a different relative molecular weight distribution. Gel permeation chromatography has been used to determine the molecular weight distribution of polyaniline [4].

Typically broad molecular weight distributions are obtained from synthetic polymer samples (Figure 2.4). As a consequence, often several parameters are defined to describe molecular weight distributions, these being number average molecular weight (M_n), weight average molecular weight (M_w), and polydispersity index.

- The Number Average Molecular Weight (M_n) is the statistical average molecular weight of all polymer chains in a sample and is defined by

$$M_n = (\Sigma N_i M_i) / (\Sigma N_i)$$

where M_i = molecular weight of a chain, and N_i = the number of chains with molecular weight M_i.

- The Weight Average Molecular Weight (M_w) of a polymer takes into account that bigger molecules contribute a larger proportion to the total mass of a polymer sample and is defined by

$$M_w = (\Sigma N_i M_i^2) / (\Sigma N_i M_i)$$

The more massive the chain, the larger the chain contributes to M_w. M_w is always higher than M_n.

- The ratio M_w/M_n is called the polydispersity index (PDI), and is a measure of the width of the molecular weight distribution. When $M_w/M_n = 1$, all polymer molecules in the sample have the same molecular weight, and the sample is said to be monodisperse. The larger the value of M_w/M_n, the greater the distribution of molecular weight within the polymer sample.

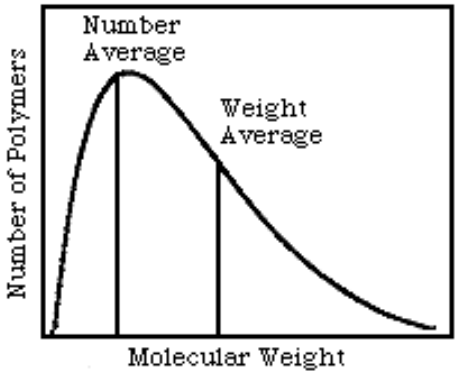

Figure 2.4. A typical molecular weight distribution curve of a polymer sample.

In some instances a peak molecular weight, M_p, may be reported and relates to the maximum, or peak, in a GPC chromatogram. When the PDI is 1 the M_p will be the same as the M_w and M_n. Typically it will fall somewhere between the two and is useful

for describing the dominant molecular weight fraction in the overall polymer distribution.

In this work, the molecular weight of PMAS samples was determined using a Waters GPC system with Millenium software using Waters Ultrahydrogel 125 and 250 columns in series held at 35°C in a column oven. A mobile phase consisting of 20 % v/v methanol and 80 % v/v aqueous solution of 0.20 M $NaNO_3$ and 0.01 M disodium hydrogen phosphate buffer (pH 9) was used at a flow rate of 0.8 mL/min. Chromatograms were recorded using a Waters 996 PDA photodiode array detector capable of providing a 3D chromatogram from which a classical 2D chromatogram could be derived. All molecular weight determinations were performed by relative calibration against poly(styrenesulfonate) standards obtained from Polymer Laboratories. Typical sample compositions analysed were 1.0 mg/mL solutions of the PMAS polymer.

2.4. Thermal analysis

Thermogravimetric analysis (TGA) was carried out to determine material stability by monitoring weight changes of a sample, resulting from chemical or physical transformations, as a function of temperature and heating rate. Thermal gravimetry was carried out using either a DTA/TGA SETARAM 92B thermoanalyzer or a DTA TA Instruments Q800 Thermal Gravimetric Analyser. A temperature programmer was used to increase temperature from 35°C to 600°C at a heating rate of 10°C per minute under nitrogen atmosphere at a flow rate of 60 mL/min. TGA was used to determine the decomposition by weight loss of the samples including MAS monomer, pure PMAS fractions and polyaniline/PMAS composite.

Differential scanning calorimetry was also used to determine decomposition point and phase transitions of the monomer and polymer by measuring the amount of energy absorbed or released during such transitions. Differential scanning calorimetery (DSC) was carried out using a Q-100 (TA series) instrument in temperature range of 20-360°C.

2.5. Electrical conductivity

The electrical conductivity of conducting polymers can be measured using a four-point probe technique. The electrical conductivities of PMAS or PAn/PMAS films cast onto ordinary glass slides were measured using a Jandel four-point probe head Model RM2. The four–point probe had a linear configuration with probe spacing of 0.635 mm (Figure 2.5a).

A constant current (0.1-100 μA, dependent on the resistivity of the material) was applied through the outermost probes and voltage measurements were made through the two inner probes. In this configuration, for a sample diameter d>>s (s = the spacing of the probe), the bulk resistivity of the sample is given by:

$$\rho = 4.532 \times (V/I) \times t$$

where t = film thickness in cm, I = applied current in amperes, and V = measured voltage in volts. The conductivity (σ) of the sample can then be calculated from the reciprocal of resistivity.

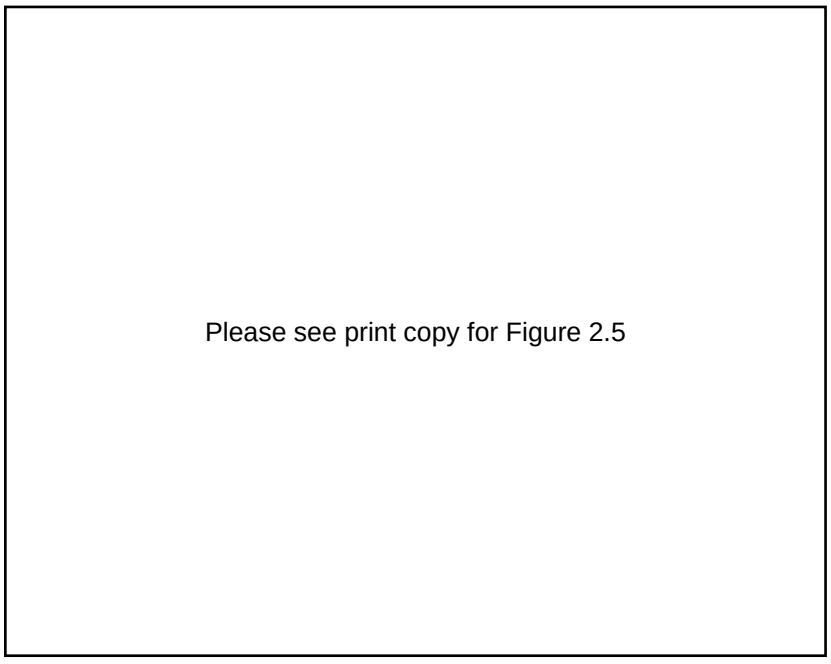

Figure 2.5. (a) Four-point probe with a linear configuration [5], (b) PMAS films evaporatively cast onto a glass substrate**.**

The films used to obtain conductivity measurements were obtained by air evaporative casting of 30 μL of either 50 mg/mL solutions of PMAS or ~10 mg/mL PAn/PMAS dispersions on glass slide substrates as seen in Figure 2.5b. The thickness of the films was approximately 0.01 mm, measured using a Mutiutoyo Digital micrometer.

2.6. UV-vis spectroscopy

UV-visible-NIR spectroscopy is a versatile and useful technique for studying the molecular structure and conformation of conducting polymers. The particular absorption bands arising from a polymer sample are indicative of the nature of the polymer, the extent of both electronic and protonic doping, the oxidation state of the polymer as well as polymer chain conformation.

UV-visible spectra of polymer thin films evaporatively cast onto glass substrates or electrodeposited onto Pt-ITO-coated glass were measured between 300 and 1100 nm using a Shimadzu UV-1601 spectrophotometer in dual beam mode or between 300 and 800 nm using a Shimadzu MultiSpec-1501 Photodiode Array with Hyper UV 1.50 software (in single beam mode). The absorption spectra over the extended region (300-2500 nm) were recorded using a Cary 500 spectrophotometer (Varian) in dual beam mode. The absorption spectra of the aqueous polymer solutions in 1.0 cm path length quartz cells were recorded between 230 and 1100 nm using a Shimadzu UV-1601 spectrophotometer.

2.7. Fluorescence spectroscopy

Molecules are excited by the absorption of a beam of electromagnetic radiation. In fluorescence, the excited species relax to the ground state via an emission process, giving up their excess energy as photons. All absorbing molecules have the potential to fluoresce, however the structure of most compounds provides radiation-less relaxation pathways.

The power of the fluorescent emission (F) is proportional to the concentration (c) of the fluorescing particle

$$F = K\,c$$

The constant K depends upon the quantum efficiency of the fluorescence, the molar absorptivity of the analyte, the power of the incident beam and the light path length. Thus, a plot of the fluorescent power of a solution versus the concentration of the emitting species should be linear at low concentrations. The linearity is lost at high concentrations as a result of self-quenching in which the fluorescence produced by analyte molecules are absorbed by other analyte molecules. Fluorescence methods are more sensitive than absorption methods.

In this thesis, the photoluminescence (PL) technique was used to study the PL properties of PMAS fractions. PL measurements were performed on aqueous solutions containing PMAS fractions at a concentration in the range 2-50 μg/mL [(0.05-1.2) x 10^{-4} M based on a dimer repeat unit] in a transparent quartz cell. Lower PMAS concentrations were employed to minimise the effect of self absorption of the emitted light. Fluorescence spectra were recorded using a JY Spex fluorescence spectrophotometer.

2.8. ESR spectroscopy

Electron spin resonance (ESR), also known as electron paramagnetic resonance (EPR), is a spectroscopic method that detects the presence of unpaired electrons in a sample. Typical examples are transition metals, organic and inorganic free radicals, and organic ion-radicals. This technique provides useful structural information about chemical and physical processes. ESR has been widely used in the characterisation of conducting polymers in order to study their magnetic properties, the nature of the charge carriers, and the mechanisms of conductivity.

ESR studies the interaction between the electronic magnetic moments of the system (with a non-zero spin) and electromagnetic radiation (microwave frequency, GHz). Because of the interaction of the unpaired electron spin moment with the magnetic field (B_0), the two spin states gain different energies. The measured energy difference depends linearly on the magnetic field. In ESR, the energy difference is given by

$$\Delta E = h \upsilon = g \mu_B B_0$$

where B_0 is the magnetic field (in Gauss) and μ_B is the Bohr magneton. The g-factor, g, is a constant and relates directly to the type of radical species. It varies depending on the electronic configuration of the radical or ion. Proton radicals have a g-factor of 2.003 and are typical of conducting polymers.

In an ESR system the sample is exposed to constant electromagnetic radiation in the microwave frequency (typically 9.8M MHz or X-band) while the magnetic field is linearly increased with an overlying 100 kHz AC perturbation of the magnetic field. When the field matches the energy level splitting, energy absorption occurs and the ESR spectrum is obtained (Figure 2.6).

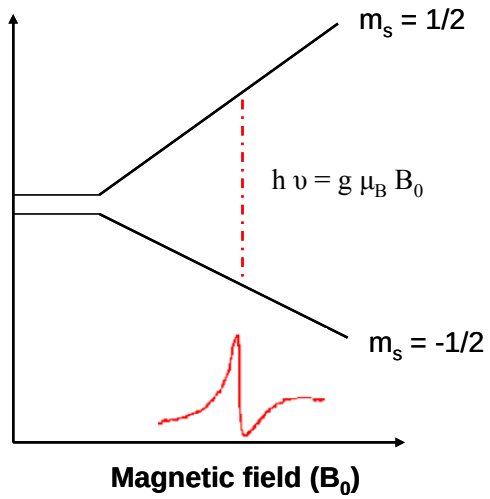

Figure 2.6. Variation of the spin state energies as a function of the applied magnetic field.

In this thesis, the ESR technique was employed to study the magnetic properties of PMAS and PAn samples. In-situ Electrochemical-ESR was also used to study the magnetic properties of PAn/PMAS in different oxidation states.

The ESR spectra of the samples were recorded on a Bruker EMX ESR spectrometer. Aqueous samples were injected into the microwave cavity via a Bruker Aqua-X™ flow cell which permitted rapid sample change over and ensured identical cell geometry and reproducible cavity tuning. The ESR spectra of solid PMAS samples were recorded either in an ESR quartz tube or using an ESR quartz flat cell with a pin hole.

2.9. Cyclic voltammetry

Cyclic voltammetry (CV) is a potentiodynamic electrochemical technique. In cyclic voltammetry, the potential is varied linearly versus time between an initial potential ($E_{initial}$) and a final potential (E_{final}) with the change in current being measured with respect to the change in voltage. The resultant current-potential plot is called a cyclic voltammogram (Figure 2.7). This technique is used to investigate the electrochemical behaviour of electroactive conducting polymers and also provides useful information on the mechanisms of polymer growth.

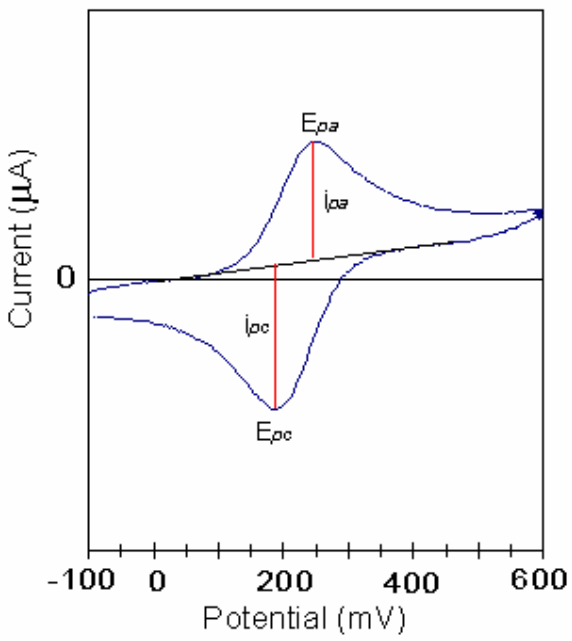

Figure 2.7. A typical cyclic voltammogram showing an oxidation peak at E_{pa} with a maximum anodic current (i_{pa}) in the forward scan, and a corresponding reduction peak at E_{pc} with a maximum cathodic current (i_{pc}) in the reversed scan.

In this thesis, cyclic voltammetry was used to investigate the redox properties of conducting polymers either in solution or as modified electrodes. This technique was also used for potentiodynamic polymerisation of aniline in the presence of different dopants. Cyclic voltammetry was carried out in a three electrode cell using a working electrode (either glassy carbon, Pt wire, or Pt-ITO coated glass) with a platinum mesh auxiliary electrode and a Ag/AgCl (3M NaCl) reference electrode using an E-Corder 401 interface and Potentiostat (EDAQ).

2.10. Contact angle measurements

Contact angle measurement is a technique used for evaluation of solid surface tension. The surface tension of a material is related to the hydrophilicity/hydrophobicity of the solid surface and can be evaluated from the contact angle of a liquid droplet with the solid surface. When a drop of liquid is lowered to the surface, it will adopt a shape under the pressure of different interfacial tensions until it reaches an equilibrium (Figure 2.8). A low contact angle (when measured using an aqueous liquid) is indicative of a solid surface that is more hydrophilic and has a high surface tension.

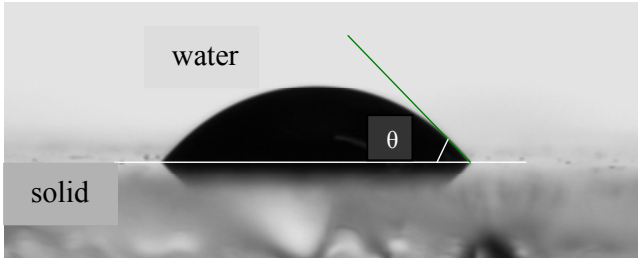

Figure 2.8. Contact angle (θ) of a 2 μL water droplet, lowered onto a polymer surface (PAn/HCl film electrodeposited onto Pt-ITO glass).

To investigate the hydrophilic properties and wettability of the polyaniline synthesised using different dopants, the contact angle of a water droplet on the polymer surface was measured. Contact angles were measured using a DataPhysics OCAZO Goniometer (employing SCAZI software). Measurements were made by lowering a 2 μL water droplet onto the polymer surface and recording the contact angle after it had reached a relatively constant value (advanced contact angle). Polymer films were prepared by evaporative casting onto a glass substrate from a dispersion in water or via electrochemical deposition onto a Pt-ITO glass substrate.

2.11. Morphology

Scanning electron microscopy (SEM) is a powerful tool for studying the surface morphology and micro/nanostructure of conducting polymers. The surface morphology of the polymer films were investigated using scanning electron microscopy (SEM, Leica

Model Stereoscan 440) with a secondary electron detector. Typical SEM images were obtained using an acceleration voltage of 20 kV. Prior to imaging, the polymer films were coated with a thin layer of gold to improve the conductivity of the sample and the resolution of the image.

Transmission electron microscopy (TEM) is used to observe the morphology and the particle size of conducting polymer nanoparticles and nanocomposites. In this thesis, TEM micrographs were obtained using a Hitachi H7000 TEM at 75 keV in order to observe the morphology of samples cast onto TEM grids from dilute aqueous solutions of PMAS or dispersions of the polyaniline/PMAS composite.

2.12. QCM

The quartz crystal microbalance (QCM) is a very sensitive mass sensor that measures mass changes in the nanogram range. QCM is used for detection of mass, density, viscosity, adsorption, desorption, and corrosion in electrochemical/chemical reactions. The mass is measured by measuring the frequency change of a piezoelectric quartz crystal. Correlation between mass and frequency is achieved by means of the Sauerbrey equation [6]:

$$\Delta m \propto - \Delta F$$

Electrochemical QCM has proved useful for studying the electrochemical synthesis of conducting polymers and electrical behaviour of the polymer films.

In this thesis, the resonance frequency of polyaniline coated quartz crystals were measured in-situ during electrochemical polymerisation of aniline, using a Stanford Research System (QCM 200) Quartz Crystal Microbalance. The quartz crystals, having an unloaded resonant frequency of approximately 5 MHz, were obtained from Stanford Research Systems. The electrochemically available surface area of the crystal (1.37 cm^2) was much larger than the oscillation surface area (0.4 cm^2), thus the edge effects on the frequency measurement were disregarded. Mass change was directly calculated from the resonance frequency change using the Sauerbrey equation [6].

2.13. References

1. Schwartz, L., *Introduction to Tangential Flow Filtration for Laboratory and Process Development Applications*, in *Scientific and Laboratory Services, Pall Corporation*.
2. Gautam Dalwadi, H.A.E.B., and Yan Chen, *Comparison of Diafiltration and Tangential Flow Filtration for Purification of Nanoparticle Suspensions.* Pharmaceutical Research, 2005.
3. Fischer, L., *Gel filtration chromatography*. 2nd fully rev. ed ed. Vol. 1. 1980, Amsterdam: Elsevier/North-Holland Biomedical Press.
4. Gordon G. Wallace, G.M.S., Peter R. Teasdale, *Conductive electroactive polymers : intelligent materials systems*. Vol. 1. 2002: Boca Raton, FL : CRC Press.
5. Pornputtkul, Y., *Development of Chiral Conducting Polymers for Asymmetric Electrosynthesis*, University of Wollongong, 2005.
6. G. Sauerbrey, Z., Phys., 1959. **155**: p. 206.

Chapter 3

Synthesis and Purification of PMAS

3.1 Introduction

Poly(2-methoxyaniline-5-sulfonic acid) (PMAS) is a water soluble, fully sulfonated, self-doped analogue of polyaniline. It can be polymerised by chemical [1] or electrochemical [2, 3] oxidation of 2-methoxyaniline-5-sulfonic acid (MAS) as shown in Scheme 3.1. Optimisation of the different reaction variables during polymerisation to produce pure high molecular weight PMAS, as well as the subsequent post-synthesis purification of the polymer, has been a major synthetic challenge.

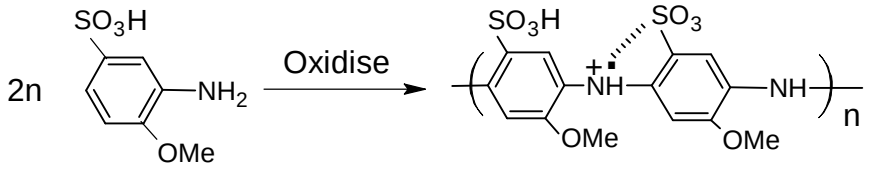

MAS PMAS

Scheme 3.1. Oxidation of MAS to form PMAS

In this work, PMAS has been produced by chemical polymerisation of MAS in NH_4OH solution using ammonium persulfate as oxidant. This process leads to a mixture of high molecular weight (HMWt) polymer *ca.* 10 kDa and low molecular weight (LMWt) oligomers, less than 2.5 kDa. These products are typical of both chemical and electrochemical synthesis [1, 2]. Due to the similar solubility characteristics of these two fractions, it has proven difficult to separate the oligomers from the polymer at the gram scale via conventional dialysis or chromatographic techniques such as gel permeation chromatography (GPC). In this work, an effective procedure has been developed for the separation and purification of these fractions using a tangential cross

flow diafiltration membrane system. Characterisation has been carried out using GPC, UV-vis spectroscopy, and cyclic voltammetry (CV). Additionally the electronic conductivity of the solid was determined using the four point probe method.

3.2 Experimental

3.2.1 Materials

2-Methoxyaniline-5-sulfonic acid (MAS), was provided by Mitsubishi Rayon, Japan and purified by acid base crystallisation before use. The purified monomer was compared with the commercially available MAS from Sigma-Aldrich. Ammonium persulfate, sodium nitrate and tetrabutylammonium dihydrogen phosphate were purchased from Sigma-Aldrich. Ammonium hydroxide (28% NH_3) and hydrochloric acid 32% (w/v) were purchased from Ajax. Methanol (HPLC grade) and disodium hydrogen phosphate were supplied by Ajax chemicals. All reagents used were of analytical grade and all solutions were prepared using Milli-Q water (18 MΩ cm).

3.2.2 Monomer purification

Crude MAS (20 g) was dissolved in 200 ml water by adding 28% (w/w) ammonia solution (~8 ml) drop wise until the pH reached 4. The solution was stirred until all of the monomer had dissolved. The solution was then passed through filter paper (1 μm). After filtering, the solution pH was reduced to less than 1 by addition of concentrated HCl and left overnight at 4°C to complete precipitation. The precipitate was then filtered and washed with 200 ml of a 70:30 mixture of methanol/water and dried in an oven at 50°C for 24 h. A white powder was obtained with a yield of 60% (w/w) (~12g). The MAS powder was then characterised by TGA, DSC and NMR. The pH of both monomer and polymer solutions was measured using a TPS Instruments Model 900-P pH meter.

3.2.3 PMAS synthesis

PMAS was chemically synthesised by polymerisation of MAS using ammonium persulfate as oxidant. MAS monomer is only slightly soluble in water in the acid form. As a consequence the MAS was dissolved via the addition of concentrated ammonia to form the ammonium salt. MAS (5.0 g) was dissolved in 50 ml water by adding approximately 2 ml $NH_4OH_{(aq)}$ 28% (w/w) slowly until the pH reached 4. Then 7.14 g $(NH_4)_2S_2O_{8(aq)}$ (APS) was dissolved in 25 mL water and was added drop wise to the monomer solution over 30 min at 16-18°C. The reaction mixture was stirred for 2 hours and then left unstirred overnight to complete the reaction. An optimisation study of the chemical synthesis of PMAS will be discussed in chapter 4.

3.2.4 Polymer purification

In order to purify the polymer and remove any residual monomer, oxidant or oligomers, two different membrane purification systems were investigated:

1. Cellulose dialysis tubing with 12 KDa molecular weight cut off (MWCO), purchased from Sigma. Dialysis was performed against Milli-Q water 3 times over 2 hours and finally 24 hours. Finally, the dialysed solution (inside the tubing) was evaporated under a fume hood for later analysis.

2. VivaFlow™ 50 and 200 polyethersulfone (PES) membranes with 5 and 10 KDa MWCO, obtained from the Sartorius Group. Prior to purification the polymerisation solution was diluted by 3 times with Milli-Q water and diafiltred by flowing through two 5 KDa MWCO VivaFlow™ 200 membranes in series for 4 hours at 400 mL/min using a Masterflex peristaltic pump (model 7518-00). A sealed sample reservoir with a water feed line was used to maintain the level of the solution. The retained polymer solution (containing the product) was then passed through two 10 kDa MWCO VivaFlow™ 50 membranes in series over 4 hours at the same flow rate.

The diafiltred solution obtained after this process was concentrated (by further filtration without the water feed line) and dried under a fume hood. The filtrate solution obtained

from the 10 KDa MWCO membrane (brown coloured fraction) was concentrated using the 5 KDa membrane and then evaporated. All samples were dried in a vacuum oven at 50°C before being characterised.

3.2.5 Characterisation

3.2.5.1 Thermal Analysis

Thermal gravimetry was carried out using a DTA/TGA SETARAM 92B thermoanalyzer. A temperature programmer was used to increase temperature from 55°C to 400°C at a heating rate of 10°C per min under nitrogen atmosphere. TGA was used to compare the decomposition by weight loss of the samples including crude MAS, pure MAS and Aldrich MAS during purification.

Differential scanning calorimetery (DSC) was carried out using a Q-100 (TA series) instrument in the temperature range 20-360°C.

3.2.5.2 Gel permeation chromatography

Molecular weight was determined using a Waters GPC system with Millenium software using Waters Ultrahydrogel 125 and 250 columns in series held at 35°C in a column oven. A mobile phase consisting of 20% v/v methanol and 80% v/v aqueous solution of 0.2 M $NaNO_3$ and 0.01 M disodium hydrogen phosphate buffer (pH 9) was used at a flow rate of 0.8mL/min. Chromatograms were recorded using a Waters 996 PDA photodiode array detector. All molecular weight determinations were performed by relative calibration against polystyrene sulfonate standards obtained from Polymer Laboratories. Throughout the thesis the peak molecular weight, M_p, has been quoted for clarity. The samples analysed were ~1 mg/mL aqueous solutions of the polymerisation product before and after purification.

3.2.5.3 UV-visible Spectroscopy during purification

UV-visible spectra were measured between 200 and 1100 nm using a Shimadzu UV-1601 spectrophotometer. The solutions were diluted in order to have an appropriate

absorbance so that they followed the Beer-Lambert law (see Figures 5.5-5.10). To measure the spectrum of the unpurified PMAS, 5 μL of the reaction solution was diluted to 3 mL with water. When absorbances were in the typically non-linear Beer-Lambert range (1-2.5), the data were interpreted in the qualitative rather than quantitative manner.

3.2.5.4 Conductivity of PMAS fractions

The electrical conductivities of PMAS films cast on ordinary glass slides were measured using a Jandel four-point probe head Model RM2. The films were obtained by air evaporative casting of 30 μL of 50 mg/mL solutions of PMAS on glass slide substrates. The thickness of the cast films were measured using a Mutiutoyo Digital micrometer and found to be ~ 0.01 mm thick.

3.3 Results and Discussion

3.3.1 Purification of monomer

In order to evaluate sample purity, DSC analysis of the monomer was carried out before and after recrystallisation (Figure 3.1). For the crude MAS, several peaks were observed in the range 100-150°C. These peaks may be attributed to the melting or release of some volatile contaminants in the crude MAS. In the recrystallised MAS sample these peaks were not observed. Both samples showed a decomposition temperature around 305-310°C although this temperature was slightly lower for the crude MAS due to the contaminants present.

The DSC of the purified MAS was then compared to that of Aldrich-MAS in the range 200-360°C. The same endothermic peak around 311°C was observed for both samples (Figure 3.2). These results confirm that the recrystallised monomer is pure and can be used for polymerisation.

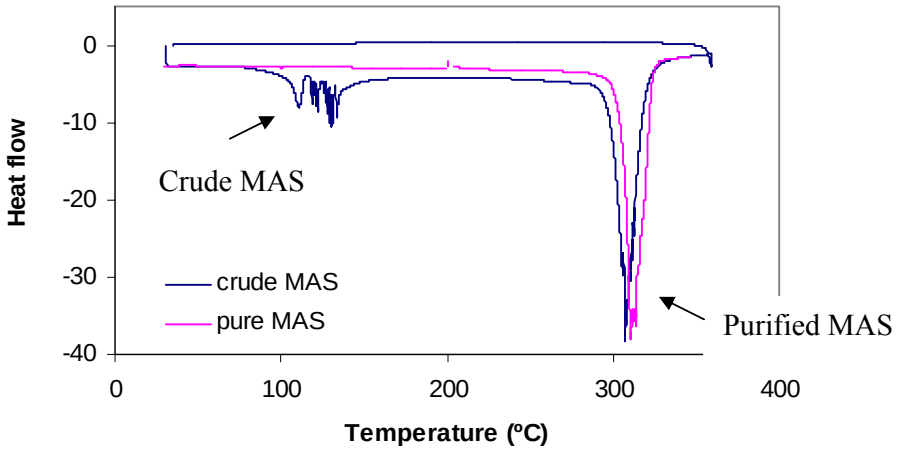

Figure 3.1. DSC curve (20-360°C) of MAS before and after purification, heating rate 10°C/min, under nitrogen atmosphere.

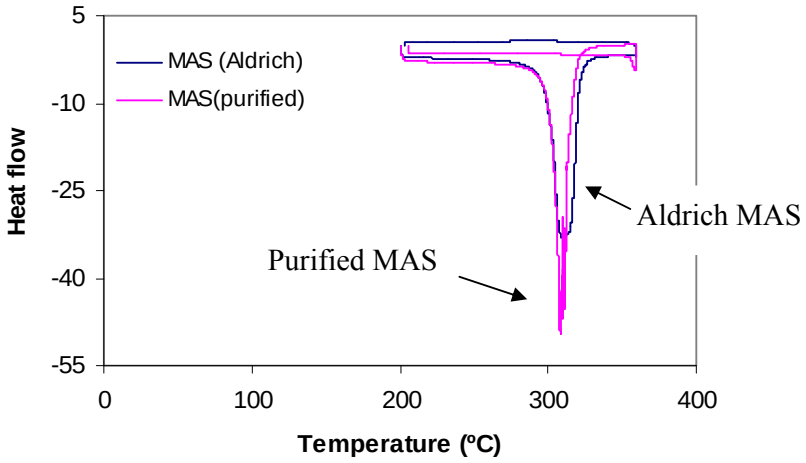

Figure 3.2. DSC curve (200-360°C) of purified MAS compared to Sigma-Aldrich MAS, heating rate 10°C/min, under nitrogen atmosphere.

TGA analysis of the purified MAS was compared to that of MAS purchased from Sigma-Aldrich. Similar thermograms were obtained with a significant weight loss (about 40%) observed around 305°C – the decomposition point (Figure 3.3). A black powder was obtained at the end of TGA experiments.

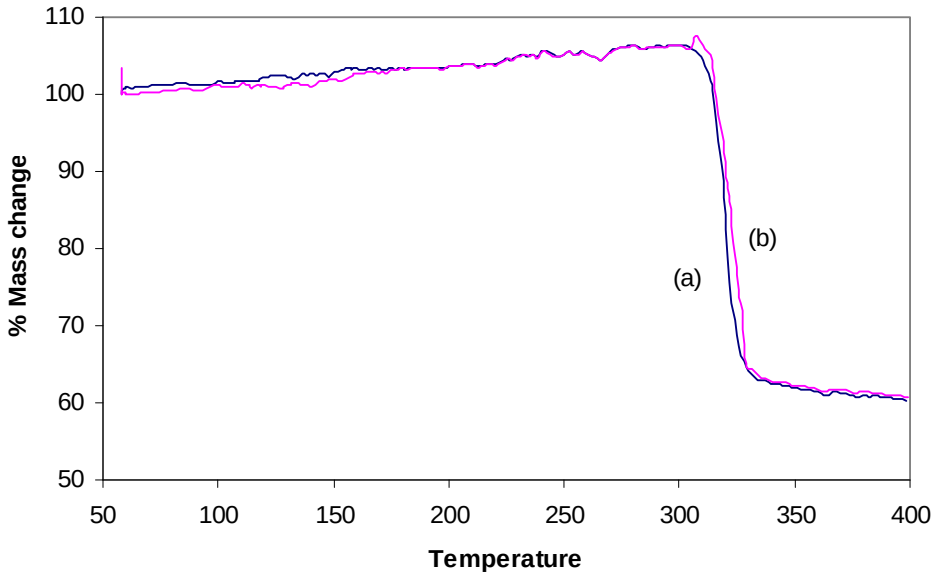

Figure 3.3. TGA curve (55-400°C) of (a) purified MAS and (b) Sigma-Aldrich MAS, heating rate 10°C/min, under nitrogen atmosphere.

3.3.2 Synthesis of PMAS

PMAS was prepared by dropwise addition of APS to the monomer solution resulting in the initially clear solution turning a dark brown colour after a few minutes. After 30 min the reaction mixture changed to a dark yellow-green colour, forming a viscous solution upon standing overnight. The initial brown colour was attributed to the formation of soluble oligomers and short polymeric chains which were converted to longer chain polymers during the reaction process (as discussed in Chapter 1, Section 1.4.1.2).

The resulting crude product from the chemical synthesis of PMAS was a mixture of polymer, low molecular weight oligomers, unreacted monomer and excess oxidant.

This crude reaction product was characterised using gel permeation chromatography (GPC) to determine the molecular weight distributions of the polymer fractions. The detector employed during this analysis was a photodiode array (PDA) capable of

providing a 3D chromatogram from which a classical 2D chromatogram could be derived. More importantly, from this 3D chromatogram, a UV-vis spectrum (300 – 800 nm) could be extracted at any given elution volume providing the capability to assess the chemical nature of the fraction being investigated. 3D and 2D chromatograms (Figure 3.4) clearly show that 3 components passed through the GPC column with different retention times as listed in Table 3.1. By employing a mobile phase buffered at pH 9, the position of the polaron band, typically observed at 473 nm for acidified PMAS, was shifted out to over 700 nm due to a polymer conformational change [4] (see Figure 3.5b).

The peak at 14-15 min (M_p = 8,740) was assigned to high molecular weight (HMWt) PMAS while the peak at 17-18 min (M_p = 1,970) was attributed to low molecular weight (LMWt) PMAS and oligomers. The last component with a retention time of 26 min (M_p = 200) is attributed to unreacted monomer retained in the polymerisation solution.

Table 3.1. Molecular weight distributions for the as-synthesised PMAS before purification. Calibration is relative to polystyrene sulfonate standards.

Component	Retention time (min)	M_n (Da)	M_p (Da)	M_w (Da)	PDI
1	14.9	7,740	8,740	11,500	1.49
2	17.7	1,700	1,970	2,100	1.21
3	26.3	-	200	-	-

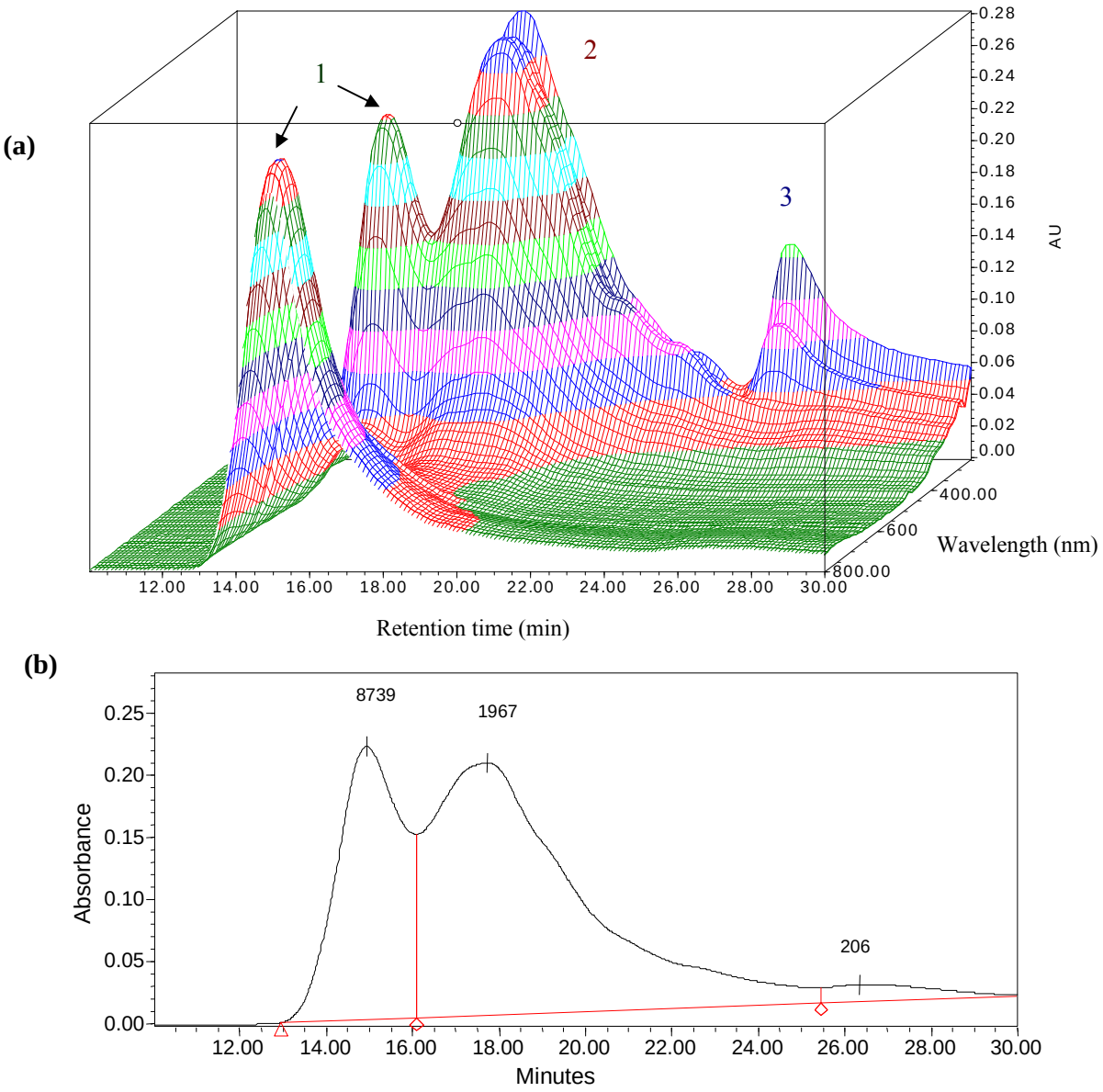

Figure 3.4. (a) 3D and (b) 2D GPC chromatograms of the as-synthesised PMAS before purification. The peak M_p values are shown on the chromatogram. The numbers refer to the three components listed in Table 3.1.

A typical UV-vis spectrum of PMAS aqueous solution at pH 3.5 exhibited a broad absorption band at 330-350 nm, attributed to π-π* transitions, a sharp band at 473 nm assigned to a low wavelength polaron band and a free carrier tail above 800 nm

attributed to a high wavelength delocalised polaron transition [4, 5]. The UV-vis spectrum of the as-synthsised PMAS before purification shows an absorption band at 473 nm and a free carrier tail in the near infrared region characteristic of PMAS polaron bands (Figure 3.5a). The broad peak situated between 280-330 nm can be attributed to π-π* transitions of PMAS, which have combined with the absorbance bands of oligomers and residual monomer in this region. The UV-vis spectrum of this sample at alkaline solutions (such as the GPC mobile phase buffered at pH 9) (Figure 3.5b) exhibits a strong absorption band at 750 nm consistent with a compact coil conformation of the PMAS chains [4] .

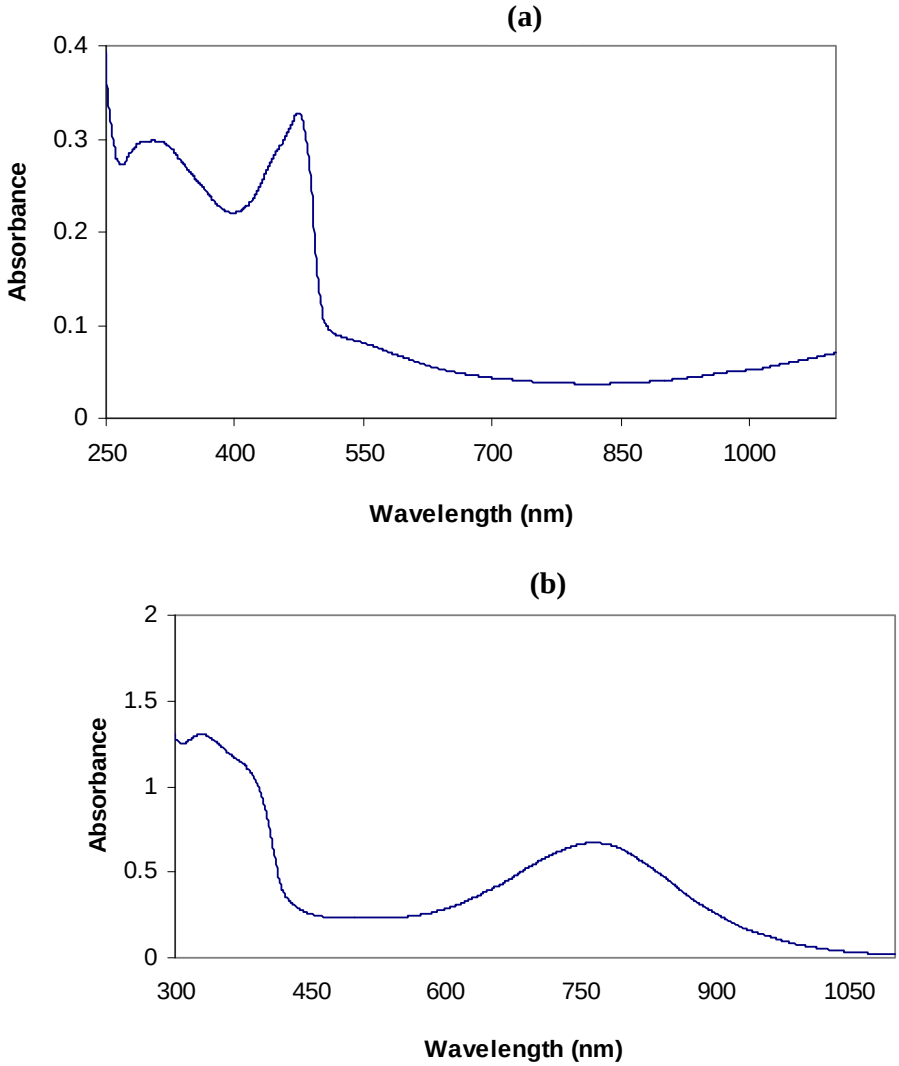

Figure 3.5. UV-visible spectrum of a dilute aqueous solution of the as-synthesised PMAS before purification: (a) at pH~3 and (b) at pH 9.

3.3.3 Purification of PMAS

Two methods were used to purify the as-synthesised PMAS, either standard dialysis using tubing, or a commercial tangential flow diafiltration system. In order to make a comparison between the two purification methods, 75 ml of crude reaction mixture was divided into two portions with each portion being purified by one of the two methods.

3.3.3.1 Purification by dialysis

Dialysis is a routine method for desalting, concentrating and separating biomolecules and macromolecules that differ substantially in molecular weight, and is a technique driven by osmotic pressure forces. Dialysis tubing is essentially a cylindrical membrane containing pores the size of which determines the "molecular weight cut-off" (MWCO) of the tubing. The MWCO describes an indicative molecular weight at which a compound will be 90% retained following overnight dialysis. Generally, molecules smaller than the MWCO will pass freely through the membrane, driven by a concentration gradient between the high concentration dialate solution inside the dialysis tube to the receiving solution which is essentially pure water.

In this work, cellulose dialysis tubing with a 12 kDa molecular weight cut off (MWCO) was used in an attempt to isolate only the high molecular weight component shown to have a 750 nm peak (polaron band) in the 3D PDA analysis above (Figure 3.4). Upon commencement of dialysis against water, a pink colour was discharged from the dialysis tubing. The dialate discharge at later stages of dialysis was predominantly dark brown in colour. The dialysis was continued for 30 hours. The dialysis bath containing 2 L MilliQ water was magnetically stirred and changed four times over the course of the 30 hours. Dialysis for longer times resulted in a light brown filtrate which turned gradually to a yellow-green solution, presumably due to penetration of some PMAS molecules through the membrane into an environment that was at pH 7. In order to avoid this, dialysis was stopped after 30 hours.

The chromatogram obtained for the polymer solution purified using dialysis tubing exhibited two distinct peaks (Figure 3.6). The first peak at retention time of *ca.* 15 min was attributed to HMWt polymer (8-9 kDa) and exhibited two absorption maxima at *ca.*

470 and 750 nm (z-axis) which are the typical π-π* and polaron transitions observed for compact coil conformation form of PMAS in the GPC buffer at pH 9 [4]. The second peak at 17 min is attributed to LMWt oligomers (2-3 kDa). The UV-vis spectra of this fraction were significantly different from HMWt fraction in that no absorption at *ca.* 750 nm, (the polaron band) was observed. Thus it was concluded that the 12 kDa MWCO dialysis tubing successfully removed the residual monomer, oxidant and pink coloured fraction containing oligomers less than *ca.* 2 kDa, but was unable to eliminate the 2-3 kDa fraction.

The UV-vis spectrum was recorded for the PMAS containing solution after dialysis using tubing (dialysed PMAS) (Figure 3.7). The spectrum clearly shows the characteristic peaks of PMAS as discussed earlier. Compared to the as-synthesised PMAS, the ratio of the intensity of the absorption band at 474 nm to the intensity at 330 nm was significantly increased due to the decrease in the concentration of oligomers and monomer absorbing in the range 300-350 nm.

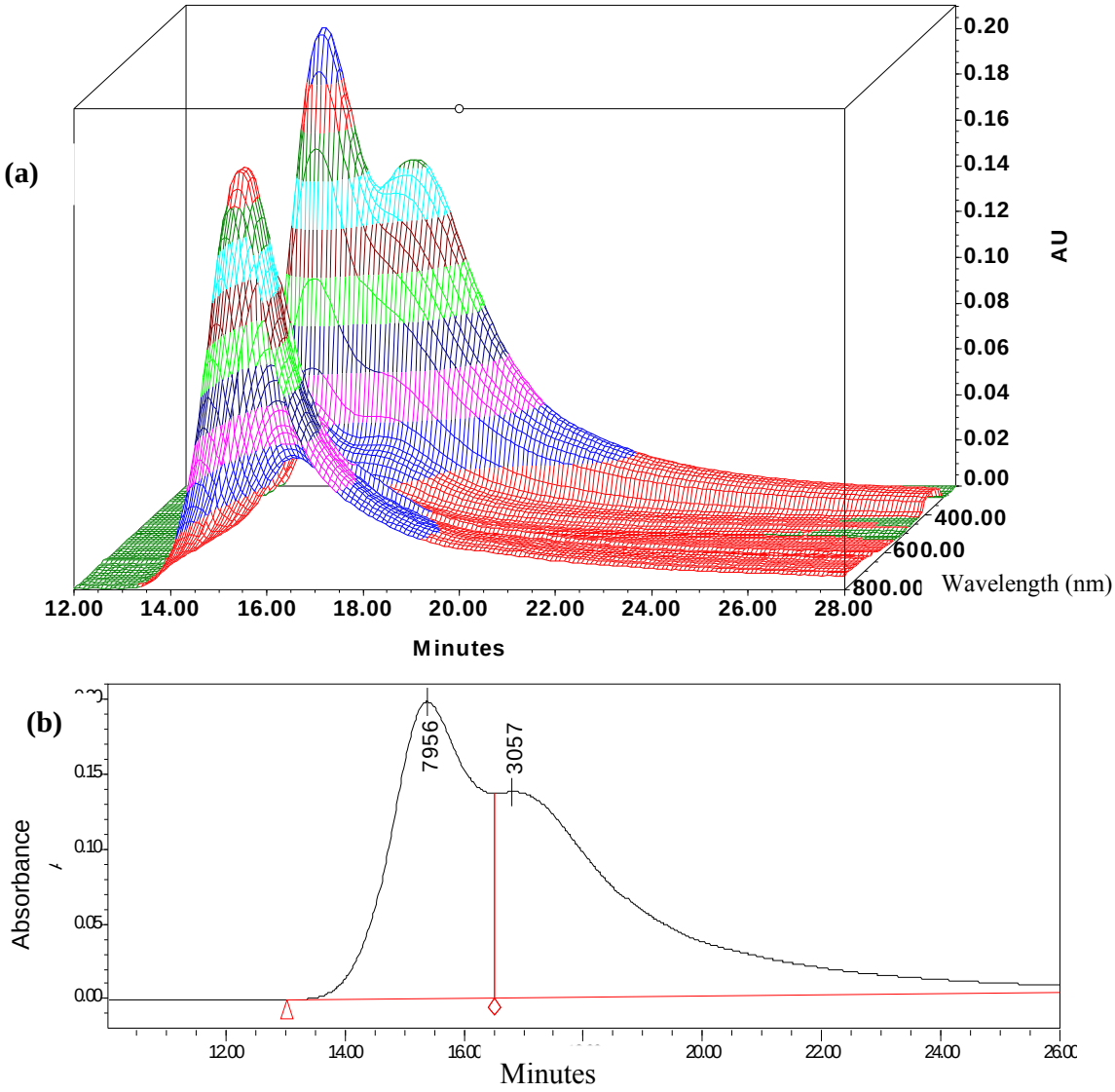

Figure 3.6. (a) 3D and (b) 2D GPC chromatograms of PMAS chemically polymerised at 16-18ºC using purified monomer and dialyzed by dialysis tubing, 12 kDa MWCO. Peak1: Retention time 15.38 min, M_n 6,870 Da, M_w 10,200 Da, M_p 7,960 Da, polydispersity 2.16. Peak2: Retention time 16.79 min, M_n 2,010 Da, M_w 2,240 Da, M_p 3,060 Da, polydispersity 1.09.

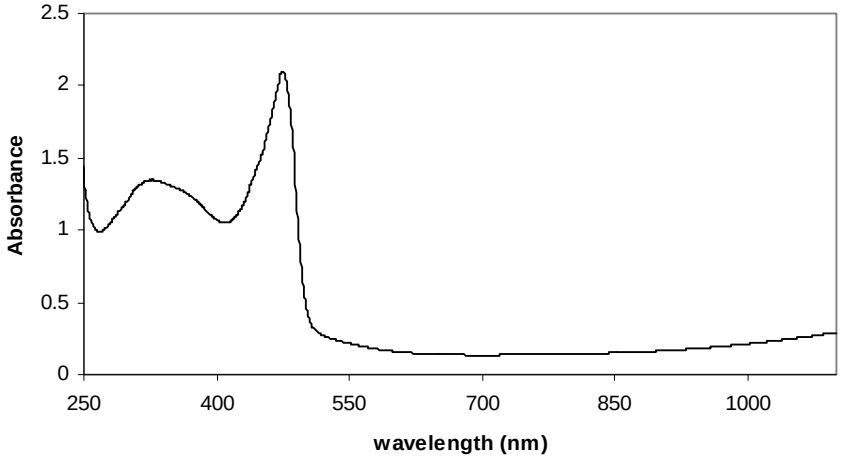

Figure 3.7. UV-visible spectrum of PMAS product dialysed using tubing.

In this thesis, the fraction with molecular weight of 8-9 kDa will be called high molecular weight PMAS (HMWt PMAS) and the fraction with molecular weight of 2-3 kDa will be called low molecular weight PMAS (LMWt PMAS).

3.3.3.2 Purification by tangential flow diafiltration

The second half of the as-synthesised PMAS was purified using the tangential flow diafiltration membrane (Scheme 3.2).

Tangential flow filtration is a rapid and efficient method for separation and purification of biomolecules. The solution to be concentrated or diafiltered is pumped across the face of a membrane filter of the desired molecular weight cut-off. A flow restrictor on the exit port supplies sufficient backpressure to force some of the solution through the membrane and into the filtrate container, the remainder is recirculated across the membrane. Recirculation is allowed to continue until the desired degree of concentration or diafiltration has taken place. Selection of the appropriate membrane and operating conditions were investigated.

Two types of membrane with different active areas and MWCO (5 kDa and 10 kDa) were used, VivaFlow™ 50 (active area 50 cm^2) and VivaFlow™ 200 (active area 200 cm^2).

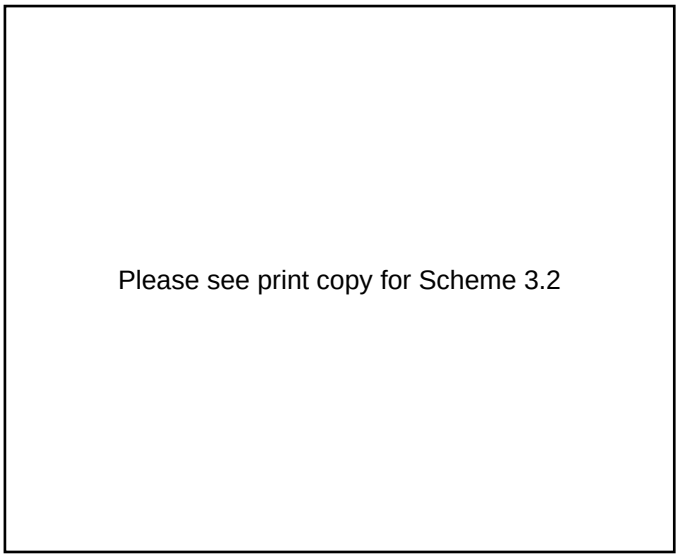

Scheme 3.2. VivaFlow™ tangential flow diafiltration system with Polyethersulfone membranes. (1) dilution reservoir, (2) sample reservoir, (3) peristaltic pump, (4) membranes, (5) filtrate collector, (6) recirculation line.

3.3.3.2.1 Using VivaFlow™ 50 membrane with 5 kDa MWCO

As recommended in the tangential flow filtration manual, 5 kDa MWCO membrane was first chosen to remove the monomer and oligomers (M_p < 2.5 kDa) and to retain HMWt PMAS (M_p 8-10 kDa). To increase the surface area, two membranes (Vivaflow 50, 5 kDa MWCO) connected in series were used. A sealed sample reservoir with a water feed line was used to maintain the level of the solution. At appropriate time intervals aliquots of sample were taken to record GPC. When diafiltration was initially started, a pink coloured solution was collected from the filtrate tubes. The diafiltration was continued for 10 hours, after this time the filtrate solution had a bright pink colour.

The GPC chromatogram obtained for the PMAS containing solution after diafiltration (5 kDa MWCO, 2 hours) exhibited two peaks assigned to two polymeric fractions having molecular weight of 8 kDa and 2 kDa (Figure 3.8a). Further diafiltration (8 hours) using this membrane removed some of the low molecular weight oligomers as evidenced by the slight increase in the M_p of the second component (Figure 3.8b). Low molecular weight oligomers and residual MAS were found in the GPC of the filtrate collected in the first 2 hours, whereas some high molecular weight fraction had started to pass through the membrane at the later stages of diafiltration (Figure 3.9).

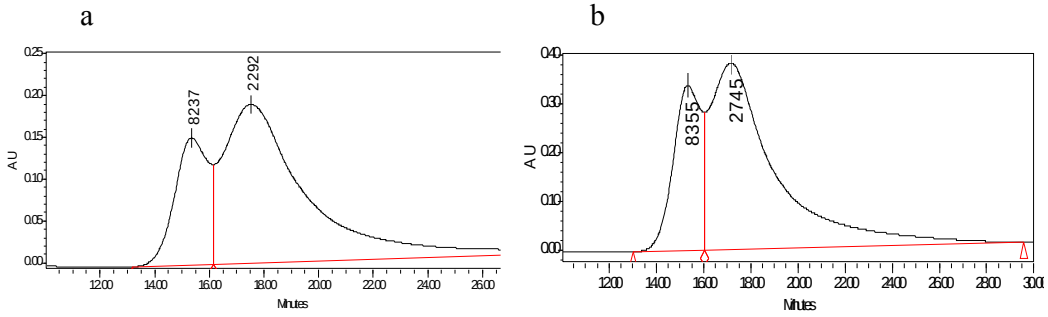

Figure 3.8. GPC chromatogram of PMAS diafiltred by 5 kDa MWCO membrane (a) after 2 hours and (b) after 10 hours. The peak M_p is shown on the plot.

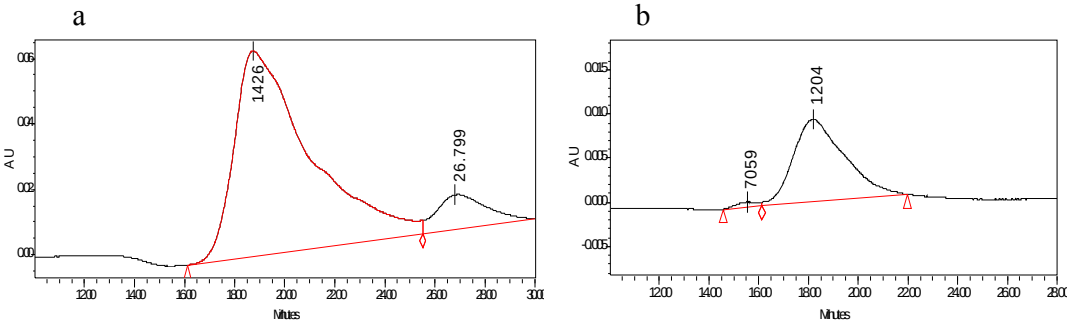

Figure 3.9. GPC chromatogram of filtrate collected from 5 kDa MWCO membrane (a) after 2 hours and (b) after 10 hours. The peak M_p is shown on the plot.

GPC analysis of the diafiltred and filtrate solutions revealed that the use of the 5 kDa MWCO membrane enabled removal of the monomer and pink-coloured low molecular weight (~1000-1500 kDa) oligomers, however two fractions with molecular weight higher than 2 kDa were also retained. As a consequence, a membrane with a higher MWCO was needed to remove all the oligomeric impurities. To confirm this, UV-

visible spectra of diafiltred PMAS and filtrate solutions obtained using the 5 kDa MWCO membrane were recorded (Figure 3.10). The intense absorption at ~300 nm in the spectrum of the PMAS containing solution confirms the presence of a significant LMWt PMAS content. A membrane with higher MWCO (10 kDa) was then chosen for further purification.

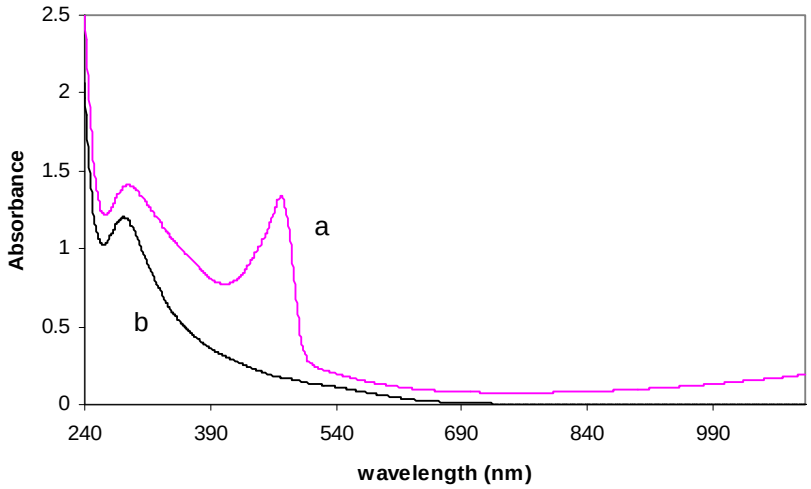

Figure 3.10. UV-visible spectra of (a) the diafiltred PMAS and (b) the filtrate solution obtained from the Vivaflow 50, 5 kDa MWCO membrane after 10 hours.

3.3.3.2.2 Using VivaFlow™ 50 membrane with 10 kDa MWCO

As the 5 kDa MWCO was unable to remove all the LMWt PMAS impurity, diafiltration was continued using 10 kDa MWCO membrane (active surface area 50 cm^2). Increased surface area was achieved by using two membrane modules (Vivaflow 50, 10 kDa MWCO) in series. A sealed sample reservoir with a water feed line was used to maintain the level of the solution as water was pumped through the membrane of the VivaFlow to the receiving side. At appropriate time intervals aliquots of sample were taken to record UV-visible spectra and chromatograms. A dark brown solution was collected from the filtrate lines. The filtration was continued for 4 hours until a light brown filtrate was obtained. When the solution was diafiltred for another 30 min, the filtrate turned to a bright yellow-green solution indicating that some HMWt PMAS passed through the membrane. This indicated that low molecular weight material was

mostly removed from the diafiltred solution, and some higher molecular weight polymers were also passed under the applied pressure. The diafiltration was then stopped and the diafiltred solution (dark yellow-green) was concentrated to ~20ml. This was achieved by removing the water feed line while continuing filtration for 10-15 min. The concentrated diafiltred solution was evaporated to get the solid PMAS.

Figure 3.11 and Figure 3.12 show the chromatograms obtained for the diafiltred polymer and filtrate solutions using the 10 kDa MWCO membrane after 4 hours. Significantly, the LMWt materials were removed and HMWt PMAS (M_p ~ 9 kDa) was retained. The filtrate obtained using this membrane contained LMWt PMAS with a molecular weight of ~ 3 kDa. No HMWt PMAS was observed in the filtrate collected during the first 3 hours. This filtrate therefore can be used as a sufficiently pure source of LMWt PMAS. The GPC of the filtrate collected after 3 hours was found to contain traces of HMWt PMAS.

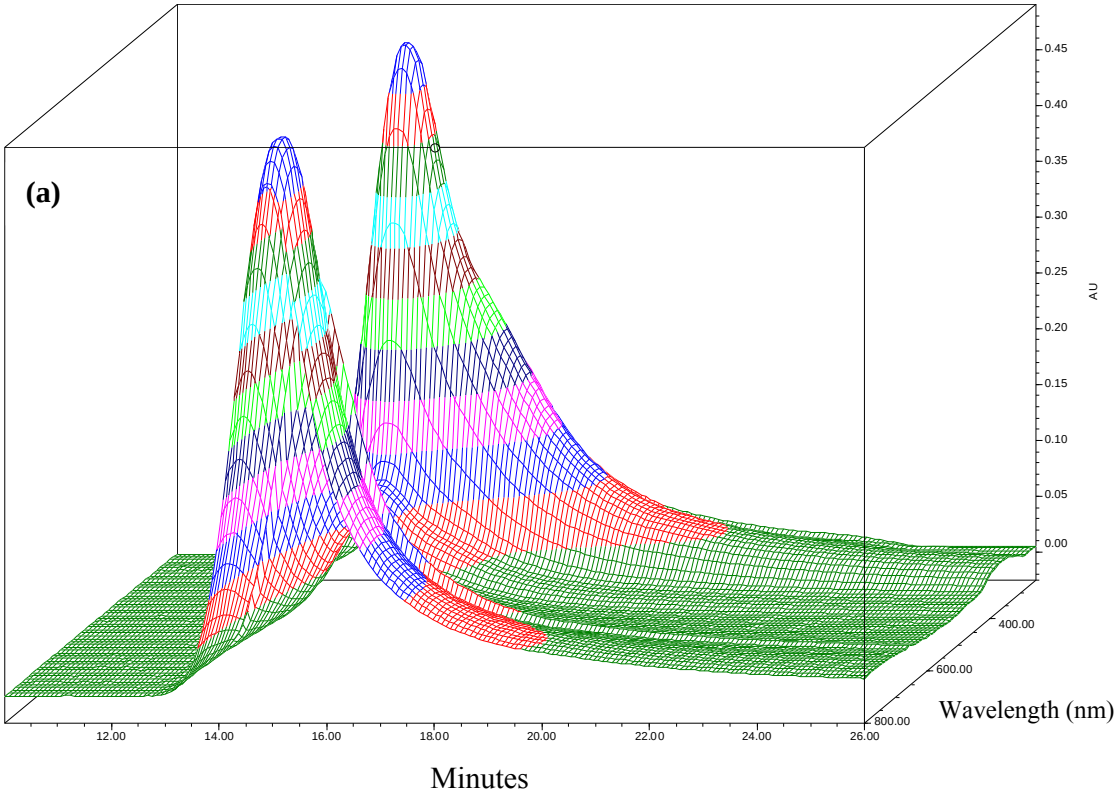

(b)

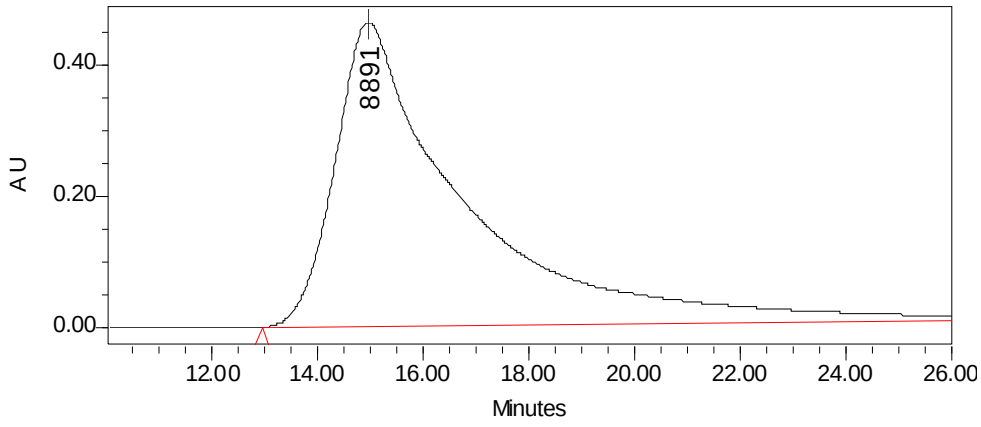

Figure 3.11. (a) 3D and (b) 2D GPC chromatograms of PMAS, chemically polymerised at 16-18 ºC, diafiltred using Viva flow 5 kDa MWCO for 4 hours, and 10 kDa MWCO for 4 hours at flow rate 400 mL/min. Peak retention time 14.96 min, M_n 3,570 Da, M_w 7,860 Da, M_p 8,890 Da, polydispersity 2.13.

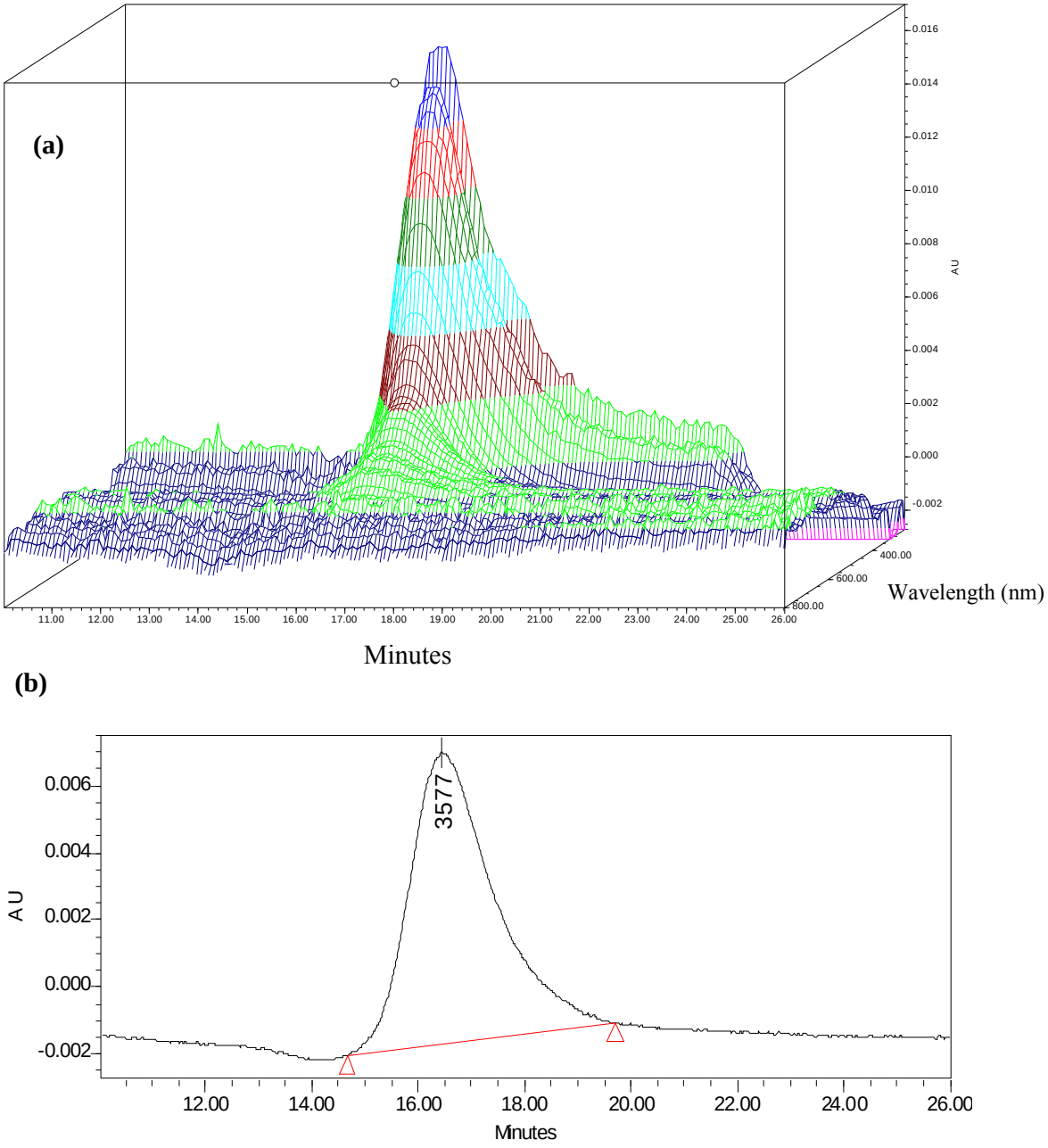

Figure 3.12. (a) 3D and (b) 2D GPC chromatograms of the filtrate solution obtained after 3 hours diafiltration using 10 kDa MWCO membrane at flow rate 400 mL/min. Peak retention time 16.44 min, M_n 2,740 Da, M_w 3,320 Da, M_p 3,580 Da, polydispersity 1.21.

3.3.3.2.3 pH changes during tangential flow diafiltration

As discussed previously in this Chapter, the polymerisation of MAS was carried out at pH 4 in order to dissolve the monomer. At the end of polymerisation, however, the solution pH was measured to be less than 1 due to release of protons during the polymerisation process. This reaction mixture was then diluted 3 times prior to it being diafiltred. As diafiltration proceeded, the pH of the dialate solution was recorded at several time periods (Table 3.2). The solution pH was found to increase slightly from 1.2 to 2.2 indicating that the excess acid had passed through the membrane.

Table 3.2. pH chages during diafiltration

dialate solution	pH
Before diafiltration	1.2
After diafiltration by 5 kDa for 7h	2.0
After diafiltration by 10 kDa for 4.5h	2.2
After diafiltration by 10 kDa for 7h	2.2
After diafiltration by 10 kDa for 10h	2.2

3.3.3.2.4 UV-visible spectroscopy during tangential flow diafiltration

The polymer mixture before diafiltration shows a strong absorption band at ~300 nm. The UV-vis spectra recorded during diafiltration (Figure 3.13) demonstrated that the intensity of 300 nm band decreased rapidly after 1 hour followed by a small decrease in the next 3 hours. This indicated that most of the LMWt PMAS was removed in the first hour. This filtrate had a strong absorption in the range 290-310 nm which decreased significantly in the first 1 hour and more slowly over the next 3 hours.

The ratio of the intensity of the absorption band situated at 473 nm band to the intensity of that at 330 nm was used as an indicator of purity. During diafiltration this ratio was found to increase steadily indicating the formation of a diafiltred product containing fewer LMWt impurities.

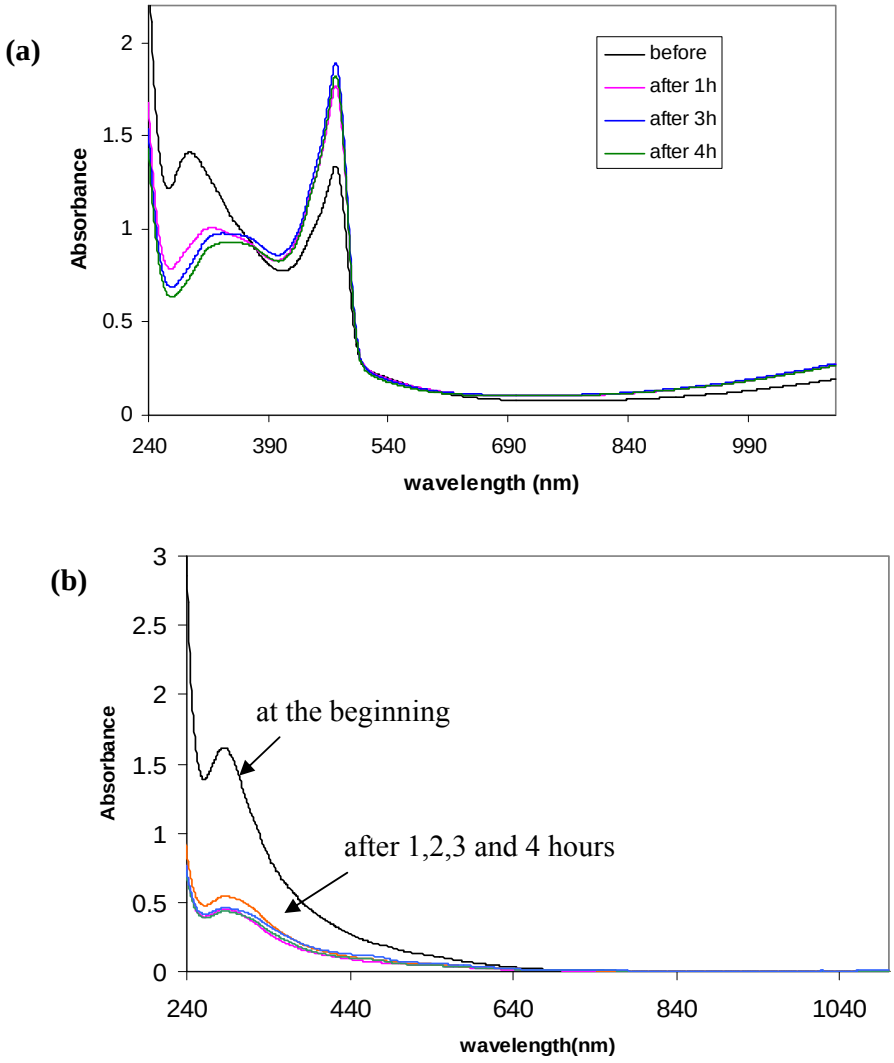

Figure 3.13. UV-visible spectra of (a) diafiltred PMAS and (b) filtrate collected from 10 kDa MWCO membrane during diafiltration using the Vivaflow 50, 10 kDa MWCO membrane.

Table 3.3. Absorbance changes for the spectra illustrated in Figure 3.13a.

Diafiltration time (hours)	A_{473}/A_{330}
0	1.13
1	1.76
3	1.93
4	1.96

The UV-visible spectrum of the pure PMAS obtained after cross flow filtration (HMWt PMAS) was compared with PMAS dialysed by conventional tubing (DPMAS) in Figure 3.14. For HMWt PMAS, the ratio of intensity at 473 nm to the intensity at 330 nm (1.96) was higher than DPMAS (1.50) and the peak at 330 nm shifts to a slightly higher wavelength. The more substantial purification of PMAS caused a 16 nm shift in wavelength from 328 nm to 344 nm.

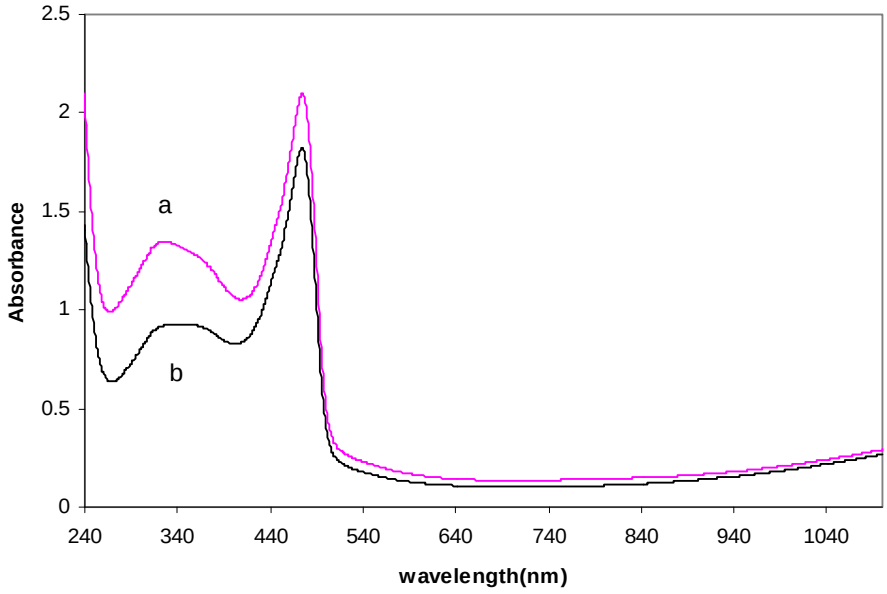

Figure 3.14. UV-visible spectra of (a) dialysed PMAS using conventional tubing and (b) pure PMAS using tangential flow diafiltration system.

The results established that the tangential flow filtration system using 5 kDa and 10 kDa MWCO membranes was able to purify and fractionate the as-synthesised PMAS mixture. In comparison to the conventional dialysis tubing, this method rapidly and effectively eliminates the LMWt materials and retains HMWt PMAS with very high recovery (>99%). Diafiltration time depends on the volume and concentration of sample, flow rate and also the active surface area of the membranes.

3.3.3.2.5 Increasing the surface area of membrane

It was shown above that it was possible to obtain pure HMWt PMAS over 10-12 hours using 5 kDa MWCO membrane and polishing for 4-6 hours using 10 kDa MWCO

membrane. In order to increase the rate of diafiltration, the large membranes (vivaflow 200) were tested. The active area of Vivaflow 200 membranes (200 cm^2) was 4 times larger than vivaflow 50 (50 cm^2).

3.3.3.2.6 Using VivaFlow™ 200 membrane with 5 kDa MWCO

GPC was recorded for the diafiltred polymer at appropriate time intervals during diafiltration. Filtration by vivaflow 200 was significantly faster and more effective than vivaflow 50. Figure 3.15 compares the chromatograms of diafiltred PMAS obtained by these two membranes. Moreover, GPC analysis of the filtrate of vivaflow 200 showed that this membrane also removed some LMWt PMAS (M_p 2-3 kDa).

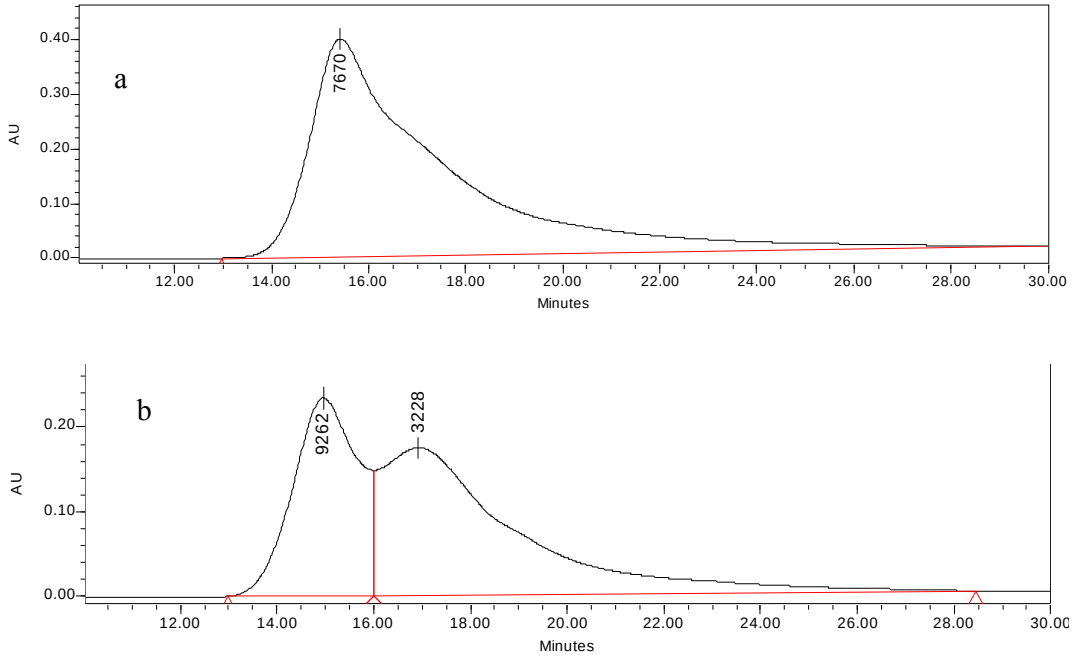

Figure 3.15. Influence of membrane surface area on purification of PMAS. (a) PMAS diafiltred by Vivaflow 200, 5 kDa MWCO for 3hours, (b) PMAS diafiltred by Vivaflow 50, 5 kDa MWCO for 7 hours. The peak M_p is shown on the plot.

GPC analysis of polymer diafiltred for 2, 3 and 4 hours (Figure 3.16) revealed that the amount of LMWT impurity decreased with time; however the rate of removal decreased so that no significant change was observed after 3 hours. This membrane did not eliminate all LMWt materials and consequently the higher MWCO membrane was required for final purification.

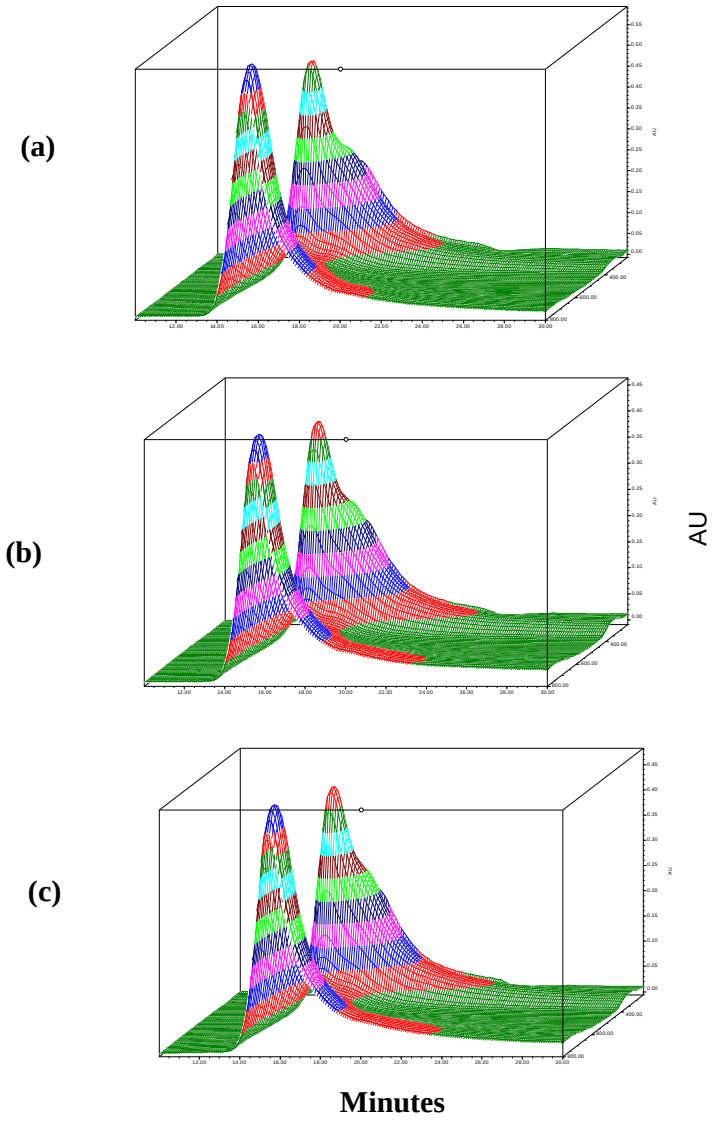

Figure 3.16. GPC recorded for diafiltred PMAS using Vivaflow 200, 5 kDa MWCO membrane during diafiltration (a) after 2 h, (b) after 3 h, and (c) after 4 h.

3.3.3.2.7 Using VivaFlow™ 200 membrane with 10 kDa MWCO

Purification of HMWt PMAS using VivaFlow™ 200 membrane (10 kDa MWCO) was investigated and found to be ineffective. When the diafiltred PMAS obtained from the 5 kDa MWCO membrane system was passed through this membrane, a concentrated yellow-green solution was collected from the filtrate lines indicative of HMWt PMAS passing freely through the membrane. Extended purification of the PMAS by this membrane system subsequently reduced the recovery of pure PMAS with respect to the smaller membrane system. As a consequence this approach was abandoned in favour of the smaller VivaFlow™ 50 membrane (10 kDa MWCO) cell.

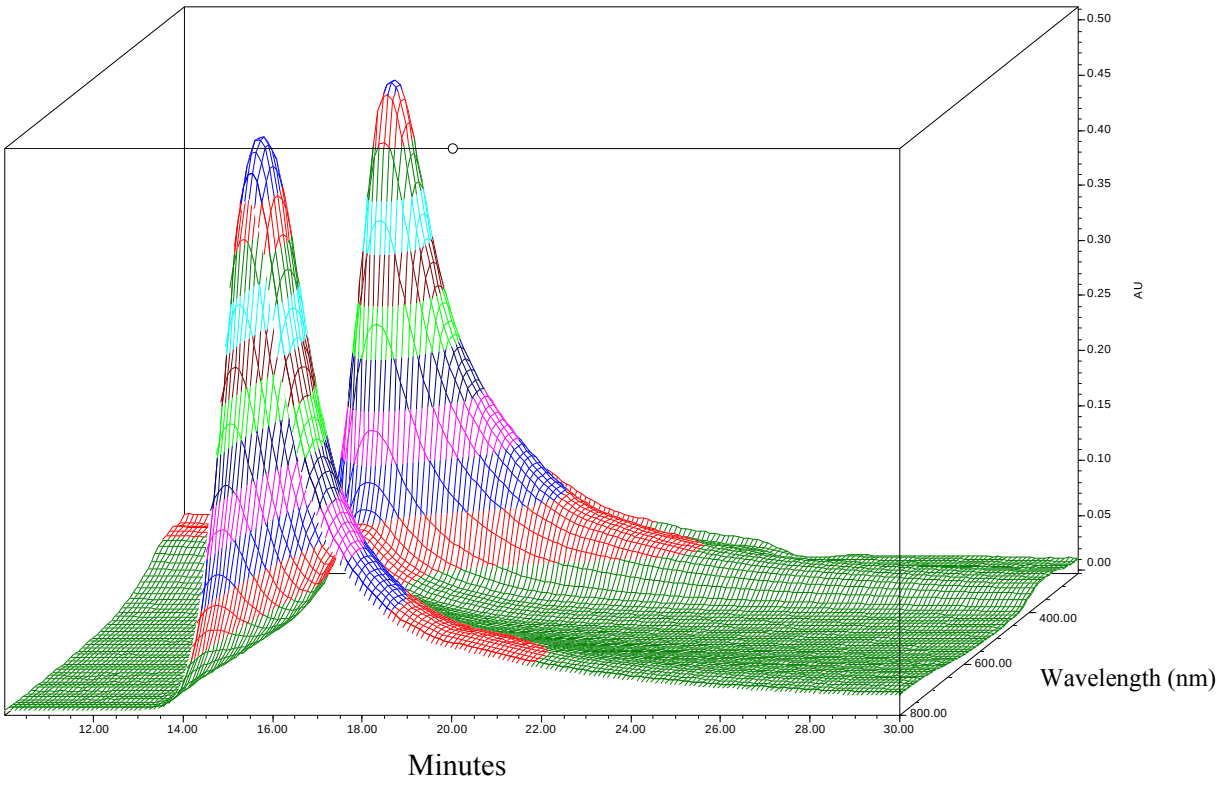

Figure 3.17. 3D chromatogram of highly pure PMAS obtained using VivaFlow™ 200, 5 kDa MWCO and VivaFlow™ 50, 10 kDa MWCO membranes. Peak retention time 15.46 min, M_n 4,010 Da, M_w 6,660 Da, M_p 7,380 Da, polydispersity 1.66.

3.3.3.2.8 Separation of LMWt fractions

The filtrate solution obtained using the VivaFlow™50, 10 kDa MWCO membrane (brown-coloured fraction) was found to have a molecular weight of 2-3 kDa and, as observed earlier, could not pass through the 5 kDa MWCO membrane. This solution was concentrated using the VivaFlow™ 50, 5 kDa MWCO membrane in order to recover the LMWt PMAS.

The filtrate obtained using the 5 kDa MWCO membrane was found to comprise of a pink coloured fraction (~1,200 Da), and the residual monomer. Monomer impurities were effectively removed within the first 3 hours of diafiltration using the 5 kDa MWCO membrane. The filtrate solution collected at the end of this diafiltration was analysed by GPC. One peak with molecular weight of ~1,200 Da (pink oligomeric fraction) was observed.

3.3.3.2.9 Optimised procedure for purification and fractionation of PMAS

Optimisation studies on the separation of PMAS fractions are presented below in Scheme 3.3 and Figure 3.18. In order to obtain the pure HMWt PMAS, the crude polymer mixture after synthesis is diafiltred for 4 h using VivaFlow™ 200, 5 kDa MWCO membrane (stage 1) and for another 4 h using VivaFlow™ 50, 10 kDa MWCO membrane (stage 2). This provides a highly pure HMWt PMAS with Mp ~ 8-10 kDa and a polydispersity of ~1.6 in only 8 hours. The LMWt PMAS with Mp ~ 2-3 kDa and a polydispersity of ~1.2 is obtained when the filtrate collected during stage 2 is concentrated using VivaFlow™ 50, 5 kDa MWCO for 1h. The filtrate collected at the end of stage 1 is defined as the pink oligomeric fraction.

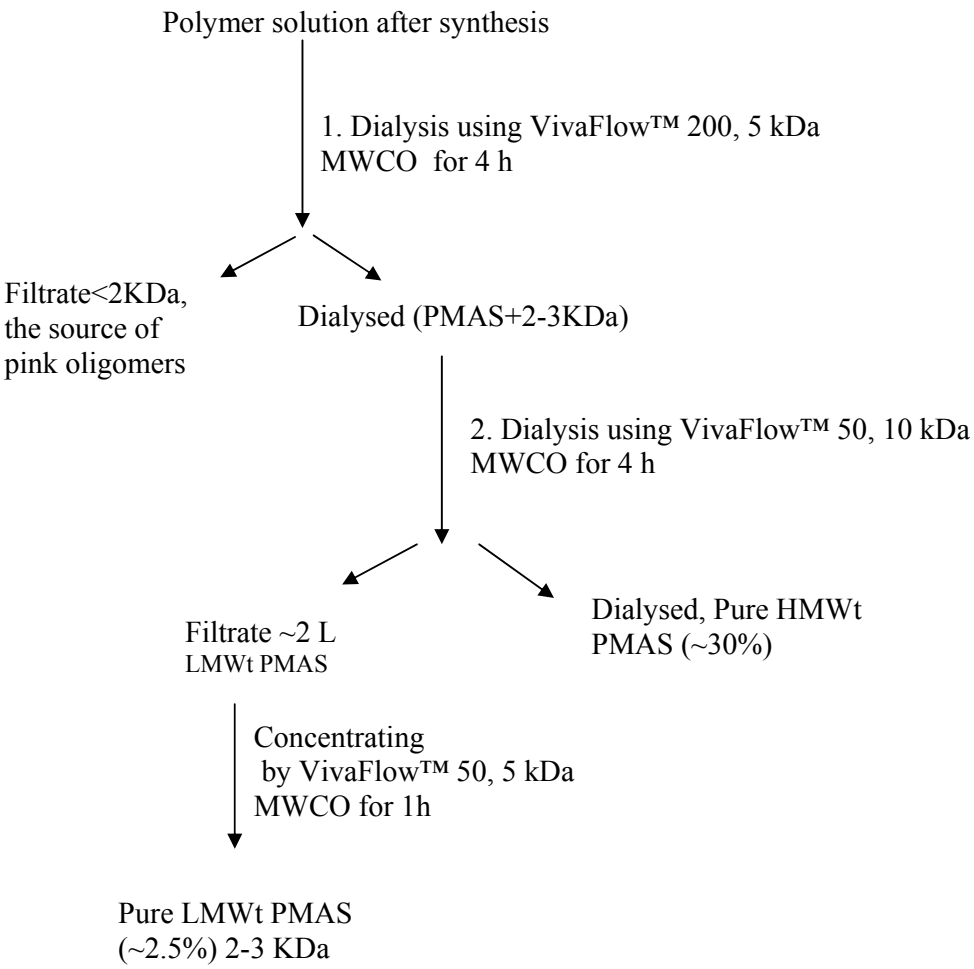

Scheme 3.3. Flowchart showing the purification and fractionation of PMAS

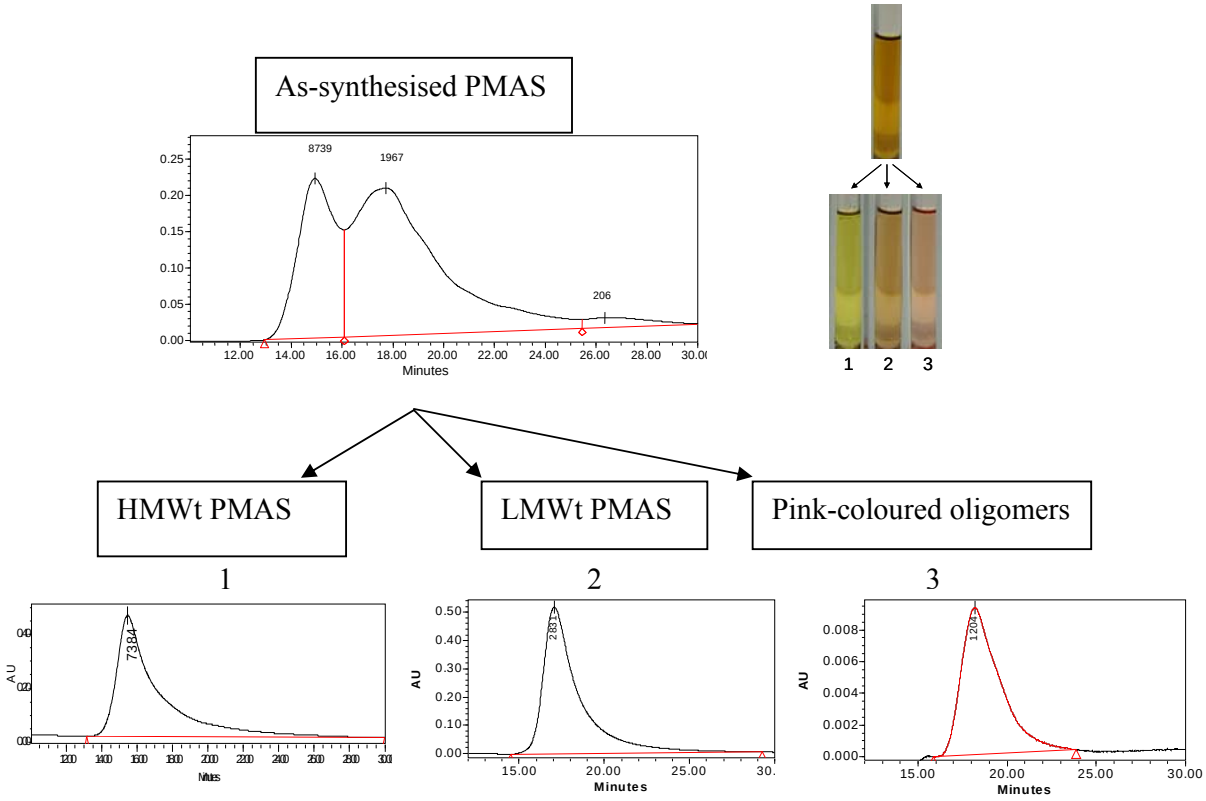

Figure 3.18. Purification and fractionation of PMAS as explained in Scheme 3.3.

3.3.3.2.10 Conductivity of the fractions

Conductivity measurements of the thin films of PMAS cast onto a glass substrate showed that the HMWt PMAS [(9 ± 1) x 10^{-2} S/cm] was more conductive than dialysed PMAS (DPMAS, obtained using conventional dialysis) [(4 ± 0.2) x 10^{-2} S/cm]. This increase in conductivity was also confirmed by measuring the conductivity of pressed pellets of PMAS obtained using the conventional and new diafiltration method. The conductivity of LMWt PMAS and pink oligomeric fractions were found to be two orders of magnitude lower than the conductivity of HMWt PMAS. As a result, the conductivity of the polymer increases substantially upon purification.

3.4 Conclusions

A new diafiltration method for purification of PMAS has been developed. This procedure provides a simple and scalable method to isolate HMWt PMAS with high purity and in a shorter time than traditional dialysis. In addition, pure oligomer fractions with different molecular weight and colour have been obtained and characterised by GPC and UV-vis spectroscopy. Results indicate that the purified HMWt PMAS has different electrical properties to the equivalent dialysed PMAS product (obtained using conventional dialysis), containing two distinctly different fractions.

The new purification system using different MWCO membranes provides a facile route for isolation and study of the pure products that are produced at different stages of polymerisation.

3.5 References

1. Shimizu, S., Saitoh, T., Uzawa, M., Yuasa, M., Yano, K., Maruyama, T., and Watanabe, K., *Synthesis and applications of sulfonated polyaniline.* Synthetic Metals, 1997. **85**(1-3): p. 1337-1338.
2. Guo, R., Barisci, J.N., Innis, P.C., Too, C.O., Wallace, G.G., and Zhou, D., *Electrohydrodynamic polymerization of 2-methoxyaniline-5-sulfonic acid.* Synthetic Metals, 2000. **114**(3): p. 267-272.
3. Zhou, D., Innis, P.C., Wallace, G.G., Shimizu, S., and Maeda, S.-I., *Electrosynthesis and characterisation of poly(2-methoxyaniline-5-sulfonic acid)-effect of pH control.* Synthetic Metals, 2000. **114**(3): p. 287-293.
4. Strounina, E.V., Shepherd, R., Kane-Maguire, L.A.P., and Wallace, G.G., *Conformational Changes in Sulfonated Polyaniline Caused By Metal Salts and OH*. Synthetic Metals, 2003. **135-136**: p. 289-290.
5. Xia, Y., Wiesinger, J.M., MacDiarmid, A.G., and Epstein, A.J., *Camphorsulfonic Acid Fully Doped Polyaniline Emeraldine Salt: Conformations in Different Solvents Studied by an Ultraviolet/Visible/Near-Infrared Spectroscopic Method.* Chem. Mater., 1995. **7**(3): p. 443-445.

Chapter 4

Chemical Synthesis of PMAS, an Optimisation Study

4.1 Introduction

Many applications of polyaniline have been limited by its lack of solubility and processability. Significant research has been directed towards developing solution processability via monomer functionalisation [1-3], copolymerisation [4], chemical modification [5-9], and the use of suitable surfactant-like acidic doping [10-13].

A successful approach to forming soluble polyaniline has been the introduction of a sulfonic acid group to the polyaniline chain to make self-doped sulfonated polyaniline (SPAN).

SPAN has been prepared by sulfonation of emeraldine base PAn using fuming sulfuric acid [7]. Elemental analysis of this SPAN has demonstrated a S/N atomic ratio of 0.48 and titration analysis has established a doping level of 0.3 [14]. The conductivity of SPAN is typically 0.1 S/cm, lower conductivity than PAn. However, unlike PANI, it remains conductive up to pH 7. In addition, SPAN is soluble in basic aqueous solutions (23 mg/ml). Treatment of leucoemeraldine base of PAn with fuming sulfuric acid has led to highly sulfonated (75%) SPAN [8], however fully sulfonated PAn has not be achieved via this approach. Highly sulfonated (75%) PAn has increased solubility (38 mg/ml) and conductivity (1 S/cm) compared to 50% SPAN and remains conductive over the pH range of 0-14.

Chemical polymerisation of sulfonated anilines such as *m*-aniline sulfonic acid has also been studied. Due to the presence of the strong electron-withdrawing sulfonate group, *m*-aniline sulfonic acid is difficult to polymerise and the formation of oligomers with molecular mass of 3000 Da and with poor electrical conductivity (3×10^{-6} S/cm)

predominates [15]. Metanillic acid has also been polymerised under high pressure but with very low yields of around 10% [16].

Substitution by an electron-donating group like methoxy [15] increases the electron density on the amino group and the reactivity of the monomer. Chemical polymerisation of 2-methoxyaniline-5-sulfonic acid [MAS] gives poly(2-methoxyaniline-5-sulfonic acid) [PMAS, Scheme 4.1] with high molecular weight (10,000 Da) and conductivity of 0.04 S/cm. The first synthesis of PMAS polymer was reported in 1997 by Shimizu *et al.* [15]. Since the MAS monomer is soluble in basic solution, polymerisation is carried out under basic conditions using pyridine, whereas the polymer is not produced under acidic conditions.

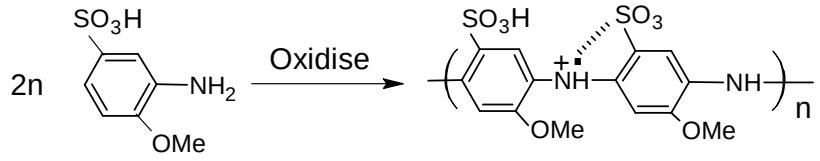

Scheme 4.1. Polymerisation of MAS to form PMAS

PMAS has been synthesised in our laboratories by electrochemical [17, 18] and chemical polymerisation of MAS in aqueous ammonia solution, which is a more "green" solvent in comparison to pyridine. A novel postsynthesis purification and fractionation method for the resultant polymer mixture has been developed using different molecular weight cut off (MWCO) polyethersulfone membranes as discussed in Chapter 3.

The influence of polymerisation parameters on chemical synthesis and properties of PMAS has to date not been systemically studied. In this chapter, studies have been undertaken to establish the most appropriate conditions to synthesise polymer with improved yield, higher conductivity and molecular weight as well as determining the influence of different reaction variables on the chemical polymerisation of MAS. In this regard, experimental parameters such as temperature reaction, time, solution pH,

monomer and oxidant concentration and the rate of addition of oxidant have been systematically varied and the effect of these variables on polymer properties analysed to establish optimal synthesis conditions.

4.2 Experimental

4.2.1 Materials

All chemicals were of analytical grade and used as received. 2-Methoxyaniline-5-sulfonic acid (MAS) was provided by Mitsubishi Rayon, Japan and purified by acid base crystallisation before use. All solutions were prepared in Milli-Q water (18 MΩ cm).

4.2.2 Monomer purification

Crude MAS (20 g) was dissolved in 200 mL water by the addition of about 8 mL 28% (w/v) ammonia solution dropwise. After filteration, the solution pH was dropped to less than 1.0 by the slow addition of concentrated HCl. The resultant precipitate was filtered and washed with 200 mL of a 70:30 mixture of methanol/water and dried in an oven at 50°C for 24 h to give a yield of 60% (w/w).

4.2.3 PMAS synthesis

Typically PMAS was chemically synthesised from 50 mL 0.50 M aqueous solution of MAS monomer (adjusted to pH 4 with 28% NH_3) by addition of 25 mL of 1.25 M aqueous solution of ammonium persulfate (APS) at a rate of 1 mL/min, giving an oxidant / monomer molar ratio of 1.25. After addition of the APS, the reaction mixture was stirred at a controlled temperature (16-18°C) for 20 hours, unless otherwise stated. A Julabo controlled temperature bath and a peristaltic pump (Minipuls 2, Gilson) were used to control temperature and the rate of addition of the oxidant during synthesis.

4.2.3.1 Purification of PMAS

After the reaction was completed, the 75 mL polymer mixture was diluted to 250 mL with water, then purified by diafiltration using the procedure developed in Chapter 3 [19]. The polymer mixture was purified using VivaFlow™ 200, 5K MWCO membrane

for 5 hours and then VivaFlow™ 50, 10 kDa MWCO membrane for 4 hours at a flow rate of 400 mL/min using a Masterflex peristaltic pump (model 7518-00). The pure concentrated polymer solution was evaporated and dried in a vacuum oven at 40-50°C before being characterised. For separation of the low molecular weight (LMWt) PMAS, the 2 liters of filtrate obtained from the VivaFlow™ 50, 10 kDa MWCO membrane was concentrated (by a factor of 1/100) using the VivaFlow™ 200, 5K MWCO membrane. The concentrate was evaporated and dried in an oven at 40-50°C.

For rapid purification of small amounts (~50 µL) of the reaction products, an equivalent Vivaspin™ 10 kDa MWCO membrane was used in a Beckman (J2-MC, rotor JA10) centrifuge centrifuge (4100 rpm) to remove the oligomers (with molecular weight less than 5 kDa). The small amount of the reaction product solution (50 µL) was diluted to 20 mL before spinning.

4.2.3.2 Synthetic conditions

In order to observe the effect of each variable in the synthesis of PMAS, all reaction parameters were systematically varied in a series of experiments, changing only one parameter at a time.

4.2.3.3 Effect of temperature

A 25 mL aliquot of 1.25 M aqueous APS was added to a 50 mL 0.50 M MAS monomer (adjusted to pH 4 with 28% NH_3) at a rate of 1 mL/min. The polymerisation temperature was varied between 0 and 20°C. The reaction was stirred at the controlled temperature for 5 hours followed by diafiltration at the same temperature for 2 hours using Vivaflow 200, 5K MWCO membrane. The solution was diafiltred further at room temperature to obtain the pure PMAS as outlined in the purification section (section 4.3.2.1).

4.2.3.3.1 Monitoring the reaction, effect of time

A 25 mL aliquot of 1.25 M aqueous APS was added to a 50 mL 0.50 M MAS monomer (adjused to pH 4 with 28% NH_3) at 10°C at a rate of 1 mL/min. Aliquots of the reaction mixture (30 µl=0.03 g) were taken at selected time intervals and diluted to 6 mL with

water to stop the reaction. Samples taken at these time intervals were characterised using GPC and UV-vis spectroscopy. Samples for UV-visible spectroscopy were prepared by diluting a further 15 times. Monomer conversion was determined by HPLC analysis of the monomer solution before polymerisation and polymer samples taken during polymerisation.

4.2.3.3.2 Monitoring the reaction, effect of pH

A 25 mL aliquot of 1.25 M aqueous APS was added to a 50 mL 0.50 M MAS monomer (adjusted to pH 4 with 28% NH_3) at a rate of 1 mL/min. Aliquots of the reaction mixture (50 µl) were taken and diluted to 20 mL with water and then concentrated using the Vivaspin 10 kDa MWCO membrane for 10 min at 4100 rpm to remove the oxidant, monomer and oligomers. The concentrated solution (~200 µl) was then diluted to 600 µl. This solution was characterised by GPC (after 2 times dilution) and UV-visible spectroscopy (after 15 times dilution). For polymerisation at controlled pH, ammonia solution (14% w/v) was added as to maintain the pH at the specified value using an in-house fabricated auto-titrator.

4.2.3.3.3 Effect of varying the monomer concentration

A 25 mL aliquot of 1.25 M aqueous APS was added to a 50 mL 0.5 M MAS monomer (adjusted to pH 4 with 28% NH_3) at a rate of 1 mL/min. The total MAS concentration was varied in the range 0.07-0.47 M. The oxidant / monomer mole ratio was 1.25 in all reactions. The reaction proceeded for 20 hours and the product was purified as outlined in the purification section (section 4.3.2.1). The pure product was dried in an oven at 40-50ºC to measure the yield. The product was then dissolved in water (0.05-1.0 mg/mL) and characterised by GPC and UV-visible spectroscopy. Monomer conversion was obtained after 20 hours for all reactions.

4.2.3.3.4 Effect of varying the oxidant to monomer molar ratio

A 25 mL APS solution was added to a 50 mL 0.5 M MAS monomer (pH 4 adjusted with NH_3 28%) at 10°C at a rate of 1 mL/min. This resulted in a final monomer

concentration of 0.33 M. The APS concentration was varied to achieve oxidant / monomer mole ratios of 0.63, 1, 1.25 and 2. The reaction solution was stirred at 10°C for 20 hours and the product was purified as outlined in the purification section. The pure product was dried to determine the yield and further characterised by GPC (molecular weight) and UV-visible spectroscopy. Monomer conversion was obtained after 20 h for all reactions.

4.2.3.3.5 Effect of oxidant addition rate

A 25 mL aliquot of 1.25 M aqueous APS was added to a 50 mL 0.50 M MAS monomer solution (adjusted to pH 4 with 28% NH_3) at 10°C. The oxidant / monomer mole ratio was 1. The addition rate of oxidant was varied from 1 mL/min to 100 mL/min (rapid mixing). The reaction was stirred at 10°C for 20 hours and the product was purified as outlined in the purification section. The pure product was dried in an oven at 40-50ºC to measure the yield. The solid was then dissolved in water (0.05-1.0 mg/mL) and characterised by GPC and UV-visible spectroscopy. The monomer conversion was obtained after 20 hours for all reactions.

4.2.4 Polymer characterisation

Molecular weight was determined using a Waters GPC system with Millenium software. Waters Ultrahydrogel 125 and 250 columns in series were held at 35°C in a column oven. A mobile phase consisting of 20% v/v methanol and 80% v/v aqueous solution of $NaNO_3$ (0.20 M) and disodium hydrogen phosphate buffer (0.01 M, pH 9) was used at a flow rate of 0.8 mL/min. Chromatograms were recorded using a Waters 996 PDA photodiode array detector. All molecular weight determinations were performed by relative calibration against polystyrene sulfonate standards obtained from Polymer Laboratories. Typically, injection volumes of 50µL of 1 mg/ml were employed for all samples and standards unless otherwise stated.

A reverse phase HPLC with a Waters Bondapak C18 column and a Linear UVIS 200 UV recorder (λ_{max}=208 nm) were used to determine residual MAS monomer. The chromatograms were recorded on a Shimadzu C-R5A Chromatopac integrator. A

mobile phase consisting of 40% v/v methanol and 60% v/v aqueous solution of 5 mM tetrabutylammonium dihydrogen phosphate was used at a flow rate of 1 mL/min. Sample injection volume was 10 μL. The concentration of aniline was measured before addition of oxidant (T_0) and after the polymerisation reaction was completed (T_x) based on the peak height of the HPLC chromatogram. The monomer conversion was calculated using the following equation:

$$\%\text{Monomer conversion} = (1-T_x/T_0) \times 100$$

UV-vis spectra were recorded using a Shimadzu UV-1601 UV-vis spectrophotometer.

Conductivity measurements were performed on dried films of 10μm thickness (obtained by evaporative casting of 30 μl of a PMAS solution (50 mg/ml) onto a glass slide substrate) using a JANDEL resistivity system (model RM2) using a linear four-point probe.

The pH of polymer solutions was measured using a TPS Instruments Model 900-P pH meter. The pH of the reaction solution was monitored using Labview 6.0 software. An in-house fabricated auto-titrator was used to control the pH during polymerisation.The potential of a platinum mesh versus a reference electrode (silver/silver chloride) was recorded to monitor the polymerisation reaction.

The viscosity of the polymer solution was measured using a Brookfield viscometer (RD-DV II+) using spindle DIN 85. Transmission electron microscopy using a Hitachi H7000 TEM at 75 keV was used to observe the morphology of samples.

4.3 Results and discussion

4.3.1 Effect of temperature

In a series of experiments, the temperature of the polymerisation reaction was varied from 0 to 20°C, with all other conditions remaining the same. The oxidation state of both reactants and products changes during the redox reactions that occur during polymerisation of MAS. The process of chemical oxidative polymerisation of MAS monomer was monitored by measuring the open circuit potential difference between a

platinum electrode and Ag/AgCl reference electrode in the reaction media. The open circuit potential (OCP) was recorded throughout the course of polymerisation as previously described by Wei et al. [20]. When a polymerisation solution reaches equilibrium, the OCP becomes constant.

The potential of the solution was found to decrease immediately after addition of oxidant from approximately 0.30 to 0.17 V (Figure 4.1). As nucleation was initiated the potential increased to about 0.51 V at the end of the oxidant addition period, followed by a slow increase to a maximum potential of 0.55-0.57 V. The rate of the potential rise was dependent on the polymerisation temperature, with slower rates noted at the lower temperatures. At longer time scales the potential was noted to decrease with a clear temperature dependence. The evolution of the potential difference during polymerisation of MAS is in general agreement with previously reported values for polyaniline in which a small decrease in potential is followed by a rapid increase, finally reaching a plateau, then a rapid decrease in potential indicative of the completion of reaction [21-23]. However, the polymerisation of aniline is generally completed in 1-2 hours; compared to the polymerisation of MAS which is not completed even after 5 hours.

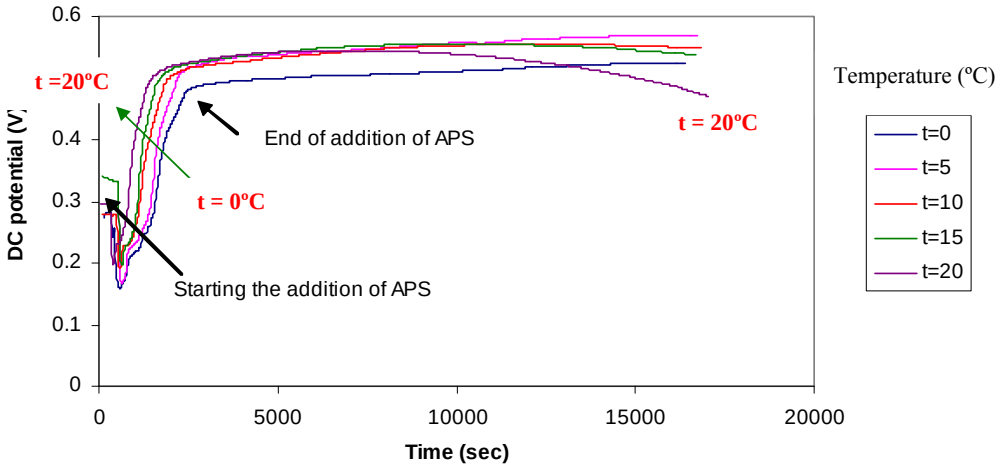

Figure 4.1. DC potential recorded for synthesis of PMAS at different temperatures.

The effect of polymerisation temperature on the products obtained is summarised in Table 4.1. Increasing the polymerisation temperature above 10°C resulted in a

significant decrease in the observed conductivity of PMAS, however no significant change was observed for temperatures in the range 0-10°C.

Table 4.1. Influence of temperature on synthesis of PMAS.

Temperature (^{0}C)	**M_w(Da) (HMWt)**	**Yield* (%)**	**M_w(Da) (LMWt)**	**Yield* (%)**	**Conductivity of HMWt PMAS (S/cm)**	**Monomer conversion (%)**
0	14,800	40.2	2,070	3.93	0.42 ± 0.04	84.0 ± 0.2
5	17,520	38.9	2,060	5.64	0.47 ± 0.03	93.0 ± 0.3
10	15,710	43.2	2,000	6.65	0.42 ± 0.05	94.0 ± 0.4
15	10,180	38.3	2,060	5.94	0.31 ± 0.04	92.0 ± 0.2
20	10,990	34.4	1,830	4.01	0.16 ± 0.02	93.0 ± 0.2

*Yield calculated after purification

The dramatic effect of temperature on the conductivity and the molecular weight of the PMAS product is shown in Figure 4.2. Polymerisation temperatures above 10°C resulted in lower MW and conductivity.

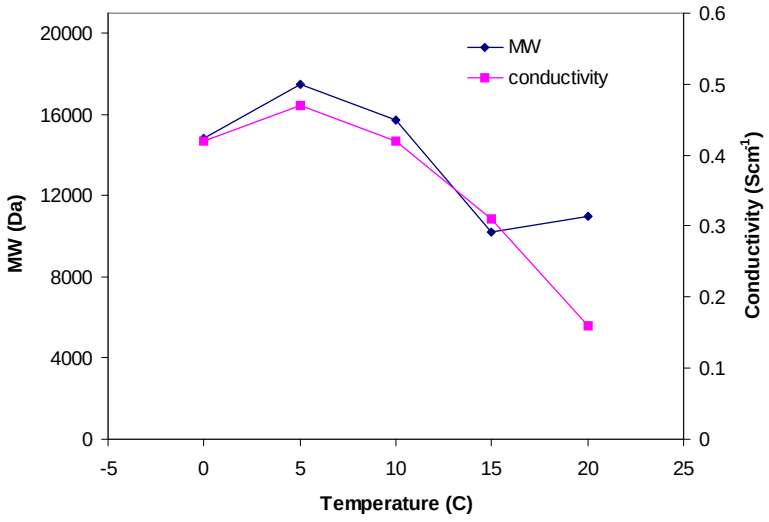

Figure 4.2. Effect of temperature on molecular weight and conductivity of PMAS. MAS 0.33 M, oxidant/monomer 1.25, reaction time 4 hours.

The influence of temperature on yield and molecular weight has been reported previously for polyaniline [24, 25]. Generally, a decrease in polymerisation temperature resulted in a higher yield and molecular weight. Adams *et al.* [26-29] found that the MW of PAn increased from 19,400 Da at 18ºC to 86,000 Da at 0ºC with further increases at sub-zero temperatures. Skejal *et al.* [30] reported that the MW of polyaniline increased as the reaction temperature was lowered. This study found that the conductivity of the resultant polymer was slightly increased as the polymerisation temperature decreased. The results observed for PMAS were in general agreement with the above findings.

A typical UV-vis spectrum of pure PMAS in the emeraldine salt form shows two peaks at 473 nm and 330 nm. The peak at 330nm may be attributed to the π-π^* transitions, and the sharp peak at 473 nm is assigned as the low wavelength polaron band [31]. Absorption of light at wavelengths higher than 700nm is the beginning of a broad band attributed to high wavelength delocalised polaron transition. The presence of the latter peak suggests the extended coil-like conformation of emeraldine base of PMAS [31]. The spectra obtained for polymer produced using polymerisation temperatures of 0 to 20ºC are presented in Figure 4.3a. Plotting the ratio of intensity at 474 nm to the intensity at 330 nm for pure PMAS synthesised at different temperatures showed a small difference (Figure 4.3b). This ratio was greatest at 10ºC, with the ratio decreasing towards both temperature extremes.

The results suggest that polymerisation of MAS at 10ºC results in a polymer with reasonably high MW, conductivity and yield. Therefore, all subsequent experiments were carried out at 10ºC.

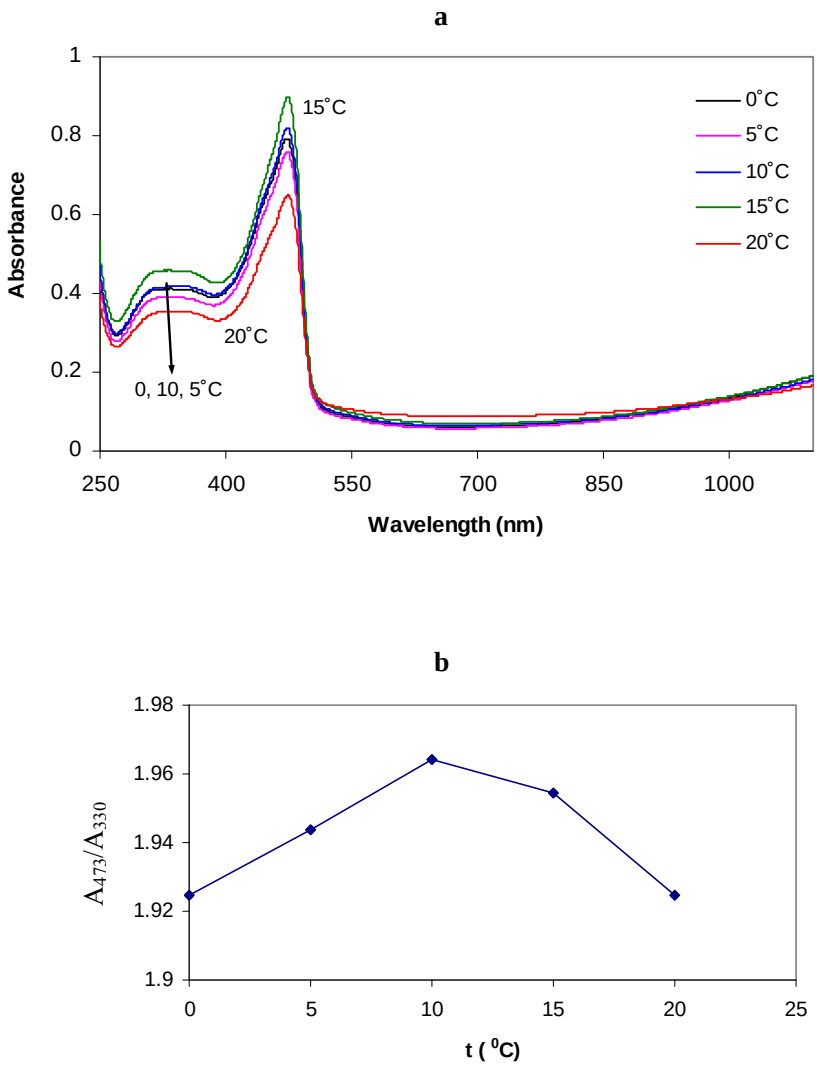

Figure 4.3. (a) UV-vis. Spectra of 0.033 mg/ml PMAS solution synthesised at different temperatures, (b) ratio of absorbance at 474 nm to 334 nm for the pure PMAS synthesised at different temperatures.

4.3.2 Effect of reaction time

Changes in potential of the solution, pH, and UV-visible spectra of the products obtained during the chemical synthesis of PAn are useful tools that have been used to determine the mechanism of polymerisation [22, 23, 32]. Here, these techniques have been used to monitor the polymerisation of MAS.

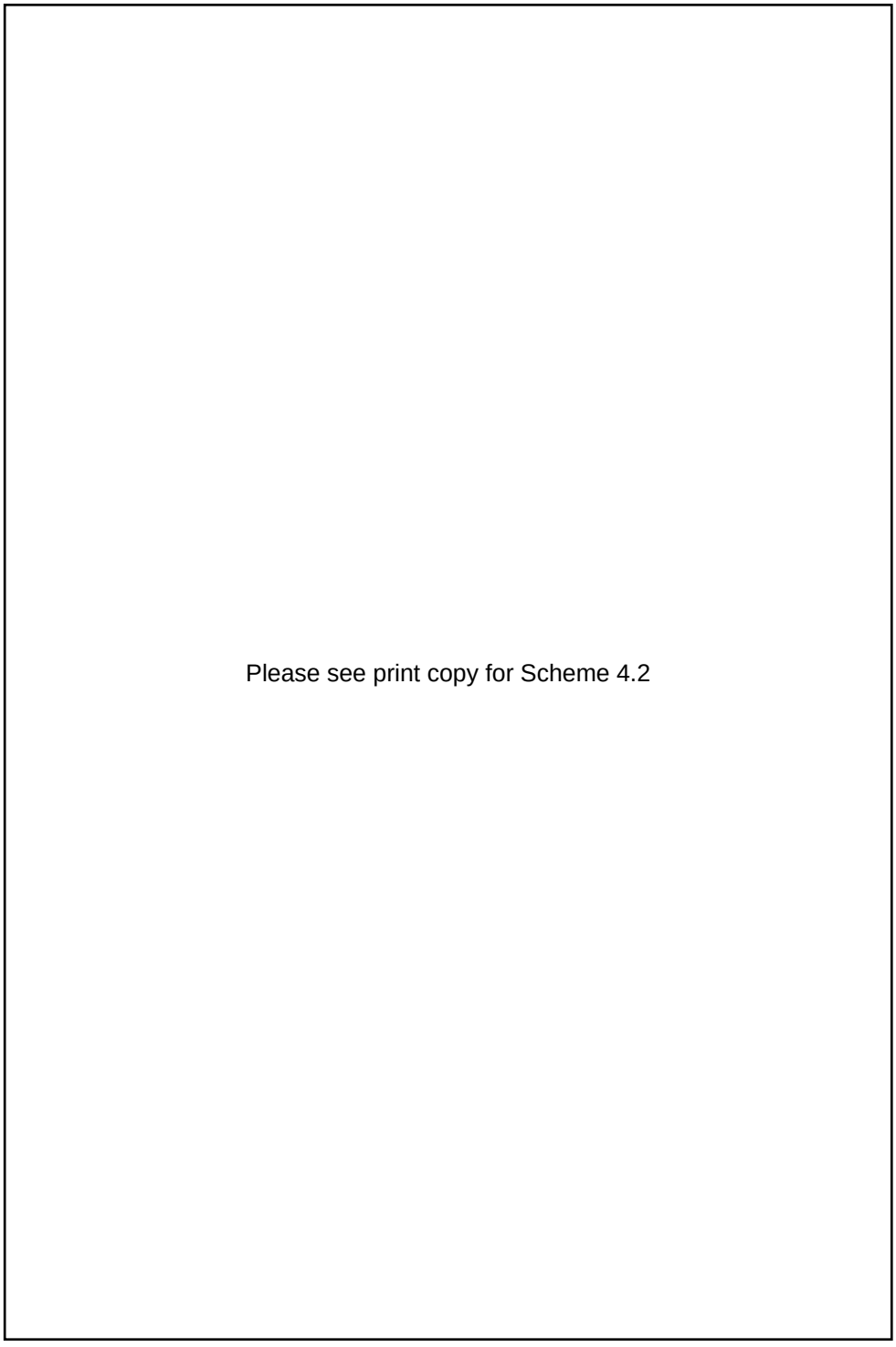

Scheme 4.2. Mechanism for chemical polymerisation of aniline, formation of polyaniline emeraldine salt [33].

The mechanism of chemical polymerisation of aniline is shown in Scheme 4.2.

The solution potential recorded during the chemical polymerisation of MAS is shown in Figure 4.4a. The open circuit potential of the solution initially decreased on addition of the oxidant from about 0.30 V to about 0.17 V (step 1) and then immediately increased indicating initial nucleation to a potential of *ca.* 0.53 V after 36 min (once all of the oxidant was added) (step 2). This process was followed by a slow increase to a maximum potential of *ca.* 0.57 V after 3 hours (step 3). The potential then dropped slowly to 0.53 V, and then steeply to about 0.46 V after 8 hours (step 4) followed by a gradual decrease to 0.41 V after 20 hours (step 5).

The pH of the polymerisation solution was monitored as a function of reaction time. Due to proton generation (see step 2 in Scheme 4.2), the pH of the reaction mixture decreases during polymerisation [32, 34]. Figure 4.4b indicates that the solution pH dropped rapidly in the first hour from 4 to 1 and then slowly to 0.6 over the next 19 hours.

The concomitant evolution of potential and pH at the early stages of polymerisation is presented in Figure 4.5. This evolution is in general agreement with that previously reported for polyaniline [22, 23, 32] and can be broken down into several steps:

Step 1. Soon after the addition of oxidant, MAS is oxidised to the radical cation of MAS. During this step the potential decreases, however the pH remains almost the same. The solution gradually develops a pink tint.

Step 2. In the next step, the potential increases and the radical cations of MAS are coupled to make dimers and oligomers. This is associated with a decrease in pH and a solution colour change to dark pink. Due to the autocatalytic polymerisation mechanism (See Chapter 1, Section 1.4.1.1), the oxidation of aniline can be accelerated by oxidised oligomers and this results in a rapid increase in potential, accompanied by a rapid decrease in pH. Reduced oilgomers can be oxidised again by the remaining APS continuing the cycle. Longer chain oligomers are produced and a dark brown colour is

observed. In the later stage of this step (potential > 0.4 V and pH < 2 the slopes of the potential and pH plots are less steep. In this stage previously made oligomers are presumably coupled and chain propagation results in PMAS (yellow green color) with molecular weight of about 6-7 kDa (Table 4.2). The monomer conversion at the end of this step was found to be 64% (Figure 4.6) corresponding to the rapid changes observed in potential and solution pH.

Step 3. In the next step the potential increases very slowly to a maximum of 0.57 V at 3 hours while the pH decreases from 1.2 to 0.7. During this step chain propagation is continued and the peak molecular weight is increased to about 9 kDa (Table 4.2). HPLC analysis revealed that 27% of the monomer was consumed in this step (Figure 4.6).

Step 4. The potential starts to drop in step 4 very slowly to 0.53 V at 5 hours and steeply to 0.46 V at 8 hours. During this step, the APS is assumed to be exhausted and the residual monomer slowly reduces the partially oxidised pernigraniline salt (PS) form of PMAS to emeraldine salt (ES) form. As the media in this stage is quite acidic, the residual MAS is in the protonated anilinium form. The oxidation of this protonated form of MAS and subsequent coupling to oligomers releases protons, which may be responsible for the small decrease in pH (decrease of 0.1 pH unit). According to the Figure 4.6, 3.2% of monomer was consumed in this step. No significant change was observed in the MW of the PMAS, however GPC 3D chromatograms of samples taken during synthesis show that the percentage of HMWt PMAS with respect to LMWt and oligomers increases up to 5 hours, providing the evidence that chain propagation is continued at the early stage of this step before the steep decrease in potential. Reduction of the PS form of PMAS to ES then becomes the dominant process which is signified by the steep decrease in potential after 5 hours of reaction.

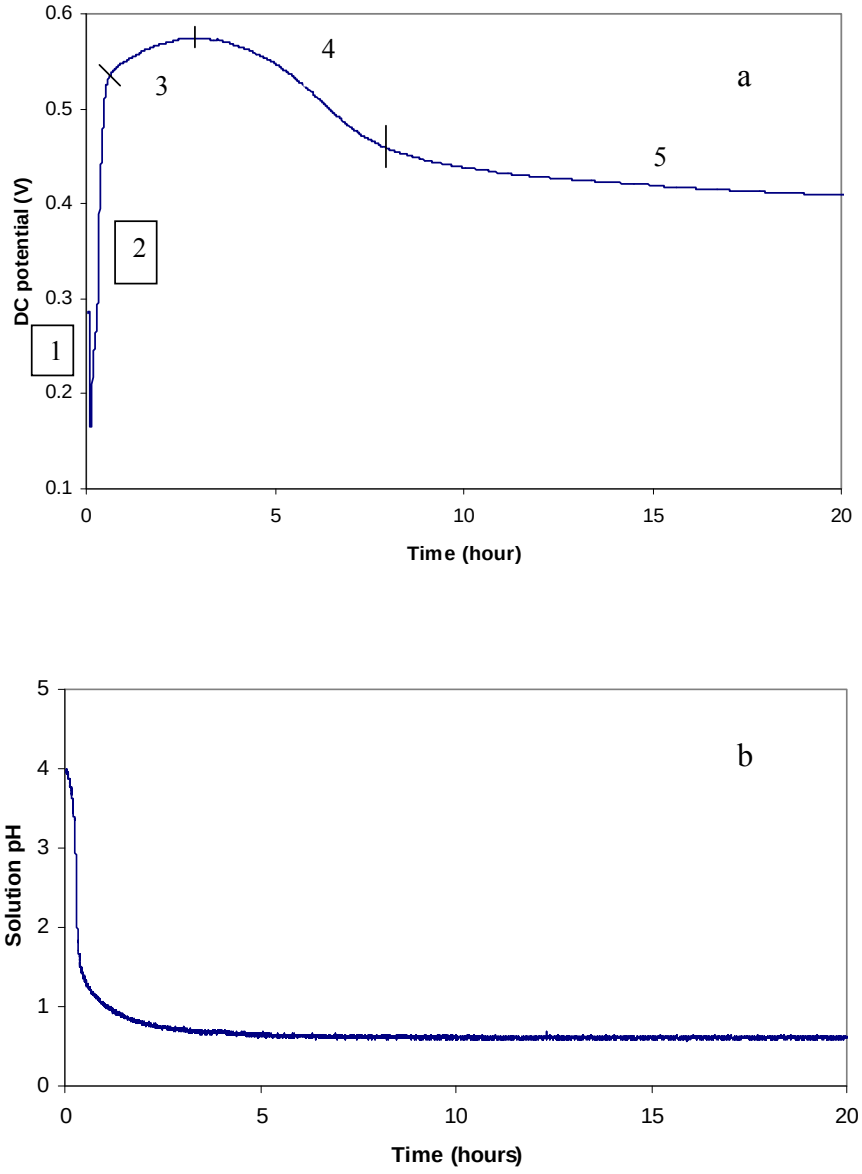

Figure 4.4. (a) DC potential (b) solution pH recorded for chemical synthesis of PMAS. Synthesis conditions: MAS 0.33 M, oxidant / monomer molar ratio 1.26, 10ºC.

Step 5. The potential change in this step is very small (0.05 V) and levels off to a final value of 0.41 V. Since the pH and monomer conversions do not change significantly from step 4, it can be said that the reaction has been completed. The small changes in

potential may be attributed to the evolution of the ES form of PMAS with time which is also observed in the UV-visible spectra (Figure 4.7). Compared to the polymerisation of aniline which is normally completed in approximately 1 h [23], the chemical polymerisation of MAS is slow and is not fully completed for approximately 10 h.

Monomer conversion was monitored using HPLC to determine residual MAS (Figure 4.6). After 3 hours, 91.0% of the monomer was consumed. The conversion reached 94.3% after 10 h.

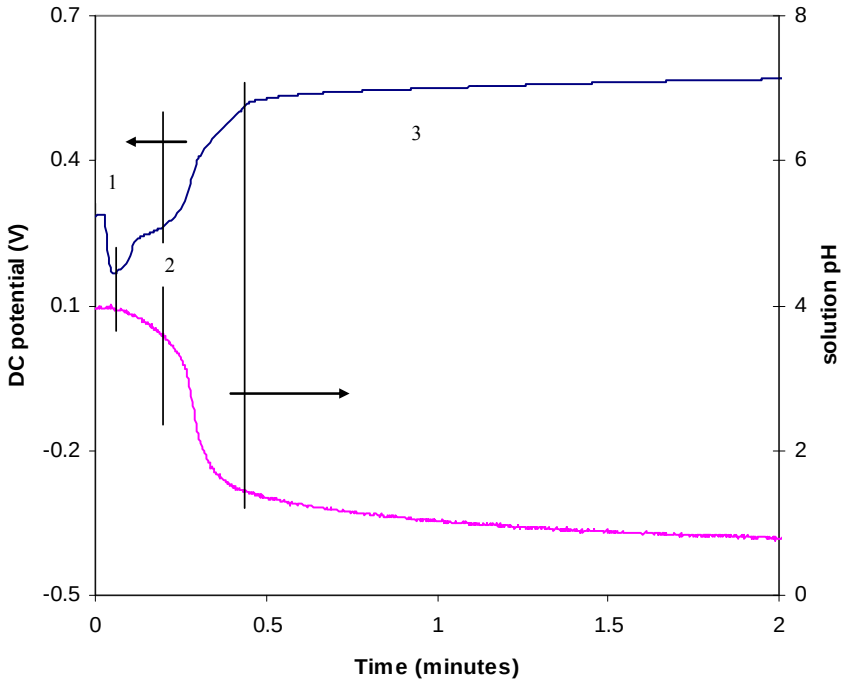

Figure 4.5. Evolution of potential and solution pH at the early stage of chemical synthesis of PMAS.

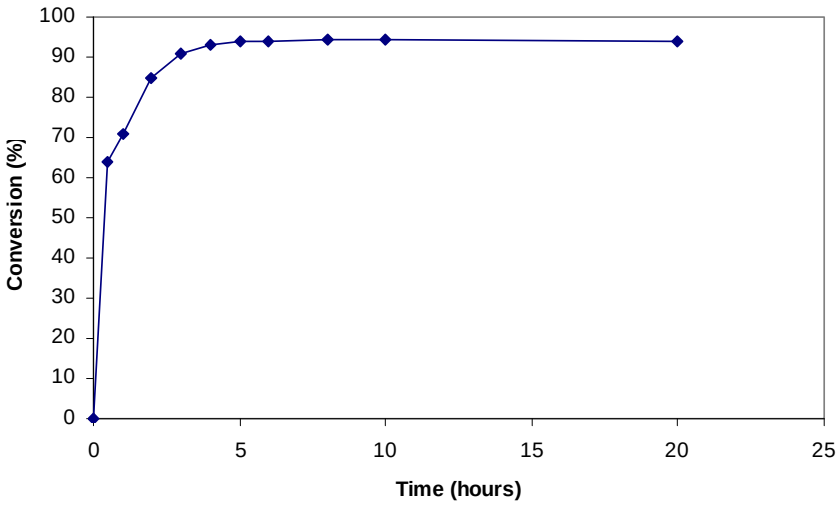

Figure 4.6. Conversion of MAS at various times during the polymerisation using 0.33 M MAS at 10ºC, starting pH 4, with a APS:MAS ratio of 1.26.

Table 4.2. Molecular weight distributions during synthesis as measured by GPC.

Time (h)	M_P (HMWT) (Da)	M_P (LMWT) (Da)
0.5	6,960	1,820
1.0	9,180	1,820
2.0	9,980	1,850
3.0	9,130	1,830
4.0	9,430	2,770 1,870
5.0	9,010	2,320 1,850
6.0	9,610	1,860
8.0	8,790	2,310 1,820
10.5	9,340	1,880
20.0	8,810	1,880

GPC analyses were performed to determine the molecular weight of the products after different reaction times (Table 4.2). Even after a 30 min reaction time the high molecular weight fraction was obvious, however the percentage of HMWT PMAS increased as the reaction continued over a period of 10 h (see later discussion for Figure 4.7).

Reaction progress was also monitored by UV-Vis spectroscopy (Figure 4.7). The absorption peak at 283 nm observed at the beginning of the reaction is attributed to the MAS monomer. At the early stages of the reaction a broad weak at 540 nm as well as an intense absorption band at 290 nm was observed. This was similar to the spectra obtained for the separated oligomers shown in chapter 3 (Figure 3.10). As the reaction proceeded the characteristic polymer bands at 473 nm and a free carrier tail in the infrared region appeared and increased with reaction time. The broad absorption band around 300-350 nm was attributed to overlapping bands due to polymer and oligomers present in the reaction mixture. The ratio of these peaks to the 473 nm peak became less at increased concentration of polymer, indicative of reaction progress. The spectra recorded during step 3 processes, discussed above (at 1-5 hours of reaction), showed the disordered peak at 473 nm and a small broad peak at 540 nm, which were characteristics of partially oxidised PMAS [33] or a mixture of PS and ES forms of PMAS. For the spectra recorded during step 4, the peak at 473 nm became sharper; suggesting that the ES form of PMAS was formed. No significant change was observed in the intensity of peaks at 330 nm and 473 nm between 8 to 10 hours of the reaction, indicating the completion of reaction. The 473 nm peak became sharper after 20 hours which may be attributed to the evolution of the ES form of PMAS with time, as explained in step 5.

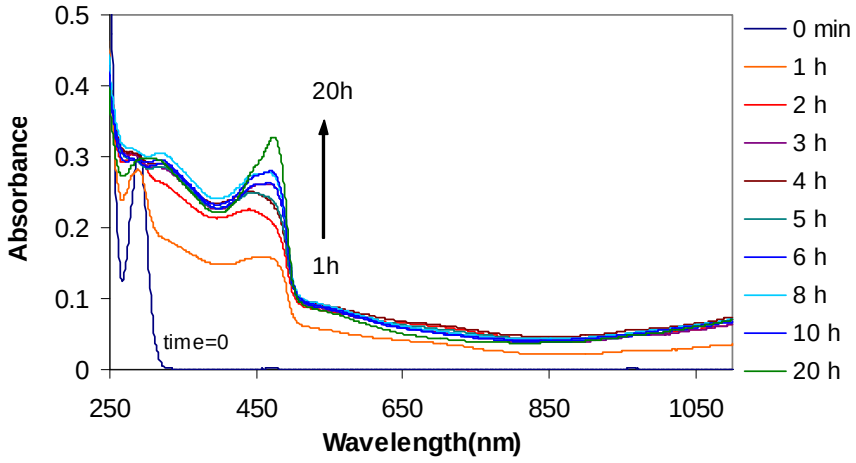

Figure 4.7. Uv-vis spectra of reaction mixture at various times during the reaction using 0.33 M MAS at 10ºC, starting pH 4, with a APS:MAS ratio of 1.26.

4.3.3 Effect of pH

4.3.3.1 Monitoring the pH

It is generally accepted that acidic conditions are required for polymerisation of aniline and result in conjugated conducting polyaniline with higher yield and conductivity [35].

To investigate the effect of pH on polymerisation of MAS, polymer properties were monitored as the pH changed. The properties of polymer product obtained with different starting pH values were also investigated. Under the conditions applied for the synthesis of PMAS, the monomer was dissolved at pH 4 (starting pH). The pH dropped rapidly to about 1.4 in less than 30 min (Figure 4.8a). No HMWt PMAS was found for the samples taken at pH values of 3.5 and 3 (Figure 4.8b). Due to the rapid pH changes, it was difficult to analyse the samples at pH values in the range 3 to 2.3. At pH values of 2.3 or lower, the characteristic band of HMWt PMAS at 473 nm was observed, increasing with decreasing pH. GPC chromatograms of the products isolated from solutions of different pH (Figure 4.9) illustrated that oligomers with Mp of 1635 at pH 3, short PMAS chains (Mp 5,515 Da, Mw 6,128 Da, PDI 1.33) at pH 2 and HMWt PMAS (Mp 14,241 Da, Mw 44,698 Da, PDI 4.29) at pH 1.2 were isolated.

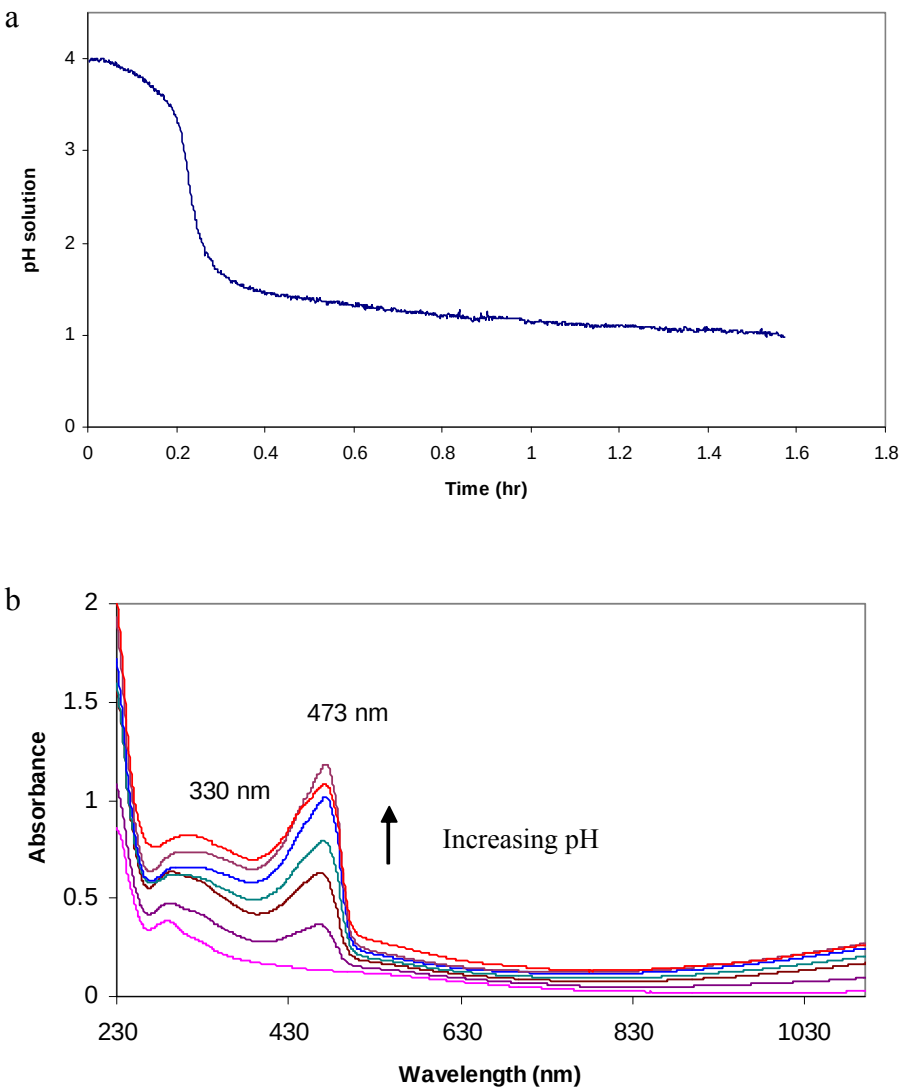

Figure 4.8. (a) pH change during polymerisation of MAS and (b) UV-vis spectra of the product at different pH solution (3, 2.3, 2, 1.7, 1.5, 1.2 and 1.07 respectively) during polymerisation of MAS after diafiltration using Viva spin 10 kDa MWCO for 10 min at 4100 rpm speed.

The LMWt PMAS and oligomers show a strong absorbance at ~300-330 nm. As a measure of the percentage of HMWt PMAS to LMWt and oligomers (see Chapter 3,

Section 3.3.3.2), the ratio of absorption at 473 nm to 330 nm (A_{473} / A_{330}) was plotted against pH (Figure 4.10). This ratio increased at lower solution pH, displaying a maximum at pH 1.2. A good correlation was found between the A_{473} / A_{330} ratio and molecular weight of the samples at different pH during polymerisation. The molecular weight also increased at lower pH, showing a maximum at pH 1.2.

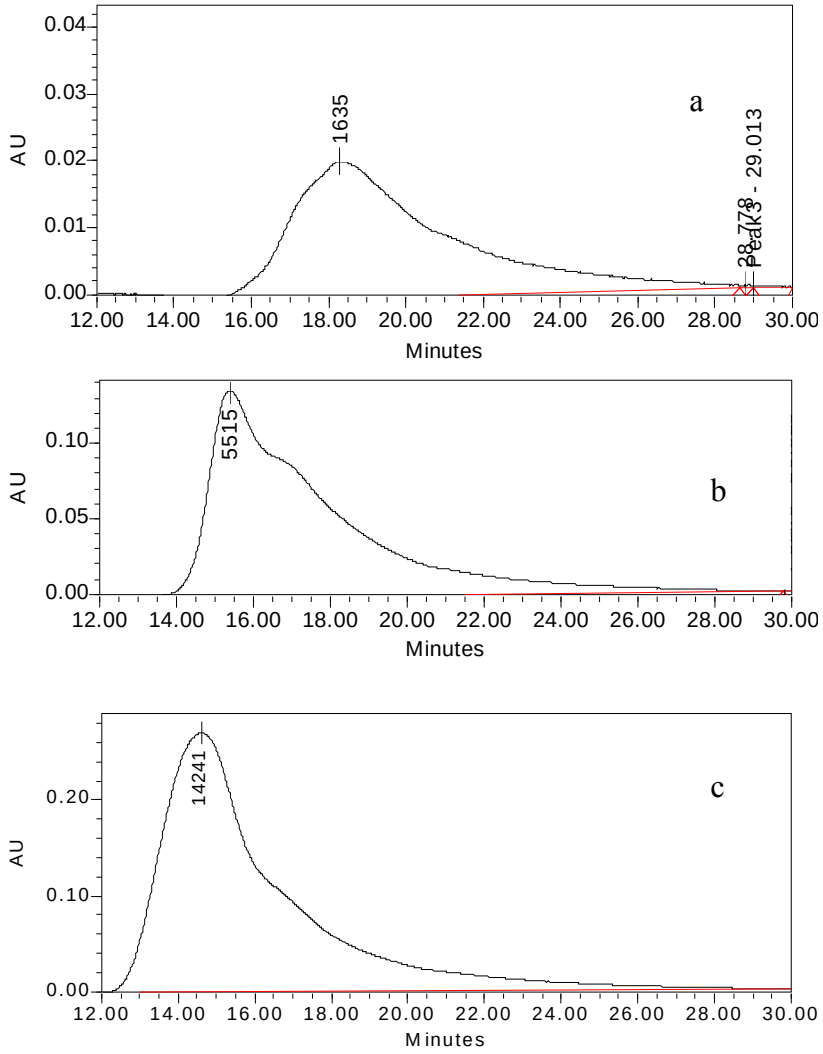

Figure 4.9. GPC chromotograms obtained at pH (a) 3, (b) 2.3 and (c) 1.2 during polymerisation of MAS.

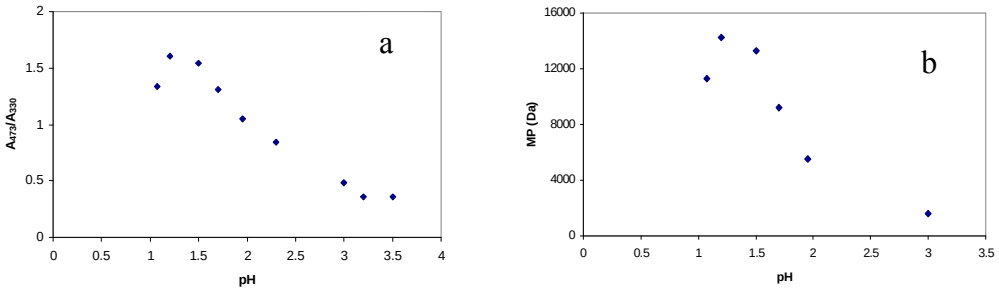

Figure 4.10. (a) The ratio of absorbance at 473 to 330 nm and (b) the molecular weight for products obtained at different pH during polymerisation of MAS.

Changes in MW and pH with time are shown in Figure 4.11. According to the results, after oxidation of MAS to radical cation, in step 1, the oligomers produced in step 2 were directly responsible for the decrease in pH to less than 3 in about 13 min. A rapid increase in molecular weight from ~1600 Da to ~13000 Da was observed during the next 8 min while the pH decreased rapidly from 3 to 1.5. As the chain propagation was very rapid and associated with the decrease in pH, it may be concluded that the automatic decrease in pH, as a result of radical coupling, accelerates the chain propagation to produce HMWt PMAS.

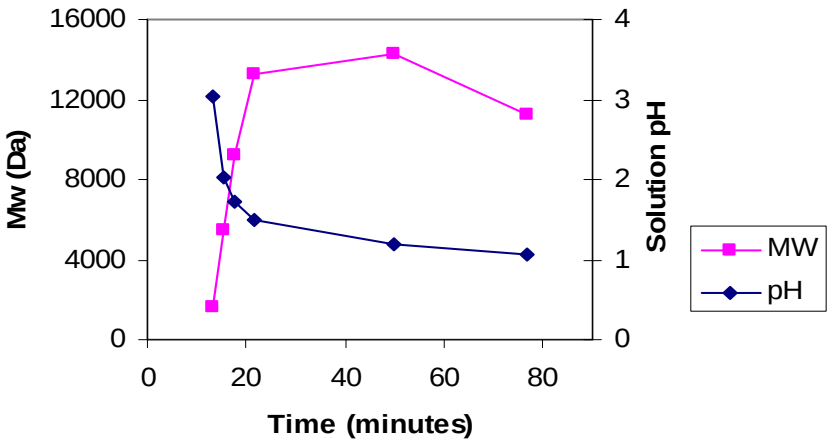

Figure 4.11. Molecular weight and pH changes during polymerisation of MAS.

4.3.3.2 Controlling the pH

An important issue in the study of pH effects in the polymerisation of MAS was the limitation in solubility of monomer. MAS solubility was pH dependent increasing with pH.

Table 4.3. Solubility of MAS at room temperature as a function of pH.

pH	Solubility of MAS (M)
1.0	0.14
2.0	0.14
2.3	0.15
3.0	0.18
4.0	0.50

The solubility of MAS was measured using HPLC. 5 mmole of MAS was added to 10 mL water with continuous stirring and the pH of the solution was adjusted to different values of 1.0, 2.0, 2.3, 3.0 and 4.0 using concentrated NH_4OH. The MAS was completely dissolved at pH 4.0 while it was partially dissolved below pH 4.0. The clear solution on the top was filtered using a 0.45 μm syringe filter and analysed by HPLC. Table 4.3 illustrates the effect of pH on solubility of MAS. A solution of 0.5 M MAS can be prepared at pH 4. Any further decrease in pH results in precipitation of MAS. With this in mind, some experiments were designed to study the effect of pH on the polymerisation of MAS.

Reducing initial pH

To further investigate the effect of pH on the polymerisation process, the initial pH of the reaction media was decreased. The monomer was initially dissolved at pH 4. Oxidant was added (1 mL/min) to monomer solution while pH was reduced manually to 3.3 by dropwise addition of 32% (w/v) HCl. The change in pH during polymerisation (Figure 4.12) was similar to that observed previously in Figure 4.6a. Upon addition of acid to pH 3, precipitation of MAS was observed; however it dissolved again as

aqueous MAS was consumed during the reaction. The UV-visible spectrum of the product showed the 473 nm peak characteristic of HMWt PMAS. However the A_{473} / A_{330} was very low indicating a low yield of high molecular weight product. A fraction with Mp less than 2000 Da was found in the GPC chromatogram. This low molecular obtained was presumably due to a decrease in the local concentration of MAS as a result of MAS precipitation (see section 4.3.4).

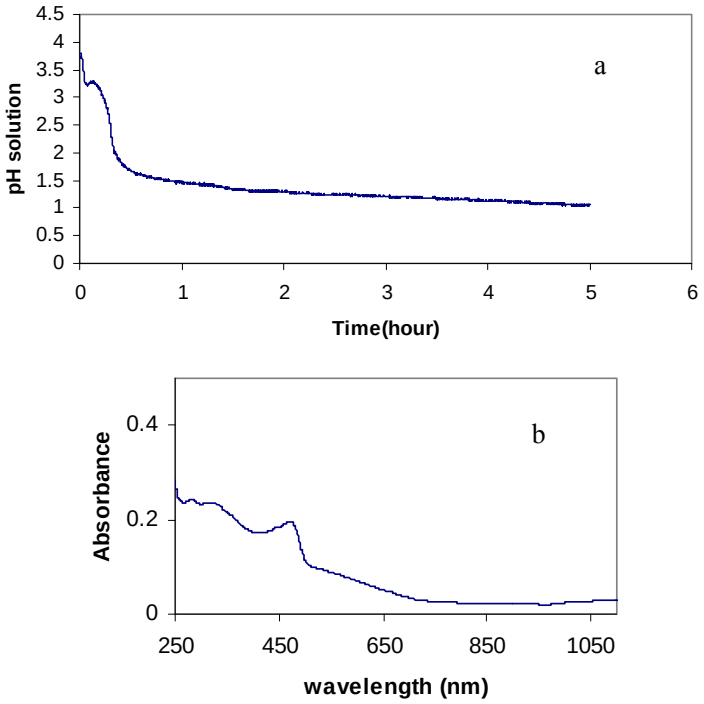

Figure 4.12. a) pH changes observed during polymerisation of 0.33 M MAS using a solution at initial pH of 3.3. (b) UV-visible spectrum of the polymer obtained after diafiltration using vivaspin 10 kDa MWCO membrane for 20 min. Adding oxidant starts at pH 3.8, decreasing to 3.3 by addition of 32% (w/v) HCl.

Controlling the pH at 4

As mentioned earlier, during the polymerisation of MAS the solution pH drops as a result of proton release in order to probe the polymerisation at constant pH, the polymerisation was started at pH 4, and kept constant (Figure 4.13) by addition of NH_4OH solution via an in-house fabricated auto-titrator. The reaction mixture had a dark brown colour and no HMWt PMAS (yellow-green solution) was produced after 4

hours. The product had a molecular weight of 1500-2700 Da (dependant on polymerisation temperature and the concentration of ammonia solution added to control the pH). The spectra of the products showed a weak band around 473 nm (Figure 4.14). This spectrum can be attributed to short chains of PMAS (probably para-coupled), terminated due to the low acidity of the media.

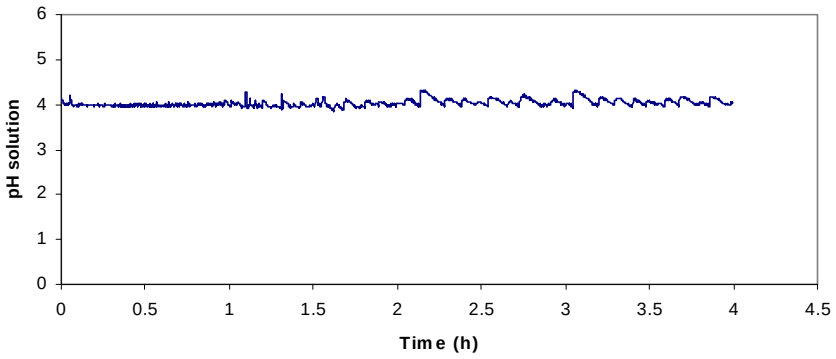

Figure 4.13. Controlling pH during polymerisation of PMAS by adding 9 mL 1:1 ammonia/ water solution.

No HMWt PMAS was found even after the pH was reduced to less than 1 overnight (Figure 4.15), indicating that the chain propagation was terminated. These results suggest that the chain propagation step only occurs in the strong acidic media created during polymerisation.

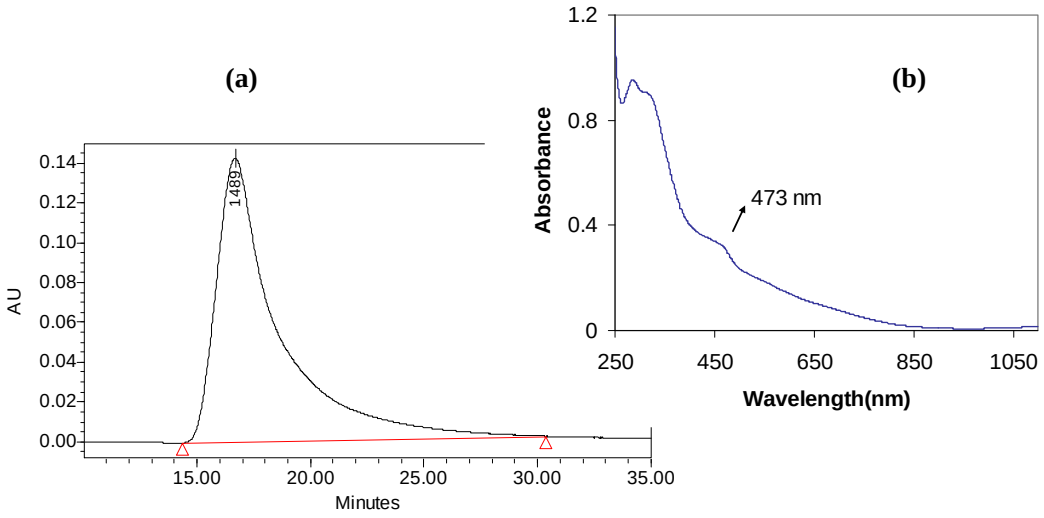

Figure 4.14. (a) GPC chromatograms and (b) UV-Vis spectra of the product obtained after cross flow filtration. Polymerisation of 0.33 M MAS at pH 4 was carried out in the temperature range 5-10ºC.

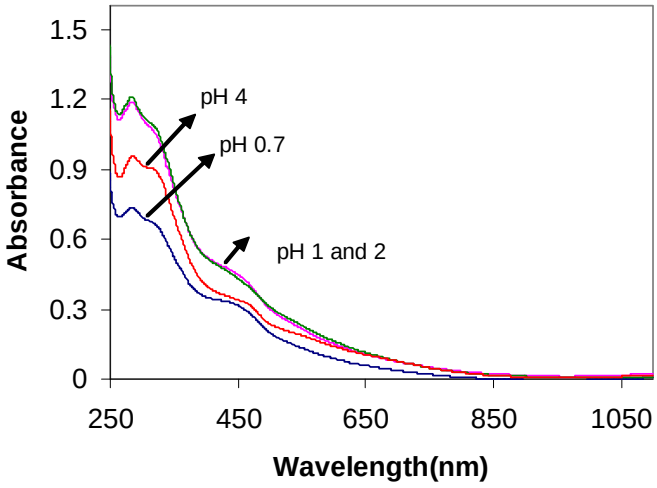

Figure 4.15. UV-Vis spectra of reaction media from polymerisation at pH 4 after the pH was reduced to different values overnight (after diafiltration using viva spin 10K).

Controlling the pH at 3

To avoid initial precipitation of the monomer due to poor solubility below pH 4, the polymerisation was started initially at pH 4. The pH dropped to 3 in the first 15 min of the reaction. This was then held constant by adding NH_4OH solution via the auto-titrator system. The viscosity of the reaction media increased after 30 min developing a yellow green colour indicative of PMAS formation. As the reaction media was heterogeneous, addition of ammonia caused local increases in pH in some areas while in some parts the pH decreased due to the polymerisation process. Thus, attempts to control pH were not successful (Figure 4.16). A mixture of HMWt PMAS (Mp 8389 Da) and LMWt fraction (Mp 2165 Da) was obtained.

Typical changes in the viscosity of the solution during polymerisation of 0.33 M MAS are shown in Figure 4.17. The viscosity increased dramatically within the first 30 min from 2.5 to 52 mPa.S, where the pH change is very rapid, although it decreased at the later stages of the reaction. The viscosity change is presumably driven be a time dependent molecular reorganisation process. Thus, controlling the pH by addition of ammonia solution proved difficult due to the heterogeneous nature of the viscous solution. In subsequent studies, pH control was investigated at lower monomer concentration to avoid the potential interference of the high viscosity of the reaction mixture.

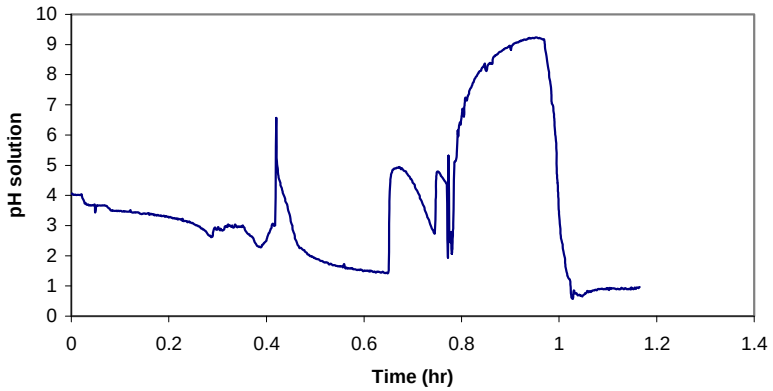

Figure 4.16. Controlling the pH during polymerisation of 0.33 M MAS by adding 3:1 ammonia / water solution.

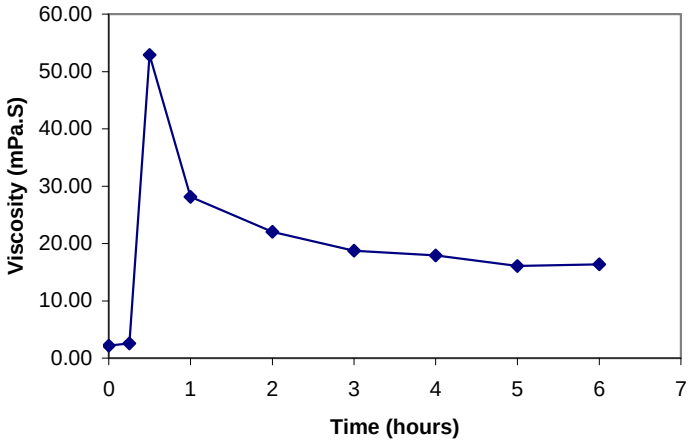

Figure 4.17. Viscosity of the reaction media at different times during the reaction. Shear rate 250 (sec^{-1}). Reaction carried out using 0.33 M MAS at 10ºC. Starting pH 4, APS:MAS 1.26.

4.3.3.3 Controlling the pH at lower monomer concentration

In order to reduce the viscosity of the reaction mixture polymerisation was carried out using a lower concentration of MAS (0.07 M and 0.13 M). This allowed control of the initial pH as well as the acidity of the media throughout the reaction. Several experiments using different conditions were carried out and are summarised in Table 4.4.

When the monomer concentration was 0.13 M with an initial pH of 3.5, a dark brown solution was obtained and the pH dropped to about 1.2 after 5 hours. The product had a molecular weight of ~1000 Da and the UV-vis spectra showed a peak at 370 nm with a broad shoulder around 540 nm (Figure 4.18). No HMWt PMAS was obtained at this monomer concentration. Controlling the pH at 3 resulted in an increase (23%) in monomer conversion into oligomers compared to Exp 1 in Table 4.4 with no pH control. The results indicate that oxidation of monomer and radical coupling is facilitated at less acidic pH (when the pH held constant at 3), however chain propagation can not proceed under these conditions.

Table 4.4. Effect of pH on polymerisation of MAS.

Exp	[MAS]	[MAS]:[APS]	Starting pH	pH controlled at	DC potential at 30 min	PH at 30 min	M_p (Da)	Monomer conversion (%)
1	0.13 M	1:1.26	3.5	_	0.42	2.8	1000	54.0 ± 0.3
2	0.13 M	1: 1.26	3	3.0	0.41	3.0	1028	77.0 ± 0.2
3	0.07 M	1: 1.26	1.5	1.5	0.34	1.5	-	7.0 ± 0.3
4	0.07 M	1 : 1.26	2.5	_	0.37	2.3	~1000	22.0 ± 0.2
5	0.07 M	1 : 2.52	2.5	_	0.41	2.1	~1000	35.0 ± 0.3
6	0.07 M	1 : 5.04	2.5	_	0.44	1.8	~1000	63.0 ± 0.2
7	0.07 M	1 : 10.08	2.5	_	0.48	1.7	~1000	80.0 ± 0.4
8	0.07 M	1 : 1.26	4.0	_	0.35	2.3	~1000	25.0 ± 0.3
9	0.07 M	1 : 3.78	4.0	_	0.43	1.8	~1000	58.0 ± 0.2
10	0.07 M	1 : 10.08	4.0	_	0.48	1.6	~1000	86.0 ± 0.3
11	**0.33 M**	**1 : 1.26**	**4.0**	**_**	**0.51**	**1.4**	**8500**	**93.0 ± 0.4**

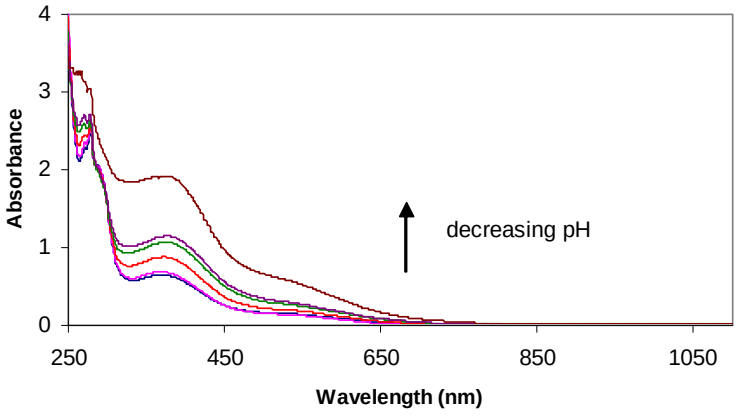

Figure 4.18. Uv-vis spectra of the product at different solution pH (2.8, 2.5, 2, 1.7, 1.65 and 1.25 respectively) during polymerisation of 0.13 M MAS before diafiltration.

Polymerisation of MAS at lower pH was carried out using 0.07 M MAS. The pH of this solution was 2.5. The product was brown in color having similar spectra to the product obtained from polymerisation of 0.13 M MAS. Zhou *et al.* [18] have shown that electrochemical polymerisation of MAS is pH dependent and the oxidation potential of MAS increases with a reduction in the initial pH. The solution potential recorded after 30 min of reaction was lower than for polymerisation of MAS (Experiment 11, 0.33 M MAS, no pH control). This may be due to insufficient concentration of oxidant or monomer. Polymerisation at higher concentration of APS caused an increase in potential and monomer conversion (Table 4.4), but no polymer was obtained. Monitoring of pH during reaction of 0.07 M MAS using different ratio of oxidant/monomer showed that the pH dropped faster and to a greater degree at higher oxidant concentrations (Figure 4.19). By maintaining the pH at 1.5 at 0.07 M MAS, the monomer conversion was only 7%. In all cases, the products were short oligomeric chains having UV-visible spectra as presented in Figures 4.18 and 4.19. The UV-vis spectra obtained here are very similar to polyazane structures that were recently reported by MacDiarmid *et al.* [36]. They found that when the conventional polymerisation solution was diluted (at a pH of 3-4) at the early stages, or when the pH of polymerisation is held constant by a buffer solution, a brown product is obtained that has different morphology (hollow microspheres) and different optical and magnetic properties from those of polyaniline. This is believed to be a member of the class of polyazanes, polymeric or oligomeric species containing a N-N backbone with three covalent single bonds for each nitrogen atom.

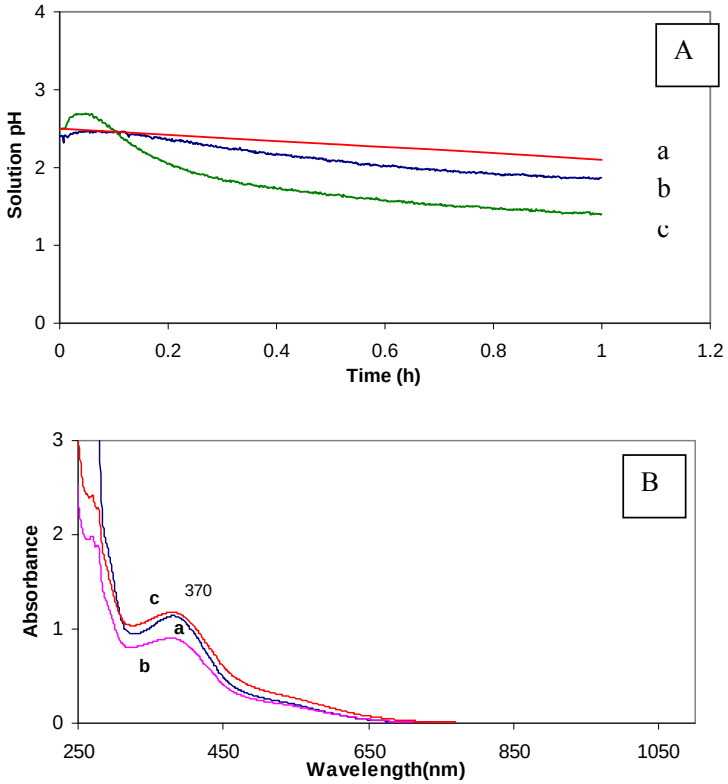

Figure 4.19. Evolution of pH (A) and UV-visible spectra (B) of the products obtained for experiments 4 (a), 5 (b) and 7 (c). Starting pH 2.5, 0.07 M MAS, different ratios of MAS:APS employed.

The first step in the polymerisation of aniline is the formation of a radical cation, which occurs in both acidic and neutral media [37-39]. It has been reported that the behavior for the oxidation products of aniline is different in acidic and neutral media [35]. The head-to-tail configuration has been attributed to the products prepared in acidic medium, while head-to-head coupling has been observed for the products prepared under neutral conditions. The oxidation potential of aniline decreases with increasing pH (50-60 mV/pH unit) [38, 39]. Thus, initiation of oxidative polymerisation of aniline is more favorable in neutral or less acidic media than strongly acidic media. This is consistent with the increase observed in monomer conversion for the polymerisation at pH 3 and 4. However, chain propagation to a conducting high molecular weight PMAS can not proceed when polymerisation is carried out using low monomer concentration and high

pH. As suggested by previous studies, a sufficiently low pH is required to protonate aniline to the anilinium cation and is critical for C-N coupling to occur during the oxidative polymerisation of aniline [25, 36].

4.3.4 Effect of varying the monomer concentration

To investigate the influence of monomer concentration on polymer properties, the concentration of MAS was varied using a constant monomer/oxidant mole ratio. By increasing monomer concentration the viscosity of the reaction media was increased so that a very viscous dark green solution was obtained using 0.47 M MAS, indicative of a high yield of HMWt PMAS.

The UV-visible spectra of the products after dilution in water (pH ~4) and in alkaline media (pH~12) are presented in Figure 4.20. HMWt PMAS has a characteristic band at 473 nm in water (pH <5) attributed to extended coil conformation and a band at 750 nm in alkaline media which is attributed to compact coil conformation [31]. When the concentration of MAS was 0.13 M, no HMWt PMAS was produced. By increasing the monomer concentration the characteristic bands of PMAS became more apparent (Figure 4.20).

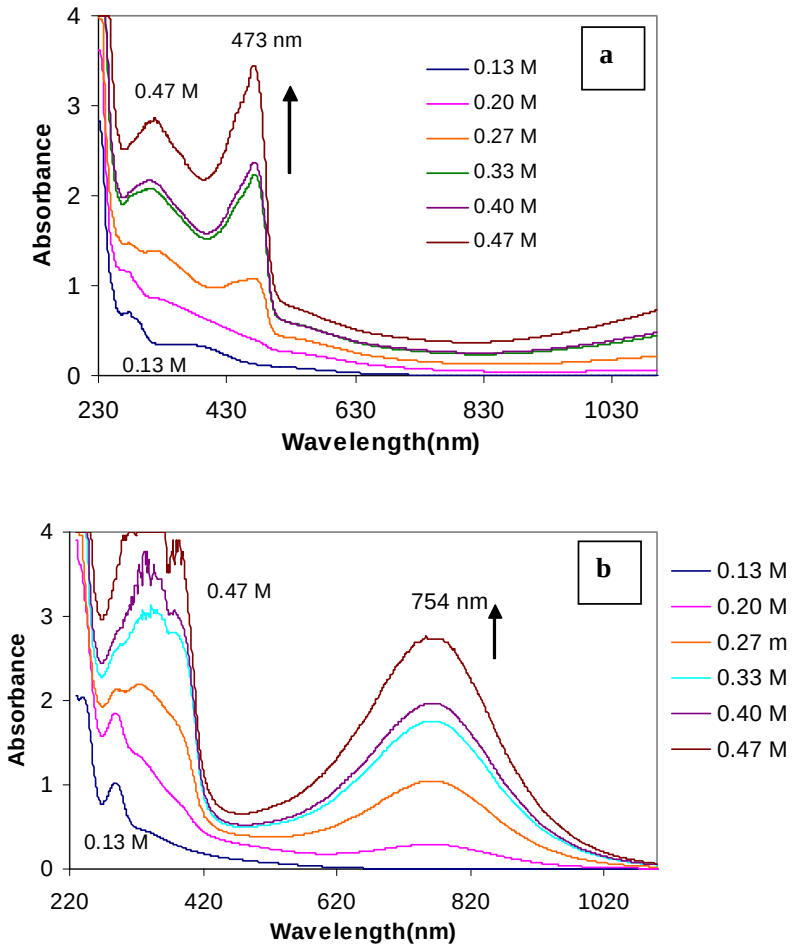

Figure 4.20. Uv-vis spectra of the reaction media after 20 hours reaction for various concentrations of MAS (a) at pH ~ 4 (by diluting 30 µl of reaction mixture in 5 mL water) and (b) at pH 12 (by diluting 30 µl of reaction mixture in 5 mL 0.1 M NaOH after standing for 1 hour to complete the conformation change).

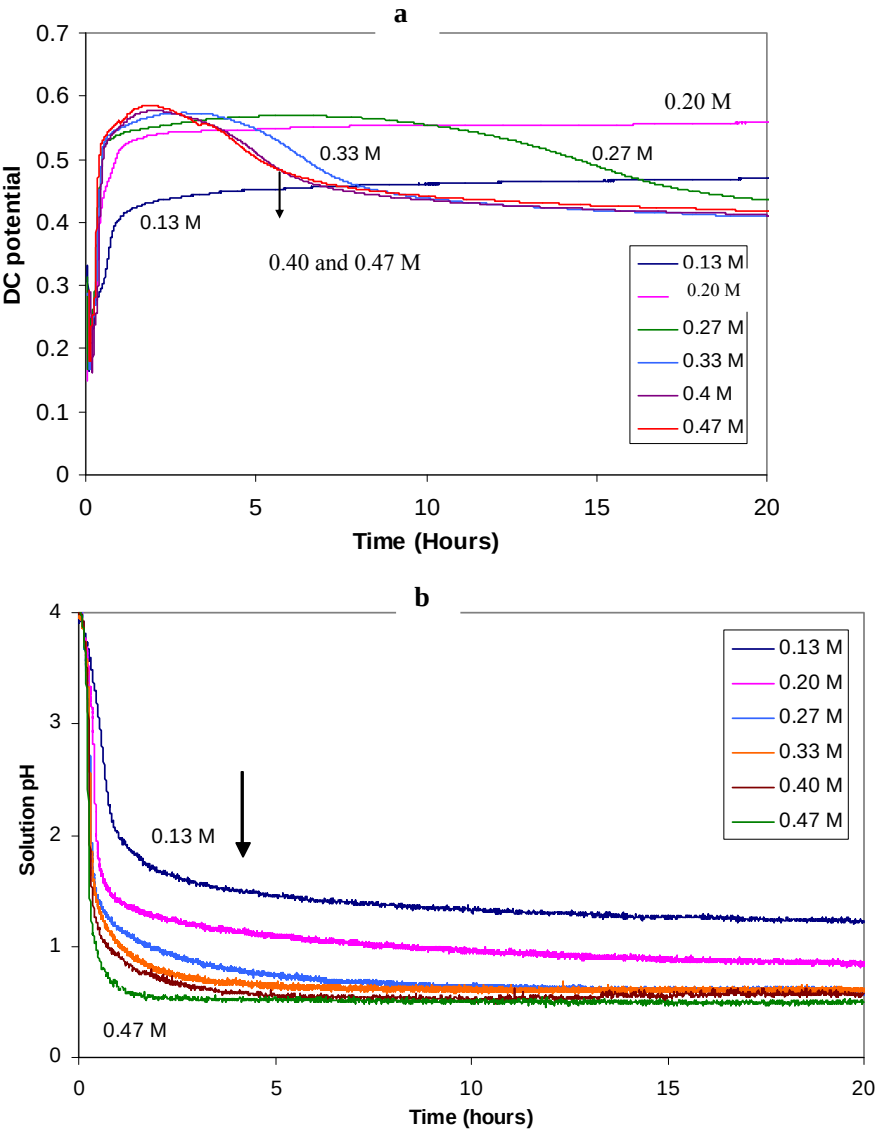

Figure 4.21. Evolution of (a) potential and (b) pH during polymerisation of MAS at different concentrations.

The evolution of potential and pH during the polymerisation of MAS using different monomer concentrations are presented in Figure 4.21. The maximum potential and the pH drop with increasing monomer concentration and consequently the reaction rate increased, accompanied by a decrease in time taken to complete the reaction. The time

to reach the maximum potential and minimum pH was greatly affected by monomer concentration. To clarify the effect of monomer concentration on pH and potential, the values of potential and pH drop after one hour of reaction (after the rapid change) are shown in Figure 4.22. For the polymerisation of 0.13 M MAS, the potential at 1 h was 0.41 V at c.a. pH 2. Under these conditions oligomers (Mp ~2,000 Da) were produced. The potential and pH value for 0.2 M MAS were 0.51 V and 1.4, respectively. Use of higher monomer concentrations resulted in increasing the potential and pH drop and subsequently increased the yield of HMWt PMAS. The results provide more evidence that propagation of oligomers and growth of longer chains occurs at potential values grater than 0.40 V and pH values less than 2.

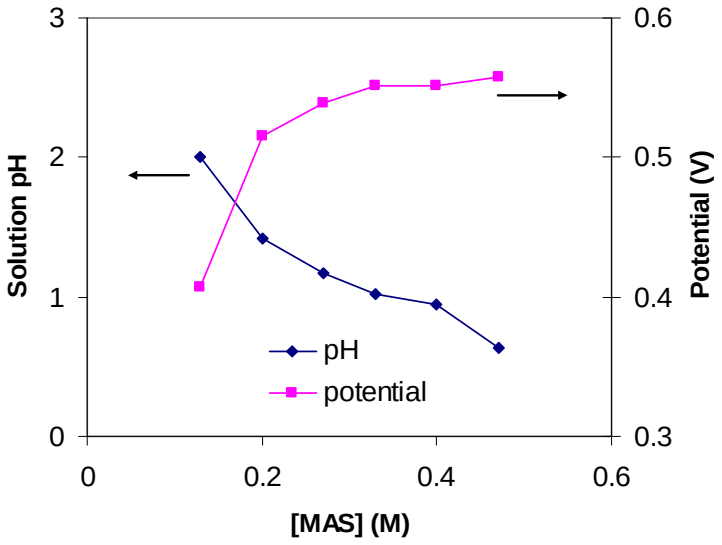

Figure 4.22. Solution pH and potential after 1 hour polymerisation of MAS with various concentrations of monomer.

Table 4.5. Influence of monomer concentration on properties of the polymer obtained. Oxidant/monomer ratio 1.26, temperature 10ºC and addition rate of oxidant 1 mL/min. Monomer conversion was measured after 20 h reaction time. The yield of pure polymer was calculated after drying in oven 45ºC overnight.

[MAS]	DC potential at 30 min	PH at 30 min	% Yield	% Monomer conversion	Mp (Da)	Mw (Da)	conductivity (S/cm)
0.13 M	0.301	3.10	0.0	11.0 ± 0.1	1,990	-	-
0.20 M	0.435	1.80	12.8	77.0 ± 0.1	11,280	2,020	0.030 ± 0.001
0.27 M	0.512	1.40	27.8	86.2 ± 0.2	11,880	21,360	0.11 ± 0.01
0.33 M	0.515	1.34	48.0	93.1 ± 0.2	9,330	12,310	0.44 ± 0.01
0.40 M	0.524	1.16	50.0	95.5 ± 0.3	8,960	11,070	0.47 ± 0.02
0.47 M	0.528	0.84	56.2	95.2 ± 0.3	8,930	10,850	0.97 ± 0.05

The yield and conductivity of HMWt PMAS were significantly increased with increased monomer concentration (Figure 4.23), without a concomitant increase in the molecular weight (Table 4.5).

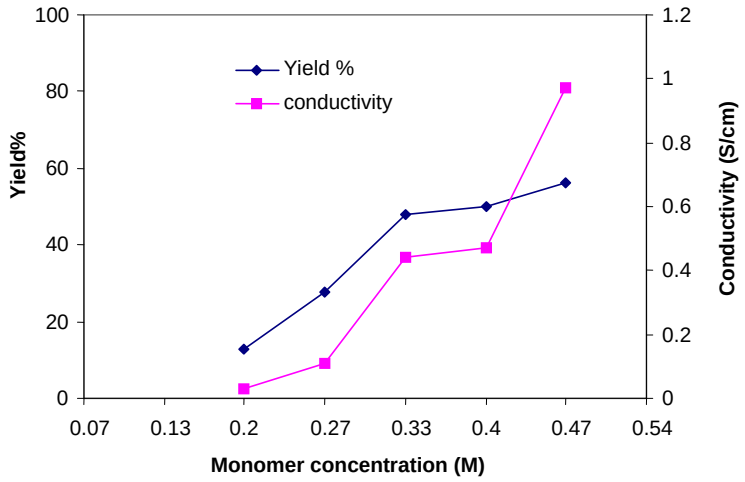

Figure 4.23. Effect of monomer concentration on yield and conductivity of PMAS.

The optimum conductivity and yield for HMWt PMAS was obtained using the highest concentration of 0.47 M MAS. The PMAS product produced at 0.47 M MAS was highly viscous, making in-situ monitoring of the potential and the pH during polymerisation impossible. In order to monitor the potential and pH in the study of the effect of other variables, the monomer concentration of 0.33 M was again used in the next experiments.

4.3.5 Effect of varying the oxidant / monomer mole ratio

The potential and solution pH monitored during polymerisation of MAS using different oxidant/monomer ratios (Figure 4.24). By increasing the ratio, the rate of oxidation of aniline and chain propagation (step 1 and 2) increased as observed in the steep positive slope of the potential change and the negative slope of the pH change.

The yield and monomer conversion as well as the molecular weight characteristics and conductivity of the resultant polymer were determined (Table 4.6). The maximum potential increased gradually as the ratio of oxidant/monomer increased to 1.26 and then dramatically at a ratio of 2, indicative of potentials likely to lead to polymer degradation. The degree of monomer conversion was directly proportional to the oxidant/monomer ratio. The yield of HMWT PMAS also increased up to the ratio of 1.26. At a ratio of 2, the final yield of HMWt PMAS was very low.

Table 4.6. Influence of oxidant/monomer mole ratio on properties of the polymer obtained. Monomer concentration 0.33 M, temperature 10ºC and addition rate of oxidant 1 mL/min. Monomer conversion was measured after 20 h reaction time. The yield of the pure polymer was calculated after drying in oven 45ºC overnight.

[APS]:[MAS]	V_{max} (V)	% Yield	MP (Da)	Mw (Da)	Conductivity (S/cm)	% Monomer conversion
0.63	0.523	17.4	8,420	11,190	0.24 ± 0.01	64.0 ± 0.2
1.00	0.551	36.7	9,230	12,320	0.72 ± 0.03	83.0 ± 0.2
1.26	0.573	48.0	8,570	10,330	0.10 ± 0.01	93.1 ± 0.3
2.00	0.680	15.0	7,560	8,590	0.02 ± 0.01	96.3 ± 0.4

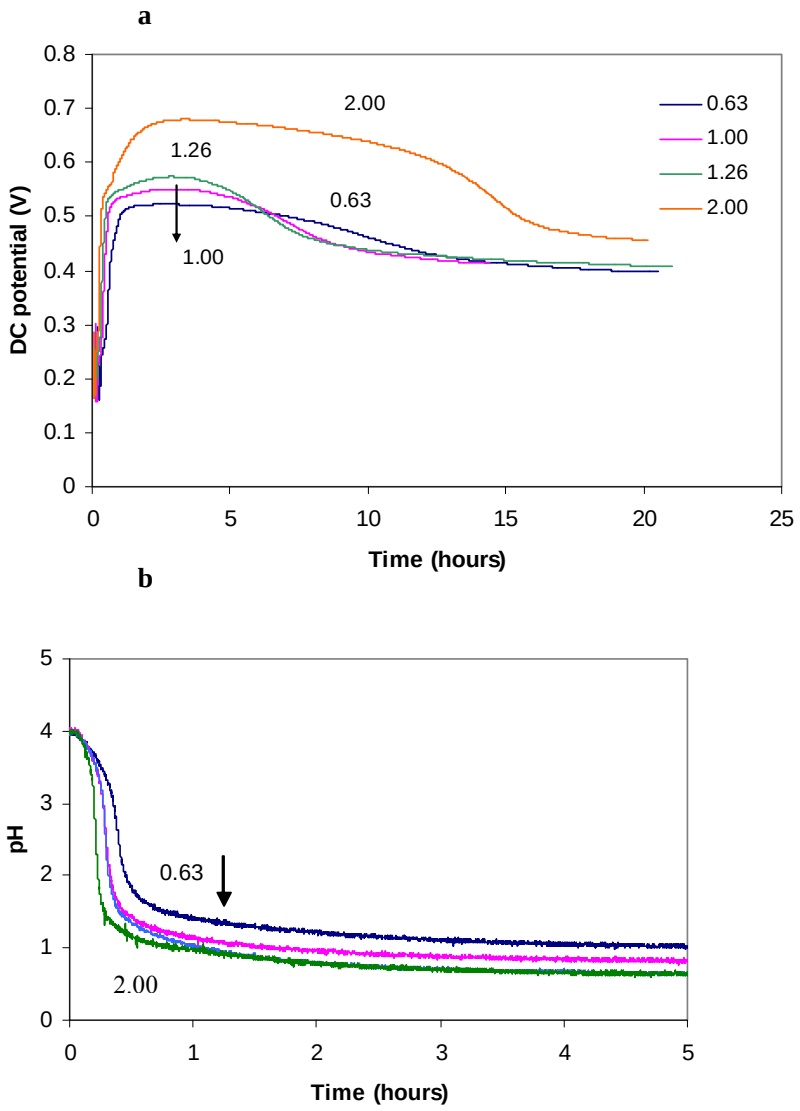

Figure 4.24. Evolution of (a) potential and (b) pH during polymerisation of 0.5 M MAS using varoius oxidant/monomer ratio (0.63, 1.00, 1.25 and 2.00).

The GPC chromatograms recorded during the synthesis of PMAS at an oxidant/monomer ratio of 2 revealed that the molecular weight and the percentage of the HMWt PMAS decreased with time presumably due to degradation processes (Figure 4.25). This corresponded with the low conductivity of the final product.

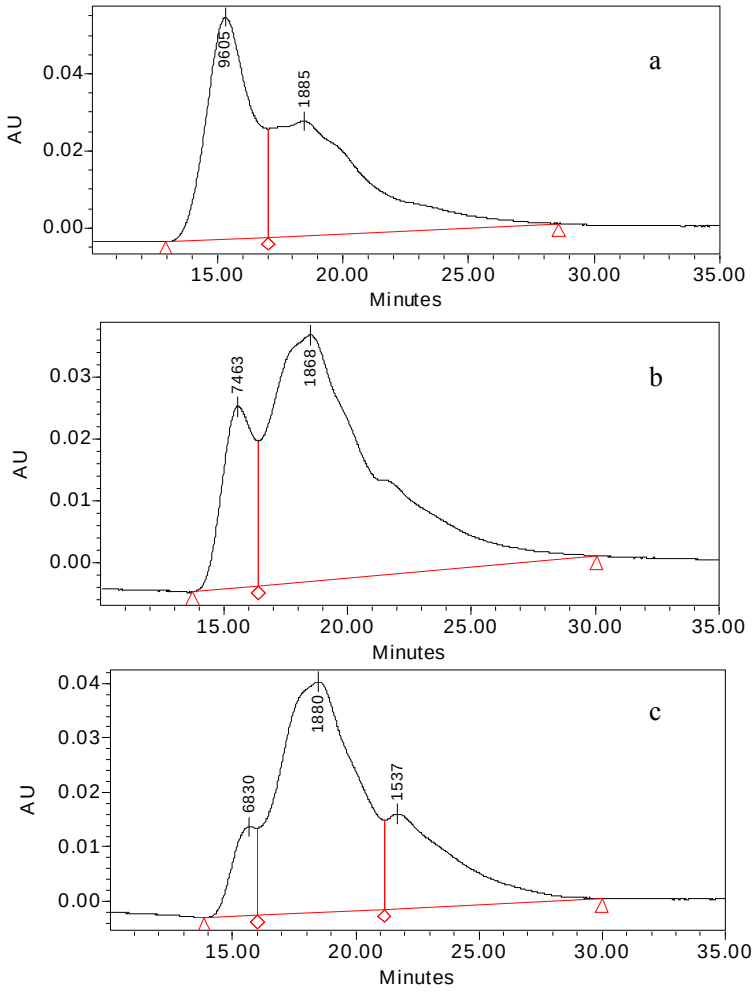

Figure 4.25. Degradation of polymer at oxidant/monomer molar ratio of 2.0. The GPC chromatograms were obtained for the reaction mixture after (a) 1.0 h, (b) 5.5 h and (c) 20.0 h of the polymerisation of MAS.

When the ratio was increased from 1 to 2, the yield (after purification) of HMWt PMAS decreased from 36.7% to 15.0%, while the yield (after purification) of LMWt materials increased from 6.5% to 11.5% as a result of polymer degradation. The time for completion of the reaction (the point at which the potential levels off) decreased when the ratio was changed from 0.63 to 1.00 or 1.26. However, for the oxidant/monomer ratio of 2.00 a much longer time was needed for this potential to become constant (Figure 4.24 a). The delayed onset was presumably due to a higher concentration of

oxidised materials (PS state) being obtained using the oxidant/monomer ratio of 2 resulting in a longer time needed for them to be reduced to the ES state. GPC results showed that degradation of polymer at the oxidant/monomer ratio of 2 commenced after 1 hour of reaction and continued during the reaction (Figure 4.25).

A good correlation was found between the molecular weight and the conductivity of the polymer (Figure 4.26). When the oxidant /monomer ratio was 1, optimum molecular weight, conductivity and yield (after purification) of HMWt PMAS were obtained. From these findings it was determined that the chemical synthesis of PMAS was optimal at oxidant/monomer mole ratios of 1.

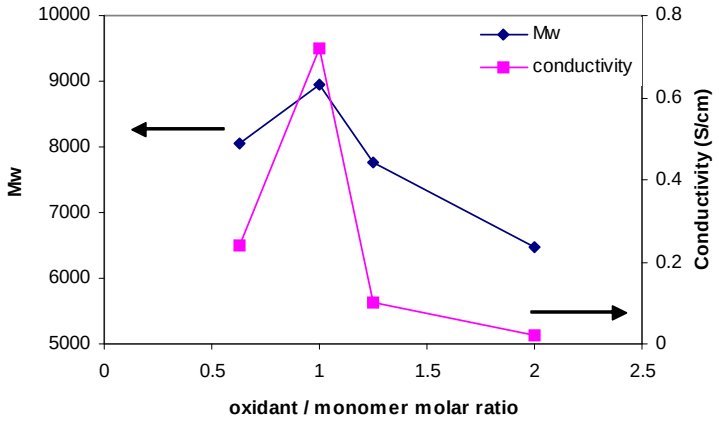

Figure 4.26. Effect of oxidant/monomer molar ratio on yield and conductivity of PMAS.

The UV-visible spectra of the pure PMAS obtained using different APS/MAS ratios is illustrated in Figure 4.27. The major difference between the spectra is the ratio of the absorption at 330 nm (π-π*) to the absorption at 473 nm (polaron band) (A_{473} / A_{330}) which correlates well with the conductivity values and has a maximum value at the ratio of 1. Similar observation was explained earlier in the effect of pH for the correlation of A_{473} / A_{330} with molecular weight of PMAS.

It was reported that the initial molar ratio of the reactants has primary influence on the properties of polyaniline. Armes and Miller [40] reported that the conductivity of

polyaniline was independent on the APS/aniline ratio for oxidant/aniline molar ratios below 1, however the yield of polyaniline increases linearly with the ratio up to 1. Both yield and conductivity decreased by over - oxidation processes of the polymer at higher

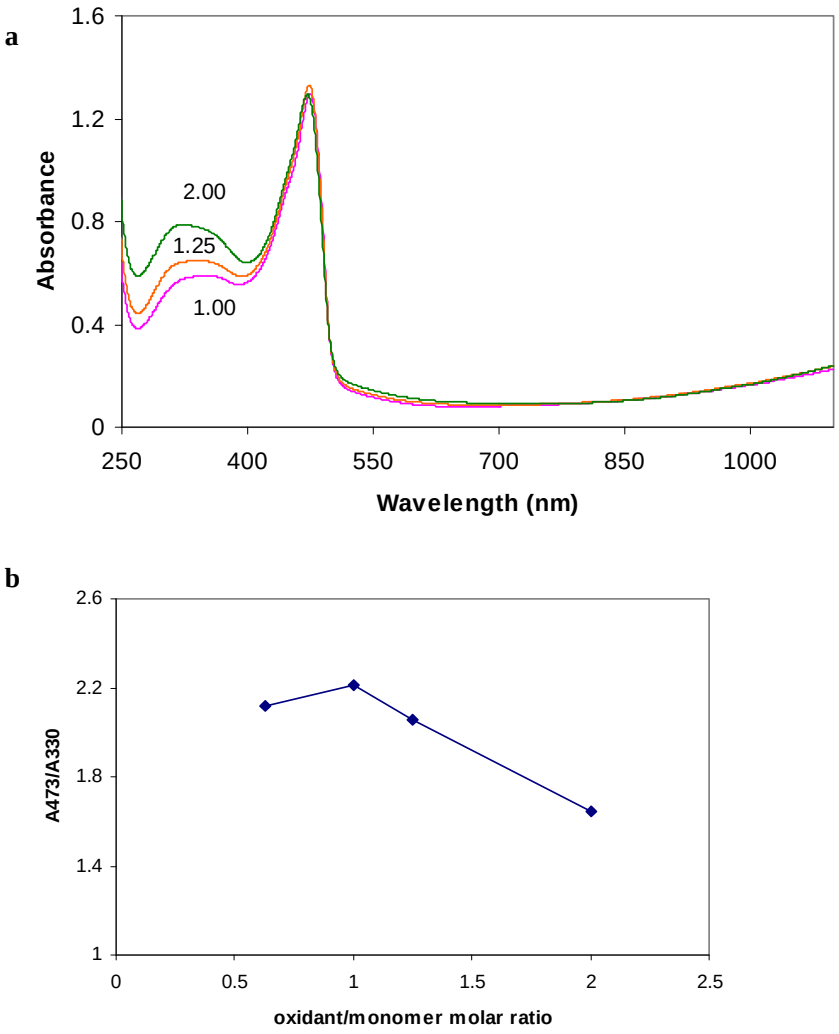

Figure 4.27. (a) UV-vis spectra of 50 ppm pure PMAS solution obtained at different oxidant/monomer molar ratios, (b) the ratio of absorption at 330 nm to 473 nm for PMAS synthesised at different APS/MAS ratios.

oxidant/monomer mole ratios. This study concluded that the most efficient ratio for polyaniline is about 1.15. Cao *et al.* [41] found that the aniline/oxidant ratio has a minor

effect on conductivity of polyaniline and a major effect on the yield of material produced. The authors concluded that the high concentration of oxidant promotes the formation of soluble oligomers that results in a lower final yield of polyaniline. A maximum molecular weight at a ratio of 1.10-1.15 and a sharp drop in molecular weight above 1.15 were reported by Adams *et al.* [26] for the polymerisation of aniline at low temperatures. Due to degradation of polymer at high concentration of oxidising agent several authors [42] have recommended the use of an oxidant/monomer ratio of 1.0 or less. In a study of chemical polymerisation of *o*-methoxyaniline by Gazotti and De Paoli [43], it was found that increasing the amount of oxidant reduced the conductivity and increased the yield of poly(*o*-methoxyaniline) due to facile oxidation of monomer and production of insoluble oligomers.

Results discussed above for chemical synthesis of PMAS using ammonium persulfate were also in agreement with the optimum oxidant/monomer reported for chemical synthesis of polyaniline. The HMWt PMAS with highest conductivity and molecular weight and good yield was obtained at oxidant/monomer molar ratio of 1.

4.3.6 Effect of varying the rate of addition of oxidant

There have been a few studies on the effect of the rate of addition of oxidant on the chemical polymerisation of aniline. Adams *et al.* [26] reported a slight increase in molecular weight and yield of polyaniline synthesised at -26ºC by increasing the time of oxidant addition from instantaneous up to 36 h. Cao *et al.* [41] have reported the effect of addition rate of oxidant on the inherent viscosity of polyaniline and the powder morphology of the precipitated polyaniline. An extremely fine morphology was obtained when the oxidant was added all at once, however coarse particles were produced at lower rates of oxidant addition. The viscosity was moderately lower for addition rates above 0.5 mL/min. The presence of more structural irregularity in the polymer chain synthesised at low temperatures was elucidated by Adams and Monkman [27] when the oxidant was added rapidly. This was thought to be due to the higher extent of formation of pernigraniline intermediate in the polymerisation of aniline with rapid oxidant addition.

In this work, the effect of the rate of addition (Figure 4.28) of APS on oxidation of MAS was investigated (from 1 ml/min to 100 mL/min (rapid mixing)). The reaction rate and completion time of reaction were affected by the rate of APS addition. The reaction rate increased with addition rate as demonstrated by the steeper slope of potential and pH changes observed at higher addition rates of oxidant. The potential drop in the step 1 was decreased by faster addition of APS and the potential rise in step 2 was faster for higher addition rates (Figure 4.28 a, inset). In rapid mixing, the evolution of potential showed a small perturbation at the end of step 2, probably due to the high extent PMAS in the oxidised sate which is formed with a high addition rate of oxidant. Increasing the addition rate up to 4 mL/min resulted in a decrease in the completion time and an increased the yield (post purification) with the same monomer conversion, however the yield was decreased when the oxidant was added more rapidly (100 mL/min). The conductivity of PMAS was substantially increased by increasing the addition rate, from 0.25 S/cm for 1 ml/min to 1.25 S/cm for rapid mixing, however monomer conversion was not affected (Table 4.7). The optimum conductivity and molecular weight were obtained when the oxidant was added rapidly (Figure 4.29). The ESR characterisation of the polymer obtained at different rates of oxidant addition is discussed in Chapter 5.

Table 4.7. Influence of oxidant/monomer mole ratio on properties of the polymer obtained. Reaction conditions were monomer concentration 0.33 M, temperature 10ºC and oxidant/monomer molar ratio 1. Monomer conversion was measured after 20 h reaction time. The yield of the pure polymer was calculated after drying in oven 45ºC overnight.

Rate of APS addition (ml/min)	M_p(Da)	% Yield	conductivity	% Monomer conversion
1	9,170	36.7	0.25 ± 0.01	84.0 ± 0.3
2	9,080	39.0	0.28 ± 0.02	83.0 ± 0.2
4	8,460	41.0	0.54 ± 0.05	84.0 ± 0.3
100	10,120	36.4	1.25 ± 0.08	85.0 ± 0.2

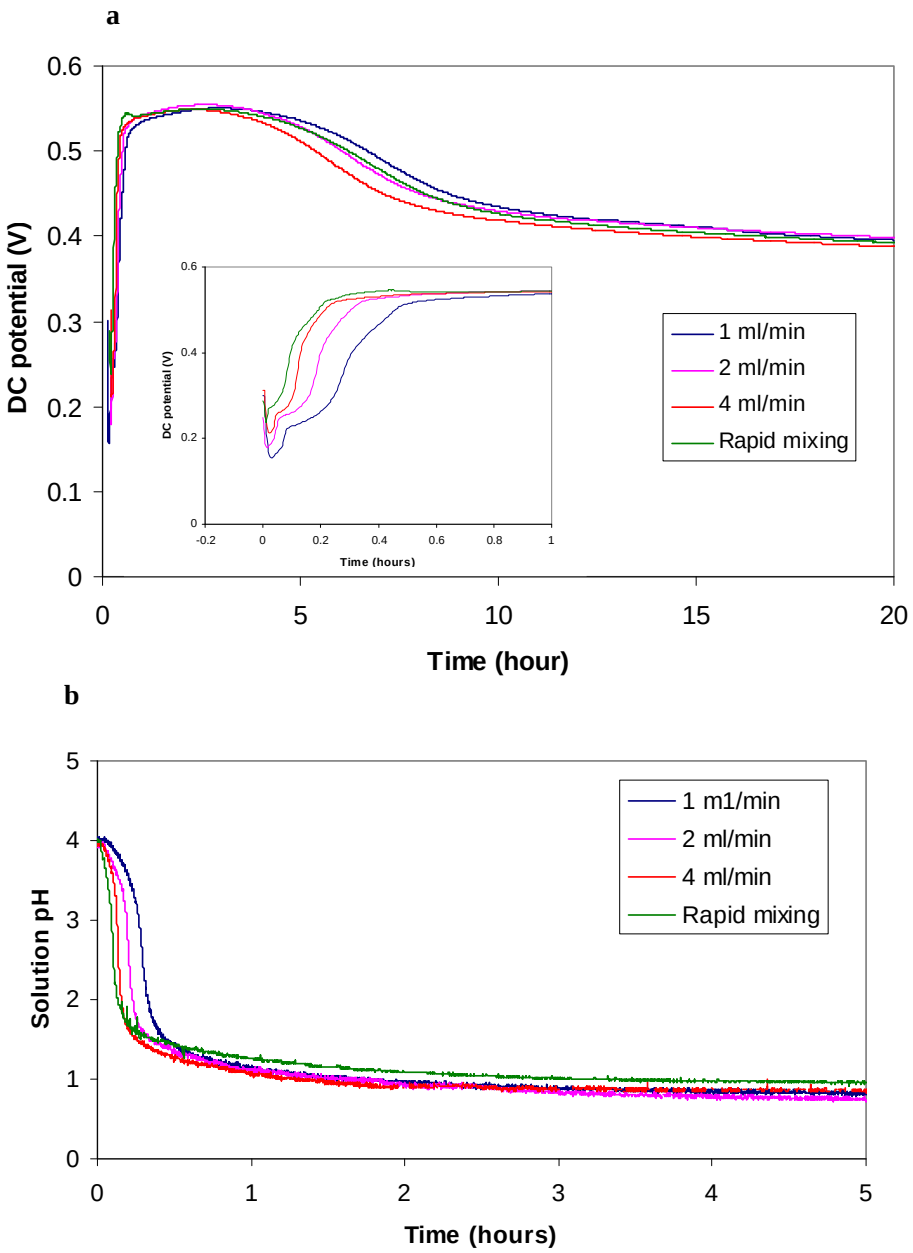

Figure 4.28. Evolution of (a) potential and (b) pH during polymerisation of 0.33 M MAS using different addition rate of oxidant. The inset in (a) illustrates the potential change during the first hour of reaction.

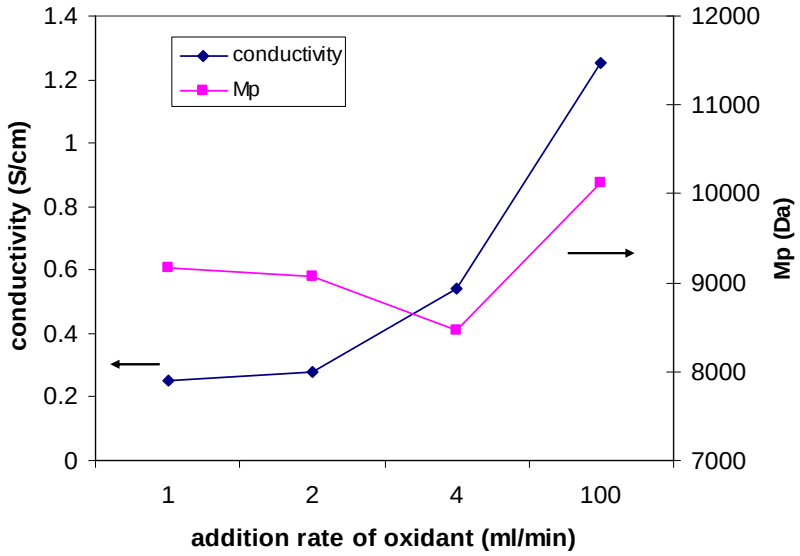

Figure 4.29. Conductivity and molecular weight of the pure polymer obtained at different rate of addition of oxidant.

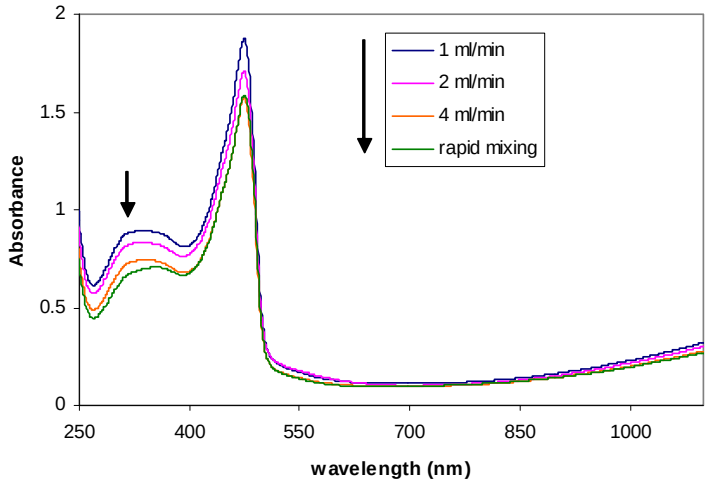

Figure 4.30. Uv-vis spectra of 50 ppm pure PMAS solution synthesised at several addition rates of oxidant.

The UV-vis spectra were recorded for the pure PMAS obtained at different APS addition rates (Figure 4.30). The absorption ratio A_{473}/A_{330} was increased slightly from

2.09 for 1 mL/min to 2.29 for rapid mixing which corresponds well with the increase in conductivity.

4.3.7 Chemical synthesis of PMAS using optimised conditions

As explained in this Chapter, the chemical synthesis of PMAS was optimised by studying the effect of a number of variables mentioned above. The optimum variable found in each step was used in the next step for study the effect of other variables, except for the concentration of monomer. A total monomer concentration of 0.33 M was used instead of the optimum of 0.47 M to overcome the viscosity problem observed with in-situ measurements of potential and pH.

The optimum reaction conditions are outlined in Table 4.8 for chemical synthesis of PMAS using ammonium persulfate oxidising agent with respect to electrical conductivity, molecular weight and reaction yield. The polymerisation of MAS under these reaction conditions results in high quality PMAS with conductivity, molecular weight and yield as high as 1.74S/cm, 16900 Da (M_w), and 49.5%, respectively (Table 4.9).

Table 4.8. Optimum conditions for the synthesis of PMAS.

Temperature	5-10ºC
Monomer concentration	0.47 M
Oxidant/monomer ratio	1:1
Addition rate of oxidant	Rapid mixing
Starting pH	4
Time	14 h

Table 4.9. Charactrisation of PMAS synthesised at optimum conditions.

PMAS synthesised at optimum conditions	**Monomer conversion**	**Yield**	**Mp (Da)**	**Mw (Da)**	**Conductivity (S/cm)**
	(81.0 ± 0.2)%	**49.5%**	**16,900**	**29,340**	**1.74 ± 0.09**

4.4 Conclusions

The influence of a range of experimental conditions on the characteristics of water-soluble conducting polymer, poly(2-methoxy-aniline-5-sulfonic acid) (PMAS), was systematically investigated in order to achieve the optimal conditions. Optimisation studies of the chemical polymerisation of MAS reveal that the experimental conditions such as temperature, pH, monomer and oxidant concentration, and the rate of addition of oxidant have a dramatic effect on properties of PMAS.

The use of synthesis temperatures lower than 10°C results in polymer with enhanced conductivity and molecular weight. However, monomer conversion and polymer yield are negligibly affected by temperature.

The optimum pH for the reaction solution at the start of the reaction is 4.0 and is required for complete solubilisation of the MAS monomer. As the reaction proceeds, a pH drop is observed resulting in the formation of conducting HMWt PMAS. Synthesis under constant pH (3 or 4) leads to formation of oligomeric products, presumably with a degree of ortho-coupling, and no conducting HMWt PMAS. It is hypothesised that as for polyaniline, the C-N para-coupling and chain propagation in polymerisation of MAS will only occur at sufficiently low pH values to from anilinium cation analogues.

Monomer concentration employed during synthesis has a dramatic effect on chemical synthesis of PMAS. Both conductivity and yield were significantly influenced by monomer concentration. The resulting polymer displays an enhanced conductivity of *ca.* 1 S/cm and yield of 56% (pure PMAS) via increasing the monomer concentration up to 0.47 M. A minimum concentration of 0.20 M MAS is required for chemical polymerisation. The synthesis rates are strongly dependent on monomer concentration, with a typical reaction time of 8 hours required for concentration range of 0.33-0.47 M.

The optimum ratio for oxidant/monomer with respect to conductivity is 1. Increasing the ratio to 1.25 is detrimental to the conductivity, however this results in an increase in

polymer yield. Using the ratios above 1.25 will result in over-oxidation and degradation of PMAS leading to a dramatic drop in both conductivity and yield.

The conductivity of PMAS is also sensitive to the rate of addition of oxidant. Increasing the addition rate of oxidant results in the PMAS product with higher conductivity. The optimum conductivity can be obtained when the oxidant solution is rapidly mixed with monomer solution.

Optimal PMAS synthesis conditions yield conductivities of 1.74 S/cm, molecular weight M_W 16900) and recovered yields of 49.5% at high monomer concentrations of 0.47 M at a temperature below 10°C, and employing equimolar oxidant/monomer ratio with rapid mixing initiated at pH 4. The conductivity of PMAS using these optimal conditions is close to two orders of magnitude higher than previously reported for PMAS (0.01-0.04 S/cm).

4.5 References

1. Chan, H.S.O., Ho, P.K.H., Ng, S.C., Tan, B.T.G., and Tan, K.L., *A New Water-Soluble, Self-Doping Conducting Polyaniline from Poly(o-aminobenzylphosphonic acid) and Its Sodium Salts: Synthesis and Characterization.* J. Am. Chem. Soc., 1995. **117**(33): p. 8517-8523.
2. Macinnes, J., David and Funt, B.L., *Poly-o-methoxyaniline: A new soluble conducting polymer.* Synthetic Metals, 1988. **25**(3): p. 235-242.
3. Leclerc, M., Guay, J., and Dao, L.H., *Synthesis and characterization of poly(alkylanilines).* Macromolecules, 1989. **22**(2): p. 649-653.
4. Kilmartin, P.A. and Wright, G.A., *Photoelectrochemical and spectroscopic studies of sulfonated polyanilines Part I. Copolymers of orthanilic acid and aniline.* Synthetic Metals, 1997. **88**(2): p. 153-162.
5. Wei, X.-L.W., Y. Z.; Long, S. M.; Bobeczko, C.; Epstein, A. J., *Synthesis and Physical Properties of Highly Sulfonated Polyaniline.* J. Am. Chem. Soc., 1996. **118**(11): p. 2545-2555.
6. Kitani, A., Satoguchi, K., Tang, H.-Q., Ito, S., and Sasaki, K., *Eletrosynthesis and properties of self-doped polyaniline.* Synthetic Metals, 1995. **69**(1-3): p. 129-130.
7. Jiang Yue, A.J.E., *Synthesis of self-doped conducting polyaniline.* J. Am. Chem. Soc., 1990. **112**(7): p. 2800-2801.
8. Wei, X. and Epstein, A.J., *Synthesis of highly sulfonated polyaniline.* Synthetic Metals, 1995. **74**(2): p. 123-125.
9. J.Y. Bergeron, J.-W.C., L.H. Dao,, J. Che. Soc. Chem. Commun., 1990. **112**: p. 180.

10. Han, M.G., Cho, S.K., Oh, S.G., and Im, S.S., *Preparation and characterization of polyaniline nanoparticles synthesized from DBSA micellar solution.* Synthetic Metals, 2002. **126**(1): p. 53-60.
11. Kohut-Svelko, N., Reynaud, S., and Francois, J., *Synthesis and characterization of polyaniline prepared in the presence of nonionic surfactants in an aqueous dispersion.* Synthetic Metals, 2005. **150**(2): p. 107-114.
12. Moulton, S.E., Innis, P.C., Kane-Maguire, L.A.P., Ngamna, O., and Wallace, G.G., *Polymerisation and characterisation of conducting polyaniline nanoparticle dispersions.* Current Applied Physics, 2004. **4**(2-4): p. 402-406.
13. Ngamna, O., Moulton, S.E., and Wallace, G.G., *Incorporation of dye into conducting polyaniline nanoparticles.* Reactive and Functional Polymers, 2007. **67**(3): p. 173-183.
14. Hwang, S.-A.C.a.G.-W., *Structure Characterization of Self-Acid-Doped Sulfonic Acid Ring-Substituted Polyaniline in Its Aqueous Solutions and as Solid Film.* Macromolecules, 1996. **29**(11): p. 3950-355.
15. Shimizu, S., Saitoh, T., Uzawa, M., Yuasa, M., Yano, K., Maruyama, T., and Watanabe, K., *Synthesis and applications of sulfonated polyaniline.* Synthetic Metals, 1997. **85**(1-3): p. 1337-1338.
16. Chan, H.S.O., Neuendorf, A.J., Ng, S.C., Wong, P.M.L., and Young, D.J., *Synthesis of fully sulfonated polyaniline: a novel approach using oxidative polymerisation under high pressure in the liquid phase.* Chemical Communications, 1998(13): p. 1327-1328.
17. Guo, R., Barisci, J.N., Innis, P.C., Too, C.O., Wallace, G.G., and Zhou, D., *Electrohydrodynamic polymerization of 2-methoxyaniline-5-sulfonic acid.* Synthetic Metals, 2000. **114**(3): p. 267-272.
18. Zhou, D., Innis, P.C., Wallace, G.G., Shimizu, S., and Maeda, S.-I., *Electrosynthesis and characterisation of poly(2-methoxyaniline-5-sulfonic acid)-effect of pH control.* Synthetic Metals, 2000. **114**(3): p. 287-293.
19. Masdarolomoor, F., Innis, P.C., Ashraf, S., and Wallace, G.G., *Purification and characterisation of poly(2-methoxyaniline-5-sulfonic acid).* Synthetic Metals, 2005. **153**(1-3): p. 181-184.
20. Wei, Y., Hsueh, K.F., and Jang, G.-W., *Monitoring the chemical polymerization of aniline by open-circuit-potential measurements.* Polymer, 1994. **35**(16): p. 3572-3575.
21. David, S., Nicolau, Y.F., Melis, F., and Revillon, A., *Molecular weight of polyaniline synthesized by oxidation of aniline with ammonium persulfate and with ferric chloride.* Synthetic Metals, 1995. **69**(1-3): p. 125-126.
22. Beadle, P.M., Nicolau, Y.F., Banka, E., Rannou, P., and Djurado, D., *Controlled polymerization of aniline at sub-zero temperatures.* Synthetic Metals, 1998. **95**(1): p. 29-45.
23. Sbaite, P., Huerta-Vilca, D., Barbero, C., Miras, M.C., and Motheo, A.J., *Effect of electrolyte on the chemical polymerization of aniline.* European Polymer Journal, 2004. **40**(7): p. 1445-1450.
24. Syed, A.A. and Dinesan, M.K., *Review: Polyaniline--A novel polymeric material.* Talanta, 1991. **38**(8): p. 815-837.
25. Mattoso, L.H.C., MacDiarmid, A.G., and Epstein, A.J., *Controlled synthesis of high molecular weight polyaniline and poly(o-methoxyaniline).* Synthetic Metals, 1994. **68**(1): p. 1-11.

26. Adams, P.N., Laughlin, P.J., and Monkman, A.P., *Synthesis of high molecular weight polyaniline at low temperatures.* Synthetic Metals, 1996. **76**(1-3): p. 157-160.
27. Adams, P.N. and Monkman, A.P., *Characterization of high molecular weight polyaniline synthesized at -40 [deg]C using a 0.25:1 mole ratio of persulfate oxidant to aniline.* Synthetic Metals, 1997. **87**(2): p. 165-169.
28. Adams, P.N., Laughlin, P.J., Monkman, A.P., and Kenwright, A.M., *Low temperature synthesis of high molecular weight polyaniline.* Polymer, 1996. **37**(15): p. 3411-3417.
29. Adams, P.M., Abell, L., Middleton, A., and Monkman, A.P., *Low temperature synthesis of high molecular weight polyaniline using dichromate oxidant.* Synthetic Metals International Conference on Science and Technology of Synthetic Metals, 1997. **84**(1-3): p. 61-62.
30. Stejskal, J., Riede, A., Hlavata, D., Prokes, J., Helmstedt, M., and Holler, P., *The effect of polymerization temperature on molecular weight, crystallinity, and electrical conductivity of polyaniline.* Synthetic Metals, 1998. **96**(1): p. 55-61.
31. Strounina, E.V., Shepherd, R., Kane-Maguire, L.A.P., and Wallace, G.G., *Conformational changes in sulfonated polyaniline caused by metal salts and OH.* Synthetic Metals, 2003. **135**(1-3): p. 289-290.
32. Stejskal, J., Kratochvil, P., and Spirkova, M., *Accelerating effect of some cation radicals on the polymerization of aniline.* Polymer, 1995. **36**(21): p. 4135-4140.
33. Pornputtkul, Y., *Development of Chiral Conducting Polymers for Asymmetric Electrosynthesis*, in *Chemistry department*. 2005, University of Wollongong.
34. Stejskal, J., Kratochvil, P., and Jenkins, A.D., *The formation of polyaniline and the nature of its structures.* Polymer, 1996. **37**(2): p. 367-369.
35. Genies, E.M., Boyle, A., Lapkowski, M., and Tsintavis, C., *Polyaniline: A historical survey.* Synthetic Metals, 1990. **36**(2): p. 139-182.
36. Venancio, E.C., Wang, P.-C., and MacDiarmid, A.G., *The azanes: A class of material incorporating nano/micro self-assembled hollow spheres obtained by aqueous oxidative polymerization of aniline.* Synthetic Metals, 2006. **156**(5-6): p. 357-369.
37. Gospodinova, N., Terlemezyan, L., Mokreva, P., and Kossev, K., *On the mechanism of oxidative polymerization of aniline.* Polymer, 1993. **34**(11): p. 2434-2437.
38. Duic, L. and Mandic, Z., *Counter-ion and pH effect on the electrochemical synthesis of polyaniline.* Journal of Electroanalytical Chemistry, 1992. **335**(1-2): p. 207-221.
39. Gospodinova, N. and Terlemezyan, L., *Conducting polymers prepared by oxidative polymerization: polyaniline.* Progress in Polymer Science, 1998. **23**(8): p. 1443-1484.
40. Armes, S.P. and Miller, J.F., *Optimum reaction conditions for the polymerization of aniline in aqueous solution by ammonium persulphate.* Synthetic Metals, 1988. **22**(4): p. 385-393.
41. Cao, Y., Andreatta, A., Heeger, A.J., and Smith, P., *Influence of chemical polymerization conditions on the properties of polyaniline.* Polymer, 1989. **30**(12): p. 2305-2311.

Chapter 5

Characterisation of PMAS fractions

5.1 Introduction

As discussed in detail earlier, the most successful route to increase the solubility and processability of polyaniline is via the introduction of sulfonate groups onto the polyaniline backbone. This can be achieved by sulfonation of pre-formed emeraldine base or leucoemeraldine base forms of polyaniline to produce 50-75% self-doped sulfonated polyaniline (SPAN, Scheme I).

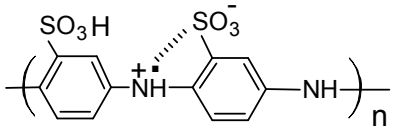

Scheme 5.1. SPAN

SPAN was the first reported self-doped, water soluble conducting polyaniline derivative which has been synthesised by sulfonation of emeraldine base using fuming sulfuric acid [1]. Elemental analysis of this SPAN demonstrated a S/N atomic ratio of 0.48 and titration analysis established a doping level of 0.3 [2]. SPAN has a conductivity of about 0.1 S/cm which is lower than PAn.HA emeraldine salts. However, unlike PAn.HA, SPAN remains conductive up to pH 7 and is soluble in basic aqueous solutions (23 mg/mL). It has been shown that SPAN has better thermal stability than the parent polyaniline doped with HCl. These properties have resulted in the use of SPAN in rechargeable batteries[3-5] with a high charge density and in light emitting diodes [6]. Treatment of leucoemeraldine base with fuming sulfuric acid leads to highly sulfonated (75%) SPAN [7]. However fully sulfonated PAn can not be achieved in this way. Highly sulfonated (75%) SPAN has increased solubility (38 mg/mL) and conductivity (1 S/cm) compared to 50% SPAN and is conductive over a wider pH range (0-14). The

optical and redox properties of these SPANs are similar to the parent polyaniline [2, 8-11].

A water soluble *N*-substituted PAn, poly(aniline-co-N-propansulfonic acid aniline) (PAPSA) has been prepared by treatment of emeraldine base with 1,3-propane sultone [12]. PAPSA has a S/N atomic ratio of 0.48, doping level of 0.33 and conductivity of 0.015 S/cm [13].

The first reported fully sulfonated water soluble polyaniline was poly(2-methoxyaniline-5-sulfonic acid) (PMAS, Scheme II). PMAS has been synthesised via chemical and electrochemical methods by polymerisation of the MAS monomer [14-16]. This self-doped polyaniline has two sulfonated groups in its dimer repeat unit. One sulfonate group is assumed to be involved in self-doping of the adjacent radical cation in the polyaniline backbone. The other sulfonate group is free and can interact electrostatically with cations such as H^+, Na^+ and NH_4^+ [17] or large positively charged moieties and polyelectrolytes (amines, amino acids, proteins and enzymes) such as phenylethylamine (PhEA) [18] , poly-L-lysine (PLL) [19] poly(4-vinylpyridine) [20] and poly(amido amine) dendrimer [21].

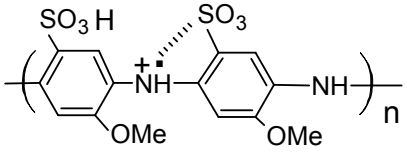

Scheme 5.2. PMAS

The UV-visible spectra obtained for PMAS in the emeraldine and leucoemeraldine states are different from SPAN and parent polyaniline. A broad absorption band at 320-390 nm observed for PMAS emeraldine salt (ES) is attributed to π-π^* transitions. The sharp peak at 474 nm and a free carrier tail in the near infrared region beginning at *ca.* 900 nm assigned as a low wavelength polaron band and a high wavelength delocalised band, respectively [22]. A film of ES (PMAS) shows an intense near-infrared band at *ca.* 2200 nm [17]. The presence of the latter peak suggests that PMAS in aqueous solution exists in an extended coil conformation [22].

The UV-vis spectrum of the leucoemeraldine base of PMAS exhibits a sharp peak at 408 nm which is different from SPAN and parent polyaniline [17], a weaker band at *ca.* 330 nm. The nature of the species with λ_{max} 408 nm is not clear, however thermochromism and salvatochromism studies by Pornputtkul *et al.* [19] have shown that the intensity of the 408 nm peak is reversibly changed with either temperature or solvent. These phenomena were attributed to a rearrangement of the PMAS chains, between two different conformations [19].

PMAS is electroactive in solution and in the solid state complexes with other materials. Similar to other polyaniline emeraldine salts, two redox peaks are observed in the cyclic voltammograms of PMAS complexes [21, 23] cast on various electrodes,. However, the shape of the first peak is dramatically different (broad and weak). When the potential is scanned above 0.8 V, a medium peak appears (as in polyaniline) presumably due to degradation and hydrolysis of the imine to form benzoquinone [21]. A cyclic voltammetry study of PMAS-PLL complex in acidic and neutral media by Pornputtkul *et al.* [19] showed that there is no proton transfer process involved in the first redox peak, while protons participate in the second redox process. In aqueous solution, PMAS shows three well defined redox peaks. Tallman and Wallace [20] attributed each of these peaks to a one electron transfer. The middle peak observed in aqueous PMAS may be attributed to additional redox processes in solution.

A charge transport and magnetic study of PMAS by Lee *et al.* [24] showed that the presence of the methoxy and sulfonate substituent leads to formation of bipolarons and a lower density of states at the Fermi level, as well as lower room temperature conductivity. The conductivity of PMAS (0.02 S/cm) is smaller than that reported for 50% or 75% SPAN (~0.1-1 S/cm).

Recently, photoluminescence and a photo-induced redox reaction have been reported for poly(2-methoxyaniline-5-sulfonic acid) (PMAS) in the emeraldine salt (ES) state by Kane-Maguire *et al.* [25]. They found that irradiation of aqueous PMAS emeraldine salt solutions at 350-450 nm (near the polaron band of PMAS) resulted in photoluminescence at *ca.* 600 nm, suggestive of emission from the polaron

chromophore of a photo-generated PMAS excited state. Based on an excited state life time of less than 40 ns, and the absence of photoluminescence enhancement upon nitrogen purging, the photoluminescence was assigned as fluorescence rather than phosphorescence. Calculations based on cyclic voltammetry of ground state PMAS led to the suggestion that photo-excited emeraldine salt PMAS is a powerful oxidizing and reducing agent, which was confirmed by photo-redox reactions of PMAS in the presence of cobalt (III) cations.

The studies outlined above were mostly carried out on commercially available PMAS prepared via chemical oxidation of the MAS monomer. It is now known that PMAS synthesised via either chemical and electrochemical oxidation possesses two distinct molecular weight fractions that can be substantially separated by membrane dialysis [15, 16]. The GPC chromatogram of dialysed PMAS exhibits an oligomer impurity shoulder with M_p 2-3 kDa. High purity (> 98%) samples of each of these PMAS fractions have become available for the first time [26], using a cross-flow dialysis system developed in Chapter 3. The high molecular weight (HMWt) PMAS fraction (obtained using the optimal procedure developed in Chapter 4) has M_p of 16.9 kDa, while the low molecular weight (LMWt) PMAS fraction is an oligomer with M_p of 2-3 kDa.

The work presented in this Chapter explores the properties of pure PMAS. UV-vis spectroscoy, cyclic voltammetry, elemental analysis, thermal analysis, photoluminescence, and ESR spectroscopy have been used to characterise the material. In addition, solubility, stability, and morphology have been determined. A comparison is also made between the properties of high and low molecular weight PMAS fractions. The photoluminescence in PMAS is reinvestigated using these pure PMAS fractions as well as mixtures, throwing new light on the origin of the photoluminescence of PMAS and on the influence of these two fractions on the unique photoredox reactions of PMAS in the ES state.

5.2 Experimental

5.2.1 Materials

2-Methoxyaniline-5-sulfonic acid (MAS) was provided by Mitsubishi Rayon, Japan and purified by acid-base crystallization before being used for polymerisation. PMAS was synthesised using the optimum conditions outlined in Chapter 4 and purified by the cross flow filtration method developed in Chapter 3 to produce fractionated polymer of distinctly different chemical and physical properties. The fractions produced were classified as HMWt PMAS, LMWt PMAS and the pink oligomeric fraction. Ammonium persulfate, hydrazine monohydrate, sodium hydroxide, sodium chloride, and sodium nitrate were purchased from Aldrich. Ammonium hydroxide (28% NH_3) and hydrochloric acid 32% (w/v) were purchased from Ajax. Amberlite IR-120 ion exchange resin was purchased from Ajax. All chemicals were of analytical grade and used as received. All solutions were prepared in Milli-Q water (18 MΩ cm). Acetonitril, chloroform, methanol, ethanol, acetone, ethylacetate, acetic acid, DMSO, THF and m-cresol were supplied by Ajax Chemicals. NMP was purchased from Aldrich.

5.2.2 Polymer characterisation

Different techniques were used to characterise the purified PMAS fractions as described below.

5.2.2.1 UV-Vis spectroscopy of PMAS fractions

The UV-Vis spectra of aqueous solutions of PMAS fractions were recorded between the wavelengths of 250 nm and 1100 nm using a Shimadzu UV-1601 UV-vis spectrophotometer. Quartz cells with 1 cm path length were used. In order to measure the molar absorptivity of the fractions, different concentrations were prepared in water or 0.02 M NaOH and the spectra recorded in the range 300-500 nm in water and in the range 250-1100 nm in 0.02 M NaOH. The concentration ranges were 3.84×10^{-6} -1.23×10^{-4} M for HMWt PMAS, 6.16×10^{-6} - 1.97×10^{-4} M for LMWt PMAS and 1.23×10^{-5} - 3.94×10^{-4} M for the pink oligomeric fraction. The absorbance values at particular wavelengths (to be discussed later in this Chapter) for different concentrations of polymer were used to calculate the molar absorptivity using the Beer-Lambert equation.

5.2.2.2 Electroactivity of PMAS fractions

5.2.2.2.1 Chemical oxidation and reduction

Aqueous solutions of PMAS fractions (0.024 mM, 10 µg/mL) were oxidised with 0.10 M ammonium persulfate and the UV-vis spectral changes monitored over 30 min at room temperature. The reductions of PMAS fractions were similarly carried out in 0.10 M hydrazine hydrate and the solution UV-vis spectra were recorded with time.

5.2.2.2.2 Cyclic volyammetry

Cyclic voltammetric studies of PMAS fractions were carried out in 0.5 mg/mL aqueous solutions of HMWt and LMWt PMAS. The potential was cycled between -0.2 and 1.0 V at a scan rate of 50 mVs^{-1}. A Pt mesh and Ag/AgCl were used as auxiliary and reference electrodes, respectively. The solutions were purged with nitrogen gas for 10 min before recording the cyclic voltammograms.

5.2.2.3 Photoluminescence spectroscopy of PMAS fractions

Photoluminescence (PL) measurements were performed on aqueous solutions containing PMAS fractions at a concentration range 2-50 µg/mL [(0.05-1.2) x 10^{-4} M based on a dimer repeat unit]. Lower PMAS concentrations were employed to minimise the effect of self-absorption of the emitted light. Fluorescence spectra were recorded using a JY Spex fluorescence spectrophotometer.

5.2.2.4 ESR spectroscopy of PMAS fractions

The ESR spectra of the PMAS fractions were recorded on a Bruker EMX ESR spectrometer under identical conditions of microwave frequency (9.87 GHz), attenuator (30.0 dB), sweep width (25 G), modulation frequency (100 KHz), modulation amplitude (0.5 G), time constant (40.96 msec), conversion time (163.84 msec), resulting in a scan sweep time of 671 sec. Aqueous samples containing 2.5 mg/mL PMAS solution were injected into the microwave cavity via a Bruker Aqua-X™ flow cell which permitted rapid sample change over and ensured identical cell geometry and reproducible cavity tuning. The ESR spectra of solid PMAS samples (~1 mg in quartz ESR tube) were recorded at different conditions of attenuator (20.0 dB), sweep width (25 G),

modulation frequency (100 KHz), modulation amplitude (0.02 G), time constant (1.28 msec), conversion time (5.12 msec) and scan sweep time (10.49 sec).

5.2.2.5 Conductivity measurements

Conductivity measurements were performed on dried films of *ca.* 10 μm thickness (obtained by air evaporative casting of 30 μL of 50 mg/mL solution of the PMAS fraction onto a glass slide substrate) using a JANDEL resistivity system (model RM2) with a linear or square four-point probe.

5.2.2.6 Thermal analysis of PMAS fractions

Thermogravimetry was carried out using a DTA/TGA SETARAM 92B thermoanalyzer. Temperature was increased from 50°C to 450°C at a heating rate of 10°C per min under a nitrogen atmosphere. Differential scanning calorimetery (DSC) was carried out using a Q-100 (TA series) instrument in the temperature range of 25-350°C. The samples were studied in aluminum pans.

5.2.2.7 Elemental analysis of PMAS

Elemental analyses were performed by the Australian National University Microanalytical laboratory using an automatic analyser, Carlo Erba, for C, H, N determinations, and a Dionex Ion Chromatography Analyser for S analysis. The samples (3 mg pure PMAS) were heated to 50ºC in a vacuum oven for 5 hours prior to analysis. The PMAS samples for elemental analysis were the pure PMAS (ammonium salt) and the acid form of PMAS. Acid form of PMAS was prepared by ion exchange of the ammonium salt using an Amberlite IR-120 ion exchange resin.

5.2.2.8 Morphology and particle size of PMAS

Transmission electron microscopy using a Hitachi H7000 TEM at 75 keV was employed to observe the morphology of PMAS cast onto TEM grids from dilute PMAS solutions.

Other instruments

Molecular weight was determined using a Waters GPC system with Millenium software using Waters Ultrahydrogel 125 and 250 columns in series held at 35°C in a column oven, with a mobile phase consisting of 20% v/v methanol and 80% v/v aqueous solution of 0.20 M $NaNO_3$ and 0.01 M disodium hydrogen phosphate buffer (pH 9) at a 0.8 mL/min flow rate. Chromatograms were recorded using a photodiode array detector, Waters 996 PDA. All molecular weight calibrations were determined via relative calibration against polystyrene sulfonate standards from Polymer Laboratories. Throughout the text the peak molecular weight, M_p, has been quoted for clarity. The pH of polymer solutions was measured by a TPS Instruments Model 900-P pH meter. A Beckman (J2-MC, rotor JA10) centrifuge at 4100 rpm was used for purification of small volumes of PMAS by vivaspin membranes.

5.3 Results and discussion

Using the purification and fractionation method developed in Chapter 3 and the syvthesis conditions optimised in Chapter 4, three fractions of HMWt PMAS, LMWt PMAS and a pink oligomeric fraction were isolated from the chemical polymerisation of MAS. Purification of PMAS by conventional dialysis tubing (DPMAS) was shown to result in a mixture of HMWt PMAS and LMWt PMAS. GPC analysis data of these fractions are summarised in Table 5.1.

Table 5.1. Molecular weight distributions for the different PMAS fractions. Calibration is relative to polystyrene sulfonate standards.

Fraction	M_n (Da)	M_w (Da)	M_P (Da)	PDI
Dialysed PMAS	12,400	30,500	14,600	2.46
	2,010	2,240	3,060	1.11
HMWt PMAS	13,400	33,600	16,900	2.50
LMWt PMAS	2,440	2,700	2,830	1.11
Pink oligomeric fraction	670	1,260	1,200	1.90

5.3.1 UV-visible spectroscopy of PMAS fractions

The UV-visible spectra of the three pure fractions in aqueous solution (pH~3.5) are presented in Figure 5.1. HMWt PMAS emeraldine salt shows two peaks at 474 nm and 330 nm. The peak at 330 nm may be attributed to π-π* transitions and the sharp peak at 474 nm is assigned as a low wavelength polaron band [22]. The absorption at wavelengths longer than 900 nm is the beginning of a broad band assigned as a high wavelength delocalised polaron band. The presence of the latter band suggests an extended coil conformation for the emeraldine salt form of PMAS [22].

The spectra obtained for the LMWt PMAS and the pink oligomeric fractions are significantly different from HMWt PMAS. The pink oligomeric fraction (about 6 monomer units, M_p *ca.* 1.2 kDa) shows a sharp π-π* band at 292 nm and a weak n-π* band at 500 nm. LMWt PMAS (M_p *ca.*2-3 kDa) shows a π-π* band at 285 nm with a shoulder at 297 nm, and the weak n-π* absorption band is red shifted to about 530 nm. A red shift in absorption with an increase in conjugation length has been reported for many types of conjugated oligomers [27]. In a study by Sein *et al.* [28] the UV-visible spectra of unsubstituted emeraldine trimers and 2,6-dialkyl-substituted aniline trimers have been reported. Two absorbance bands at about 270-300 nm and 530-585 nm were dependent on the substituent on the aniline rings.

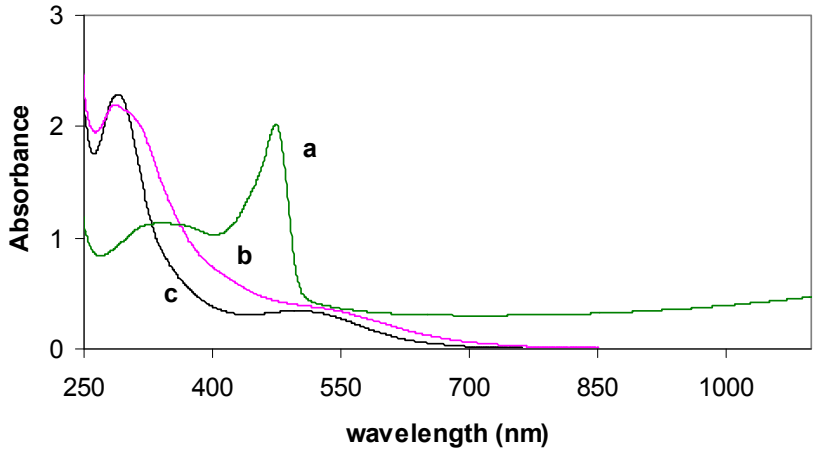

Figure 5.1. UV-vis spectra of 70 µg/mL aqueous solutions of (a) HMWt PMAS, (b) LMWt PMAS and (c) pink oligomeric fraction.

The effect of fraction composition

The influence of the low molecular weight LMWt fraction on the UV-vis spectrum of high molecular weight HMWt PMAS was examined (Figure 5.2) using mixtures of pure HMWt and LMWt PMAS samples obtained via the cross-flow dialysis purification method. For each of the aqueous mixtures, the total concentration of PMAS was kept constant at 1.0 mg/mL (2.4 x 10^{-3} M). The presence of an isosbestic point at *ca.* 315 nm is indicative that the two PMAS species are interacting additively. This approach therefore provides a simple and quantitative tool for the rapid estimation of polymer composition without the need to resort to time consuming chromatographic (GPC) analysis [16, 26]. For example, the spectrum (Figure 5.3a) of aqueous dialysed polymer (DPMAS) obtained in Chapter 3 indicates that this sample is composed of approximately 80% HMWt PMAS and 20% LMWt PMAS.

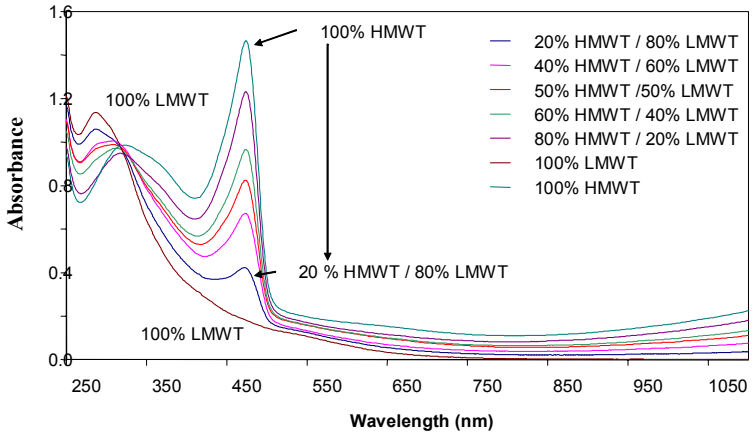

Figure 5.2. UV-visible spectra of various aqueous mixtures of high and low molecular weight PMAS (total [PMAS] = 2.4 x 10^{-3} M in each case).

Effect of pH

The natural pH of aqueous HMWt PMAS was *ca.* pH 3.5. In more acidic aqueous solution (1.0 M HCl) the π-π^* band shifted to 296 nm (Figure 5.3b), while the position of all other peaks remained unchanged (although decreased in intensity). This suggests only minor structural changes in the PMAS polymer chains, presumably arising from more extensive protonation of the sulfonate substituents on the polymer backbone.

However, in aqueous 1.0 M NaOH significant changes were observed in the spectrum of HMWt PMAS. As seen in Figure 5.3b, the π-π^* transition broadened and underwent a bathochromic shift to 358 nm, while the 472 nm polaron band disappeared. Additionally, the near infrared absorption disappeared and a new strong peak appeared at 750 nm. These observations are inconsistent with alkaline de-doping of PMAS to the emeraldine base form which would be expected to give rise to a characteristic exciton band at *ca.* 600 nm [29, 30]. Instead, they are suggestive of a change in conformation of the PMAS chain in aqueous NaOH to a compact coil arrangement [22]. Similar observations were noted for the dialysed (DPMAS) sample upon addition of NaOH (Figure 5.3a).

In contrast, LMWt PMAS and the pink oligomeric fraction was found to be inert to changes in pH. It exhibited only a single broad absorption band at *ca.* 282 nm in water, 1.0 M HCl and 1.0 M NaOH (Figure 5.3c). The slight increase in the intensity of 282 nm band in 1.0 M NaOH may possibly be due to trace impurities of the HMWt PMAS fraction.

(a)

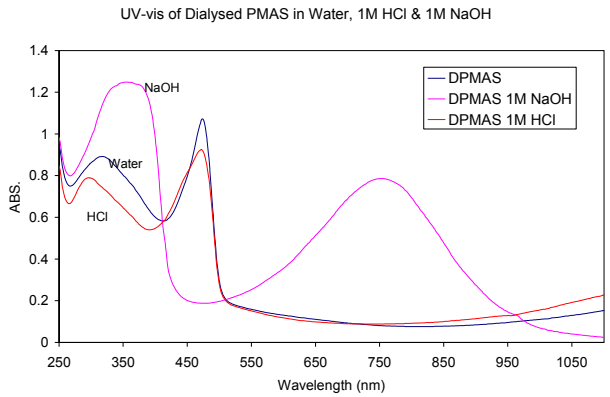

(b)

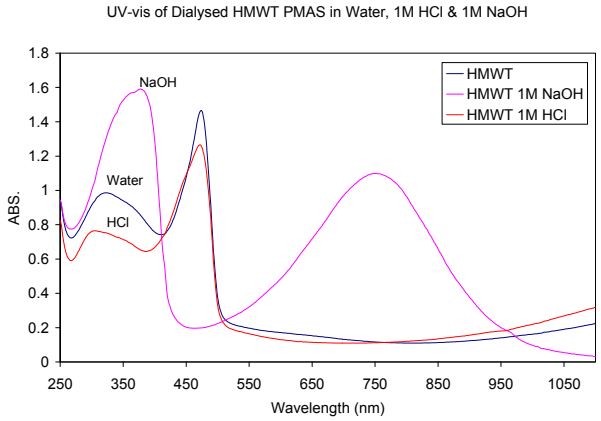

(c)

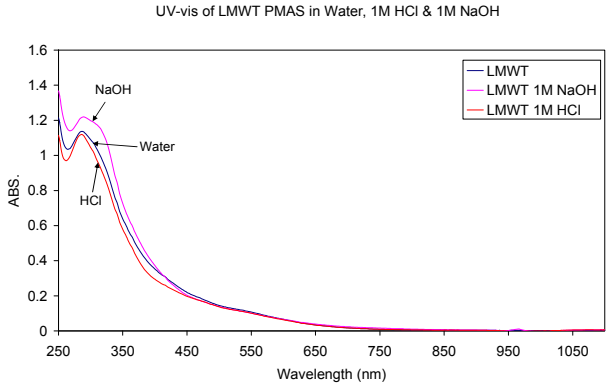

Figure 5.3. UV-vis spectra 0.024 mM solutions of : (a) dialysed PMAS, (b) high molecular weight PMAS and (c) low molecular weight PMAS in water, 1.0 M HCl(aq) and 1.0 M NaOH(aq).

Molar absorptivity of fractions (Beer-Lambert Equation)

Using the Beer-Lambert equation (eq. 1), it is possible to calculate the molar absorptivities of the pure PMAS fractions at various wavelength maxima.

$$A=\varepsilon bC \quad (1)$$

By recording the UV-visible spectra for PMAS at various concentrations (Figure 5.4), the absorption at 350 nm (A_{350}) and 473 nm (A_{473}) can be determined for each PMAS concentrations. Figure 5.5 shows that the relationship between the absorbance at 473 nm and PMAS concentration is linear over a wide concentration range up to 1.8 x 10^{-4} M, with a slight deviation from Beer's law at higher concentrations. Plotting A_{350} and A_{473} versus concentration results in a linear plot with slope of εb, in which b is the light path length, 1 cm. From the slope values of the linear plots shown in Figure 5.6, the molar absorptivities of HMWt PMAS at 350 nm and 473 nm were calculated and are summarised in Table 5.2.

The concentration of PMAS solutions therefore can be estimated using the Beer-Lambert equation by knowing the molar absorptivity and measuring the absorbance at the particular wavelength maximum.

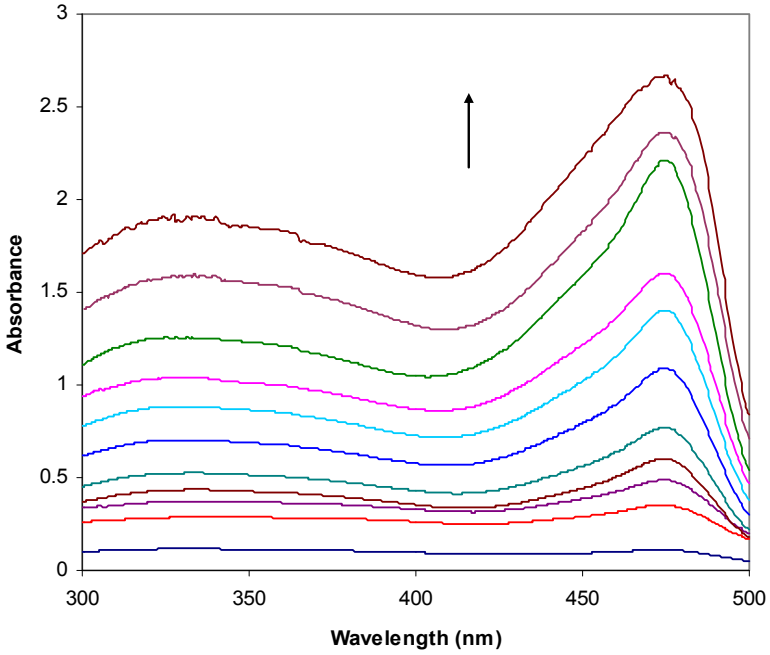

Figure 5.4. UV-vis spectra of aqueous HMWt PMAS at concentrations from 6×10^{-6} to 2.6×10^{-4} M.

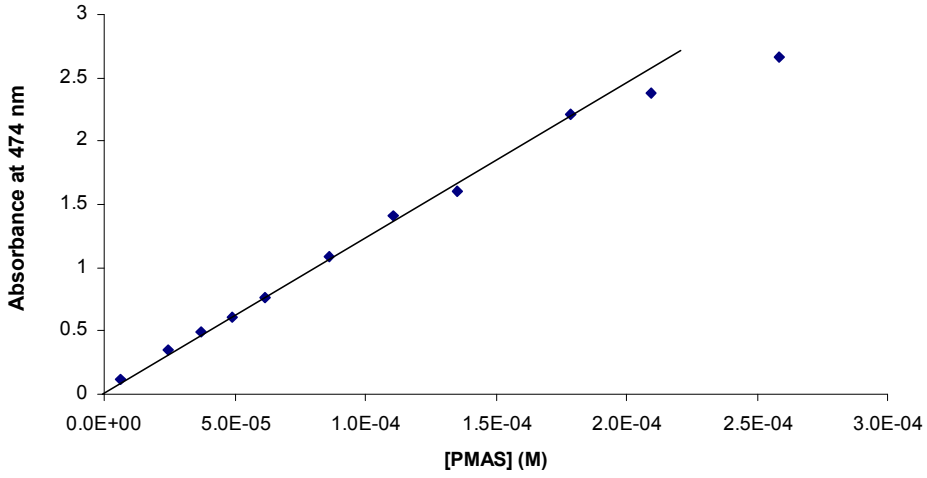

Figure 5.5. Calibration curve for HMWt PMAS and 474 nm maximum at concentrations from 6×10^{-6} to 2.6×10^{-4} M.

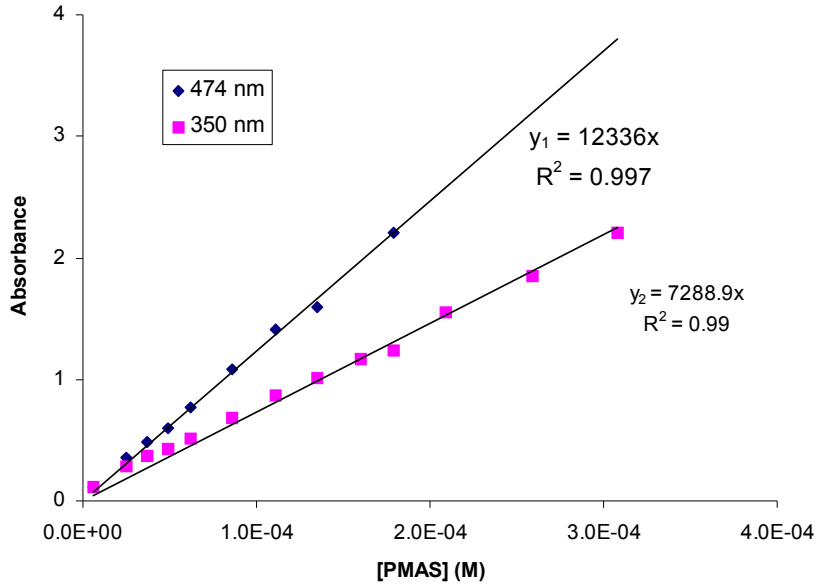

Figure 5.6. Calibration curve at 350 nm for HMWt PMAS at 350 nm maximum at concentrations from 6 x 10^{-6} to 2 x 10^{-4} M.

Table 5.2. Molar absorptivities of PMAS fractions at various wavelengths in aqueous solution.

Wavelength (nm)	Molar Absorptivity (M^{-1} cm^{-1})
474	**12,000**
350	**6,800**

Stejskal *et al.* [31] have reported an estimated absorption coefficient value of ε = 31,500 ± 1700 cm^2 per gram of PAn.HCl emeraldine salt for the absorption maximum between 380 and 420 in 1.0 M hydrochloric acid.

When there is more than one absorbing species in the solution, A is the sum of the absorbances for each individual compound.

$$A=A_1+A_2+A_3= b\,(\varepsilon_1 C_1 + \varepsilon_2 C_2 + \varepsilon_3 C_3) \qquad (2)$$

The composition of a mixture of PMAS fractions can be determined by using two or more wavelengths and by knowing the molar absorptivity of all fractions at each wavelength. These wavelengths are usually the λ_{max} of the individual compounds and cannot be an isosbestic point for any pair of species. Choosing these wavelengths in the spectra of PMAS fractions in water is difficult since the fractions have similar absorbance in some areas. At the λ_{max} of HMWt PMAS, other fractions absorb light. Moreover, the absorption spectra of LMWt PMAS and pink oligomeric fractions are similar. The ideal wavelength to choose is a wavelength maximum for a fraction at which the absorption of the other fractions is nearly zero. These requirements are found in the spectra of the fractions in alkaline solution. HMWt PMAS in 0.02 M NaOH (pH~12) shows an absorbance band at 740 nm and the other fractions have no significant absorption at this wavelength (Figure 5.7).

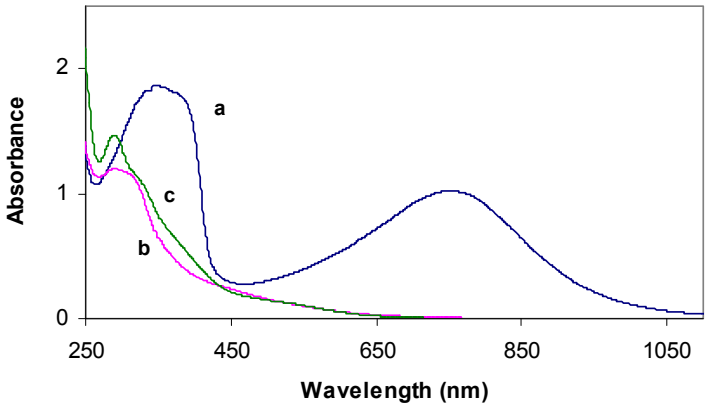

Figure 5.7. UV-vis spectra of (a) HMWt PMAS (50 µg/mL), (b) LMWt PMAS (40 µg/mL) and (c) pink oligomeric fraction (80 µg/mL) in 0.02 M NaOH (pH~12) after standing for 1 hour.

Based on these considerations, the three wavelengths 750, 340 and 290 nm were selected and the calibration curves at these wavelengths were obtained for PMAS

fractions in aqueous 0.02 M NaOH (Figure 5.8-10). Molar absorptivities of PMAS fractions at different wavelengths were determined from slopes of the Beer-Lambert plots (Table 5.3). It should be noted that since the spectral changes of PMAS in alkaline NaOH solution are completed over one hour, the absorbance values of the PMAS fractions were recorded after the fraction was treated with 0.02 M NaOH for one hour.

Table 5.3. Molar absorptivities of PMAS fractions at different wavelengths in 0.02 M NaOH aqueous solution.

Wavelength (nm)	**Molar Absorptivity (M^{-1} cm^{-1})**		
	HPMAS	**LPMAS**	**Pink oligomers**
290	**10,700**	**11,400**	**7,200**
340	**15,000**	**7,400**	**4,600**
750	**8,400**	**80**	**20**

The practical use of this is shown in the example discussed below. The UV-vis spectrum of PMAS dialysed by conventional dialysis tubing (DPMAS) was comprised of HMWt PMAS and LMWt PMAS fractions, as confirmed by GPC (see Chapter 3). In this instance, the contribution of the "pink oligomeric" fraction is considered to be nil as it was effectively removed via dialysis tubing. The UV-vis spectrum of this sample was recorded in 0.02 M NaOH after standing for one hour. The absorbance values at 290 nm (A_{290}=1.66) and 750 nm (A_{750}=1.087) were extracted from the spectrum and substituted in Eqn. 2, where a and b refer to the HMWt PMAS and LMWt PMAS fractions, respectively.

$$A_{290} = A_{a,290} + A_{b,290} = b\,(\varepsilon_{a,290}\,C_a + \varepsilon_{b,290}\,C_b) \qquad (3)$$

$$A_{750} = A_{a,750} + A_{b,750} = b\,(\varepsilon_{a}\,C_{a,750} + \varepsilon_{b,750}\,C_b) \qquad (4)$$

Since the molar absorptivity of LMWt PMAS at 750 nm is very low compared to HMWt PMAS, the absorption observed at 750 nm can be attributed to HMWt PMAS

alone. The term "$\varepsilon_{b,750}\ C_b$" can then be ignored and the concentration of HMWt fraction is easily calculated from Eqn. 4. The concentration of LMWt PMAS can be calculated from Eqn. 3.

Following the above calculation, the composition of DPMAS was estimated to be 84 % w/w HMWt PMAS and 16 % w/w LMWt PMAS.

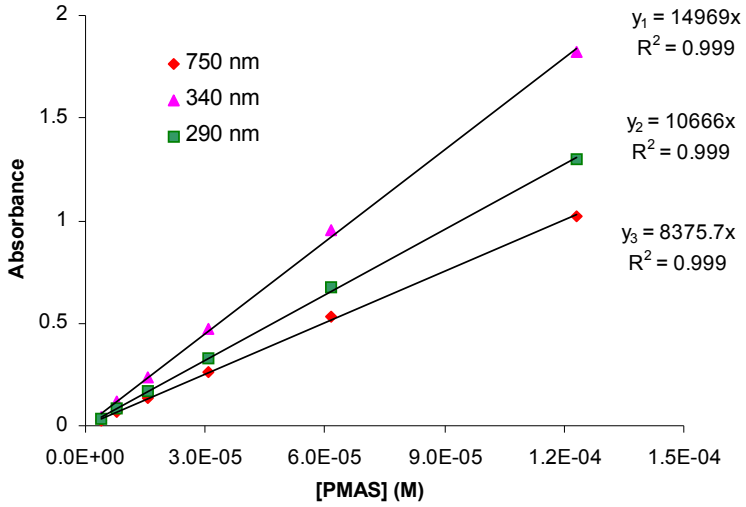

Figure 5.8. Calibration curve for high molecular weight PMAS at different wavelengths: 750 nm(♦), 340 nm (▲) and 290 nm(▪). Concentrations 3.8 x 10^{-6} to 1.2 x 10^{-4} M.

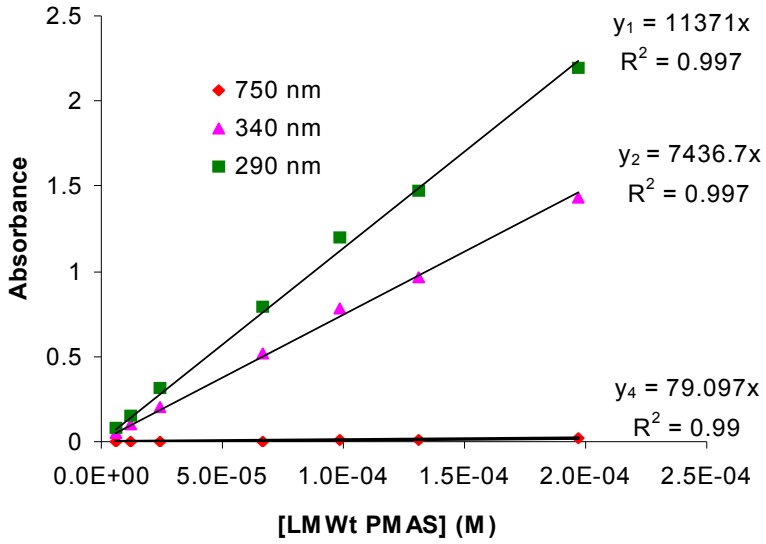

Figure 5.9. Calibration curve for brown colored oligomer at different wavelengths: 750 nm(♦), 340 nm (▲) and 290 nm(▪). Concentrations 6 x 10^{-6} to 2 x 10^{-4} M.

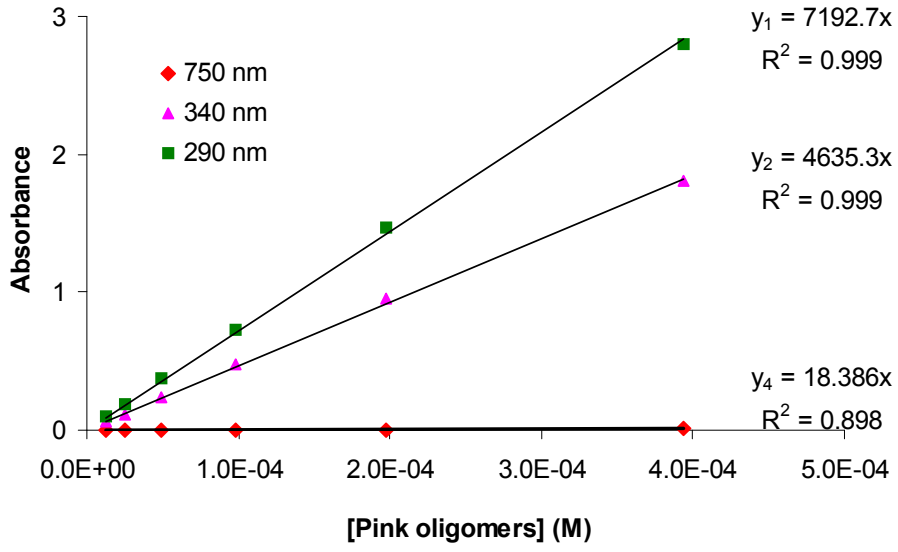

Figure 5.10. Calibration curve for pink colored oligomer at different wavelengths: 750 nm(♦), 340 nm (▲) and 290 nm(▪). Concentrations 1.2 x 10^{-5} to 4 x 10^{-4} M.

5.3.2 Electroactivity of fractions

Polyaniline is unique among inherently conducting polymers in that it has three readily accessible oxidation states. Similar behavior is confirmed here for fully sulfonated polyaniline HMWt PMAS.

5.3.2.1 Chemical oxidation and reduction

Treatment of aqueous HMWt PMAS emeraldine salt solution (0.024 mM) with 0.10 M ammonium persulfate resulted in the disappearance of the absorbance bands of the original emeraldine salt, over a 30 min period, and their replacement by new bands at *ca.* 290 and 550 nm (Figure 5.11). These peaks are very similar to those reported previously for the oxidation of unsubstituted polyaniline emeraldine salt [32, 33], indicating oxidation of HMWt PMAS to the fully oxidised pernigraniline form.

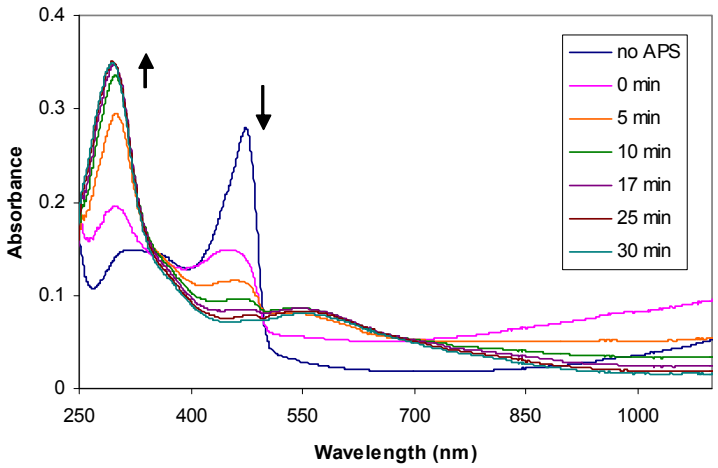

Figure 5.11. UV-vis spectral changes upon oxidation of 10 µg/mL (0.024 mM) aqueous HMWt PMAS emeraldine salt to pernigraniline base using 0.10 M ammonium persulfate.

Reduction of HMWT PMAS was similarly readily achieved by treatment with 0.10 M hydrazine hydrate. As seen in Figure 5.12, within 1 min the bands of the original emeraldine salt were replaced by a new strong band at 405 nm and a shoulder at *ca.* 315 nm. Interestingly, this spectral behaviour upon reduction of sulfonated HMWt PMAS is

different to that reported for unsubstituted polyaniline emeraldine salt, where the leucoemeraldine base product shows only a single peak at *ca.* 320 nm. In other studies [19], it has been demonstrated that the ratio of the 405 nm and 315 nm reduction products for PMAS are very sensitive to the temperature and solvent employed, suggesting reversible interconversion of PMAS leucoemeraldine base between two conformations.

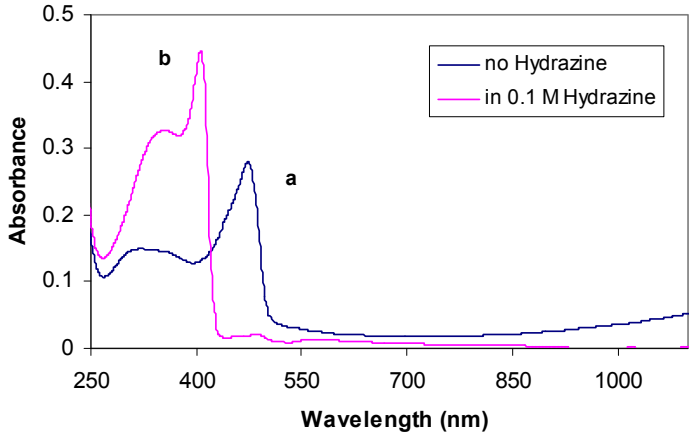

Figure 5.12. UV-vis spectral changes after treating aqueous 10 µg/mL HMWt PMAS with 0.10 M aqueous hydrazine for 1 min.

The above ability of the HMWt PMAS fraction to undergo facile oxidation and reduction provides strong evidence that it is indeed in the emeraldine salt state of the polymer. This is further confirmed with cyclic voltammetry studies.

In contrast, aqueous LMWt PMAS and the pink oligomeric fraction underwent negligible UV-vis spectral changes upon similar treatment with either 0.10 M ammonium persulfate (Figure 5.13) or 0.10 M hydrazine (Figure 5.14), i.e. they are redox inactive. This shows conclusively that the oligomeric form of PMAS is not an emeraldine salt. This result, together with the insensitivity of LMWt towards acid and base (see Figure 5.3c) explains why mixtures of LMWt and HMWt PMAS, as in commercially available PMAS or samples that have been subjected to standard dialysis (e.g DPMAS), exhibit similar UV-vis spectral changes upon redox and alkaline treatment [17, 34] to that found here for pure HMWt PMAS.

The redox inactivity of LMWt and oligomers of PMAS is in contrast with parent aniline tetramer and pentamer [27] or phenyl-capped aniline heptamer [35]. These para-coupled aniline oligomers showed electroactivity towards oxidation and reduction. This suggests that the LMWt fractions of PMAS may be formed by different types of ring couplings, e.g. *ortho* or *meta*, resulting in the loss of electroactivity.

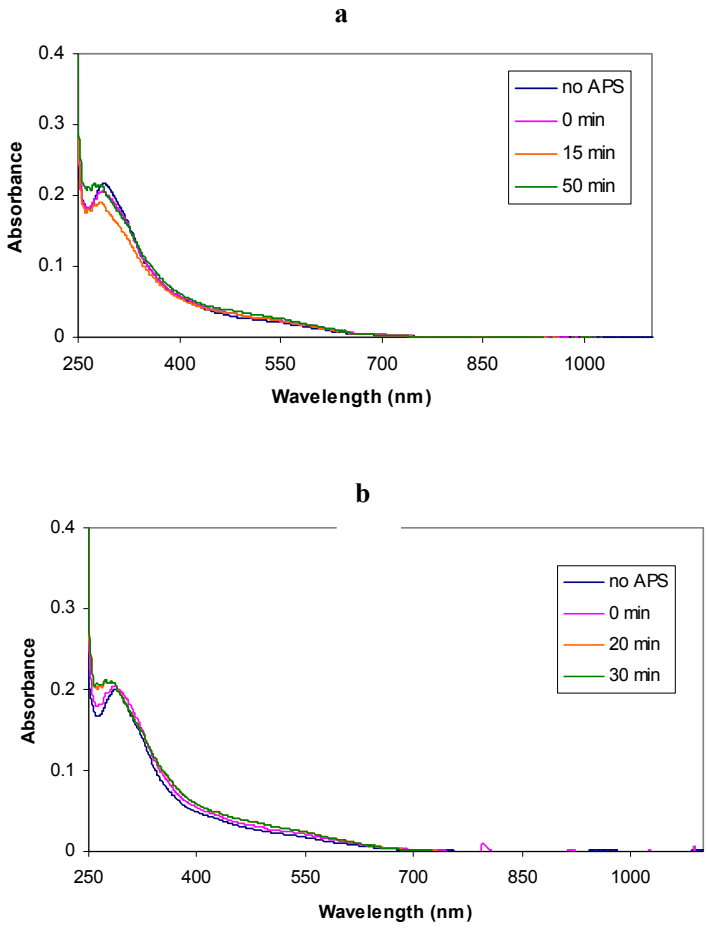

Figure 5.13. UV-vis spectral changes after treating a 10 µg/mL aqueous solution of (a) LMWt PMAS and (b) pink oligomeric fractions with 0.10 M aqueous ammonium persulfate.

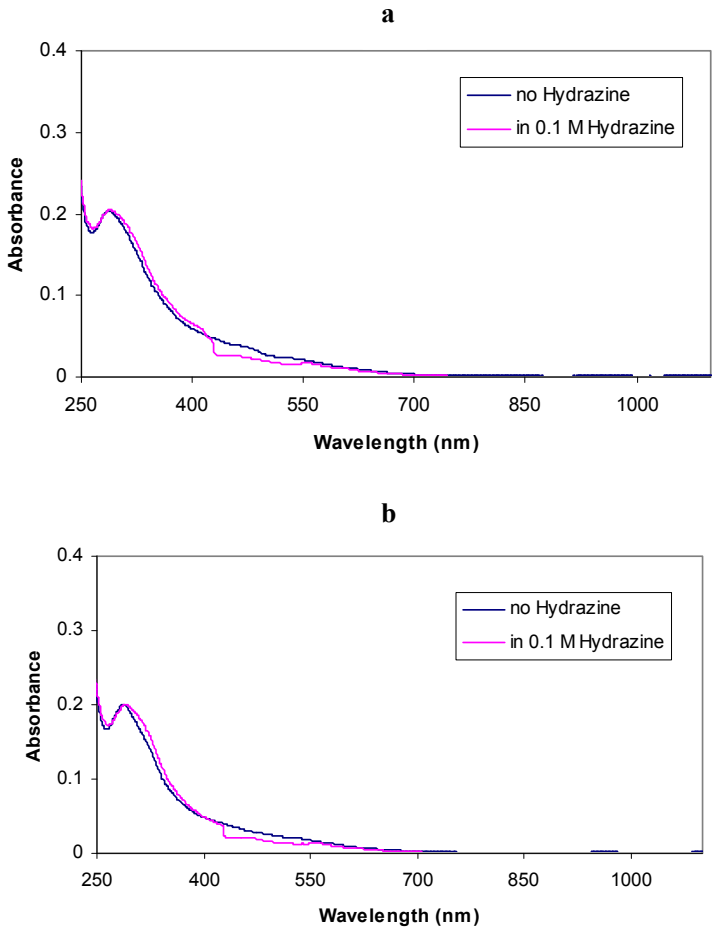

Figure 5.14. UV-vis spectral changes after treating a 10 µg/mL aqueous solution of (a) LMWt PMAS and (b) pink oligomeric fractions with 0.10 M aqueous hydrazine for 1 min.

5.3.2.2 Cyclic voltammetry of PMAS

Electroactivity of the HMWt PMAS, dialysed PMAS (DPMAS) and LMWt PMAS aqueous solutions was further investigated by cyclic voltammetry (CV).

The cyclic voltammogram of an aqueous solution of HMWt PMAS (0.5 mg/mL=0.05% w/v) at a glassy carbon electrode showed three redox couples (Figure 5.15). The anodic peaks were observed at 0.08, 0.55 and 0.78 V, with the corresponding cathodic peaks at

-0.11, 0.26 and 0.65V. The middle peak appears to be a combination of two peaks. Similar results with slightly less-defined peaks were obtained for DPMAS (Figure 5.15).

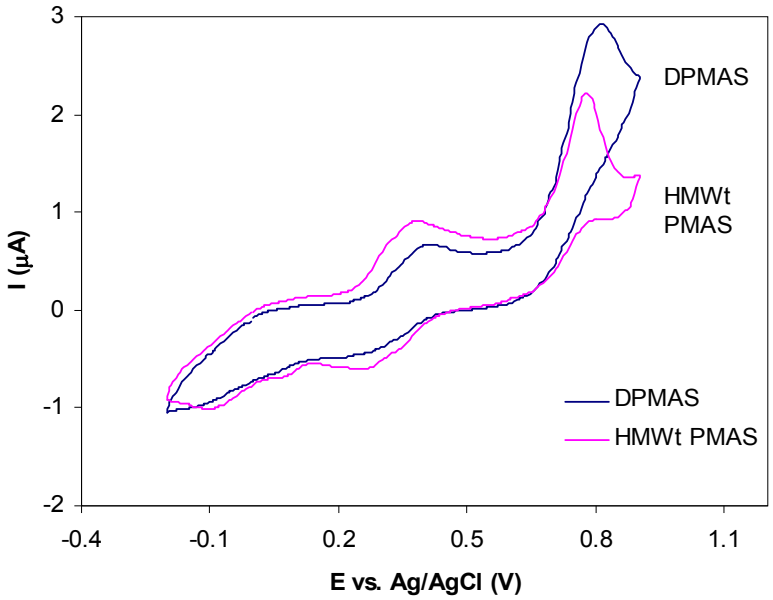

Figure 5.15. Cyclic voltanmmograms of dialysed PMAS (DPMAS) and pure HMWt PMAS aqueous solutions (0.5 mg/mL). Scan rate 20 mV/s, second scan.

As seen in the chemical oxidation and reduction of the PMAS fractions (Section 5.3.5.1), the CVs confirmed that the HMWt PMAS and DPMAS are redox active. The impurity of redox inactive LMWt PMAS in DPMAS had no major effect on the electroactivity of the PMAS, except in smoothing the peaks and reducing the current to some extent (see Figure 5.15).

5.3.2.2.1 Effect of electrolyte on cyclic voltammograms of PMAS

PMAS is a polyelectrolyte with its ionic conductivity dependent on concentration. A 0.5 mg/mL aqueous PMAS solution has an ionic conductivity of 2.98 µS/cm (the conductivity of deionised water is 0.18 µS/cm). The cyclic voltammetry of PMAS was further investigated with the addition of supporting electrolytes to increase the ionic strength (*I*) and the conductivity of the solution for electrochemical reactions. The

conductivity of a 1.0 M NaCl(aq) solution is 1.068 x 10^5 µS/cm. The effect of supporting electrolyte concentration on the CV of PMAS is shown in Figure 5.16. The oxidation peak in the range 0.3-0.5 V was partially resolved into two peaks in the presence of 0.10 M $NaNO_3$ (I = 0.10 M) and completely resolved in the presence of 1.0 M $NaNO_3$ (I =1.0M). The CV of PMAS(aq) was also recorded in 1.0 M NaCl and 1.0 M Na_2SO_4. The CVs obtained in these latter electrolytes were similar (Figure 5.17); however the peaks were shifted to negative potentials in 1.0 M Na_2SO_4. Shifting the second oxidation peak towards negative potentials has also been reported for a parent polyaniline film upon potential cycling in H_2SO_4 solution [36]. The enhanced current responses were a result of the higher concentrations of supporting electrolyte carrying the bulk of the charging current between the counter and working electrodes, rather than relying on the analyte (PMAS) being responsible for the mass transport processes within the cell.

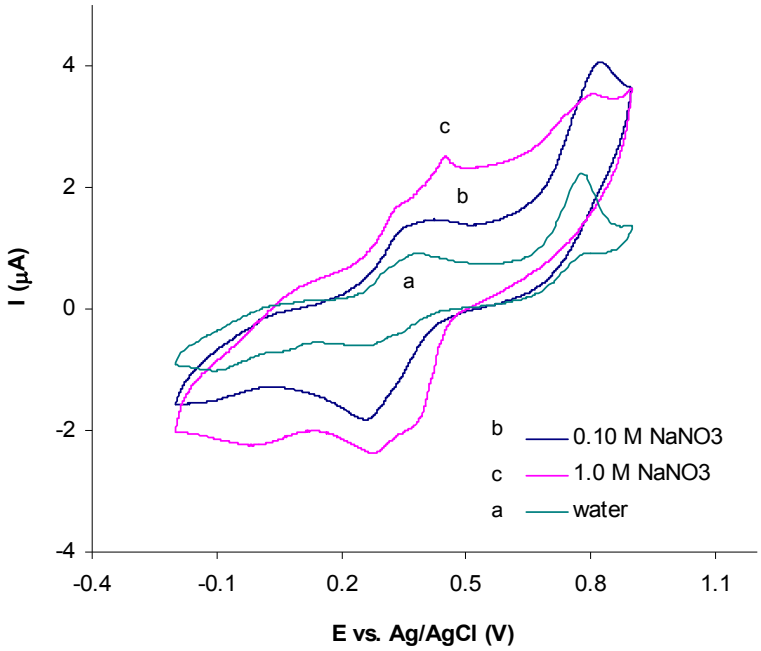

Figure 5.16. Effect of electrolyte concentration, (a) 0.0 M, (b) 0.1 M and (c) 1.0 M $NaNO_3$, on the CV of aqueous PMAS (0.5 mg/mL). Scan rate 50 mV/s; second cycle.

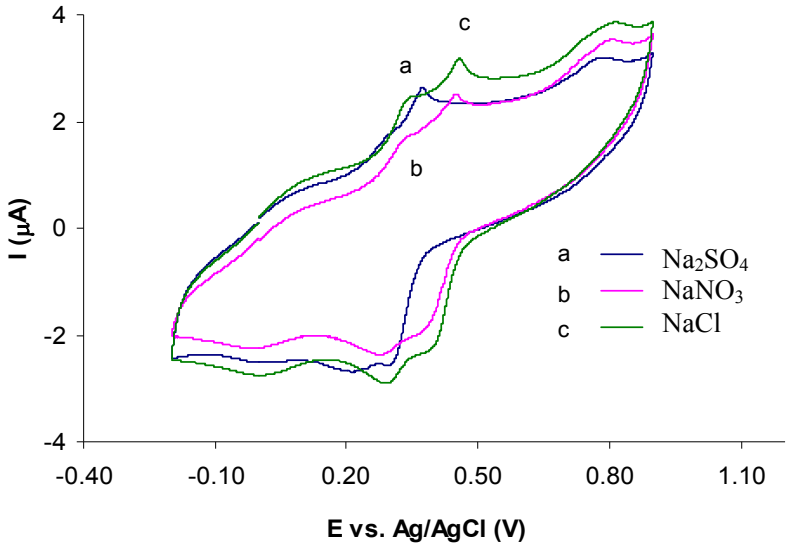

Figure 5.17. CV of aqueous PMAS (0.5 mg/mL) in 1.0 M of various electrolytes (pH~3.5), (a) Na_2SO_4, (b) $NaNO_3$ and (c) NaCl. Scan rate 50 mV/s. Second cycle.

5.3.2.2.2 Scan rate dependence studies

In order to further investigate the electrochemistry of PMAS, the scan rate dependence of the current magnitudes observed during cyclic voltammetry was determined. In a Nernstian system, the reversibility of the electrochemical reaction, the number of electrons involved and the diffusion constant of the redox material can be determined using Equation 5. The peak current, i_p, in amperes for a Nernstian reaction is defined as

$$i_p = (2.69 \times 10^5) n^{3/2} A D^{1/2} \nu^{1/2} c_0 \qquad (5)$$

where n is the number of electrons in the reaction, A (m^2) is the area of the electrode, ν (Vs^{-1}) is the sweep rate of the voltage, D (m^2 s^{-1}) is the diffusion coefficient and C_0 (mol m^{-3}) is the concentration of the reactant. From the above relationship it can be seen that i_p varies linearly with the square root of the sweep rate. If the effective surface area of the electrode (A) is known, the diffusion constant can consequently be determined from the slope.

Measuring the effective surface area of glassy carbon electrode using potassium ferrocyanide K_4 Fe CN_6

Potassium ferrocyanide is a simple system which has one redox couple in its cyclic voltammogram. By plotting i_p as a function of square root of the sweep rate in this system, the (effective) area of the electrode can be obtained from the slope.

To measure the electrochemically active surface area of the glassy carbon electrode using the above equation, cyclic voltammograms of a 5.56 mM potassium ferrocyanide in 1.0 M Na_2SO_4 were recorded at different scan rates (Figure 5.18a) and i_p was plotted against the square root of the sweep rate. A slope of 0.0002 $A/(Vs^{-1})^{1/2}$ was obtained from the linear plot (Figure 5.18b). The diffusion coefficient for potassium ferrocyanide at the concentration of 5.56 mM is 1.178 x 10^{-5} cm^2 s^{-1}. Considering n=1 in the redox reaction of ferrocyanide, the surface area of the glassy carbon electrode was calculated from the slope to be 0.039 cm^2. This value is smaller than the geometrical surface area of the electrode which was ~0.07 cm^2.

(a)

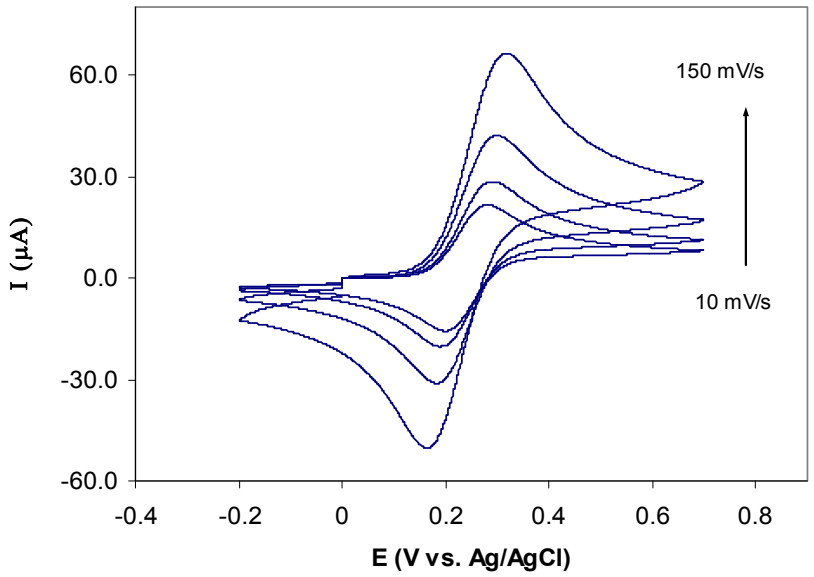

(b)

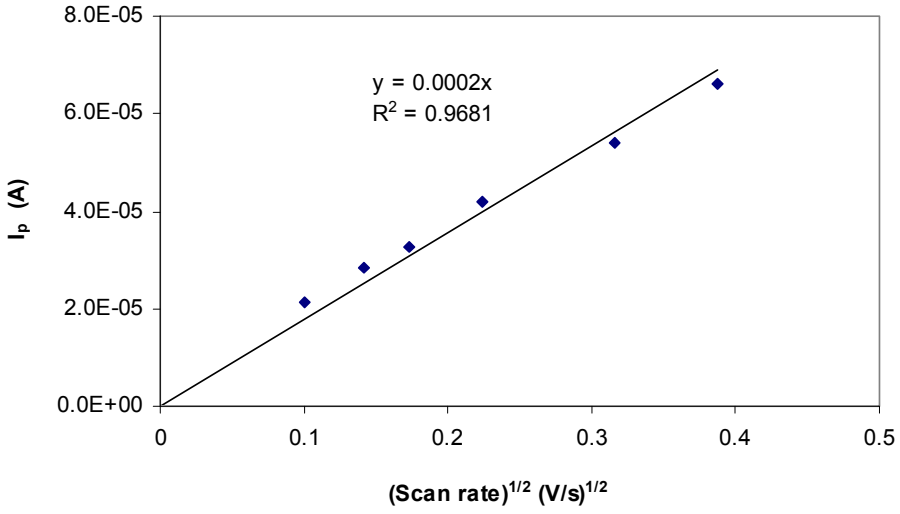

Figure 5.18. (a) Cyclic voltammograms of 5.56 mM $K_4Fe(CN)_6$ in 1.0 M Na_2SO_4 on a glassy carbon electrode in the potential range –0.2 to 0.6 V using 10, 20, 50 and 150 mV/s scan rates. (b) Plot of peak current against square root of sweep rate (0.01, 0.02, 0.03, 0.05, 0.1 and 0.15 V/s) in the cyclic voltammograms of potassium ferrocyanide.

Measuring the diffusion coefficient of PMAS

As seen earlier in this section, the cyclic voltammograms of PMAS in electrolytes such as inorganic sodium salts showed well-defined redox peaks due to redox reactions of PMAS. To further explore the electrochemical reactions of PMAS, the scan rate dependence of the system was studied and the diffusion constant of 0.05% (w/v) (1.2 mM) PMAS was calculated using Equation 5.

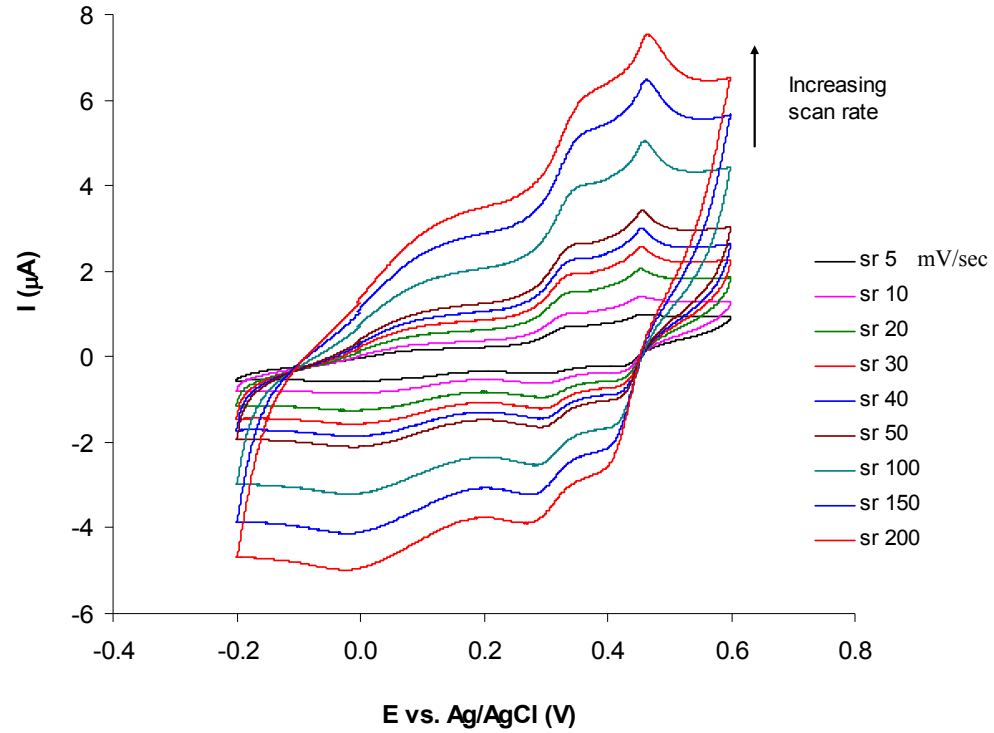

Figure 5.19. Cyclic voltammograms of aqueous 0.5 mg/mL PMAS in 1.0 M NaCl at different scan rates (5 to 200 mV/sec).

In linear sweep voltammetry (LSV), if the position of the peak does not vary with sweep rate and if the difference between the anodic and cathodic peaks is a multiple of 0.059 V, the reaction is said to be reversible and we can find the number of electrons in the reaction according to Equation 6.

$$E_{p,a} - E_{p,c} = 2.303\ R\ T/nF = 0.059/n \qquad (6)$$

The cyclic voltammetry of 0.05% (w/v) (1.2 mM) aqueous PMAS in 1.0 M NaCl was carried out at a glassy carbon electrode using different potential sweep rates (Figure 5.20). Three redox couples were observed with anodic potentials of ~0.10 V, 0.35 V, and 0.46 V and the corresponding cathodic peaks at -0.02 V, 0.28 V, and 0.41 V. The peak at 0.46 V was sharp; where as the peak at 0.10 V was weak and broad.

The reversibility and the number of electrons involved in the reactions occurring at E_p (anodic) = 0.35 V and E_p (anodic) = 0.35 V were investigated. The anodic and corresponding cathodic peak, and their separation, were measured at different sweep rates (Table 5.4 and). The peaks are seen to be separated by ~0.04 -0.07 V and their positions are approximately constant with varying scan rate. Given that PMAS is a macromolecular system with diffusional restriction in solution the deviation from an idealised 59 mV was not unexpected. These observed redox processes were therefore considered to be single electron reversible process. In addition, for these reversible reactions the plots of peak anodic current versus square root of the scan rate were linear (Figure 5.20). The slopes of the linear plots were measured as 6.0×10^{-6} $A/(Vs^{-1})^{1/2}$ and 3.0×10^{-6} $A/(Vs^{-1})^{1/2}$, respectively, for E_p (anodic) = 0.35 and E_p (anodic) = 0.46. Using these slopes in Equation 5, in which the surface area of the GC electrode was previously measured (0.039 cm^2), the diffusion constant (D) for 0.05% (w/v) (1.2 mM) PMAS was calculated as $D = (1.4 \pm 0.9) \times 10^{-7}$ $cm^2 s^{-1}$.

The origin of these multiple redox waves in solution is not fully understood. The more extensive solvation and/or greater conformational flexibility of the solution phase polymer may result in resolving individual one electron transfer steps [20].

Table 5.4. Effect of scan rate on redox peak at E_p (anodic) = 0.35 V of aqueous 1.2 mM PMAS in 1.0 M NaCl.

Scan rate (mV/s)	E_p (anodic) (V)	E_p (cathodic) (V)	{E_p (anodic)- E_p (cathodic)} (V)
5	0.34	0.29	0.05
10	0.34	0.29	0.05
20	0.35	0.30	0.05
30	0.35	0.29	0.06
40	0.35	0.29	0.06
50	0.35	0.29	0.06
100	0.35	0.28	0.07
150	0.36	0.28	0.08
200	0.36	0.27	0.09

Table 5.5. Effect of scan rate on redox peak at E_p (anodic) = 0.46 V of aqueous 1.2 mM PMAS in 1.0 M NaCl

Scan rate (mV/s)	E_p (anodic) (V)	E_p (cathodic) (V)	{E_p (anodic)- E_p (cathodic)} (V)
5	0.456	0.41	0.046
10	0.455	0.41	0.045
20	0.454	0.41	0.044
30	0.455	0.41	0.045
40	0.456	0.41	0.046
50	0.457	0.41	0.047
100	0.460	0.40	0.060
150	0.463	0.40	0.063
200	0.466	0.40	0.066

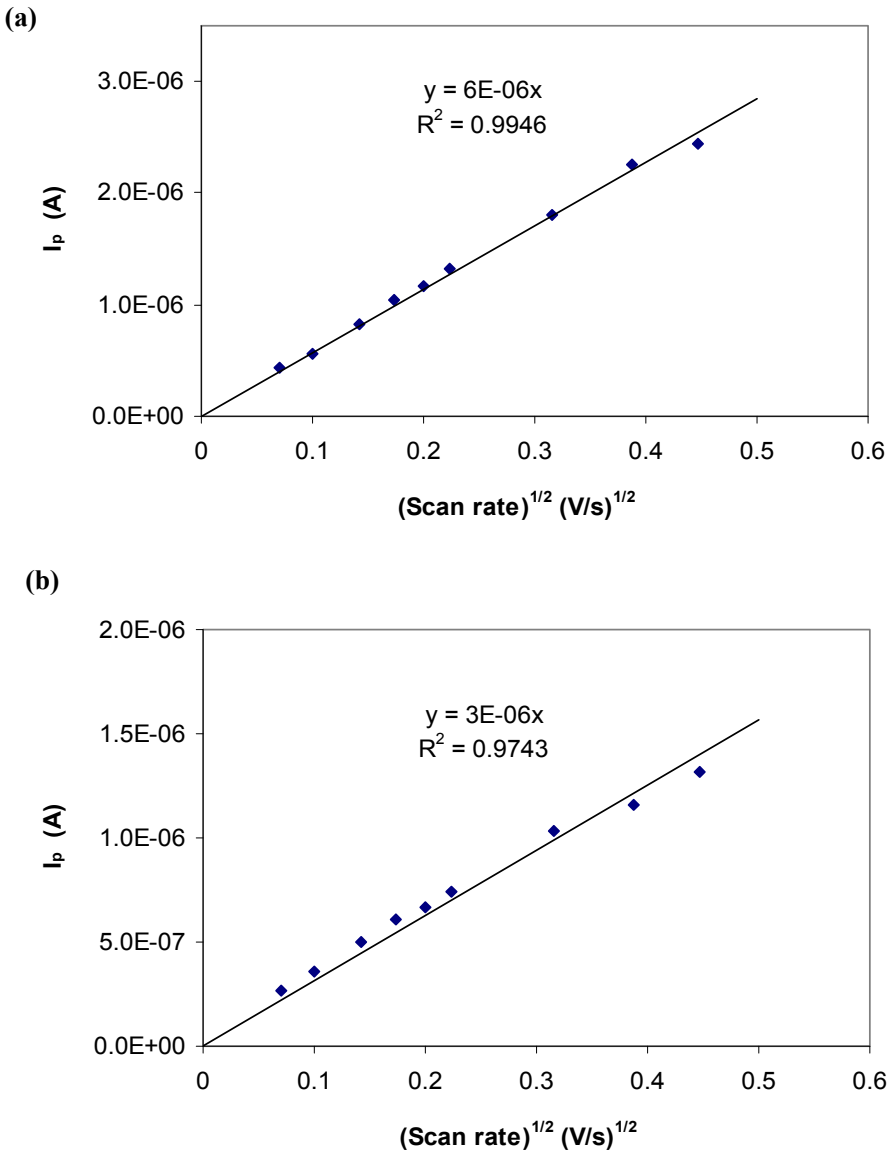

Figure 5.20. Plots of peak current against square root of sweep rate in the cyclic voltammograms of aqueous 0.5 mg/mL PMAS in 1.0 M NaCl (scan rates 5 to 200 mV/s) at (a) E_p (anodic) = 0.35 V, and (b) E_p (anodic) = 0.46 V (see Figure 5.19).

Effect of pH on the CV of HMWt PMAS

Cyclic voltammograms were recorded at different pH solutions. Since PMAS showed a well-defined redox peaks in the presence of a supporting electrolyte, in these experiments the PMAS was dissolved in 1.0 M NaCl (a final pH 3.5) and the pH was further adjusted with HCl and NaOH.

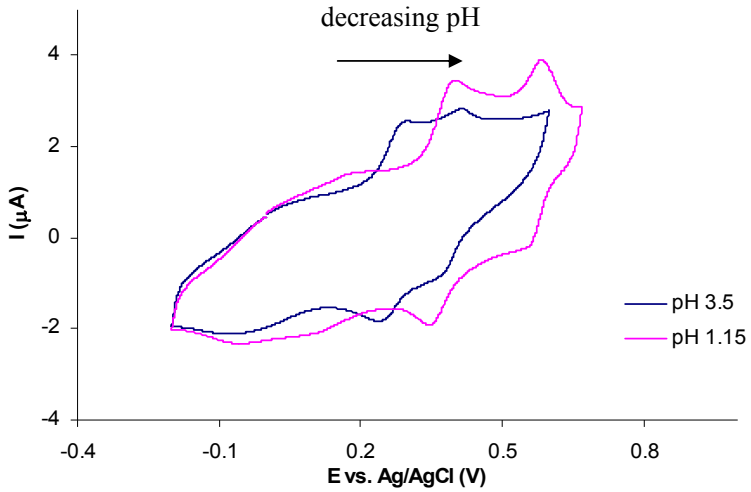

Figure 5.21. CV of PMAS aqueous solution (1.0 mg/mL) in 1.0 M NaCl (pH 3.5) and after pH dropped to 1.15 by addition of a few drops HCl 3M. Scan rate 50 mV/s. Second cycle.

The cyclic voltammograms obtained using PMAS in 1.0 M NaCl (pH 3.5) and after the pH decreased to 1.15 are shown in Figure 5.21. The oxidation peaks at 0.31 and 0.43 V were shifted positive to 0.41 and 0.6 V at pH 1.15. The peak at 0.43 V showed more shift to positive potentials and a better separation was indeed observed in the redox peaks.

The multiple redox peaks in Figure 5.21 were no longer observed when the CV of PMAS was recorded in neutral media (Figure 5.22); however, an anodic peak at 0.18V and a corresponding cathodic peak at -0.04V were clearly observed at pH 7.15.

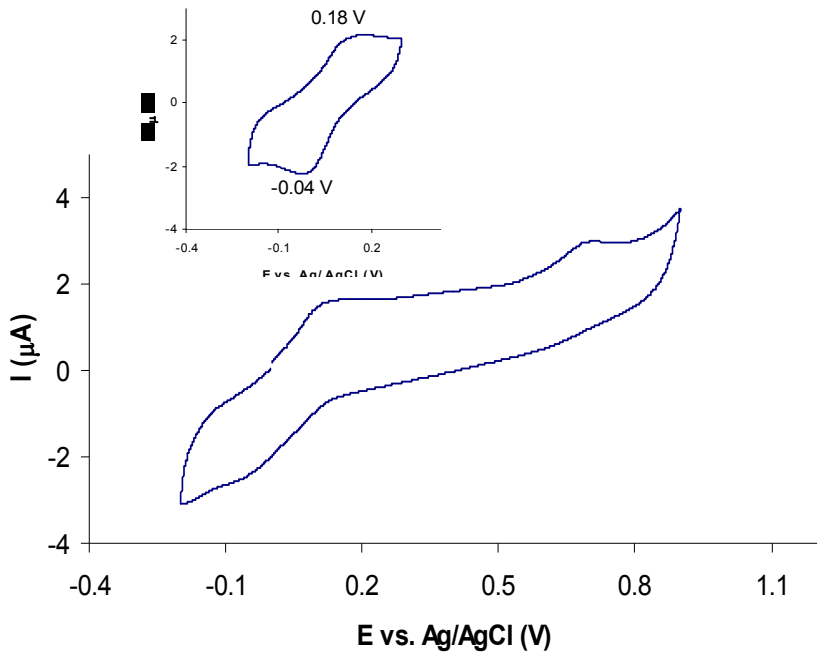

Figure 5.22. CV of aqueous PMAS solution (1.0 mg/mL) in 1.0 M NaCl after pH was increased to 7.15 by addition of a few drops of 3.0 M NaOH. Scan rate 50 mV/s. Second cycle.

The results show that PMAS is electroactive in acidic and neutral aqueous solutions. The first redox peak was observed in acid and neutral solutions with slight shift to negative potentials with pH. This shows that this process is not a proton transfer process. The disappearance of the peaks at 0.31 and 0.43 V in neutral solution indicates that protons participate in these redox reactions. Similar pH dependence behavior was recently reported for a PMAS-PLL complex film [19, 23]

5.3.3 Thermal analysis of PMAS fractions

Oligomer impurities had no significant effect on the thermal behaviour of PMAS (Figure 5.23). Thermogravimetric analysis (TGA) of HMWt PMAS polymer and LMWt PMAS oligomer (Figure 5.23 and Figure 5.24) showed that in each case weight loss occurred in two steps. The first weight loss observed between 100° and 150°C represents the removal of moisture adsorbed by the polymer powder. The major second weight loss (above 200°C) is due to decomposition of the sample. This result is in agreement with the themogravimetric analysis of SPAN reported by Chen and Hwang [2] in which the weight loss was attributed to the elimination of some sulfonic acid groups. The TGA of the three PMAS fractions separated by cross flow filtration (see Chapter 3) indicated that the pure HMWt PMAS, the LMWt PMAS and a pink oligomer fraction had decomposition temperatures of *ca.* 255°C, 285°C and 250°C, respectively (Table 5.5).

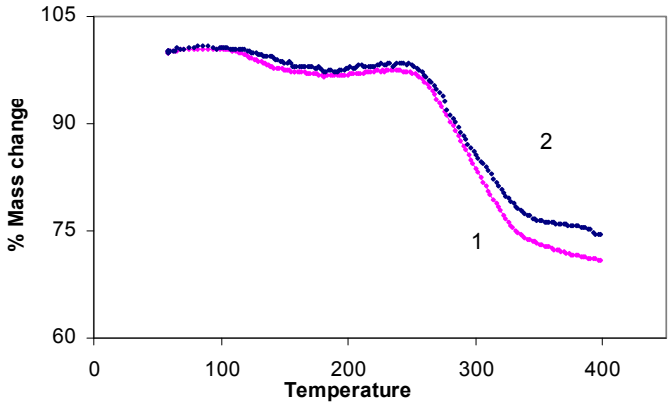

Figure 5.23. TGA curve of: (1) impure PMAS dialysed by tubing and (2) pure HMWt PMAS dialysed by cross flow membrane, using a heating rate of 10°C/min under nitrogen atmosphere.

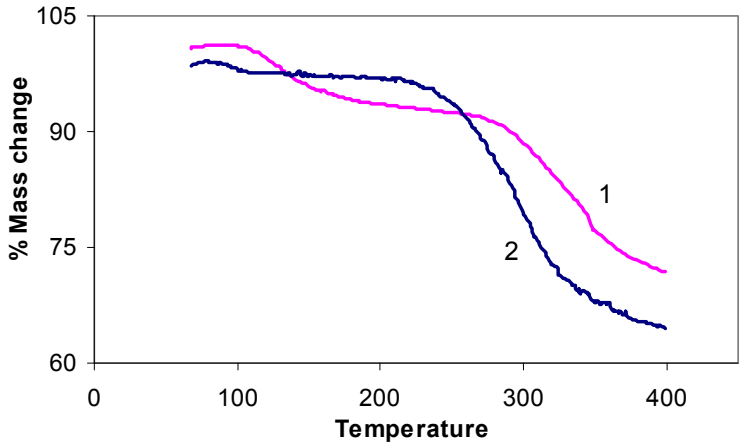

Figure 5.24. TGA curve of: (1) brown coloured LMWt PMAS oligomer, and (2) pink coloured oligomers, using a heating rate of 10°C/min under nitrogen atmosphere.

Table 5.6. Decomposition points of PMAS fractions

Fraction	Decomposition point (ºC)
HMWt PMAS	255
LMWt PMAS	285
Pink oligomers	250

Similar results were obtained using differential scanning calorimetry. The DSC thermograms of PMAS fractions were recorded using a scan rate of 10°C/min under N_2 atmosphere and are illustrated in Figure 5.25. Two endotherms were observed in the heating half-cycle. The first endothermic peak in the temperature range of 110-160°C is attributed to the vaporization of water and most probably ammonia associated with ammonium ions bound to the sulfonate groups of PMAS. The second endothermic peak can be attributed to melting and immediate degradation of HMWt and LMWt PMAS. This peak appeared at a higher temperature for LMWt PMAS (~280°C) compared to HMWt PMAS (~255°C), which is in agreement with the TGA results. No exotherm was observed in the cooling sweep indicating that the sample was decomposed in the heating sweep to 325°C.

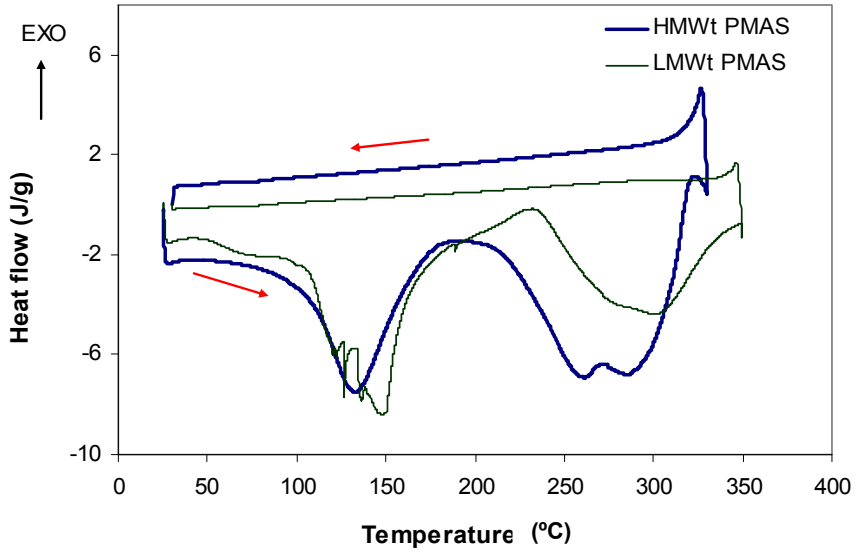

Figure 5.25. DSC thermal analysis curve of HMWt PMAS (thick line) and LMWt PMAS (thin line) under N_2 atmosphere.

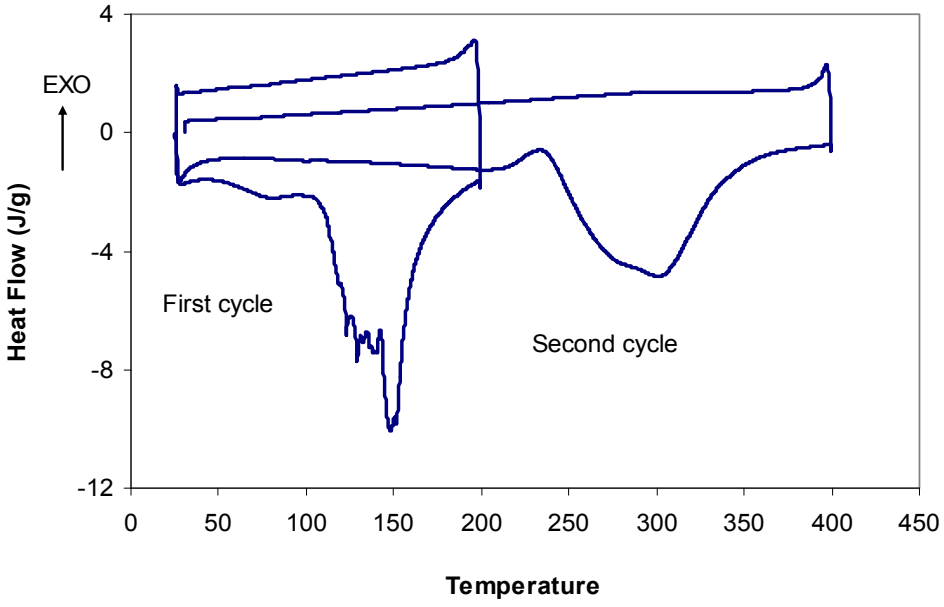

Figure 5.26. DSC thermal analysis curve of LMWt PMAS under N_2 atmosphere. The sample was heated to 200ºC in the first cycle and then to 400ºC in the second cycle at a heating rate of 10ºC/min.

In another experiment a sample of LMWt PMAS was heated to 200ºC in the first cycle and then heated to 400ºC. The first cycle (Figure 5.26) exhibited endothermic peak in the range 110-170ºC. This endothermic peak was no longer observed in the second cycle indicating that it was due to the vaporization of water or elimination of ammonia gas. A similar result was obtained for HMWt PMAS.

5.3.4 Elemental analysis of HMWt PMAS

The elemental analyses for pure HMWt PMAS are summarised in Table 5.6. The C/S molar ratio had the expected value of ~7, considering seven carbon atoms per each sulfur in the monomer unit of PMAS. However, the N/S ratio was found to be ~1.4 indicating excess nitrogen in the PMAS structure. This excess presumably comes from ammonium ions in the ammonia salt form of PMAS arising from the ammonia and ammonium persulfate used in the chemical polymerisation of MAS. In other words, the amount of N in the N/S ratio is the sum of the nitrogen atom along the chain (N_{amine}) and the nitrogen of the ammonium salt ($N_{ammonium}$) of PMAS.

$$N/S = (N_{amine} + N_{ammonium})/S = (S + N_{ammonium})/S = 1.397$$

$$N_{ammonium} = 0.4\ S$$

$$N_{ammonium} = 0.4\ N_{amine}$$

The results suggest that in the PMAS structure, *ca*. 80% of the free sulfonate groups along the chain are associated with ammonium ions (ammonium salt form of PMAS) and 20% are in the acid form. The ammonium ions can be exchanged by hydrogen ions (H^+) using a proton exchange resin. To further explore this, the pure HMWt PMAS was passed through a proton exchange resin twice before elemental analysis. The N/S ratio found for this (H^+) PMAS was found to be *ca*. 1 (Table 5.7). Under these conditions, all the ammonia ions were effectively exchanged by protons. Elemental analysis of the pure HMWt PMAS before and after passing through the proton exchange resin confirmed that it was partly in the ammonia salt form, with the excess of the nitrogen arising from ammonium ions associated with the free sulfonate groups of the PMAS. It should be noted that the ratio of the acid to ammonia salt forms of PMAS can be different from batch to batch and would be affected by the synthesis conditions.

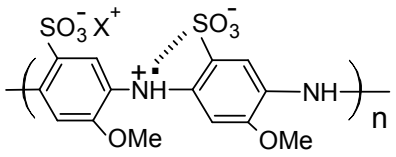

$X^+ = NH_4^+$ or H^+

Table 5.7. Elemental analysis of the pure HMWt PMAS (before proton exchange)

Specifications	%	Mole %	N/S ratio	C/S ratio
C	**36.71**	**3.06**		
H	**4.15**	**4.15**	**1.40**	**7.03**
N	**8.51**	**0.61**		
S	**13.92**	**0.435**		

Table 5.8. Elemental analysis of the pure HMWt PMAS after passed through the proton exchange resin.

Specifications	%	Mole %	N/S ratio	C/S ratio
C	**36.01**	**3.001**		
H	**3.99**		**0.972**	**7.08**
N	**5.77**	**0.412**		
S	**13.56**	**0.424**		

5.3.5 Conductivity of PMAS fractions

HMWt PMAS is conductive. As explained in the previous Chapter, the conductivity of PMAS depends on the synthetic conditions and lies in a range between 0.02-1.74 S/cm. The conductivities of LMWt PMAS (the filtrate from the 10 kDa MWCO membrane)

and the pink oligomeric fraction (the filtrate from the 5 kDa MWCO membrane) are less than 1 mS/cm (10^{-4} S/cm). Therefore the conductivity of PMAS is also affected by the extent of the low molecular weight impurities and increases upon dialysis and purification. It should be noted that pure HMWt PMAS has a conductivity about two fold higher than the dialysed PMAS (DPMAS).

5.3.6 ESR spectroscopy of PMAS fractions

ESR studies in the early 1960s have shown polyaniline to be paramagnetic [37]. The magnetic properties of polyaniline originate from radical cations (polarons with spin of 1/2) in the protonated form [38]. The ESR spectrum of polyaniline typically shows a single signal without hyperfine structure. The g value is *ca.* 2.003, close to that of a free electron [39-42]. A line width in the range 1-3 G has been reported for solid polyaniline PAn.HA emereldine salts [38, 43] and SPAN [44].

ESR spectra of aqueous PMAS fractions (2.5 mg/mL) are shown in Figure 5.27. PMAS exhibits a single signal without hyperfine structure similar to polyaniline with a g value of 2.00295 and a line width of ~2.55 G. The magnetic properties of HMWt PMAS are due to polaron spins (radical cations). X.-L. Wei *et al.* [44] have reported a g value of ~2.0026 for SPAN at room temperature, consistent with the presence of electrons that are unpaired and delocalised primarily on phenyl rings . This value increases to 2.003 at 70 K which is typical for hetero-atom systems, indicating localisation of spins at the nitrogen sites [44]. Considering the g value of PMAS (2.00295), the spins are apparently more localised on the nitrogen sites. This is presumably due to the electron-withdrawing nature of the sulfonate groups and steric strain induced by substituents on the phenyl ring increasing the torsional angle between the adjacent rings [44, 45]. The measured ESR spin intensity of aqueous PMAS was found to be much lower than that of an aqueous dispersion of PAn/HCl nanofibres (see Chapter 6). A magnetic and charge transport study of PMAS by Lee *et al.* [24] has shown that the density of states at the Fermi level, the density of Curie spin and room temperature conductivity, are smaller than for SPAN. The larger twist of the phenyl rings and increased interchain separation induced by the methoxy side groups of PMAS and the higher density of

sulfonate groups have been suggested as the origin of this lower density and conductivity favoring the formation and stabilisation of bipolarons.

The LMWt PMAS and pink oligomeric fractions showed no ESR signal, indicating that there were no paramagnetic polarons in LMWt PMAS and oligomeric fractions (Figure 5.27). It should be noted that the LMWt PMAS in this experiment was highly purified using 5 kDa and 10 kDa MWCO vivaspin membranes, as trace impurity of HMWt in this fraction results in a weak ESR signal. The absence of an electron spin in these materials is also consistent with their poor redox properties and electrical conductivity, as discussed above.

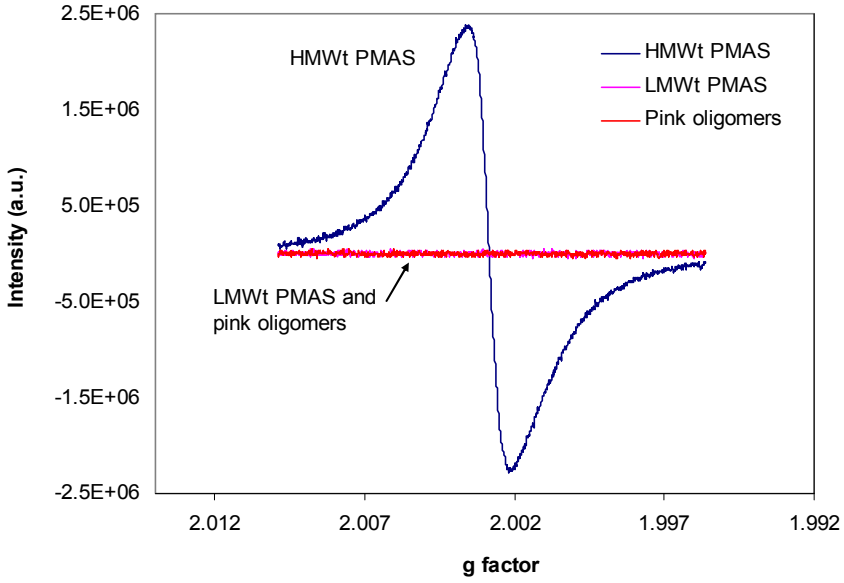

Figure 5.27. ESR spectra of aqueous solutions of PMAS fractions (2.5 mg/mL).

5.3.6.1 Effect of LMWt impurity on the conductivity and ESR of PMAS

Dialysed PMAS (containing *ca.* 20% LMWt PMAS) has a significantly lower electrical conductivity (typically 4 to 5 times less) than the purified HMWt PMAS fraction. This significant difference in electrical conductivity was probed by preparing mixtures (solid) of the conducting HMWt and non-conducting LMWt PMAS forms containing 0, 25, 50, 75 and 100% w/w HMWt. ESR, and electrical conductivity studies were performed on

these mixtures simulating the as-synthesised PMAS. Films of these mixtures were obtained by evaporative casting of 1 μL of 2.5 mg/mL onto an ESR flat quartz cell (for ESR measurements), or 30 μL of 50 mg/mL onto a glass slide (for conductivity measurements).

The HMWt fraction was observed to have a conductivity of 260 mS/cm while the 50:50 mixture had a conductivity of 2.6 mS/cm, considerably lower than would be expected for the addition of an insulating filler. Clearly, the LMWt fraction interacts strongly with the electronic structure of the HMWt PMAS in addition to functioning as insulating filler. ESR on films cast from these mixtures when compared to pure HMWt PMAS, at equivalent dilution levels, exhibited a lower level of electron spin in the presence of LMWt PMAS (Figure 5.28). This result suggests that the presence of the LMWt PMAS converts the HMWt PMAS from a high-spin polaron state into a low-spin bipolaron state. The chemical similarity of the LMWt and HMWt fractions would suggest that the non-electroactive LMWt fraction interacts strongly with the charge carriers in the HMWt PMAS, presumably via intercalating between adjacent HMWt PMAS chains via π-stacking, inhibiting intrachain charge transfer and resulting in the observed loss of electrical conductivity.

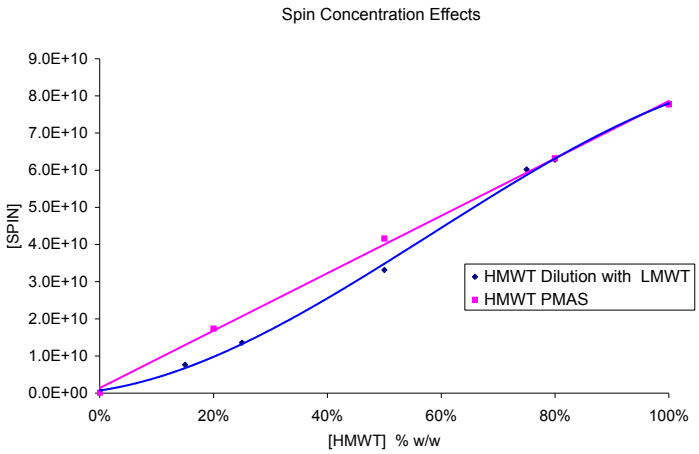

Figure 5.28. Spin concentration effects for mixtures (solid state) of HMWt and LMWt PMAS.

5.3.6.2 Effect of synthetic conditions on ESR spectra of PMAS

As explained in detail in Chapter 4, the physical properties of PMAS were significantly affected by synthetic conditions. For instance, oxidant concentration and addition rate had a major effect on the polymer properties such as electrical conductivity. In order to explore the paramagnetic properties of PMAS polymer and establish the relationship between conductivity and ESR parameters at different synthetic conditions, ESR experiments were carried out.

oxidant addition rate

The ESR spectra were recorded for aqueous solutions of HMWt PMAS (2.5 mg/mL) synthesised at different oxidant addition rates, Figure 5.29. The ESR parameters are given in Table 5.8. The g value of the samples was *ca.* 2.003 close to that of a free electron. The peak to peak line width of the ESR signal can be related to the spin localisation in the polymeric chain [46, 47].

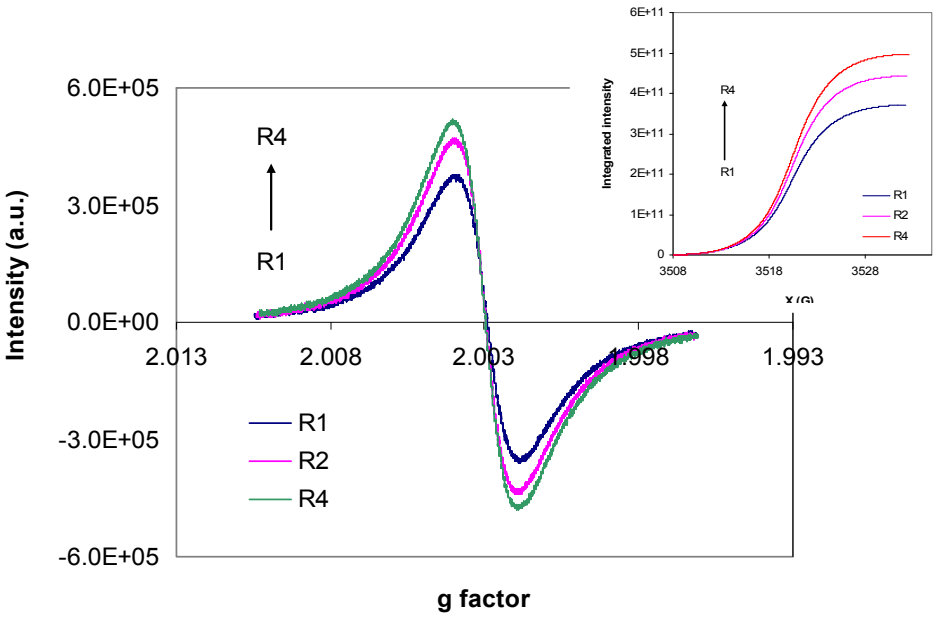

Figure 5.29. The ESR spectra of aqueous HMWt PMAS (2.5 mg/mL) synthesised at different oxidant addition rates: R1 (1mL/min), R2 (2 1mL/min) and R4 (4 1mL/min). The inset shows the integrated intensity (relative spin population) of the PMAS ESR signal at different oxidant addition rates.

An increase in the ESR integrated intensity with oxidant addition rate was observed over the oxidant addition rate range of 1 to 4 mL/min. However, the line width was not affected significantly by oxidant addition rate. This indicates that the samples have similar spin diffusions [47]. By increasing the rate of oxidant addition the spin density on the polymer backbone increased, which was consistent with the observed increased conductivity of the polymer.

Table 5.8. ESR data for aqueous PMAS (5.0 mg/mL solution) prepared using various oxidant addition rates

APS addition rate	g value	ΔH (G) [line width]	Conductivity (S/cm)
1 ml/min	2.00294	2.13	0.25 ± 0.01
2 ml/min	2.00295	2.20	0.28 ± 0.02
4 ml/min	2.00296	2.33	0.54 ± 0.05
100 ml/min	2.00295	2.45	1.25 ± 0.08

Oxidant / monomer ratio

The ESR spectra were also recorded for HMWt PMAS synthesised at different oxidant/monomer molar ratio (Figure 5.30 and Table 5.9). Increasing the oxidant concentration resulted in peaks with broader line width, and with spin concentration remaining approximately the same. This indicates that spin delocalisation decreases with increasing oxidant concentration while the spin concentration is not affected by the oxidant/monomer molar ratio over the range 1 to 2. An oxidant/monomer molar ratio of 1:1 resulted in the narrowest line width and consequently the most delocalised spin, which is in good agreement with the electrical conductivity recorded for PMAS synthesised using this ratio of reactants. Langer *et al.* studied the ESR of microporous polyaniline samples of various electrical conductivity [42]. The narrowest line width was found for the sample of the highest conductivity. They also observed that an increase in oxidation potential for electrochemical polymerisation of aniline from 0.8 to 1.2 V resulted in broadening the ESR line from 1.8 G to 2.4 G.

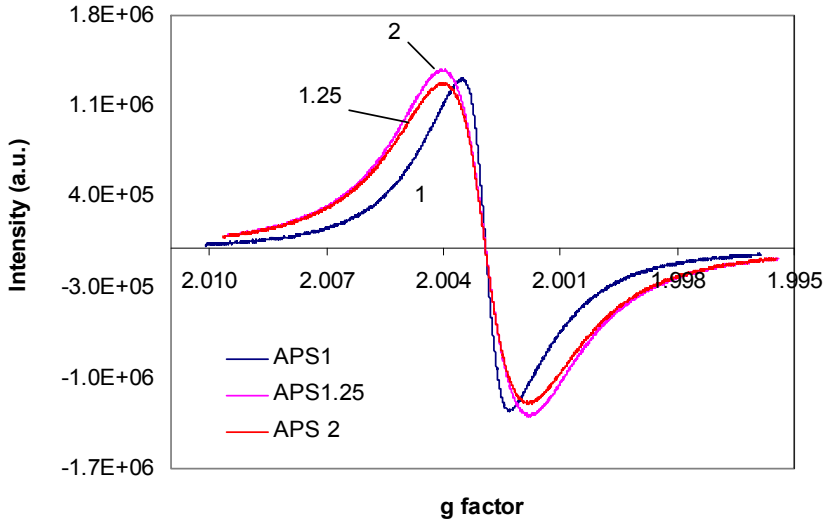

Figure 5.30. ESR spectra of aqueous HMWt PMAS (5.0 mg/mL) synthesised at oxidant/monomer molar ratios of 1, 1.25 and 2.

These results suggest a good correlation between the ESR and conductivity of PMAS polymer synthesised under different conditions, and explain the influence of oxidant concentration and addition rate used in the synthesis, on the spin concentration and delocalisation in the polymer obtained.

Table 5.9. ESR data for PMAS (5.0 mg/mL solution) prepared using various oxidant/monomer ratios

APS/MAS molar ratio	g value	ΔH (G) [line width]	conductivity (S/cm)
1 : 1	2.00294	2.13	0.72 ± 0.03
1.25 : 1	2.00295	3.87	0.10 ± 0.01
2 : 1	2.00295	3.82	0.02 ± 0.01

5.3.7 Photoluminescence

To date, the majority of photochemical and photoelectrochemical studies on inherently conducting polymers have concentrated on poly(phenylenevinylene)s, polyphenylenes and polythiophenes, which have exciting potential applications in areas such as light emitting diodes, photovoltaics and photoelectrochemical cells [48]. Relatively few photobehavioural studies have been carried out on polyaniline (PAn, **1,** Scheme 5.3). Initial studies focused on the fully reduced (y =1) leucoemeraldine base (LB) form [49, 50], which exhibits a strong emission centred at ca 410 nm when irradiated at 300-350 nm. These excitation wavelengths are close in energy to the π - π^* absorption band of LB at ca 330 nm associated with its benzenoid repeat units. The emission observed for LB at 410-420 nm equates to *ca.* 3.0 eV. Combining this value with corresponding cyclic voltammetry data suggests that the thermally equilibrated photoexcited state (*LB) should be a powerful reducing agent (Eqn. 7) [25].

$$*LB + S \rightarrow EB + Sred \quad (7)$$

1

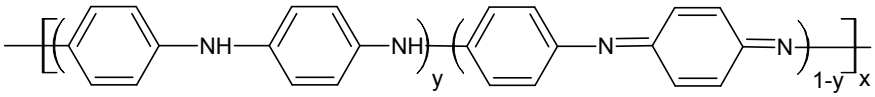

y= 1.0 (leucoemeraldine), 0.5 (emeraldine) and 0 (pernigraniline) as base forms

2

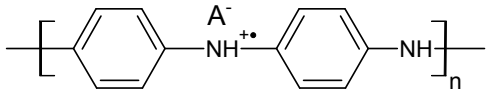

Emeraldine salt (ES), PAn.HA

Scheme 5.3. Polyaniline (1) different oxidation states as base forms, (2) emeraldine salt form.

Early studies [49] suggested that the half-oxidised (y = 0.5) emeraldine base (EB) form of PAn does not photoluminesce (PL). Emission from the EB excited state was believed to be self-quenched by adjacent quinoid groups in its structure (see Scheme 5.3). However, several recent studies by MacDiarmid [51] and others [52, 53], have reported photoluminescence from EB films cast from solvents such as N-methylpyrrolidinone

(NMP). As with LB, the emitting units in photoactivated *EB were considered to be the benzenoid groups.

More recently, photoluminescence and photo-redox induced reactions have been reported for poly(2-methoxyaniline-5-sulfonic acid) (PMAS) in the emeraldine salt (ES) state [25]. These studies were carried out on commercially available PMAS prepared via chemical oxidation of the MAS monomer. It is now known that PMAS synthesised via either chemical or electrochemical oxidation results in two distinct molecular weight fractions that can be substantially separated using a cross-flow dialysis system for separation following chemical polymerisation (Chapter 3). The high molecular weight PMAS fraction has M_p of 16.9 kDa (obtained using the optimal procedure developed in Chapter 4), while the low molecular weight PMAS fraction is an oligomer with M_p of *ca.* 2-3 kDa. The photoluminescence in PMAS has now been reinvestigated using these pure PMAS fractions and mixture, throwing new light on the origin of the photoluminescence of PMAS and of the influence of these two fractions on the unique photoredox reactions of PMAS in the ES state.

Initial studies were carried out on a PMAS sample purified by standard dialysis (12 kDa cellulose membrane). This (DPMAS) form of PMAS was shown from the above UV-vis spectral studies to contain approximately 80% HMWt and 20% LMWt PMAS. A 3D photoluminescence study was carried out to map the emission responses for this material. As seen in Figure 5.31. three excitation wavelengths centred at 280-300, 350-360 and 510-520 nm resulted in photoluminescence (PL) emissions. Excitation at *ca.* 300 nm resulted in emissions centred at 355 and 510 nm, 355 nm excitation resulted in emissions at only 510 and 590 nm, while 520 nm excitation gave an emission at 590 nm.

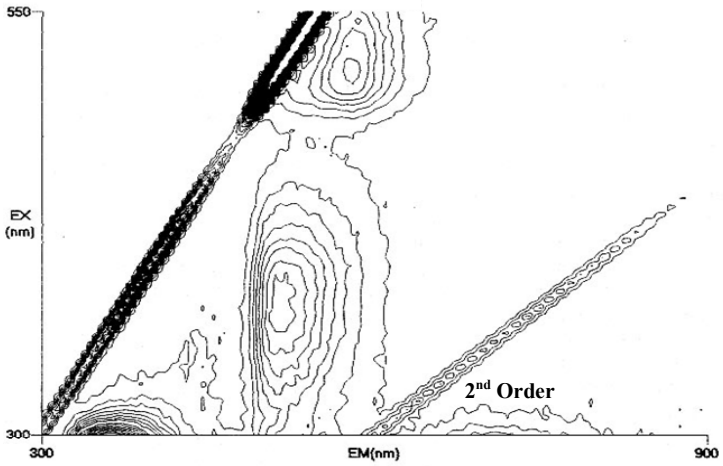

Figure 5.31. Fluorescence map of aqueous DPMAS (1.2 x 10^{-4} M based on dimer).

The PL resulting from the emeraldine salt form of the PMAS known to be in this DPMAS sample was surprising, since the emeraldine salt state of unsubstituted polyaniline is reported to be a quencher [54]. The quenching has been attributed to the interaction of singlet excitons in the photoexcited state with polarons [54-56]. In order to explain this unexpected photoluminescence observed for the mixed DPMAS, detailed PL studies were then carried out on pure HMWt and LMWt PMAS. Excitation wavelengths of 290, 355 and 520 nm were employed. Figure 5.32 shows the PL spectra of aqueous solutions (50 µg/mL) of pure HMWt and LMWt PMAS fractions, as well as the dialysed DPMAS sample at excitation wavelength of 355 nm (excitation of the polymer π-π^* band which is relatively independent of the oxidation state and protonation levels of the polymer). The emissions from other excitation sources were interrelated and not shown for the sake of simplicity. In all spectra a Raman scattering peak was observed at *ca.* 410 nm. The LMWt fraction exhibited a strong, broad emission with a peak maximum at *ca.* 525 nm. On the other hand, the HMWt sample displayed a very weak PL emission, as expected for an emeraldine salt. The weak emission band observed for this HMWt fraction at *ca.* 515 nm (with a long high wavelength tail) is believed to be due to a trace impurity (≥ 5%) of LMWt PMAS. Dialysed DPMAS presented a similar but more intense PL spectrum to that observed for the HMWt sample, with a medium intensity emission band at *ca.* 525 nm (Figure 5.32).

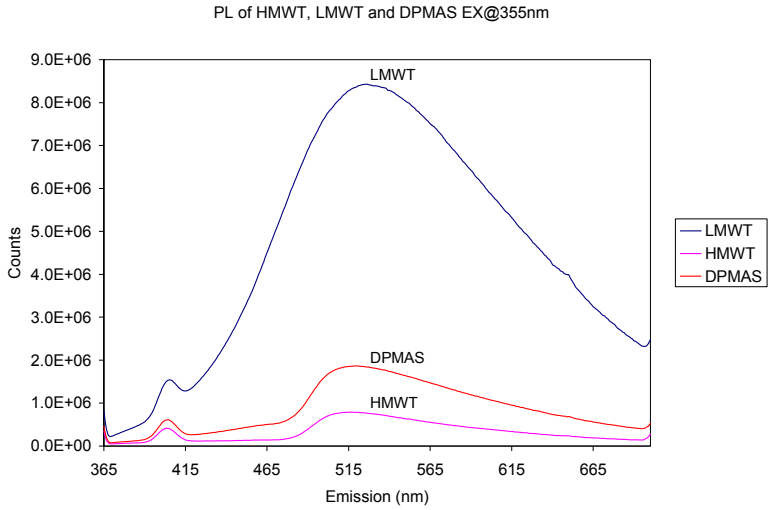

Figure 5.32. PL spectra of aqueous HMWt, LMWt and dialysed PMAS ([PMAS] = 50 μg/mL, λ_{ex} = 355 nm).

The PL spectra of three different fractions of HMWt and LMWt PMAS and pink oligomeric fractions were also compared at various excitation wavelengths (Figure 5.33). The oligomeric fraction and the HMWt PMAS showed the strongest and weakest luminescence, respectively.

The PL spectra were recorded at a range of different concentrations of LMWt PMAS, the most fluorescent material, in order to establish a calibration curve at different excitation wavelengths. This calibration curve can be used later to estimate the concentration of LMWt PMAS. A plot of fluorescence intensity versus concentration was linear at low concentrations and showed departure at high concentrations. This non-linearity at higher concentrations is the effect of self-quenching (or self-absorption) in which the fluorescence emitted by analyte molecules is absorbed by other analyte molecules.

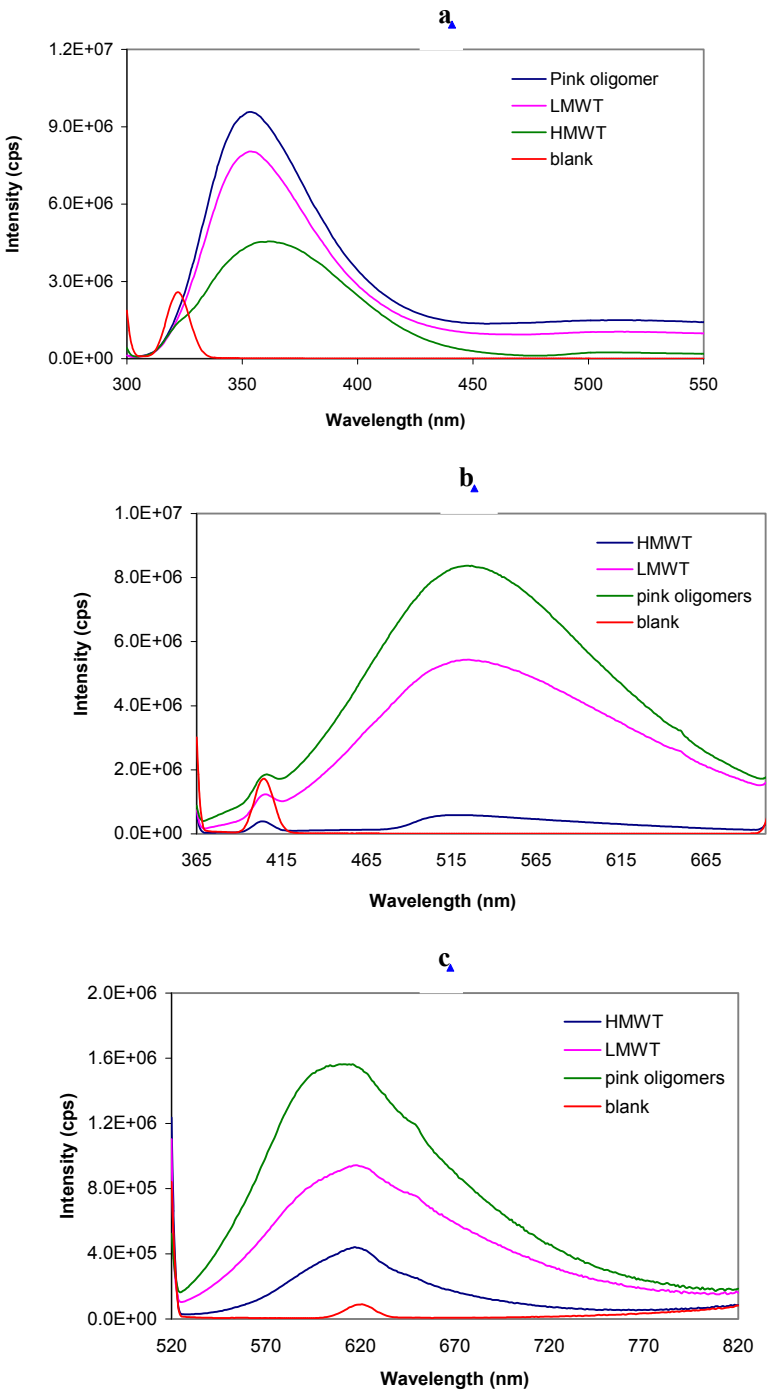

Figure 5.33. PL spectra of aqueous HMWt, LMWt and pink oligomeric fractions of PMAS (50 µg/mL), (a) λ_{ex} = 290 nm, (b) λ_{ex} = 355 nm λ_{ex} = 510 nm. The PL spectrum of water as blank is also shown.

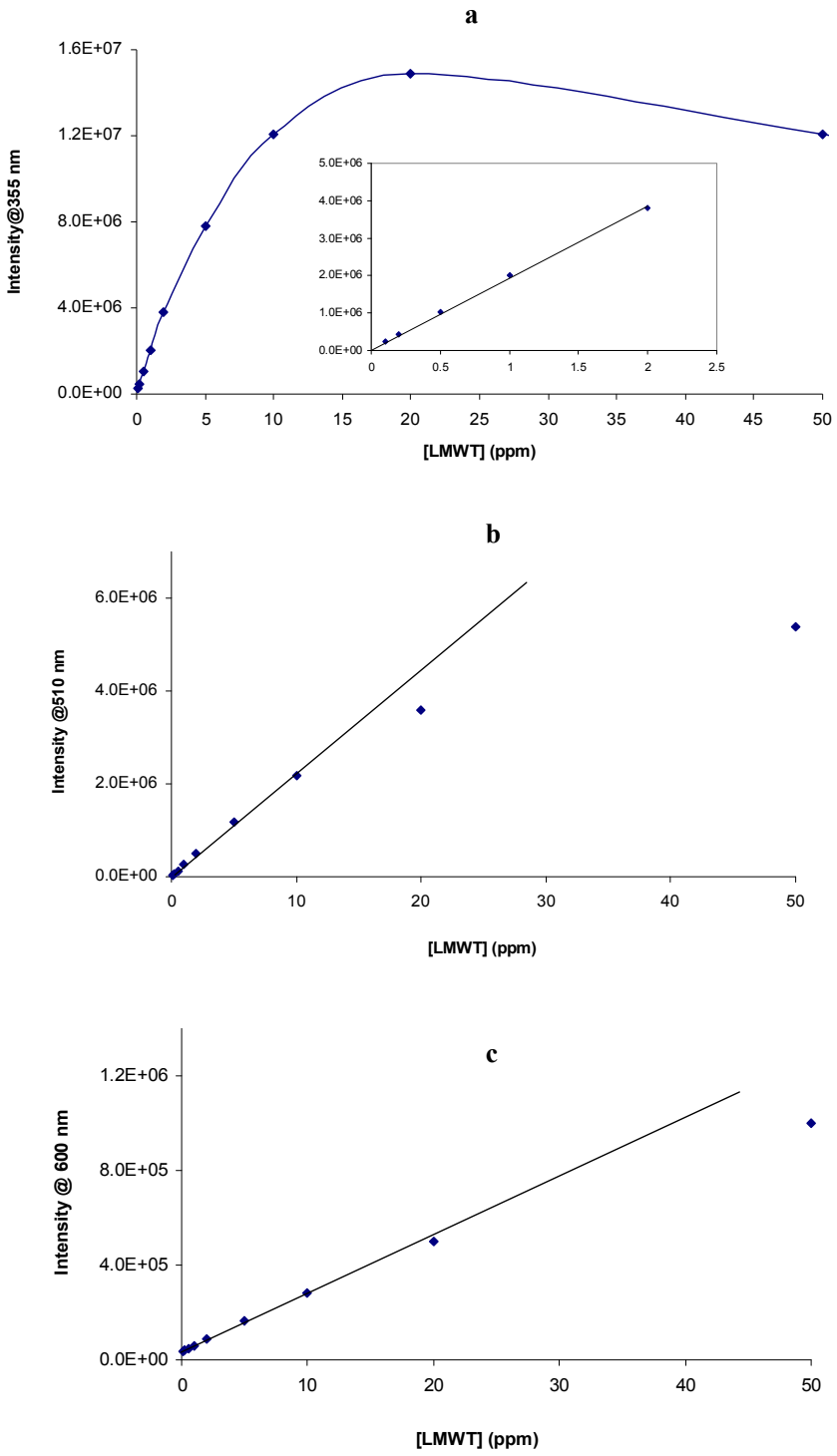

Figure 5.34. Calibration curves for LMWt PMAS at different excitation wavelengths: (a) 290 nm (Inset shows the linear range), (b) 355 nm, and (c) 510 nm.

Based on the calibration curves of LMWt PMAS at excitation wavelengths of 290, 355 and 510 nm (Figure 5.34), the concentration range of LMWt PMAS for fluorescence study at different excitation wavelengths were obtained. The LMWt PMAS concentration was dependent upon the wavelength of the exciting light. The maximum concentrations for PL studies were determined as 2 μg/mL (= 2 ppm) for 290 nm, 10 μg/mL for 355 nm and 20 μg/mL for 510 nm excitations.

As seen in Figure 5.33, the fraction with higher molecular weight and conductivity had weaker fluorescence. This HMWt PMAS fraction (M_p 11,000 Da) was subsquently fractionated by splitting the GPC chromatogram into segments of different molecular weight collected via a fraction collector attached to the GPC (Figure 5.35). Samples GPC 1 to GPC 5 were collected at different retention times as summarised in Table 5.9. The samples with higher molecular weight were collected at lower retention times. The gel permeation chromatography analysis of GPC 3 and GPC 4 showed peak molecular weights (M_p) of 15,200 and 11,500, respectively. The PL spectra were recorded for the GPC 2 to GPC 5 fractions after desalting against water, Figure 5.36. The strongest fluorescence was obtained for GPC 5 which had the lowest molecular weight. The results clearly suggest that fluorescence properties of the PMAS are affected by the molecular weight of the sample.

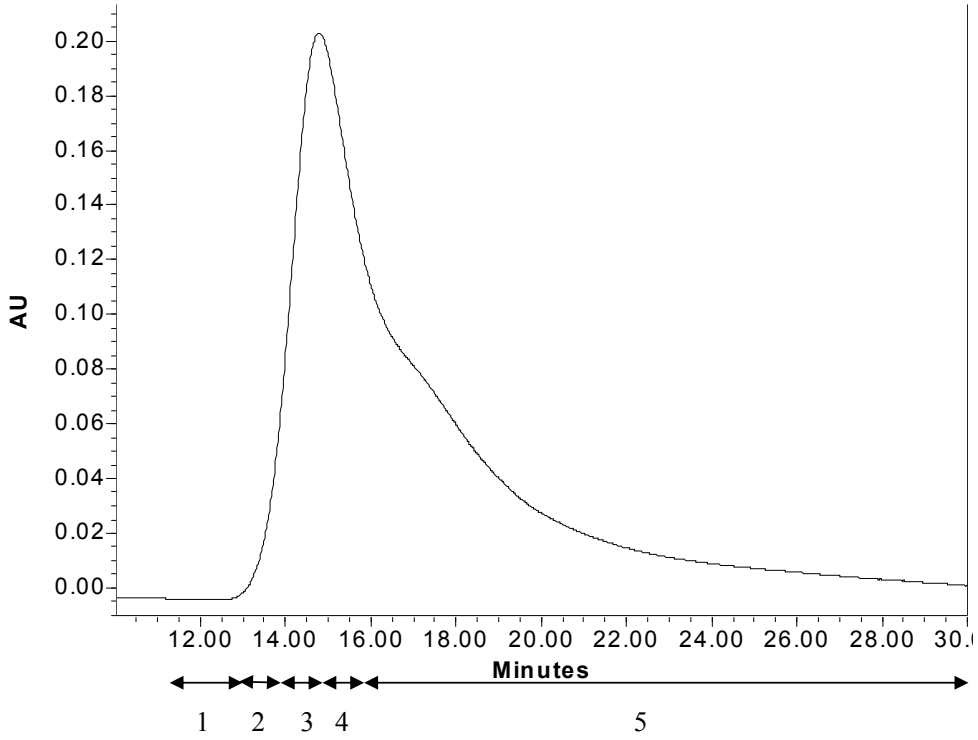

Figure 5.35. Fractionation of HMWt PMAS by GPC.

Table 5.9. Table showing the fractionation of HMWt PMAS using GPC (see Figure 5.35)

Collected time (min)	11.30-13.24	13.25-14.5	14.51-15.29	15.30-16	16.01-30

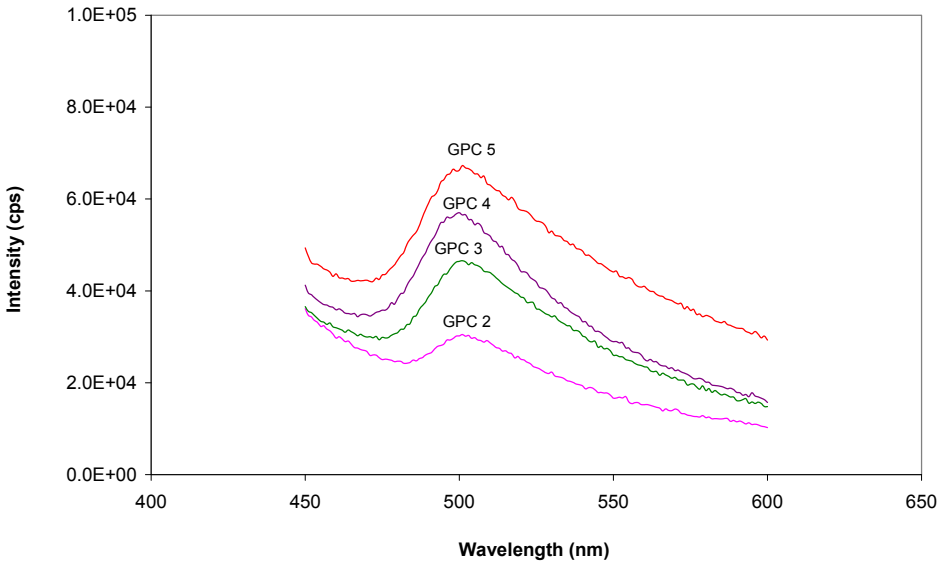

Figure 5.36. PL spectra of PMAS samples (10 µg/mL) fractionated by GPC at 355 nm excitation wavelength.

Quench study

The PL study of different fractions of PMAS (Figure 5.33) confirmed that the emission at 520 nm arises entirely from the LMWt PMAS component and the fluorescence of this fraction is quenched significantly in the presence of HMWt PMAS near the polaron absorption band (450-475 nm).

This quenching was probed in more detail by a study of the LMWt PMAS emission with addition of HMWt PMAS. The PL spectra of mixtures containing increasing amounts of HMWt PMAS from 0 to 61 µg/mL (0 to 1.51 x 10^{-4} M) while maintaining a constant LMWt PMAS concentration of 10 µg/mL (2.47 x 10^{-5} M) were obtained. In this study, high purity HMWt PMAS (quencher) was essential as the presence of LMWt PMAS impurities would interfere with the quenching of HMWt PMAS and subsequently increase the observed PL. In order to minimise this complication, the HMWt PMAS was further purified using vivaspin 10 kDa MWCO membrane to ensure the removal of all trace amounts of LMWt PMAS. The LMWt PMAS oligomer emission decreased markedly as the HMWt PMAS concentration was increased (Figure 5.37a). Two characteristic quenching behaviours were observed: from 460 to 500 nm;

and from 500 nm and higher, with a maxima at ~510 nm. The distortion of the 460 – 479 nm emission band with loss of intensity in the high energy end of the band is attributed to absorbance quenching by the polaron absorption band of the conducting HMWt PMAS (see Figure 5.1).

There is almost certainly an element of absorbance quenching of LMWt PMAS by the HWMt PMAS fraction as a result of an inner filter effect (trivial quenching process), whereby the photon released by the luminophore is simply reabsorbed by an adjacent chromophore. This type of quenching does not usually affect the emission intensity outside of the absorbance region of the chromophore, resulting in distortion of the observed emissions Figure 5.37a. In radiative, or trivial energy transfer the luminophore emits via its usual mechanism, but the emitted photon is reabsorbed before it reaches the fluorimeter detector. The effect of increasing radiative energy transfer acceptor on the emission of a donor would be expected to be linear, through a relationship similar to the Beer Lambert Law. Interestingly, reduction of luminescence intensity of LMWt PMAS with increasing concentrations of HMWt PMAS is distinctly non-linear, as shown in Figure 5.37b, even though preliminary studies showed that these systems were maintained at concentrations that obey the Beer-Lambert law. Clearly other quenching mechanisms contribute to the observed responses.

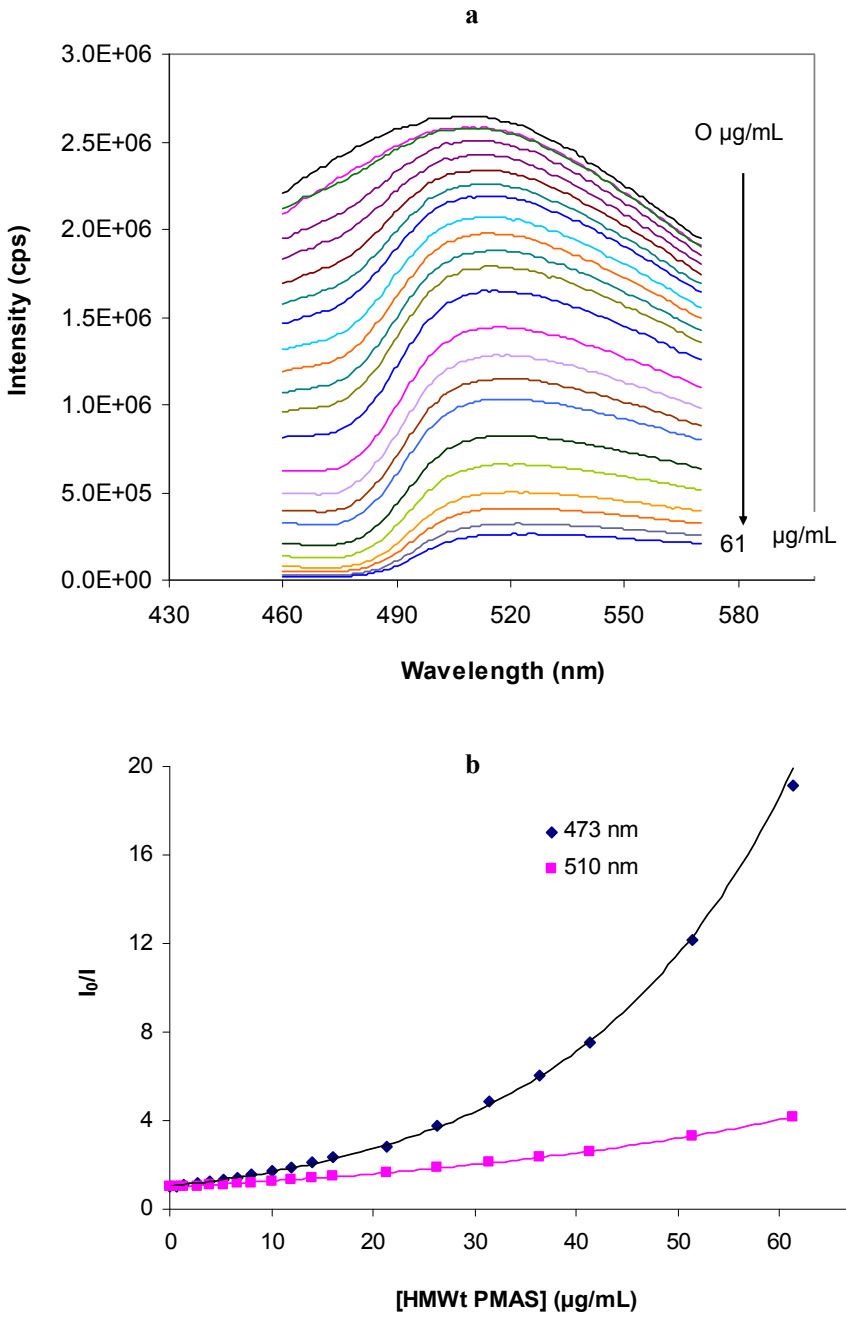

Figure 5.37. (a) Photoluminescence spectra of various aqueous mixtures of LMWT PMAS (10 µg/mL) increasing the HMWT PMAS (0 to 61 µg/mL) were added, λex = 355 nm., (b) Stern-Volmer plot of the fluorescence quenching in (a) at emission wavelengths of 473 nm and 510 nm.

Dynamic fluorescence quenching, arising from a molecular collision, can be modeled using the Stern-Volmer equation (Equation 8), where I and Io are the fluorescence intensities with and without a quencher, and the concentration of the quencher is denoted as [Q]. A plot of I_o/I versus [Q] will yield a slope of $k_q\tau_o$, where the collision quenching rate constant, k_q, can be determined if the fluorescence lifetime, τ_o, can be measured

$$\frac{I_o}{I} = \frac{\Phi_o}{\Phi} = 1 + k_q \tau_o [Q] \qquad (8)$$

If the fluorophore can form a stable complex with a quenching molecule, the resultant ground state of the fluorophore-quencher complex is said to be statically quenched. In this case the Stern-Volmer equation is modified where the slope of a plot of I_o/I versus [Q] will be proportional to the association constant, K_a, of the fluorophore-quencher complex. In the static (complexation) quenching model the lifetime of the fluorophore will be unchanged since the fluorophores that are not complexed (and therefore able to emit after excitation) will have normal excitation/emission properties. This model assumes that the resulting complex is non-luminescent and the fluorescence intensity of the sample is reduced since the quencher is essentially reducing the number of fluorophores that can emit. The Stern-Volmer plot of the observed fluorescence data for both static and dynamic models gave a poor fit to the model as the behaviour was non-linear (Figure 5.37b).

Alternatively, since the quencher is polymeric and therefore diffusionally restricted in fluid media, the Perrin Model (Equation 9) [57-59] may provide a better interpretation of the fluorescence behaviour. In Equation 3, I_o and I are as described above, while the term *c* describes the quenching volume of action. The Perrin model applies if diffusion is sufficiently restricted such that the time taken for collision between donor and acceptor exceeds the lifetime of the excited state. Further, quenching behaviour only occurs within a set volume containing the excited state species. Static quenching behaviour, conforming to the Perrin Model, is not expected to exhibit changes in the lifetime of the fluorphore. The model assumes that once the quencher resides within the

effective quenching volume, the excited state is completely extinguished, while fluorophores outside this volume have unimpeded behaviour.

$$\ln\left(\frac{I_o}{I}\right) = c[Q] \qquad (9)$$

A plot of the Perrin model is shown in Figure 5.38 and exhibits an excellent fit at selected emission wavelengths of 473 and 510 nm. Significantly, quenching is far more efficient around 460 nm associated with the non-spin paired electron of the mobile polaron charge carrier sited upon the conducting HMWt PMAS conjugated backbone. The interactions of the HMWt PMAS to the LMWt PMAS are characteristic of a non-radiative energy transfer. The association of the LMWt and HMWt PMAS fractions in solution is not surprising given the very significant effort required to separate these isomeric fractions (see Chapter 3).

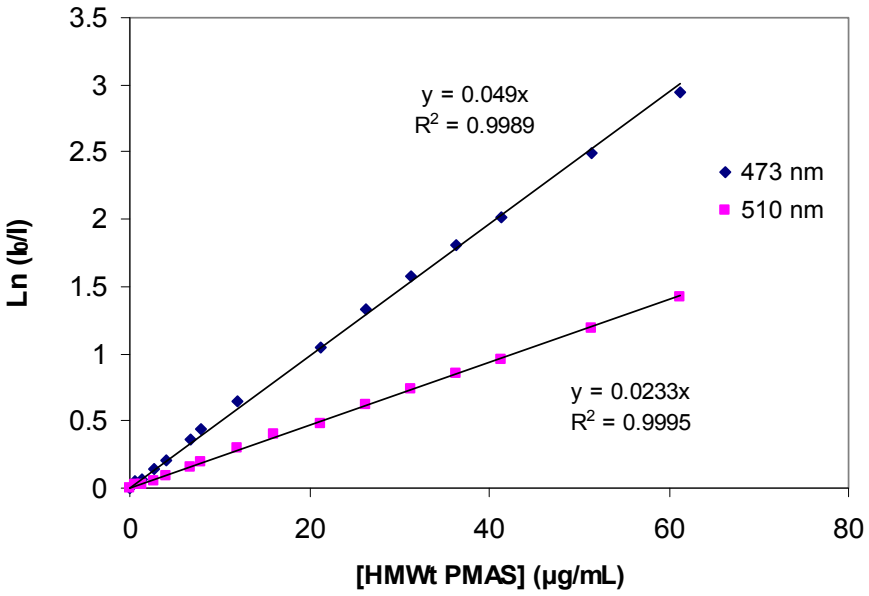

Figure 5.38. Perrin plot of the fluorescence quenching ratio of aqueous mixtures of LMWt PMAS (10 µg/mL) with increasing amounts of HMWt PMAS (0 to 61 µg/mL). λex = 355 nm.

Life time measurements

The lifetime measurements were performed in collaboration with Prof Robert Forster and Dr Tia Keyes from Dublin City University on HMWt and LMWt PMAS materials.

In order to further elucidate the nature of the observed LMWt PMAS photoluminescence, fluorescence lifetime studies were carried out for LMWt PMAS and HMWt PMAS, as well as the mixed DPMAS sample. A time-correleated single photon counting (TCSPC) system was employed using 280, 370 and 450 nm pulsed laser sources. Cut-on filters of 400, 475 and 530 nm were used to separate out the effects of the multiple photoluminescence emission bands.

Typical TCSPC responses for HMWt PMAS and LMWt PMAS are shown in Figure 5.39. In each case the upper trace relates to the TCSPC output and resultant model fit. The underlying curve relates to the background signal from the excitation laser source, which is subtracted from the TCSPC output when estimating fluorescence lifetime. The TCSPC responses in each case were collected to the same photon count intensity, with collection times varying from 120 sec typically for LMWt PMAS to 400 sec for HMWt PMAS.

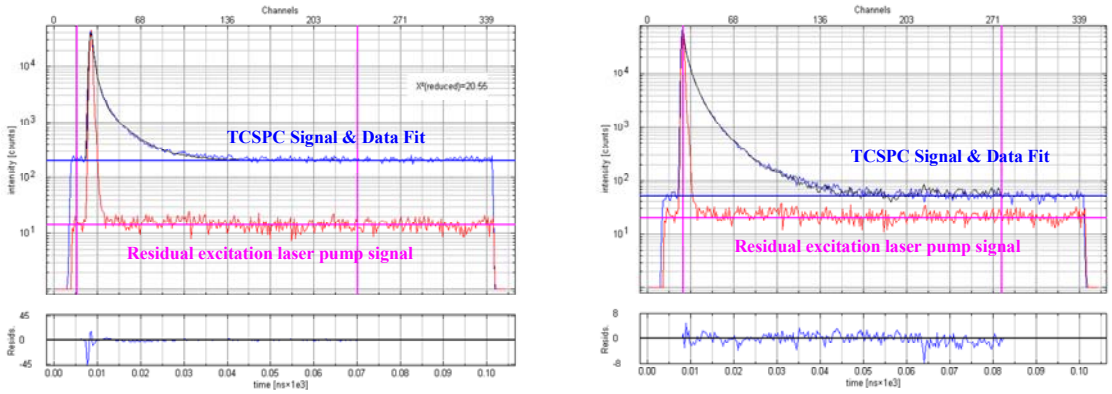

Figure 5.39. Typical TCSPC emission response curves for HMWt PMAS and LMWt PMAS using a 370 nm excitation source with no emission filters employed.

Emission responses were analysed using PicoQuant FluoFit software employing a fitting function containing three time constants. The first order decay function was typically a residual instrumental laser plus response of less than < 0.25 ns, and was rejected. For both PMAS samples, second- (τ_2) and third- (τ_3) order lifetime responses were 1-2 ns and 6-8 ns, respectively. A typical Stern–Volmer plot for the fluorescence lifetime, τ_0/τ vs [Q], of HMWt PMAS exhibited clear independence of quencher concentration, Figure 5.40. This observation was also consistent for all PMAS forms as well as for the order of the modeled lifetime response. As discussed above, the observed independence for the fluorescence lifetime was inconsistent with the Stern-Volmer dynamic quenching collision model. In contrast, this independence was predicted for the Perrin model where diffusionally restricted behaviour can be anticipated for the polymer in solution.

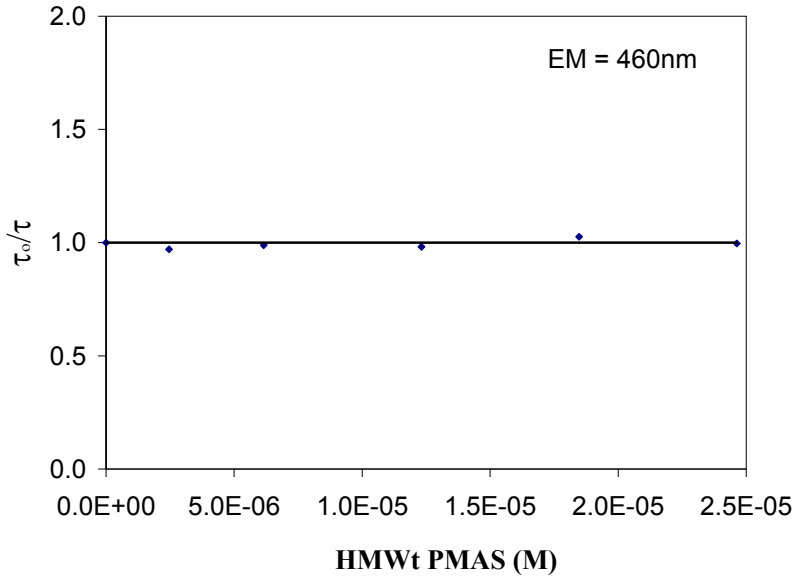

Figure 5.40. Typical Stern-Volmer fluorescence lifetime ratio τ_o/τ dependence of τ_2 on HMWt PMAS quencher concentration.

The observed TCSPC behaviour was also consistent with the occurrence of both radiative energy transfer and static quenching in a restricted environment. The fluorescence lifetime of the LMWt PMAS was independent of the HMWT concentration, (see Figure 5.40). This condition arises since the LMWt PMAS

fluorophores that are not associated are able to emit after excitation in the normal fashion. The fluorescence of the sample is reduced since the quencher is essentially reducing the number of fluorophores that can emit, consistent with the increasing time required to acquire lifetime signals at higher HMWt PMAS concentration.

Influence of synthetic conditions on PL properties of PMAS

As discussed in Chapter 4, the rate of oxidant addition in chemical polymerisation of PMAS has a significant effect on the conductivity of PMAS, as polymer with increased conductivity was obtained at higher addition rates of oxidant. PL spectra were therefore recorded for PMAS synthesised at different addition rates of oxidant. As seen in Figure 5.41, the PL intensity of the HMWt PMAS decreased with increasing oxidant addition rate. In the other words, the weakest fluorescence was obtained for the polymer with the highest conductivity. The PL quenching of LMWt PMAS was also studied in the presence of PMAS synthesised at different oxidant addition rate (Figure 5.42). The polymer obtained using higher addition rate (with higher conductivity) was found to be the best quencher. These results suggest that there is a relationship between conductivity and PL properties of PMAS, i.e. polymers with higher conductivity have reduced PL properties presumably via self-quenching.

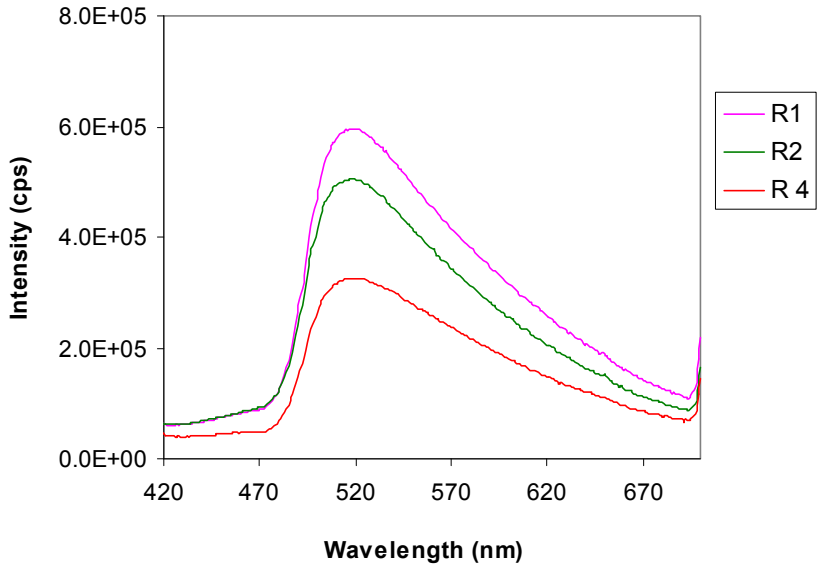

Figure 5.41. PL spectra of aqueous HMWt PMAS (50 µg/mL) synthesised at different oxidant addition rates. Excitation at 355nm.

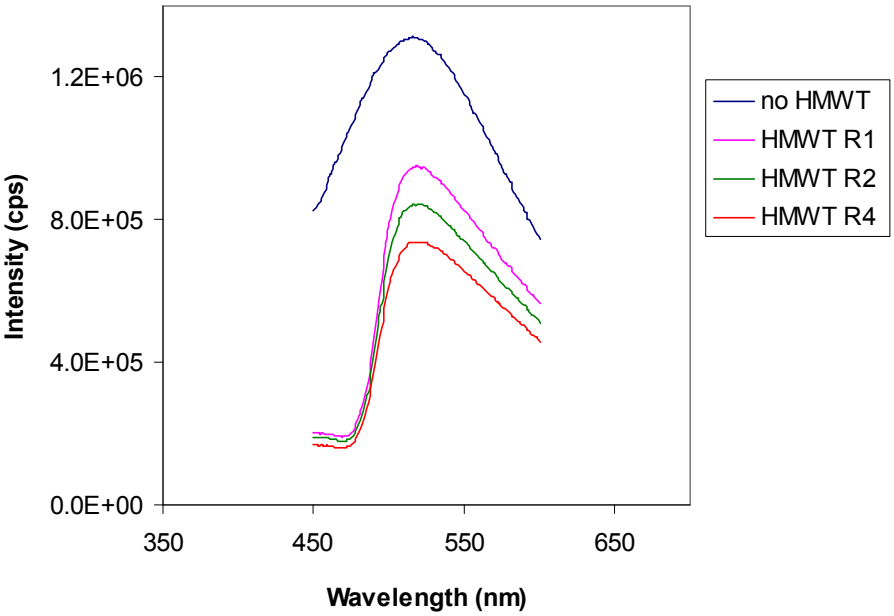

Figure 5.42. PL quenching of LMWt PMAS (10 µg/mL) by pure HMWt PMAS (100 µg/mL) synthesised at different addition rates of oxidant: R1=1 mL/min, R1=2 mL/min, R4=4ml/min and RM=rapid mixing.

Influence of Oxidation and Reduction on PL of HMWt PMAS

(i) Oxidation

Treatment of aqueous LMWt PMAS with ammonium persulfate as potential oxidant caused little change in the PL spectrum in water. This is consistent with the UV-vis spectral studies above which showed this oligomeric form of PMAS to be inert to oxidation. Similar treatment of aqueous HMWt PMAS caused oxidation to pernigraniline, as evidenced by UV-visible spectral changes. With unsubstituted polyaniline, the fully oxidised pernigraniline state is reported not to photoluminesce [49]. Unfortunately, oxidised HMWt PMAS solutions were too unstable to permit reliable PL spectra to be obtained.

(ii) Reduction

The PL of aqueous PMAS fractions was studied after treatment with hydrazine. Not surprisingly, the LMWt PMAS sample exhibited the same PL response as seen in water, since the earlier UV-Vis spectral studies had shown it was inert to reduction. HMWt PMAS emeraldine salt was reduced to the leucoemeraldine base form by stepwise addition of hydrazine. Figure 5.43a illustrates the spectral changes of HMWt PMAS during reduction probed by UV-vis and fluorescence spectroscopy. The hydrazine treatment resulted in a strong PL response at 423 nm (Figure 5.43b) accompanied by the appearance of a 410 nm absorption band and gradual disappearance of the 473 nm band in the UV-vis spectrum. The strong PL contrasts with the extremely weak emission of the initial emeraldine salt. It is very similar, however, to the behaviour of polyaniline where the reduced leucoemeraldine base photoluminesces strongly [49-51, 60].

In order to find the excitation wavelength at which the emission of the LB form of PMAS is strongest, a PL study was carried out at different excitation wavelengths near the maximum absorbance (410 nm), Figure 5.44. The emission wavelength and the PL shape were similar for excitation in the range 300-410 nm. However, the PL intensity was highly affected and the strongest emission was achieved using 400 nm excitation. This excitation wavelength can be used for qualitative and quantitative fluorescence analysis of the leucoemeraldine base form of PMAS.

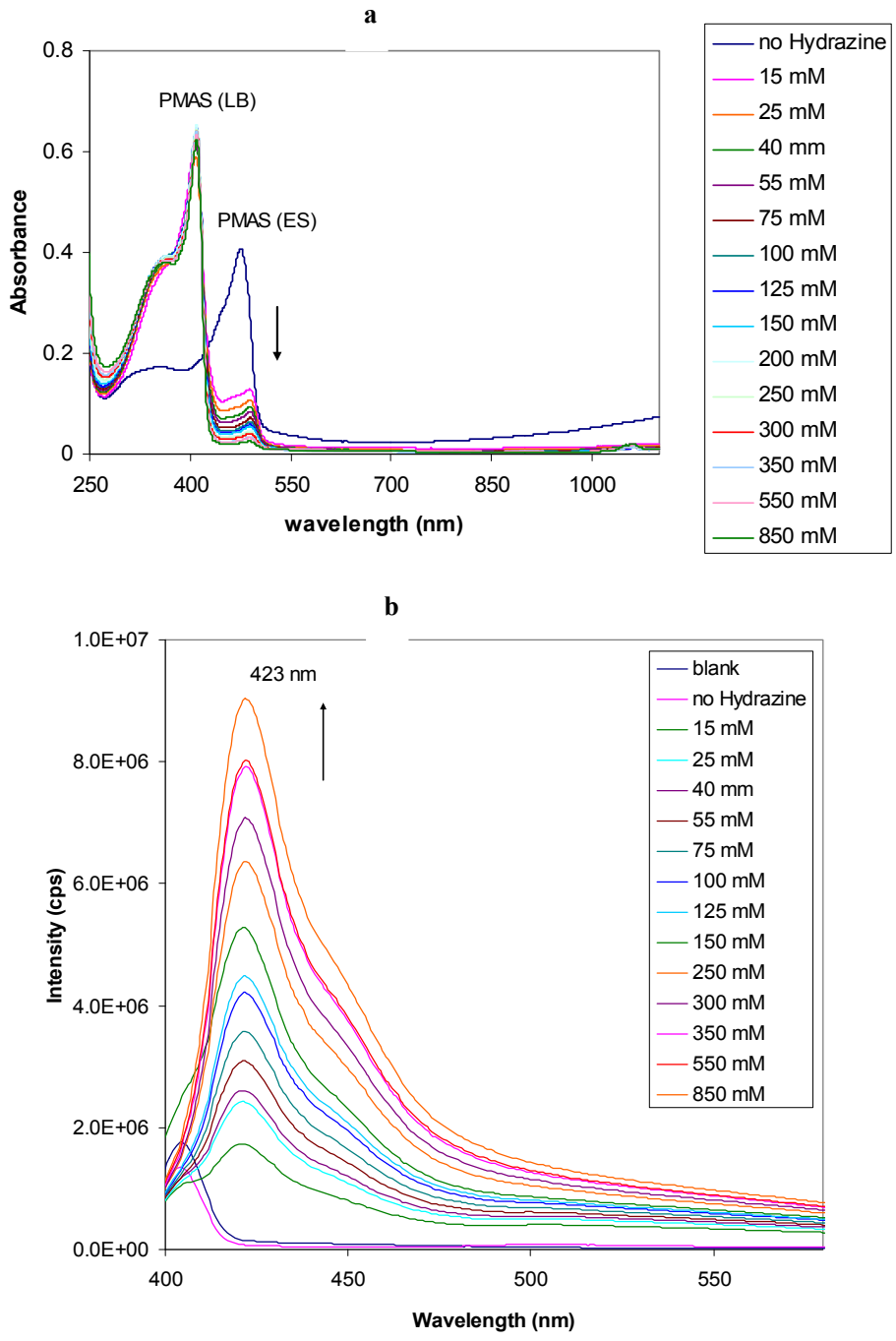

Figure 5.43 (a) UV-vis spectral changes and (b) PL spectra of HMWt PMAS during reduction by hydrazine. The hydrazine concentration was increased by stepwise addition of 3 to 170 µL of 10 M hydrazine aqueous solution to 3 mL of aqueous 10 µg/mL HMWt PMAS.

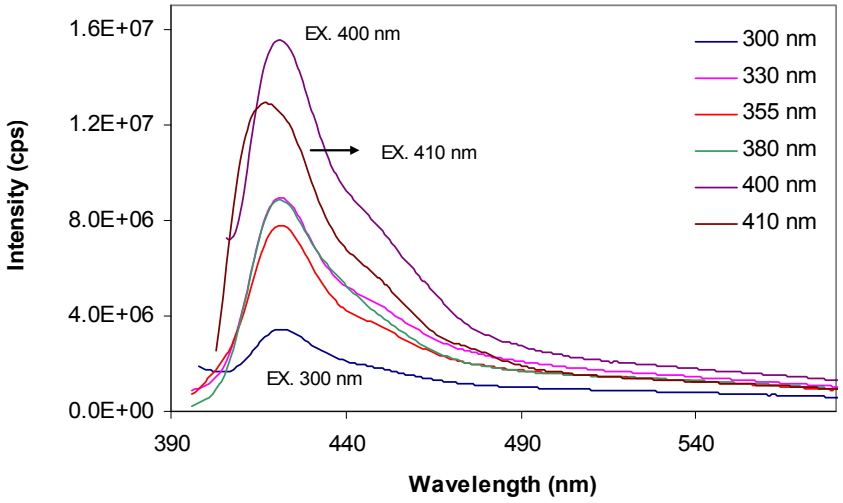

Figure 5.44. PL of the LB form of aqueous HMWt PMAS (10 µg/mL) in 0.10 M hydrazine) using different excitation wavelengths.

From these results it can be concluded that the unexpected photoluminescence of commercially available, as-synthesised PMAS reported previously [25] does not originate from the conductive HMWt PMAS, but rather from a low molecular weight, redox inactive component present in the sample. In turn, the mechanism for the fascinating photo-electron transfer reactions recently reported [25] with PMAS will require reassessment.

5.3.8 PMAS morphology and particle size

The morphology of HMWt PMAS was also found to be affected by synthetic conditions, varying from rod-like to spherical nanoparticles. Rod-like morphology, with a typical nanorod diameter of 100 nm, was obtained for PMAS synthesised using low addition rate of oxidant (1mL/min) (Figure 5.45). The length of the nanorods varied with oxidant concentration. Typical lengths were 1 to 1.5 µm for an APS/monomer ratio of 1 and were smaller (<0.5 µm) for an APS/monomer ratio of 1.25.

a

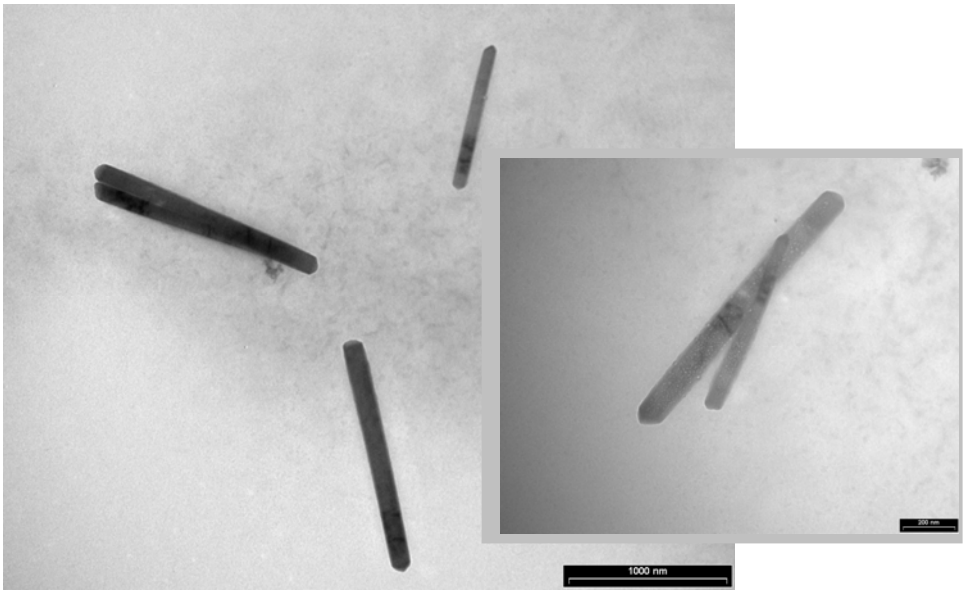

b

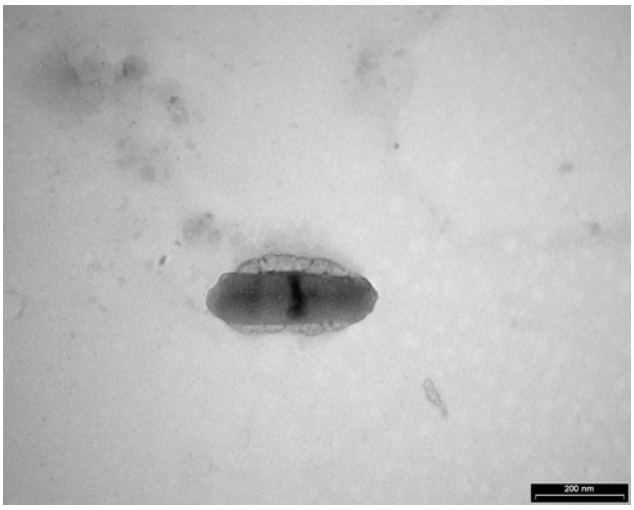

Figure 5.45. TEM micrographs of pure HMWt PMAS synthesised with an oxidant addition rate of 1 mL/min using an APS/MAS molar ratio of (a) 1, and (b) 1.25. The monomer concentration and reaction temperature were 0.33M and 10°C, respectively.

Synthesis of PMAS at optimum conditions (as discussed in Chapter 4) with rapid addition of oxidant resulted in polymer with a different morphology. Nanospheres with diameters less than 50 nm and their agglomerations, or probably together with some

small rods, were observed in the TEM micrograph of the polymer (Figure 5.46). Casting the film from a dilute PMAS solution (~100 μg/mL) containing these nanospheres on TEM grids resulted in an ultra thin film that was continuously deposited onto the grid. This may be applicable when a thin film of conducting polymer is required (Figure 5.46 inset).

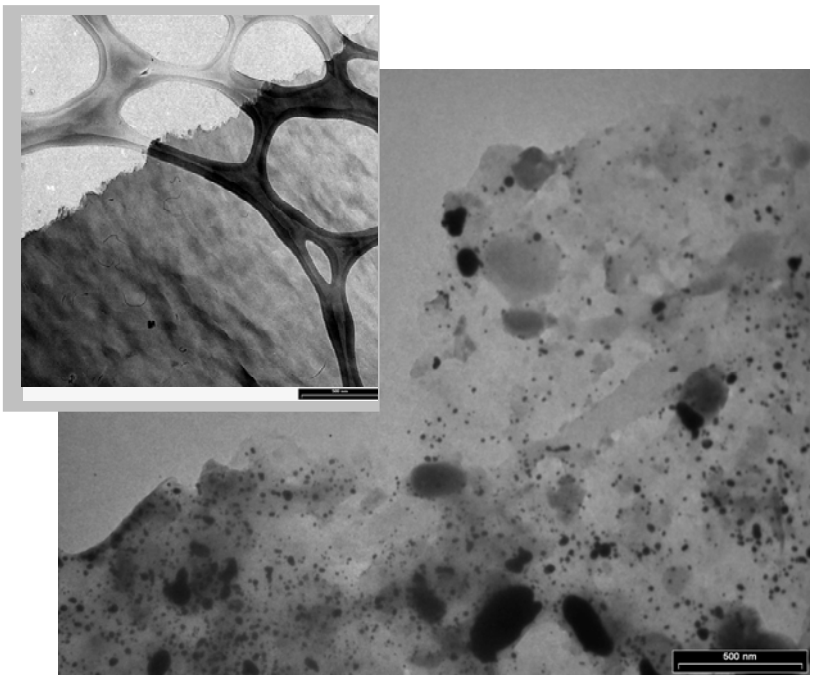

Figure 5.46. TEM micrographs of pure HMWt PMAS synthesised using rapid mixing. The oxidant/monomer molar ratio was 1, and the monomer concentration and reaction temperature were 0.47M and 10°C, respectively. Scale bar 500 nm. The inset shows an ultra thin film of PMAS cast on TEM grids from the dilute solution, scale bar 500 nm.

A SEM image of the HMWt PMAS film cast onto glass (10 μm thickness) showed a smooth surface (Figure 5.47).

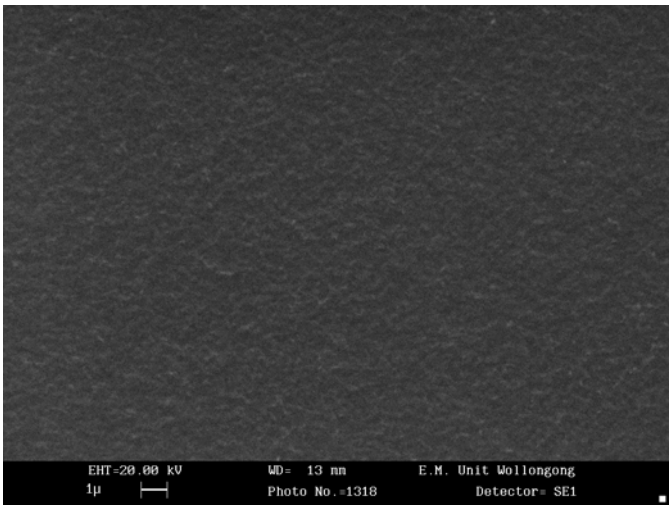

Figure 5.47. SEM of PMAS film cast onto glass (10 µm thickness), scale bar 1µ.

A TEM of LMWt PMAS showed a mixture of nanoparticles with a size ranging from 20-100 nm and needles with diameter about 20 nm (Figure 5.48). Similar morphology has been observed by Stejskal *et al.* [61] for the precipitate isolated from the initial stages of oxidative polymerisation of aniline in 0.4 M acetic acid (pH ~4). This semi-crystalline oligomer exhibits rod-like objects with dimensions of several micrometres.

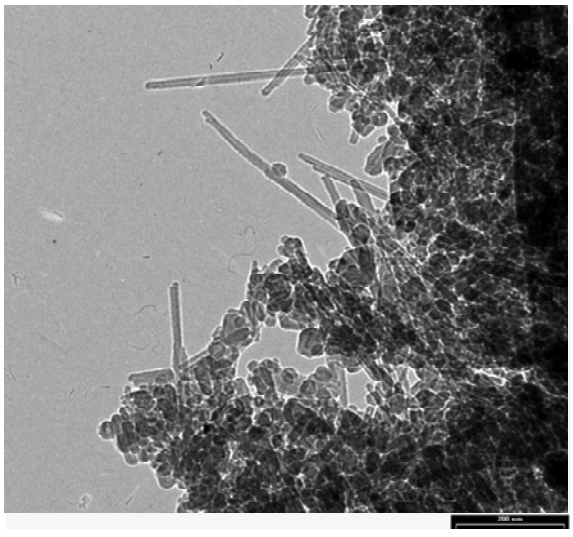

Figure 5.48. TEM micrograph of LMWt PMAS, scale bar 200 nm**.**

5.3.9 Solubility of PMAS

Polyaniline has limited solubility in common organic and aqueous solvents. Substitution of polyaniline by alkyl, alkoxy chains or polar substituents has been used to improve the solubility of polyaniline in both organic and aqueous solvents. Introduction of sulfonate group in the polyaniline results in water soluble polymers. SPAN (50% sulfonated polyaniline is appreciately soluble in 0.10 M NaOH or NH_4OH in the corresponding salt forms, and is partly soluble in DMSO (in green protonated form) and in NMP (in blue deprotonated form) [1]. PMAS, which is a fully sulfonated polyaniline, has a much higher solubility in water (up to ~ 30%) [14].

Table 5.10. Solubility of PMAS in solvents

	Solvent	**Dielectric constant (ε)**	**Polarity index**	**Solubility of PMAS**
Protic solvents	Water	80	9	>10% (w/v)
	Methanol	32.9	5.1	-
	Ethanol	24.6	5.2	-
	Acetic acid	6.2	6.2	-
Aprotic solvents	DMSO	46.7	7.2	>2% (w/v)
	Acetonitrile	36.6	5.8	-
	NMP	32.0	0.7	-
	Acetone	20.7	5.1	-
	m-Cresol	11.5		-
	THF	7.5	4	-
	Ethyl Acetate	6.0		-
	Chloroform	4.8	4.1	-

The solubility of PMAS in a number of protic and aprotic solvents with different polarity was investigated (Table 5.10). Pure HMWt PMAS is soluble to more than 10% (w/v), i.e. more than 100 mg/mL, in water in its emeraldine salt protonated form with a dark yellow-green colour. PMAS slowly dissolves in DMSO {~2 % (w/v), 20 mg/mL}, giving a dark green colour instead of yellow-green colour which PMAS shows in water. This may be due to the extended coil conformation of PMAS in aqueous solution being

changed to compact coil in DMSO. Water is a protic solvent with high polarity ($\varepsilon = 80$), and DMSO is a polar aprotic solvent ($\varepsilon = 46.7$). PMAS was found to be insoluble in common organic solvents with lower polarity such as methanol, ethanol, acetic acid, acetonitrile, NMP, acetone, *m*-cresol, THF, ethyl acetate and chloroform.

5.3.10 Stability of PMAS

The stability of PMAS in solution and solid states, which is critical to its storage and its applications, can be assessed by aging experiments using UV-vis spectroscopy and gel permeation chromatography (GPC).

The UV-vis spectrum of PMAS was gradually affected by aging for more than 10 days (Figure 5.49). The absorption band at 320 nm increased in intensity and slightly blue-shifted with time. The free carrier tail in the near infrared decreased and a new broad absorption band slowly appeared at about 550-580 nm. The ratio of the absorptions at 473 nm to 330 nm (A_{473}/A_{330}) decreased with time. The absorption peak at 473 nm remained unaffected after 2 months and the colour of the solution also remained yellow-green. This peak slightly decreased after longer storage and vanished after 27 months and the colour of PMAS solution was turned to yellow.

In contrast, it was observed (Chapter 3, section 3.3.3.2) that the intensity of 330 nm band decreased with dialysis of an impure PMAS solution due to removal of oligomers and LMWt PMAS. Shortening of the PMAS chains by breaking some N-C bonds presumably caused by hydrophilic attack of hydroxide ions in water molecules may be responsible for the observed spectral changes. A similar explanation was suggested for the spectral changes of SPAN solutions with time [11]. The bands in the UV-vis spectrum of SPAN solutions were blue-shifted with time, since shorter chains have higher transition energy due to a reduced delocalisation of electrons.

Aging processes in polyaniline can lead to the generation of phenazine units [61, 62]. The formation of “phenazine-like” structures formed by cross linking has also been reported for thermally treated polyanilines [63].

The similarity of the UV-vis spectra of the aged degradation products of PMAS to that of PMAS samples containing the LMWt PMAS fraction suggest the possibility of phenazine structures [61] in LMWt PMAS, arising from *ortho*-coupling of MAS monomers during the polymerisation at pH ~4, as discussed in section 5.3.11.

PMAS in the solid state was more stable, with no significant change observed in the UV-vis spectrum upon storage in dessicator after a few months. However, some small spectral changes (decrease of A_{473}/A_{330} ratio) were also observed for the solid PMAS stored in the ambient conditions for more than 1 year. The GPC of pure HMWt PMAS after 2.5 years showed some impurity of LMWt species, which appeared as a small hump nearby the peak of HMWt PMAS (Figure 5.50). The polydispersity of the peak also increased slightly from 2.03 for the fresh polymer to 2.83 after aging for 2.5 years, presumably due to degradation and shortening of polymer chains to some extent.

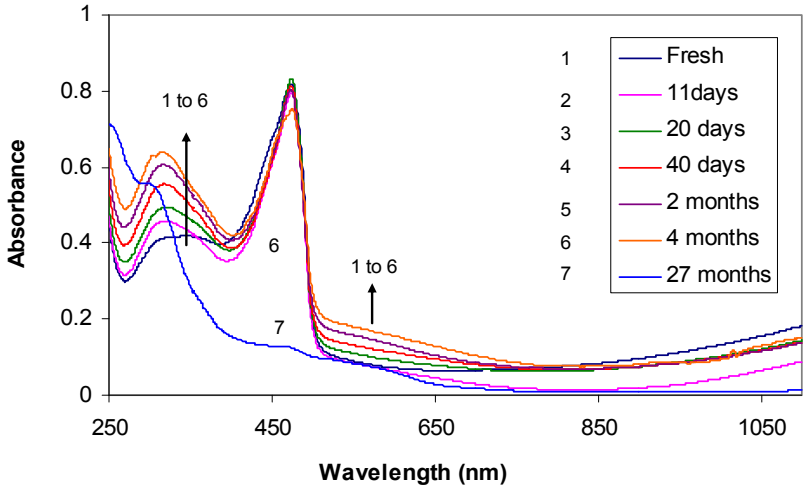

Figure 5.49. UV-vis spectral changes of dilute aqueous PMAS dilute solution (33 µg/mL) with aging.

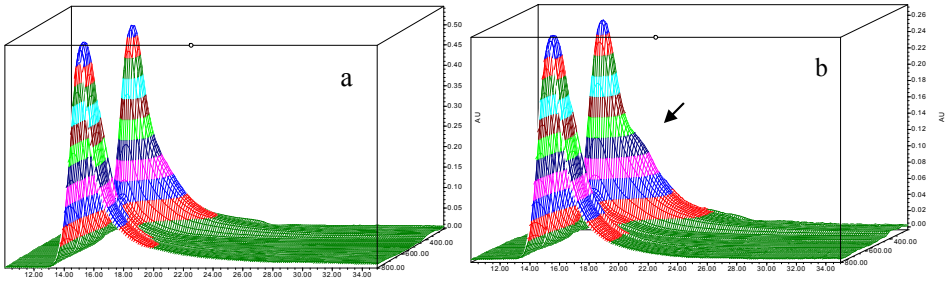

Figure 5.50. Aging effect on the 3D GPC chromatogram of pure HMWt PMAS: (a) pure fresh PMAS, and (b) HMWt PMAS after 2.5 years storage in a dessicator.

The stability of PMAS aqueous solution with storage was also studied by conductivity studies on films cast from fresh and old solutions. The conductivity of PMAS films deposited from the 50 mg/mL solution were significantly decreased by solution storage, from 0.71 S/cm for a fresh solution to 0.38 S/cm after 5 hours and 0.16 S/cm after 4 days (Figure 5.51). This decrease in conductivity can be attributed to the breaking of some chains due to hydrophilic attack of water molecules on the aminic bonds, as suggested by Barbero *et al.*[11].

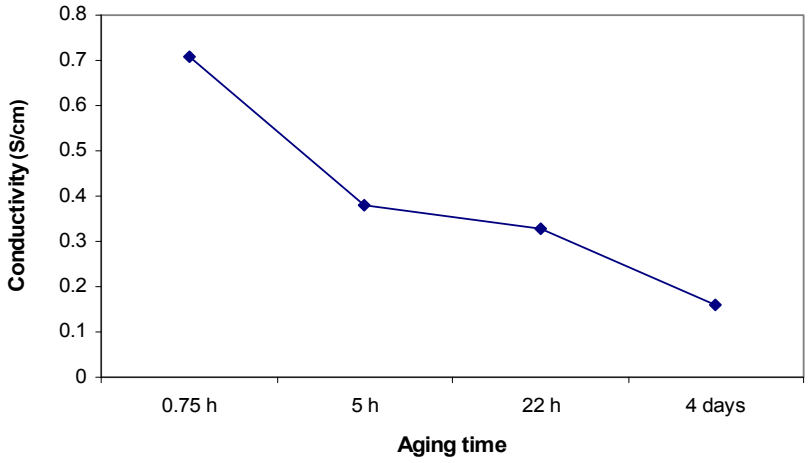

Figure 5.51. Effect of storage time of aqueous PMAS on the conductivity of drop-cast PMAS films. The films were dried by evaporating in air and storing in a desiccator for 3h.

The slow UV-vis spectral changes of aqueous PMAS with aging indicate oxidation and degradation of polymer under the open environment, and suggest that storage of PMAS solutions should be in the dark and under sealed conditions.

5.3.11 The nature of LMWt PMAS

Characterisation of LMWt PMAS showed that this material is distinctly different from the conducting emeraldine salt form of PMAS, exhibiting a different UV-vis spectrum and different morphology. LMWt PMAS is non-conducting, shows no ESR signal (i.e. no electron spin), and no electroactivity. The redox inactivity of LMWt and oligomers of PMAS is in contrast with para-coupled parent aniline tetramer and pentamer [27] or phenyl-capped aniline heptamer [35]. This suggests that the LMWt fractions of PMAS may be formed by different couplings between the phenyl rings, resulting in the loss of electroactivity and conductivity.

Very recently a study of the genesis of polyaniline nanotubes by Stejskal *et al.* [61] has shown that at the beginning of aniline oxidation in 0.40 M acetic acid (pH ~4), semi-crystalline oligomers, rod-like objects with dimensions of several micrometers, precipitate from the reaction medium. FTIR study of this precipitate separated at the beginning of oxidative polymerisation of aniline revealed the presence of phenazine-like structures, as a result of some *ortho*-coupling of aniline molecules. The phenazine units are produced from oxidation of *ortho*-coupled anilines combined with intramolecular cyclisation. It is suggested that the nano-sized oligomer crystallites serve as starting templates for the nucleation of PAn nanotubes. The oligomeric product is non-conducting (2.4×10^{-10} S/cm) and results in a lower conductivity for the final polyaniline nanotubes (0.078 S/cm) compared to polyaniline synthesised in more acidic media.

Aging processes in PMAS also lead to formation of products with similar properties to LMWt PMAS. Formation of phenazine units by aging processes has been reported for polyaniline [61, 62]. The observed morphology of LMWt PMAS, together with its non-conducting behaviour, reveals some similarities between this fraction and the

phenazine-like oligomeric products obtained at the beginning of polymerisation of aniline at pH~4 [61].

The results obtained here therefore suggest the possible existence of phenazine-like structures (Figure 5.52) in the LMWt PMAS fraction as a result of *ortho*-coupling of MAS monomer units during the polymerisation at pH ~4, as discussed in Chapter 4.

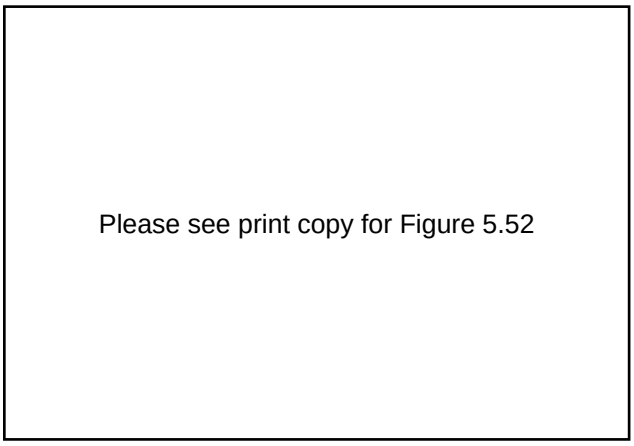

Figure 5.52. (A) coupling of aniline molecules in both *ortho*- and *para*-positions during the oxidative polymerisation in mildly acidic media., (B) Formation of a phenazine unit by further oxidation of *ortho*-coupled units [61].

5.4 Conclusions

The separation via cross-flow dialysis of high molecular weight (HMWt) and low molecular weight (LMWt) fractions from previously described poly(2-methoxyaniline-5-sulfonic acid) (PMAS) has permitted a detailed characterisation of these pure PMAS fractions. The high molecular weight PMAS fraction has M_p of 16.9 kDa, while the low molecular weight PMAS fraction is an oligomer with M_p of *ca.* 2-3 kDa

The UV-visible spectrum of LMWt PMAS is unaffected by changes in pH or treatment with oxidizing or reducing agents, confirming its chemical inertness. In contrast, aqueous HMWt PMAS emeraldine salt is oxidised to its pernigraniline base form by persulfate ions and reduced to PMAS leucoemeraldine base by hydrazine, consistent with it being an emeraldine salt.

Scan rate studies on the cyclic voltammetry of the electroactive HMWt PMAS reveal that the redox reactions of aqueous HMWt PMAS are reversible with one electron transfer involved. A diffusion constant of (0.57-2.3) x 10^{-7} cm^2s^{-1} is estimated for 1.2 mM HMWt PMAS.

In contrast to HMWt PMAS (with a conductivity of 0.02-1.74 S/cm depending on the synthetic conditions), the LMWt PMAS is not conducting and has no ESR signal. The ESR spectrum of aqueous PMAS shows a symmetric line similar to parent polyaniline emeraldine salt, with a g value of 2.00295 and a line width of ~2.55 G. Dialysed PMAS (containing *ca.* 20% LMWt PMAS) has a significantly lower electrical conductivity (typically 4 to 5 times less) than the purified HMWt PMAS fraction. The ESR spectra of the PMAS mixtures when compared to pure HMWt PMAS, at equivalent dilution levels, exhibit a lower level of electron spin in the presence of LMWt PMAS. This result suggests that the presence of the LMWt PMAS converts the HMWt PMAS from a high-spin polaron state into a low-spin bipolaron state. The observed loss of electrical conductivity is presumably caused by interaction of the LMWt fraction with the charge carriers in the HMWt PMAS, inhibiting interchain charge transfer.

The photochemical properties of PMAS reassessed in this Chapter. The LMWt PMAS fraction is shown to be the source of the unexpected photoemission recently reported for aqueous PMAS. Pure HMWt PMAS does not photoluminesce, and is shown to statically quench the photoluminescence of LMWt PMAS. Fully reduced HMWt PMAS leucoemeraldine base (LB) strongly photoluminesces, in common with the LB form of unsubstituted polyaniline. The observed fluorescence lifetime for both HMWt and LMWt PMAS samples originates from the LMWt fraction. Because of this, longer sample acquisition times are required to collect a signal from the HMWt PMAS fraction as it has low trace level concentrations of the emitting LMWt component. As a result, for both PMAS samples the second- (τ_2) and third- (τ_3) order lifetime responses have lifetimes of 1-2 ns and 6-8 ns, respectively.

Mixtures of the high and low molecular weight fractions display a distortion to the luminescence spectra and decreased luminescence intensity, without accompanying

changes in luminescent lifetime. This behaviour is consistent with absorption of emitted light from the LMWt PMAS fraction by the HMWt PMAS fraction via an inner filter quenching (or radiative energy transfer) effect. Results suggest that a second quenching process occurring between the HMWt and LMWt PMAS fractions further complicates the interpretation. Based on relative absorbance and emission properties of the two fractions, a second non-radiative energy transfer is likely to occur and the quenching data correspond well to a static quenching model in a diffusionally restricted polymer environment. The non-linear fluorophore-quencher behaviour is successfully described via a Perrin quenching model. The static quenching behaviour suggests strong association of the two distinct PMAS fractions and also sheds further light on why extraordinary purification methods are required for their separation.

PMAS is soluble in water (>100 mg/mL) and DMSO (~20 mg/mL), which are highly polar protic and aprotic solvents, respectively. It is insoluble in other common protic and aprotic solvents.

Elemental analysis of PMAS reveals that the HMWt PMAS is an ammonium salt and *ca*. 80% of the free sulfonate groups along the chain are associated with ammonium ions. The ammonium ions are exchanged by hydrogen ions (H^+) using a proton exchange resin.

A HMWt PMAS film shows a smooth surface. PMAS is a nanostructured fully-sulfonated polyaniline. The morphology of HMWt PMAS is affected by synthetic conditions, varying from rod-like (diameters about 100 nm) to spherical nanoparticles (with diameters less than 50 nm). A TEM micrograph of the LMWt PMAS shows a mixture of nanoparticles and needles with diameters less than 100 nm.

The HMWt and LMWt PMAS are thermally stable up to *ca.* 250°C and 280°C, respectively. HMWt PMAS in the solid state is stable over a year, with some degradation to low molecular weight materials observed by GPC after longer storage. An aqueous solution of HMWt PMAS is stable for a few weeks. Small changes in the UV-vis spectrum of this solution is observed in which the intensity of the 300 nm peak

increases with storage time, presumably due to degradation of the polymer chains in the presence of water.

Characterisation of LMWt PMAS shows that this material is distinctly different from the conducting emeraldine salt form of PMAS, exhibiting different optical and electrical properties. The non-conducting behaviour of LMWt PMAS and some similarities of this fraction with the phenazine-like oligomeric products of polyaniline suggest the possible existence of phenazine-like structures in the LMWt PMAS fraction as a result of *ortho*-coupling of MAS monomer units during polymerisation at pH ~4.

5.5 References

1. Yue, J. and Epstein, A.J., *Synthesis of self-doped conducting polyaniline.* J. Am. Chem. Soc., 1990. **112**(7): p. 2800-2801.
2. Chen, S.-A. and Hwang, G.-W., *Structure Characterization of Self-Acid-Doped Sulfonatic Acid Ring-Substituted Polyaniline in Its Aqueous Solutions and as Solid Film.* Macromolecules, 1996. **29**: p. 3950-3955.
3. Barbero, C., Miras, M.C., Kotz, R., and Haas, O., *Sulphonated polyaniline (SPAN) films as cation insertion electrodes battery applications Part II: Exchange of mobile species in aqueous and non-aqueous solutions.* Journal of Electroanalytical Chemistry, 1997. **437**(1-2): p. 191-198.
4. Barbero, C., Miras, M.C., Kotz, R., and Haas, O., *Comparative study of the ion exchange and electrochemical properties of sulfonated polyaniline (SPAN) and polyaniline (PANI).* Synthetic Metals, 1993. **55**(2-3): p. 1539-1544.
5. Hwang, K.S., Lee, C.W., Yoon, T.H., and Son, Y.S., *Fabrication and characteristics of a composite cathode of sulfonated polyaniline and Ramsdellite-MnO2 for a new rechargeable lithium polymer battery.* Journal of Power Sources, 1999. **79**(2): p. 225-230.
6. Rubner, M.F.a.M.F., *Molecular-Level Processing of Conjugated Polymers. 1. Layer-by-Layer Manipulation of Conjugated Polyions.* Macromolecules, 1995. **28**(21): p. 7107-7114.
7. Wei, X. and Epstein, A.J., *Synthesis of highly sulfonated polyaniline.* Synthetic Metals, 1995. **74**(2): p. 123-125.
8. Wei, X.-L., Wang, Y.Z., Long, S.M., Bobeczko, C., and Epstein, A., *Synthsis and Physical Properties of High Sulfonated Polyaniline.* J. Am. Chem. Soc., 1996. **118**: p. 2545-2555.
9. Yue, J., Wang, Z.H., Cromack, K.R., Epstein, A., and MacDiarmid, A.G., *Effect of Sulfonic Acid Group on Polyaniline Backbone.* J. Am. Chem. Soc., 1991. **113**: p. 2665-2671.
10. Barbero, C., Salavagione, H.J., Acevedo, D.F., Grumelli, D.E., Garay, F., Planes, G.A., Morales, G.M., and Miras, M.C., *Novel synthetic methods to produce functionalized conducting polymers I. Polyanilines.* Electrochimica Acta, 2004. **49**(22-23): p. 3671-3686.

11. Cesar Barbero, Maria.C. Miras., Bernhard Schnyder, Otto Hass and Rüdiger Kötz, *Sulfonated polyaniline films as cation insertion electrodes for battery applications. Part 1.—Structural and electrochemical characterization.* J. Mater. Chem.,, 1994. **4**(12): p. 1775-1783.
12. Hwang, S.-A and Chen, G.-W., *Synthesis of Water-Soluble Self- Acid-Doped Polyaniline.* J. Am. Chem. SOC., 1994. **116**(17): p. 7939-7940.
13. Hwang, S.-A and Chen, G.-W., *Water-Soluble Self-Acid-Doped Conducting Polyaniline: Structure and Properties.* J. Am. Chem. SOC., 1995. **117**(40): p. 10055-10062.
14. Shimizu, S., Saitoh, T., Uzawa, M., Yuasa, M., Yano, K., Maruyama, T., and Watanabe, K., *Synthesis and applications of sulfonated polyaniline.* Synthetic Metals, 1997. **85**(1-3): p. 1337-1338.
15. Innis, P.C., Chen, Y.C., Ashraf, S., and Wallace, G.G., *Electrohydrodynamic polymerisation of water-soluble poly((4-(3-pyrrolyl))butane sulfonate).* Polymer, 2000. **41**(11): p. 4065-4076.
16. Zhou, D., Innis, P.C., Wallace, G.G., Shimizu, S., and Maeda, S.-I., *Electrosynthesis and characterisation of poly(2-methoxyaniline-5-sulfonic acid)-effect of pH control.* Synthetic Metals, 2000. **114**(3): p. 287-293.
17. Strounina, E.V., *Synthesis and Characterisation of Chiral Substituted Polyanilines*, in *Chemistry Department*. 2001, University of Wollongong.
18. Strounina, E.V., Kane-Maguire, L.A.P., and Wallace, G.G., *Optically active sulfonated polyanilines.* Synthetic Metals, 1999. **106**(2): p. 129-137.
19. Pornputtkul, Y., *Development of Chiral Conducting Polymers for Asymmetric Electrosynthesis*, in *Chemistry department*. 2005, University of Wollongong.
20. Tallman, D.E. and Wallace, G.G., *Preparation and preliminary characterization of a poly (4-vinylpyridine) complex of a water-soluble polyaniline.* Synthetic Metals, 1997. **90**(1): p. 13-18.
21. Li, C., Mitamura, K., and Imae, T., *Electrostatic Layer-by-Layer Assembly of Poly(amido amine) Dendrimer/Conducting Sulfonated Polyaniline: Structure and Properties of Multilayer Films.* Macromolecules, 2003. **36**(26): p. 9957-9965.
22. Strounina, E.V., Shepherd, R., Kane-Maguire, L.A.P., and Wallace, G.G., *Conformational changes in sulfonated polyaniline caused by metal salts and OH.* Synthetic Metals, 2003. **135**(1-3): p. 289-290.
23. T. Tatsuma, T.O., R. Sato, and N. Oyama, J. Electroanal. Chem., 2001. **501**: p. 180-185.
24. Lee, W., Du, G., Long, S.M., Epstein, A.J., Shimizu, S., Saitoh, T., and Uzawa, M., *Charge transport properties of fully-sulfonated polyaniline.* Synthetic Metals, 1997. **84**(1-3): p. 807-808.
25. Kane-Maguire, L.A.P., Causley, J.A., Kane-Maguire, N.A.P., and Wallace, G.G., *Photoluminescence and photo-redox reactions of poly(2-methoxyaniline-5-sulfonic acid).* Current Applied Physics, 2004. **4**(2-4): p. 394-397.
26. Masdarolomoor, F., Innis, P.C., Ashraf, S., and Wallace, G.G., *Purification and characterisation of poly(2-methoxyaniline-5-sulfonic acid).* Synthetic Metals, 2005. **153**(1-3): p. 181-184.
27. Chen, L., Yu, Y., Mao, H., Lu, X., Zhang, W., and Wei, Y., *Synthesis of parent aniline tetramer and pentamer and redox properties.* Materials Letters, 2005. **59**(19-20): p. 2446-2450.

28. SeinJr., L.T., Duong, T., Wei, Y., and Jansen, S.A., *Theoretical analysis of 2,6-dialkyl-substituted aniline trimers.* Synthetic Metals, 2000. **113**(1-2): p. 145-149.
29. P.M. McManus, S.C.Y.a.R.J.C., Chem. Soc., Chem. Commun., 1985: p. 1556.
30. S. Stafsrtom, J.L.B., A.J. Epstein, H.S. Woo, D.B. Tanner, W.S. Huang and A.G. MacDiarmid, Phys. Rev. Lett., 1987. **59**: p. 1464-1467.
31. Stejskal, J., Kratochvil, P., and Radhakrishnan, N., *Polyaniline dispersions 2. UV--Vis absorption spectra.* Synthetic Metals, 1993. **61**(3): p. 225-231.
32. Huang, W.S. and MacDiarmid, A.G., *Optical properties of polyaniline.* Polymer, 1993. **34**(9): p. 1833-1845.
33. Albuquerque, J.E., Mattoso, L.H.C., Balogh, D.T., Faria, R.M., Masters, J.G., and MacDiarmid, A.G., *A simple method to estimate the oxidation state of polyanilines.* Synthetic Metals, 2000. **113**(1-2): p. 19-22.
34. Strounina, E.V., Shepherd, R., Kane-Maguire, L.A.P., and Wallace, G.G., *Conformational Changes in Sulfonated Polyaniline Caused By Metal Salts and OH-.* Synthetic Metals, 2003. **135-136**: p. 289-290.
35. Chen, L., Yu, Y., Mao, H., Lu, X., Zhang, W., and Wei, Y., *Synthesis of phenyl-capped aniline heptamer and its UV-vis spectral study.* Synthetic Metals, 2005. **149**(2-3): p. 129-134.
36. Tawde, S., Mukesh, D., and Yakhmi, J.V., *Redox behavior of polyaniline as influenced by aromatic sulphonate anions: cyclic voltammetry and molecular modeling.* Synthetic Metals, 2001. **125**(3): p. 401-413.
37. Engelhardt, H.A.P.a.E.H., *SYNTHESIS AND CHARACTERIZATION OF SOME HIGHLY CONJUGATED SEMICONDUCTING POLYMERS.* Journal of Physical Chemistry, 1962. **66**(11): p. 2085-2095.
38. Jayashree Anand, S.P., and D. N. Sathyanarayana, *Variable-Temperature EPR and Transport Studies on Poly(4,4'-methylenedianiline): Evidence for Bipolarons.* J. Phys. Chem., 1995. **99**(25): p. 10324 - 10328.
39. Krinichnyi, V.I., Konkin, A.L., Devasagayam, P., and Monkman, A.P., *Multifrequency EPR study of charge transport in doped polyaniline.* Synthetic Metals, 2001. **119**(1-3): p. 281-282.
40. Lin, D.-S. and Yang, S.-M., *Syntheses of ethyl and ethoxy-substituted polyaniline complexes.* Synthetic Metals, 2001. **119**(1-3): p. 111-112.
41. Sakharov, I.Y., Ouporov, I.V., Vorobiev, A.K., Roig, M.G., and Pletjushkina, O.Y., *Modeling and characterization of polyelectrolyte complex of polyaniline and sulfonated polystyrene produced by palm tree peroxidase.* Synthetic Metals, 2004. **142**(1-3): p. 127-135.
42. Langer, J.J., Krzyminiewski, R., Kruczynski, Z., Gibinski, T., Czajkowski, I., and Framski, G., *EPR and electrical conductivity in microporous polyaniline.* Synthetic Metals, 2001. **122**(2): p. 359-362.
43. Rao, P.S., Anand, J., Palaniappan, S., and Sathyanarayana, D.N., *Effect of sulphuric acid on the properties of polyaniline-HCl salt and its base.* European Polymer Journal, 2000. **36**(5): p. 915-921.
44. Wei, X.-L., Wang, Y.Z., Long, S.M., Bobeczko, C., and Epstein, A.J., *Synthesis and Physical Properties of Highly Sulfonated Polyaniline.* J. Am. Chem. Soc., 1996. **118**(11): p. 2545-2555.
45. Jiang Yue, Z.H.W., Keith R. Cromack, Arthur J. Epstein, Alan G. MacDiarmid, *Effect of sulfonic acid group on polyaniline backbone.* J. Am. Chem. Soc., 1991. **113**(7): p. 2665-2671.

46. Kahol, P.K., Perera, R.P., Satheesh Kumar, K.K., Geetha, S., and Trivedi, D.C., *Electron localization length in polyaniline.* Solid State Communications, 2003. **125**(7-8): p. 369-372.
47. Kahol, P.K., Satheesh Kumar, K.K., Geetha, S., and Trivedi, D.C., *Effect of dopants on electron localization length in polyaniline.* Synthetic Metals, 2003. **139**(2): p. 191-200.
48. Heeger, A.J., *Semiconducting and Metallic Polymers: The Fourth Generation of Polymeric Materials.* J. Phys. Chem. B, 2001. **105**(36): p. 8475-8491.
49. Thorne, J.R.G., Masters, J.G., Williams, S.A., MacDiarmid, A.G., and Hochstrasser, R.M., *Time-resolved fluorescence of polyaniline.* Synthetic Metals, 1992. **49**(1-3): p. 159-165.
50. Kim, K., Lin, L.B., Ginder, J.M., Gustafson, T.L., and Epstein, A.J., *Luminescence and picosecond photoinduced absorption of polyaniline.* Synthetic Metals, 1992. **50**(1-3): p. 423-428.
51. Shimano, J.Y. and MacDiarmid, A.G., *Polyaniline, a dynamic block copolymer: key to attaining its intrinsic conductivity?* Synthetic Metals, 2001. **123**(2): p. 251-262.
52. Cochet, M., Buisson, J.-P., Wery, J., Jonusauskas, G., Faulques, E., and Lefrant, S., *A complete optical study of the conductive form of polyaniline: the emeraldine salt.* Synthetic Metals, 2001. **119**(1-3): p. 389-390.
53. Chen, S.-A., Chuang, K.-R., Chao, C.-I., and Lee, H.-T., *White-light emission from electroluminescence diode with polyaniline as the emitting layer.* Synthetic Metals, 1996. **82**(3): p. 207-210.
54. Son, Y., Patterson, H.H., and Carlin, C.M., *Potential-dependent photoluminescence of conductive polymers: Simple quenching model and experimental results for poly(aniline).* Chemical Physics Letters, 1989. **162**(6): p. 461-466.
55. Lee, S., Lee, J.Y., and Lee, H., *Solvent effects on the characteristics of conductive and luminescent polymers.* Synthetic Metals International Conference on Science and Technology of Synthetic, 1999. **101**(1-3): p. 248-249.
56. Peter Åsberg, P.N., and Olle Inganäs, *Fluorescence quenching and excitation transfer between semiconducting and metallic organic layers.* Journal of Applied Physics, 2004. **96**: p. 3140.
57. Yang, J., Winnik, M.A., Ylitalo, D., and DeVoe, R.J., *Polyurethane-Polyacrylate Interpenetrating Networks. 2. Morphology Studies by Direct Nonradiative Energy Transfer Experiments.* Macromolecules, 1996. **29**(22): p. 7055-7063.
58. Suppan, P., *"Chemistry of Light",*. 1994, Cambridge: The Royal Society of Chemistry. 70.
59. Sluch, M.I., Samuel, I.D.W., Beeby, A., and Petty, M.C., *Photoinduced Electron Transfer between 16-(9-Anthroyloxy)palmitic Acid and Fullerene C60 in Langmuir-Blodgett Films.* Langmuir, 1998. **14**(12): p. 3343-3346.
60. Antonel, P.S., Molina, F.V., and Andrade, E.M., *Fluorescence of polyaniline films on platinum surfaces. Influence of redox state and conductive domains.* Journal of Electroanalytical Chemistry, 2007. **599**(1): p. 52-58.
61. Stejskal, J., Sapurina, I., Trchova, M., Konyushenko, E.N., and Holler, P., *The genesis of polyaniline nanotubes.* Polymer, 2006. **47**(25): p. 8253-8262.

62. Mathew, R., Mattes, B.R., and Espe, M.P., *A solid state NMR characterization of cross-linked polyaniline powder.* Synthetic Metals, 2002. **131**(1-3): p. 141-147.
63. Pereira da Silva, J.E., de Faria, D.L.A., Cordoba de Torresi, S.I., and Temperini, M.L.A., *Influence of Thermal Treatment on Doped Polyaniline Studied by Resonance Raman Spectroscopy.* Macromolecules, 2000. **33**(8): p. 3077-3083.

Chapter 6

Chemical synthesis and characterisation of PAn/PMAS

6.1 Introduction

Routes to enhancing the processability of ICP's have been an ongoing challenge. In this regard, a number of strategies aimed at improving the processability of polyaniline have been investigated. Chemical and electrochemical synthesis of appropriate substituted monomers such as aniline carboxylic acid [1], o-aminobenzylphosphonic acid [2], or methoxyaniline sulfonic acid [3-5], as well as post synthesis chemical modification of polyaniline [6-9] have resulted in self-doped polyanilines with improved solubility and redox activity over a wide pH range. However, these polymers have low electrical conductivity as these modifications distort the molecular structure from the ideal conformation. In a recent review by Malinauskas [10] the synthesis and properties of self-doped polyanilines have been presented, reviewing some aspects of polymerisation and properties of these materials [10].

An alternate route to solution processing has been the formation of nanostructured colloidal dispersions with conductivities lower than the bulk material by using a range of steric stabilisers. These include surfactants, micelles and dispersed templates such as dodecylbenzene sulfonic acid [11, 12], naphthalenesulfonic acid [13] polyethylene oxide [14, 15], water soluble polymers such as poly(N-vinyl-pyrrolidone) [16, 17], organic dopants [18], and silica colloids [19]. In these cases the stabilising material has the inherent limitation of preventing ICP particle interaction, thereby reducing the conductivity of cast films with respect to a bulk system.

Recently, polyaniline nonofibers have been synthesised using interfacial polymerisation at aqueous/organic interfaces or via rapid mixing of monomer and oxidant solutions in a controlled ratio[20, 21]. These methods have the advantage of providing a facile

stabiliser and template-free polymerisation that subsequently simplifies purification. The nanofibers formed via the rapid mixing route have diameters between 30 and 50 nm forming relatively stable dispersions at pH around 2-3 [22].

The fully sulfonated polyaniline, poly(2-methoxyaniline-5-sulfonic acid) (PMAS) (Scheme 6.1 shown below), has one free negatively charged sulfonate group per dimer unit with the second involved in the self-doping of the polymer. This polymer has characteristics similar to polyaniline. Due to these unique properties, PMAS has been used to make complexes with positively charged materials such as chiral amines [23]. It has also been used as a molecular dopant for preformed polyaniline [24]. PMAS has also been used as a molecular dopant for polypyrrole being incorporated during electrosynthesis [25]. A novel route was developed in Chapter 3 for purification and fractionation of this polymer [26]. The highly pure PMAS (obtained using the optimal procedure developed in Chapter 4) has a molecular weight (M_p) of 16.9 kDa and significantly enhanced conductivity compared to the (tubular) dialysed PMAS published previously [3-5].

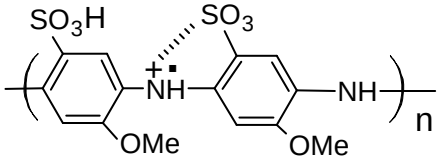

Scheme 6.1. Structure of PMAS

In the course of this work the synthesis of polyaniline in the presence of PMAS was investigated. The polyelectrolyte PMAS rendered the polyaniline soluble or dispersible in water. Additionally, since PMAS is also a conducting polyelectrolyte it has the advantage of not introducing an insulating component to the resultant material, which has been a major limitation of previous surfactant based studies [27].

In this chapter the synthesis of PAn/PMAS (Scheme 6.2) by chemical oxidation of aniline in the presence of PMAS was investigated while monitoring the effect of pH and

PMAS concentration on the conductivity, electroactivity and physical properties of the resultant material.

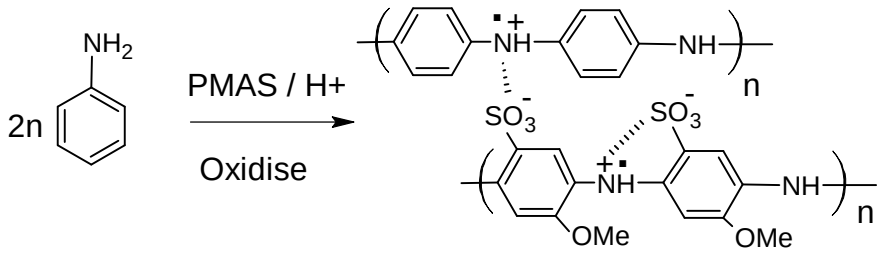

Scheme 6.2. Chemical polymerisation of aniline in the presence of PMAS.

6.2 Experimental

6.2.1 Materials

Aniline was purchased from Aldrich and was distilled and stored at -4ºC (freezer) prior to use. Ammonium persulfate, hydrazine monohydrate and tetrabutylammonium dihydrogen phosphate were purchased from Aldrich. Ammonium hydroxide (28% w/v NH_3) and hydrochloric acid 32% (w/v) were purchased from Ajax. Methanol (HPLC grade) was supplied by Ajax chemicals. PMAS (conductivity ~0.25 S/cm and MW ~10,000 Da) was synthesised and purified in house [25]. Amberlite cation exchange resin (IRA-400), obtained from BDH chemicals, was exposed to HCl 2M and used to convert PMAS to the acid form. All reagents used were of analytical grade and all solutions were prepared in Milli-Q water (18 MΩ cm).

6.2.2 Synthesis and purification of PAn/PMAS

A polymerisation procedure similar to that used by Huang and Kaner [21] was employed. A 5 mL aqueous solution of aniline in PMAS and another 5 mL of ammonium persulfate (APS) in PMAS were prepared and mixed rapidly together followed by rapid stirring. For the polymerisation of aniline in the presence of PMAS and HCl (0.10 or 1.0 M), 200 μL of APS was added rapidly to a 10 mL aqueous solution of aniline, PMAS and HCl. The reaction mixture was left stirring overnight at

room temperature. The aniline concentration was 0.08 M or 0.16 M and the PMAS concentration varied from 0 to 1.60% (w/v). The aniline to APS molar ratio was 4 to 1 unless otherwise stated (see Tables 6.1 and 6.2 later in the results). A concentrated dark green dispersion (suspension) was produced overnight. The polymerised dispersion was diluted six times in water and purified using a Beckman (J2-MC, rotor JA10) centrifuge at 4100 rpm for 15 min. The supernatant was decanted and retained for characterisation. The precipitate was redispersed by shaking in water, followed by centrifuging/decantation 3 times. The final precipitate was diluted to 10 mL for characterisation. The yield was measured by drying the pure product. PAn/HCl dispersion was prepared under identical conditions but in the absence of PMAS.

6.2.3 Polymer characterisation

Contact angle measurements

Contact angles were measured using DataPhysics OCAZO Goniometer (employing SCAZI software). A 2 μL water was lowered onto the polymer surface and the contact angle was recorded after the angle reached to a relatively constant value (advanced contact angle). The polymer films were prepared by evaporative casting onto glass substrate from the dispersion in water or electrochemical deposition onto Pt-ITO glass substrate.

HPLC analysis

Reverse phase HPLC was carried out to determine residual aniline. A Waters Bondapak C_{18} column and a Linear UVIS 200 UV detector (λ_{max} = 208 nm) were employed. The chromatograms were recorded on a Shimadzu C-R5A Chromatopac integrator. A mobile phase consisting of 40% v/v methanol and 60% v/v aqueous solution of 5 mM tetrabutylammonium dihydrogen phosphate was used at a flow rate of 1 mL/min. Sample injection volume was 10μL. The concentration of aniline was measured before addition of oxidant (T_0) and after the polymerisation reaction was completed (T_x). Monomer conversion was calculated using the following equation:

$$\%\text{Monomer conversion} = (1-T_x/T_0)x100$$

Thermal analysis

Thermogravimetry was carried out using a DTA TA Instruments Q800 Thermal Gravimetric Analyser. Temperature was increased from 35 °C (equilibrated for 20 min) to 600 °C at a heating rate of 10 °C per minute under nitrogen atmosphere at a flow rate of 60 mL/min.

UV-Vis spectroscopy

The UV-Vis spectra of aqueous dispersions of PAn/PMAS were recorded between the wavelengths of 250 nm and 1100 nm using a Shimadzu UV-1601 UV-vis spectrophotometer. The quartz cells with 1 cm path length were used. For base treatment experiments, the spectra of PAn/PMAS were recorded in 0.06 M NaOH. The concentration of PAn/PMAS and PAn/HCl dispersions were 0.0025% w/v (25 μg/mL).

Elemental analysis

Elemental analyses were performed by the ANU (Australian National University) Microanalytical laboratory using an automatic analyser, Carlo Erba for C, H, N determinations, and a Dionex Ion Chromatography Analyser for S and Cl analysis. The samples (3 mg of powder materials) were heated to 50 ºC in a vacuum oven for 5 hours prior to analysis. The PMAS samples for elemental analysis were PAn/PMAS samples obtained using different concentrations of PMAS.

ESR

The ESR spectra of the samples were recorded on a Bruker EMX ESR spectrometer under identical conditions of microwave frequency (9.87 GHz), attenuator (30.0 dB), sweep width (25 G), modulation frequency (100 KHz), modulation amplitude (0.5 G), time constant (10.24 mSec), conversion time (40.96 mSec) resulting in a scan sweep time of 671s. Aqueous samples consisting of 1.5 mg/mL polyaniline dispersion were injected into the microwave cavity via a Bruker Aqua-X™ flow cell which permitted rapid sample change over and ensured identical cell geometry and reproducible cavity tuning.

Morphology

Transmission electron microscopy was carried out using a Hitachi H7000 TEM at 75 KeV in order to observe the morphology of samples cast onto TEM grids from dilute PAn/PMAS aqueous dispersions of approximately 0.02 mg/mL.

Conductivity

Conductivity measurements were performed on dried films of about 10 μm thickness using a JANDEL four-point probe resistivity system (model RM2). These were formed by drop casting onto glass slides from a ~1% w/v dispersion solutions. For conductivity measurements at different pH, the PAn/PMAS film was cast onto a glass substrate, immersed in buffer solutions and dried in a fume hood for 5 hours.

Electroactivity

Cyclic voltammetry (CV) was carried out in a three electrode cell using a glassy carbon working electrode with platinum mesh auxiliary and Ag/AgCl (3M NaCl) reference electrodes using an E-Corder 401 interface and Potentiostat (EDAQ). The CVs were recorded for the films cast onto a GC electrode (~250 $\mu g/cm^2$) from a PAn/PMAS dispersion. A 0.10 M HCl solution was used as electrolyte and a scan rate of 50 mV/sec was employed.

Other Characterisation

The pH of the polymer solutions was measured using a TPS Instruments Model 900-P pH meter. The open circuit potential of a platinum mesh versus a reference electrode (silver/silver chloride) was monitored in order to track the progression of the polymerisation reaction.

Particle size measurements were performed using a DLS (dynamic light scattering) Nano-ZS Zetasizer, Malvern Instruments.

6.3 Results and discussion

6.3.1 Doping PAn film with PMAS solution

In order to determine whether PAN could be doped with PMAS, electrochemically polymerised PAn films were dedoped/deprotonated in $NaOH_{(aq)}$ 0.30 M solution and re-doped in PMAS 0.50% w/v and HCl 1.0 M solutions respectively over 10 minutes. Both films turned from blue to green colour. UV-vis spectroscopy (Figure 6.1) showed that PMAS effectively re-doped the emeraldine base form of polyaniline. The broad band at 600 nm was replaced by a free carrier tail above 900 nm, indicative of doped emeraldine salt polyaniline films.

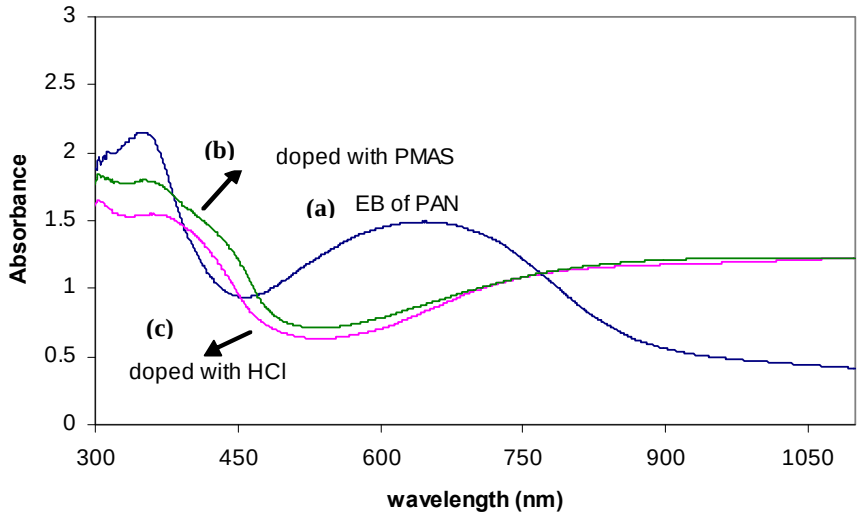

Figure 6.1. UV-vis spectra of (a) PAn EB film on ITO glass after doping with (b) PMAS 0.50% (w/v) and (c) HCl 1.0 M.

6.3.2 Chemical polymerisation of aniline in the presence of PMAS

After the successful doping of polyaniline film with PMAS, aniline was polymerised using PMAS as dopant. Reaction conditions are summarised in Table 6.1. Oxidation of aniline in the presence of 0.50% (w/v) PMAS resulted in the formation of a dark yellow-green dispersion which settled after centrifugation. After decanting off the supernatant the sediment was redispersed in Milli-Q water with shaking. This process was repeated 4 times. No PMAS was observed in the UV-vis spectrum of the first

supernatant indicating the incorporation of all PMAS in the PAn/PMAS product. UV-Vis spectra of the washed material were obtained (Figure 6.2). The UV-vis spectra of the product clearly showed that polyaniline in the emeraldine salt form was produced, although the doping level was lower than observed in Figure 6.1. The absorption bands at 430 and 810 nm are attributed to polyaniline [28] and the peak at 473 nm and the free carrier tail above 900 nm are attributed to the polaron bands of PMAS [29].

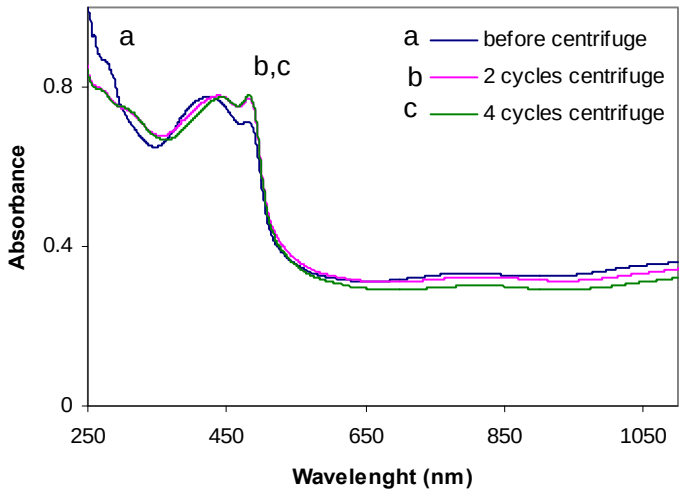

Figure 6.2. UV-vis spectra of PAn/PMAS dispersion before and after subsequent washing / centrifugation.

UV-vis spectra of the washed PAn/PMAS showed that the dopant was stable upon centrifugation (Figure 6.2). As the PAn/PMAS product became more pure, the intensity of bands at 276 nm and 390-400 nm which are related to residual aniline and oligomers decreased. (See also Figure 6.3). Increasing the number of washes resulted in a more intensely green supernatant such that dark green solutions with a pH about 4 to 5 were obtained after 4 and 5 cycles of washing/centrifugation. The pure precipitate was also redispersed in water.

When a higher ratio of oxidant to monomer was used, lower concentration of aniline remained in the first supernatant (see peak at 278 nm) (Figure 6.3). The UV-vis spectrum of the product clearly showed that polyaniline in the emeraldine salt form was produced as evidenced by the presence of a small band at 810 nm, although clearly the

doping level was low based on the weak nature of this feature (Figure 6.4 and Figure 6.5). The absorption bands at 430 and 810 nm are attributable to polyaniline while the peak at 473 nm and the free carrier tail above 900 nm are related to the polaron bands of PMAS.

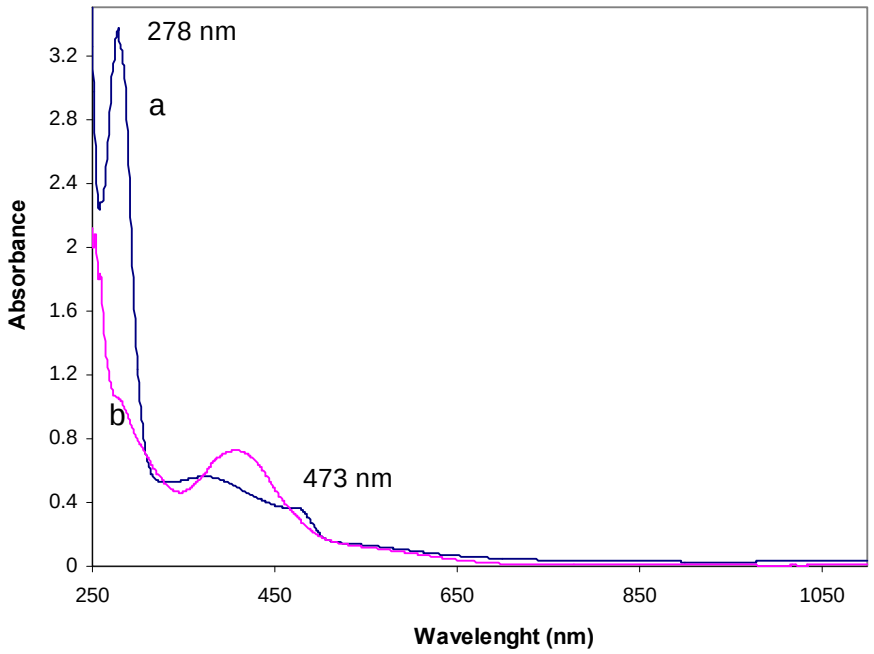

Figure 6.3. UV-vis spectra of filtered supernatant (second cycle of centrifugation) of the product obtained using different oxidant/aniline molar ratios, (a) 1:4, (b) 1:2. The supernatant was filtered by 0.45μm PTFE syringe filter.

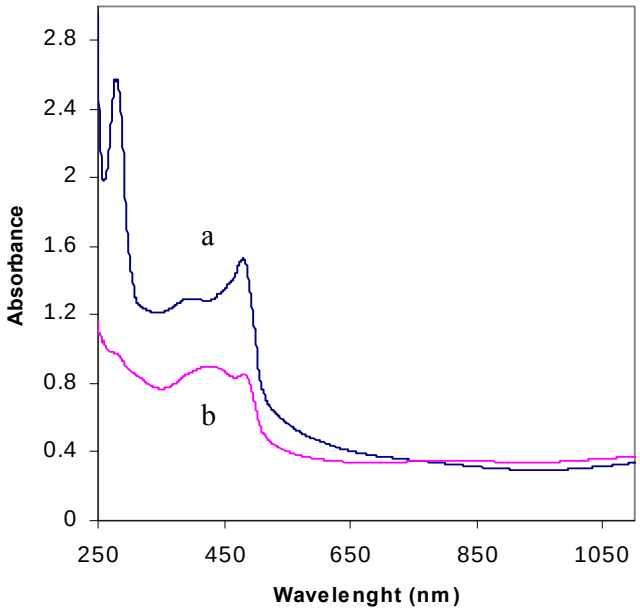

Figure 6.4. UV-vis spectra of PAn/PMAS dispersion before purification obtained using different oxidant/aniline ratios, (a) 1:4 and (b) 1:2.

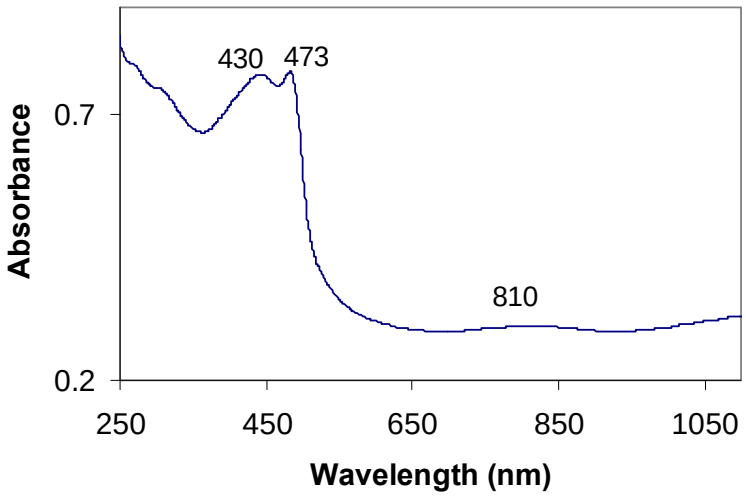

Figure 6.5. UV-vis spectrum of PAn/PMAS dispersion after purification (5 cycles of centrifugation/washing). The polymer was synthesised using 0.16 M aniline, 0.08 M APS (An/APS 1:2) and 0.50% w/v PMAS.

A thin film of PAn/PMAS was deposited onto a GC electrode by cycling the potential between -0.5 V and 1.1 V for 10 cycles at 50 mV/sec in an aqueous dispersion of the product at ~1% w/v. Characterisation of this polymer film by cyclic voltammetry showed two clear redox peaks attributed to switching between the oxidation states of PAn (Figure 6.6) according to Scheme 6.3.

leucoemeraldine salt (LS)

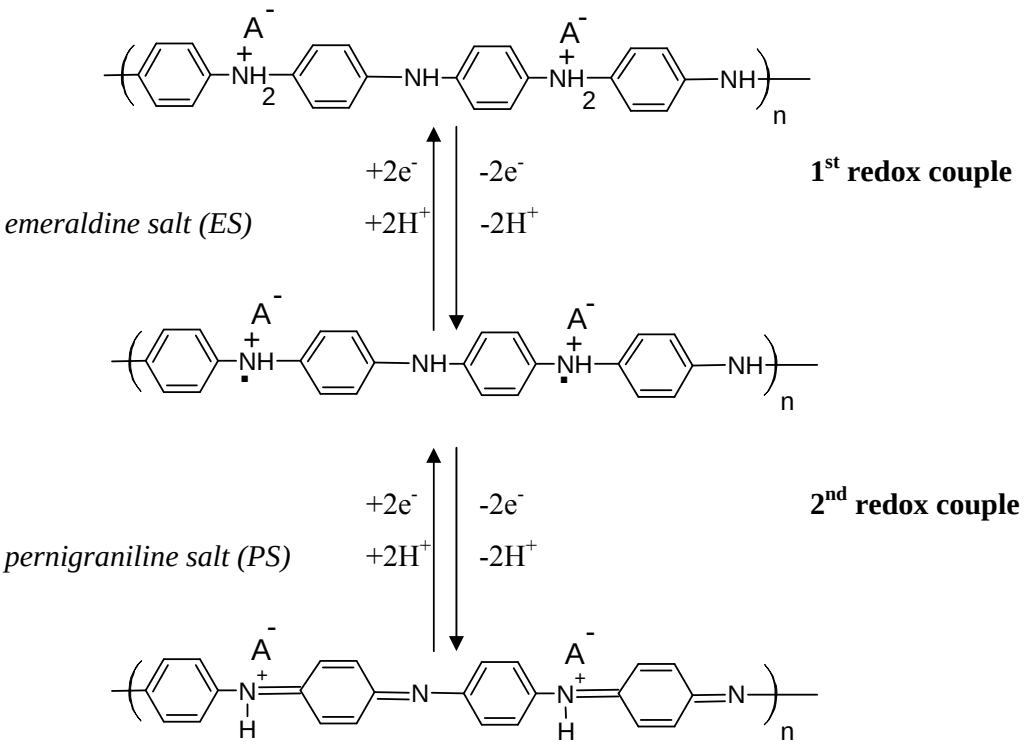

Scheme 6.3 Switching of polyaniline between redox states

The anodic peaks were observed at 0.2 V and 0.48 V with the corresponding cathodic peaks appears at 0.07 V and 0.43 V respectively. An additional weak oxidation wave observed at ca 0.64 V with the corresponding cathodic peak at 0.53 V. The well-defined oxidation waves were observed at more negative potential and are clearly different from the parent polyaniline.

A number of studies have shown that sulfonation of polyaniline alters the electrochemical behavior with respect to unsubstituted polyaniline. A shift toward more negative potentials has been reported for electrochemical doping of un-doped polyaniline with polyaniline-sulfonic acid [30]. A more negative second redox pair (ES to PS transition) has also been reported for the self-doped copolymer of aniline and m-aminobenzenesulfonic acid (metanilic acid) [31]. Doping of polyaniline by potential cycling in some aromatic sulfonate anions such as naphthalene sulfonic acid has also been reported to result in a shift of the second oxidation pair toward more and more negative direction with time [32].

As PMAS is itself electroactive, the redox pairs observed in the voltammogram is a combination of redox peaks of polyaniline and PMAS.

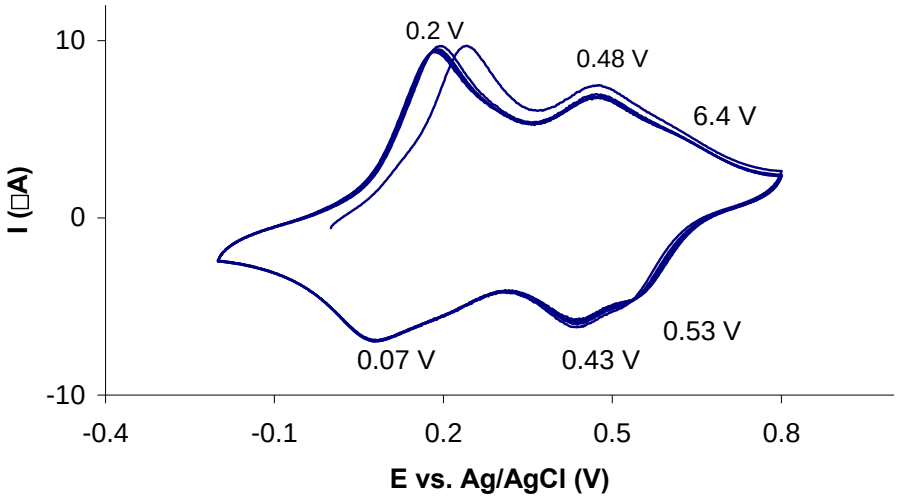

Figure 6.6. Cyclic voltammogram of a thin film of PAn/PMAS in 0.10 M HCl solution. Scan rate 50 mV s^{-1}. The polymer was deposited onto a GC electrode by cycling the potential between -0.5 V and 1.1 V for 10 cycles at 50 mV/sec.

In order to increase the doping level, the PMAS concentration was increased up to 3.00% (w/v). This increase resulted in a stable dispersion formation. This corresponded to a stochiometric ratio of aniline to PMAS (dimer unit) of 2:1. UV-visible spectra obtained on this material displayed an intense peak at 473 nm indicative of the presence

of PMAS. The increased intensity of the free carrier tail (λ > 900 nm) and the absence of a peak at 810 nm suggest that the polyaniline was in the extended coil conformation. Since PMAS has an extended coil conformation [29], the conformation of the PAn may have been induced by the PMAS. The conductivity was found to increase 10 fold (0.75 S/cm) using this higher concentration of PMAS.

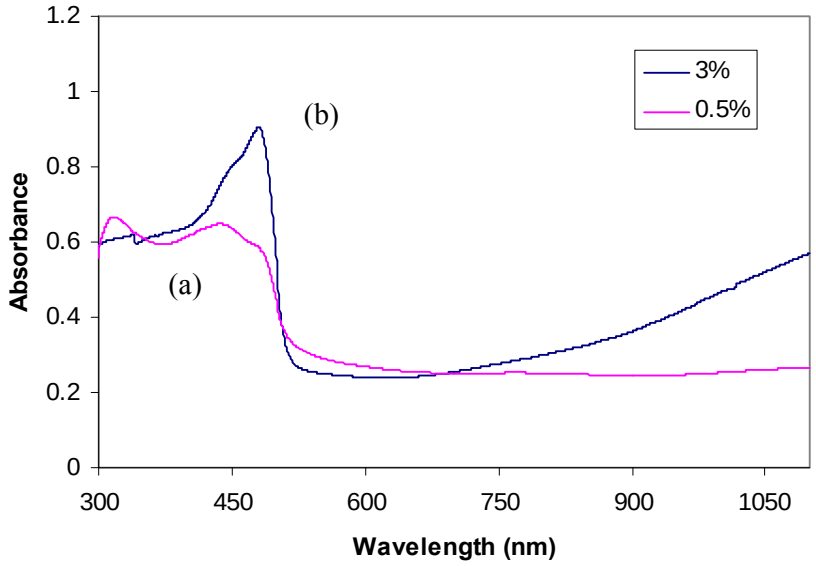

Figure 6.7. UV-vis spectra of PAn/PMAS film cast onto glass from aqueous dispersion (0.50 mg/mL) obtanied using different concentration of PMAS (a) 0.50% and (b) 3.00% w/v after purification.

Transmission electron micrographs of the PAn/PMAS were obtained (Figure 6.8). Rods with diameters less than 100 nm surrounded by aggregated particles were observed when the aniline/oxidant ratio was 4:1, however, aggregation of particles was observed when an aniline/oxidant ratio of 2:1 was employed.

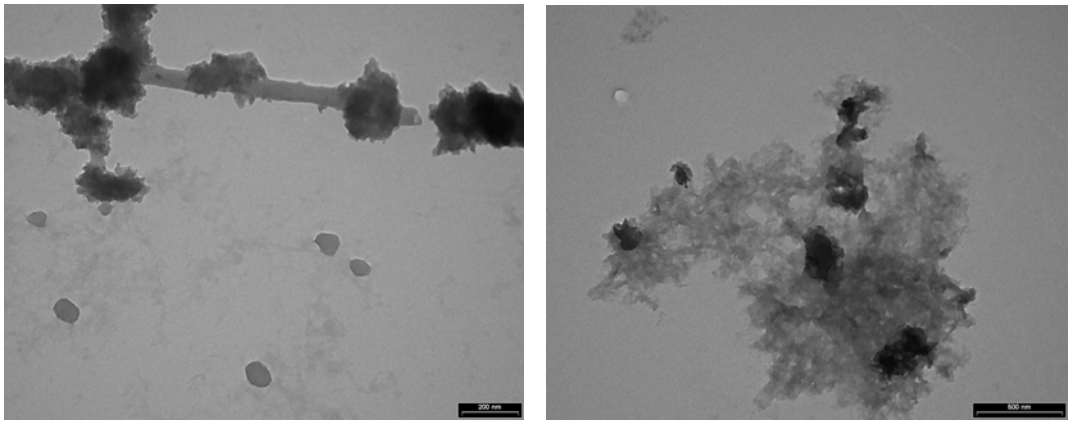

a **b**

Figure 6.8. TEM images of PAn/PMAS cast from purified dispersion synthesised using different ratio of aniline to oxidant (a) 4:1 (scale bar 200 nm) (b) 2:1 (scale bar 500 nm).

All the dispersions showed a size less than 1 micron. The size was apparently sensitive to the aniline/oxidant ratio and was smaller for the higher ratio. An average particle size of 160 ± 15 nm was obtained using an aniline/oxidant ratio of 4:1 (Figure 6.9), however an average size of 600 ± 45 nm , indicative of coagulation, was observed using the ratio of 2:1 (Figure 6.10). The results suggest that at the higher ratio of aniline/oxidant, the ability of PMAS to function simultaneously as a dopant and stabiliser was diminished. Increasing the concentration of PMAS however resulted in experimental difficulties due to increasing solution viscosity. As a consequence, a compromise between the oxidant ratio and PMAS concentration was considered.

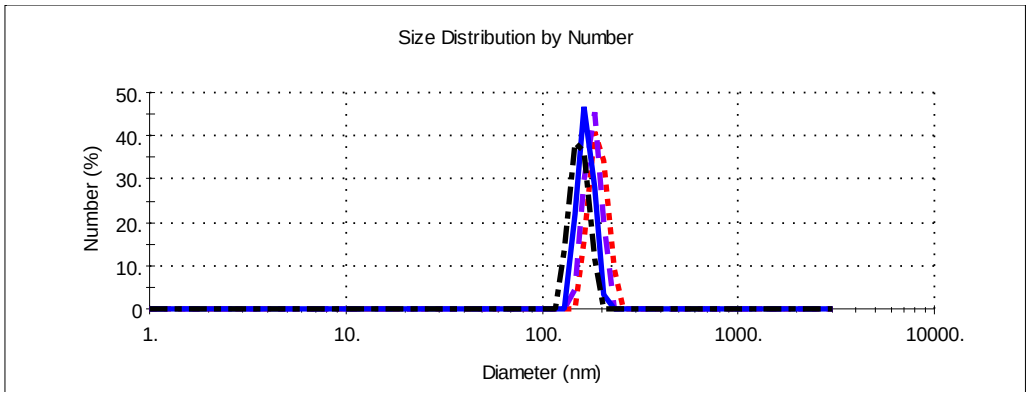

Figure 6.9. The average particle size of PAn/PMAS dispersion synthesised using an aniline/oxidant ratio of 4:1.

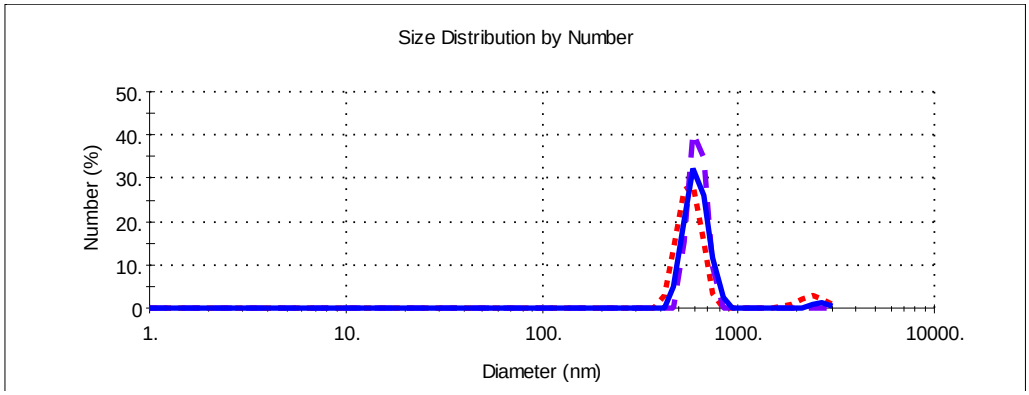

Figure 6.10. The average particle size of PAn/PMAS dispersion synthesised using an aniline/oxidant ratio of 2:1.

6.3.3 Chemical synthesis of PAn/PMAS in the presence of acid

Polymerisation of PAn/PMAS in 0.10 M HCl

In order to investigate the effect of pH on chemical polymerisation of PAn/PMAS material, the polymerisation was carried out in 0.10 M HCl and the results compared to HCl doped polyaniline (Table 6.1). For this comparison, aniline was polymerised in 0.10 M HCl while equimolar HCl as PMAS (12 mM) was added to the reactants. The reaction conditions have been summarised in Table 6.1.

Table 6.1. Reaction conditions for the synthesis of PAn/PMAS.

Exp.	HCl (M)	[Aniline] (M)	[PMAS] (mM)	[PMAS] %w/v	Aniline/APS ratio	Starting pH	pH (end)	Conductivity (S/cm)
1	-	0.16	12	0.5	4:1	6.0	2.5	0.007 ± 0.001
2	-	0.16	12	0.5	2:1	6.0	2.5	0.008 ± 0.001
3	-	0.16	60	3	2:1	5.4	1.65	0.77 ± 0.13
4	-	0.08	60	3	2:1	5.2	1.6	0.76 ± 0.05
5	0.10 M +12 mM (excess)	0.16	-		2:1	4.4	1.5	0.036 ± 0.001
6	0.10 M	0.16	12	0.5	2:1	4.4	1.5	0.12 ± 0.02
7	0.10 M	0.08	12	0.5	4:1	2.5	1.5	2.5 ± 0.5

To explore the effect of PMAS in the polymerisation of aniline the open circuit potential (OCP) was recorded during polymerisation (Figure 6.11). During the polymerisation of aniline/HCl, the potential increased over 40 min to a maximum of 625 mV, droping slowly to 354 mV in 80 min. This result was consistent with a number of earlier studies [33-35]. As discussed in detail in Chapter 4, the increase in potential can be attributed to coupling of radicals (preformed in the early stage of the reaction) leading to the propagation of oligomers and finally polymer in the fully oxidised pernigraniline state. The subsequent decrease in potential has been attributed to the reduction of pernigraniline to the emeraldine salt state through reaction with the residual monomer in the reaction mixture. At longer reaction times, when the potential levels off, the reaction was considered to be completed. These changes in potential were observed to occur very rapidly for PAn/PMAS. In the presence of PMAS the OCP quickly reached a maximum of 619 mV within 9.5 min and then dropped to 354 mV over 36 min. The rapid increase in potential observed for the templated polymerisation of aniline with PMAS indicated that the radical coupling to produce dimers and oligomers leading to the subsequent chain propagation were strongly facilitated by the templating of the anilinium radicals to the host PMAS template. This PMAS template effect provided a

proximity reaction enhancement effect while the PMAS simultaneously functioned as an effective dopant.

Polymerisation of aniline/PMAS was also faster than aniline/HCl, even at the lower concentrations of aniline and oxidant. The low V_{max} observed (for 0.08 M aniline and 0.02 M APS) in Figure 6.11 was due to the lower concentration of oxidant (experiment 7).

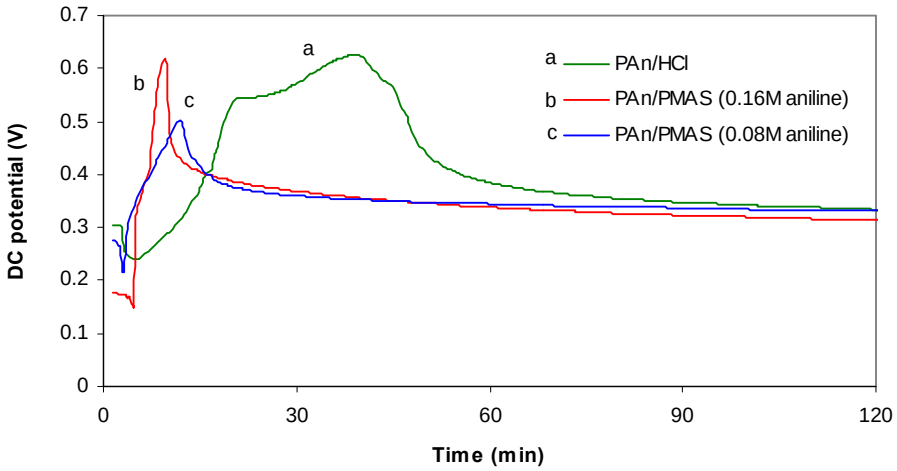

Figure 6.11. DC potential recorded for polymerisation of 0.16 M aniline in 0.10 M HCl (a) in the absence and (b) the presence of 0.50% w/v PMAS. (c) Polymerization of 0.08 M aniline in 0.10 M HCl and 0.50% w/v PMAS.

The UV-vis spectra of polyaniline in the absence (exp 5) and in the presence of PMAS (exp 6,7) have been shown in Figure 6.12. HCl doped polyaniline exhibited polaron bands around 870 nm and 410 nm and π-π* band at approximately 350-360 nm. In the presence of PMAS, an extra peak at 473 nm and free carrier tail at higher wavelengths appeared. By increasing PMAS the free carrier tail and thus the extended coil conformation became dominant. Also a clear band at 440-450 nm was observed. No PMAS was observed in the first supernatant indicating the incorporation of all PMAS in the product (Figure 6.13).

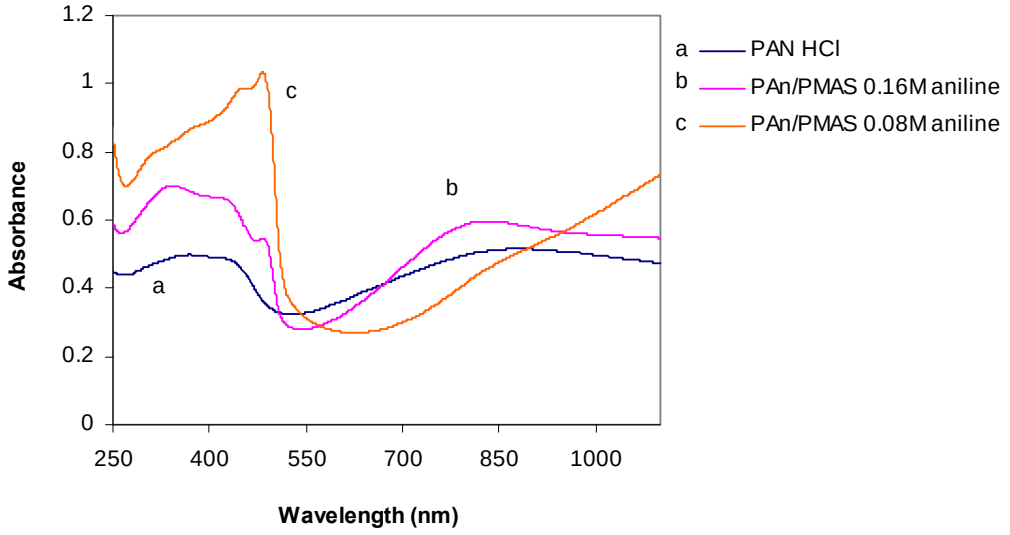

Figure 6.12. UV-vis spectra of aqueous dispersions (~25 ppm) of (a) PAn/HCl (exp 5), (b) PAn/PMAS (exp 6) and (c) PAn/PMAS (exp 7). The conditions are as Figure 6.11).

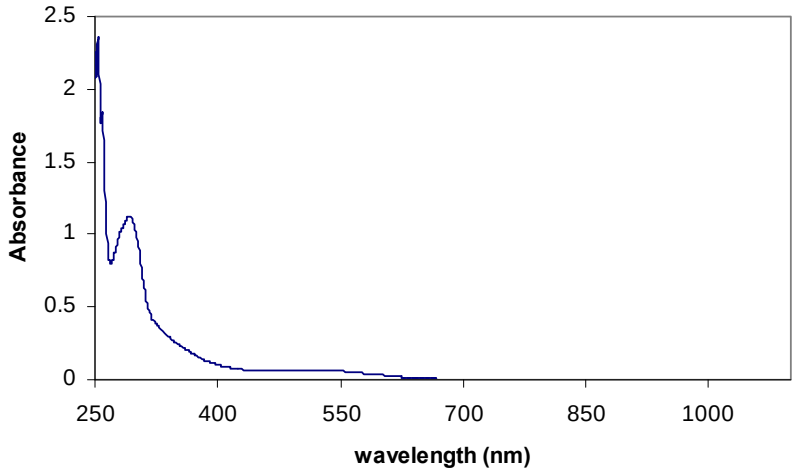

Figure 6.13. UV-vis spectra of the first supernatant of PAn/PMAS (exp7) after filtering by 0.45µm PTFE syringe filter. Note that PMAS can pass through the filter.

Conductivity measurements of the polymer synthesised in 0.10 M HCl showed that addition of 12 mM (0.50% w/v) PMAS before polymerisation resulted in a 3 fold higher conductivity. The high conductivity of 2.5 S/cm was obtained by reducing the aniline and oxidant concentration at the same concentration of PMAS (Table1).

Particle size was again found to be affected by the aniline to PMAS ratio and the aniline to oxidant ratio. By keeping the PMAS concentration constant, smaller particles were obtained using low concentration of aniline and oxidant (Figure 6.14 and Figure 6.15).

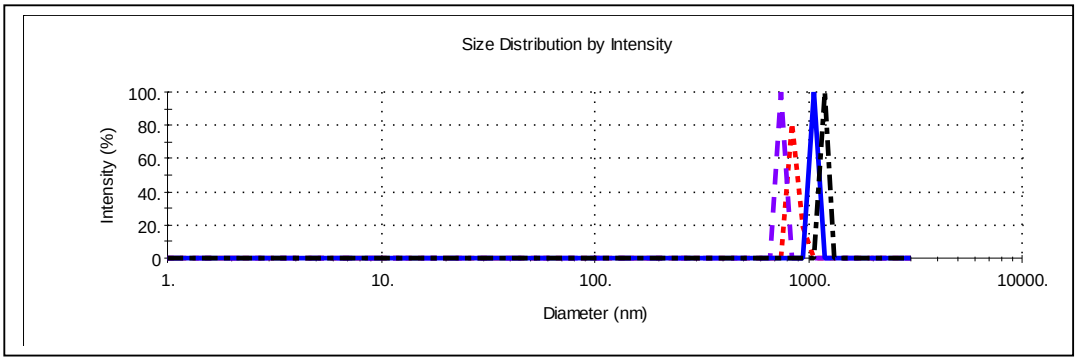

Figure 6.14. The average particle size of PAn/PMAS dispersion. The polymer was synthesised from 0.16 M aniline in 0.10 M HCl, 0.50% w/v PMAS and an aniline/oxidant ratio of 2:1 (exp 6).

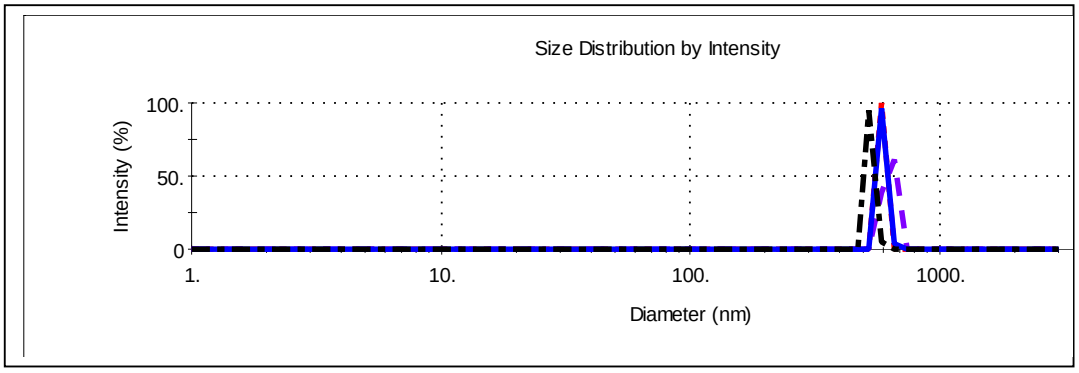

Figure 6.15. The average particle size of PAn/PMAS dispersion. The polymer was synthesised from 0.08 M aniline in 0.10 M HCl, 0.50% w/v PMAS and aniline/oxidant ratio of 4:1 (exp 7).

In order to confirm the templating of polyaniline onto PMAS, the PAn/PMAS dispersion was treated with NaOH. In alkaline solutions, polyaniline undergoes dedoping which is characterised by a shift in the π-π* band to ca. 320 nm and accompanied by the evolution of a characteristic exciton band of the EB at ca. 600 nm [12]. Treating PMAS with NaOH solution results in replacement of these initial bands by two bands at 350-390 nm and 750 nm consistent with a compact coil conformation for PMAS [29].

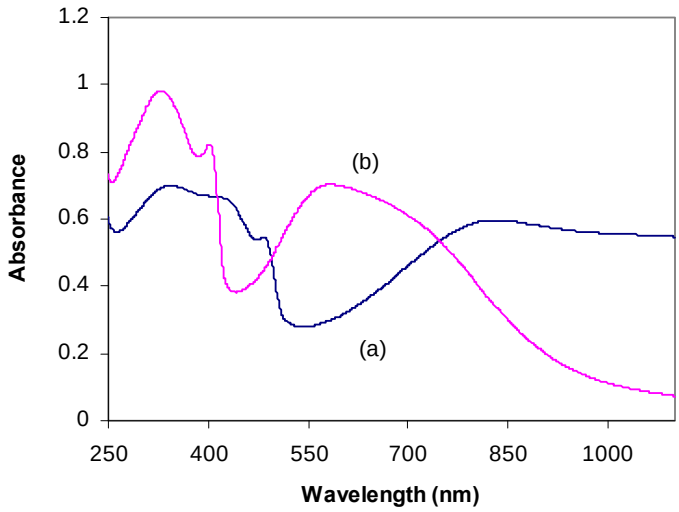

Figure 6.16. UV-vis spectra of PAn/PMAS (exp 6) dispersion in (a) water and (b) in 0.06 M NaOH.

Upon base treatment of the PAn/PMAS dispersion, four bands appeared in the UV-vis spectra, two peaks at ca. 330 nm and 400 nm and the other two overlapping bands between 570 and 750 nm (Figure 6.16 and Figure 6.17). By increasing the PMAS concentration, the absorption intensities at 400 nm and 750 nm increased confirming the incorporation of more PMAS in the product.

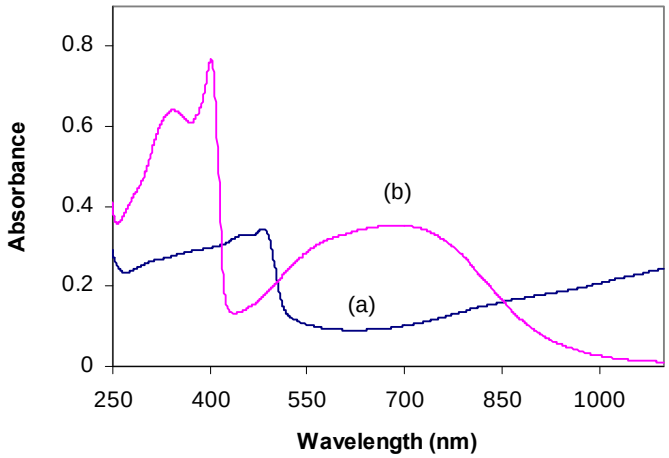

Figure 6.17. UV-vis spectra of PAn/PMAS (exp 7) dispersion in (a) water and (b) in 0.06 M NaOH.

Effect of 0.10 M HCl

Polymerisation of aniline/PMAS in the presence of 0.10 M acid (by dropping the initial pH from 6 to 4.43) results in a higher doping level as evidenced by the appearance of a well-defined band at 800 nm (Figure 6.18) and overlapping of peaks at 330 and 410 nm [12]. The characteristics of PAn are more pronounced in the presence of acid, however the free carrier tail above 900 nm associated with the band at 825 nm suggest a partially extended-coil conformation presumably induced by PMAS. The conductivity also increased from 0.008 to 0.115 S/cm (14 fold).

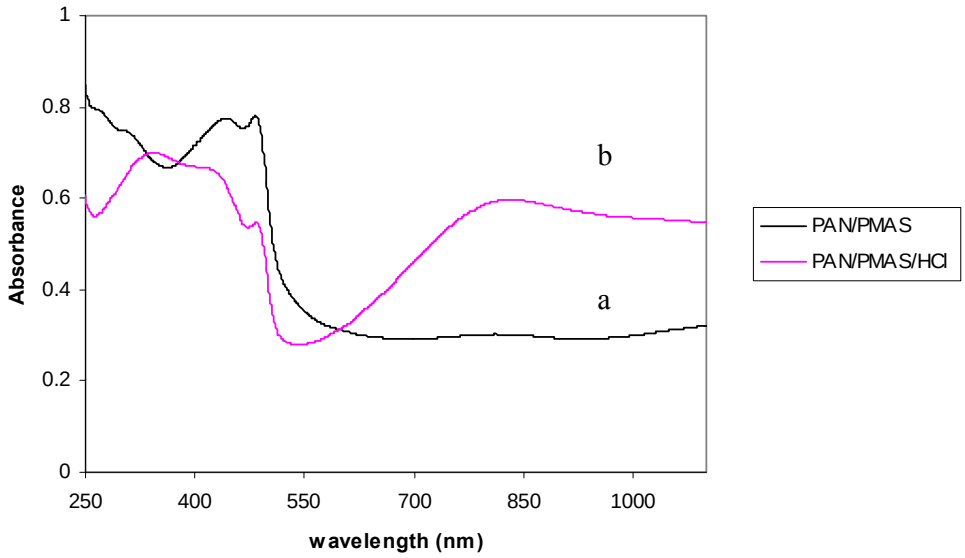

Figure 6.18. Effect of pH on the polymerisation of 0.16 M aniline in the presence of 12 mM PMAS (a) in the absence of acid (pH 6) and (b) in 0.10 M HCl (pH 4.43). The aniline to oxidant ratio was 1:2.

Polymerisation of PAn/PMAS in 1.0 M HCl

Following the successful chemical polymerisation of aniline in the presence of PMAS as dopant, in slightly acidic media, and to investigate the effect of solution pH, PAn/PMAS was synthesised in 1.0 M HCl. Furthermore, to study the effect of PMAS incorporation, the concentration of PMAS was varied from 0 to 38.4 mM equivalent to the stochiometric ratio of aniline to the PMAS dimer unit (Table 6.2). Figure 6.15 shows the open circuit potential (OCP) recorded during polymerisation. Recording OCP during polymerisation of PAn/PMAS in 1.0 M HCl shows different behavior to that observed with 0.10 M HCl (Figure 6.19). Addition of PMAS in the polymerisation of aniline in 1.0 M HCl clearly reduced the maximum potential needed for polymerisation, however the reaction was observed to be slower. In the polymerisation of aniline/HCl, the potential reached a maximum of 0.76 V in *ca.* 8 minutes. Upon addition of 0.25, 0.50, 1.0 and 1.60% w/v PMAS prior to polymerisation, a reduction in the maximum OCP potential was noted at 0.635, 0.576, 0.518 and 0.519 V respectively. The pH of the polymerisation solution using 1.0 M HCl (comprising aniline, PMAS and APS in 1.0 M HCl) was less than 1. At this pH both aniline monomers and sulfonic acid groups

of PMAS were in the protonated form. As a consequence the interaction of the aniline monomer and PMAS would not be via simple electrostatic interaction, and therefore under these conditions it had no effect upon reaction rate. In this case, PMAS functioned as a steric stabilizer, providing a site for the adsorption of aniline and oligomeric intermediates [16].

Table 6.2. Reaction conditions for the polymerisation of aniline in 1.0 M HCl and in the presence of PMAS.

Experiment	HCl (M)	[Aniline] (M)	[PMAS] (mM)	Aniline/APS	Aniline/PMAS dimer unit
1	**1.0**	**0.08**	**0**	**4:1**	**-**
2	**1.0**	**0.08**	**6**	**4:1**	**2 : 0.15**
3	**1.0**	**0.08**	**12**	**4:1**	**2 : 0.3**
4	**1.0**	**0.08**	**24**	**4:1**	**2 : 0.6**
5	**1.0**	**0.08**	**38.4**	**4:1**	**2 : 1**

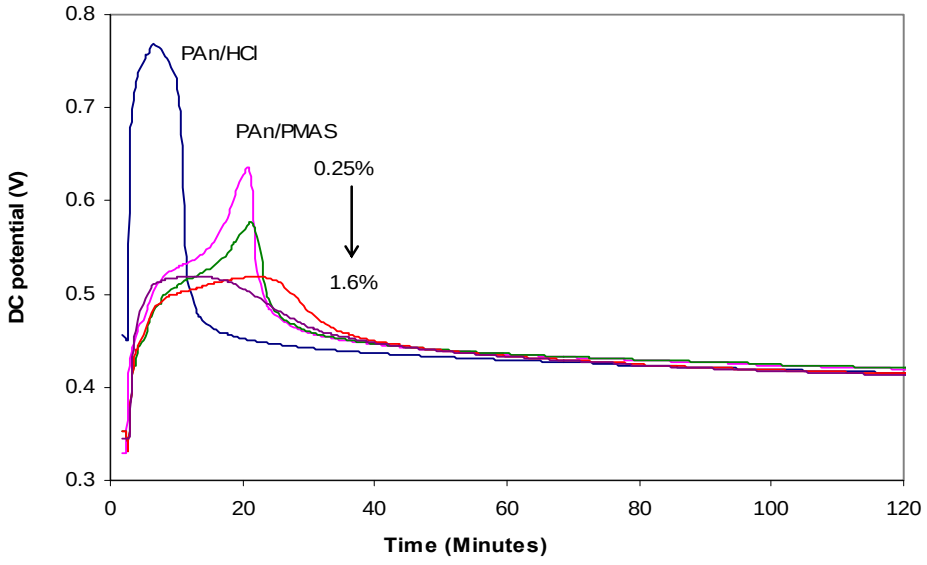

Figure 6.19. DC potential recorded for aniline polymerisation using different concentration of PMAS (0, 0.25, 1.00 and 1.60% w/v) in 1.0 M HCl (experiments as Table 6.2).

After the first supernatant filtration using a 0.45 µm PTFE syringe filter no significant amount of PMAS was observed in solution, indicating the near complete incorporation of PMAS in the product (Figure 6.20). The peak at 276 nm is attributed to the residual monomer in the first supernatant and decreases with the number of centrifuge cycles and almost disappears in the fourth supernatant. Therefore, centrifuging for 4 cycles would be enough to remove the residual monomer. For the PMAS concentration above 12 mM the filtrate solution was green in colour. The green colour can be attributed to small particles of PAn/PMAS which are not spinning down by centrifuging.

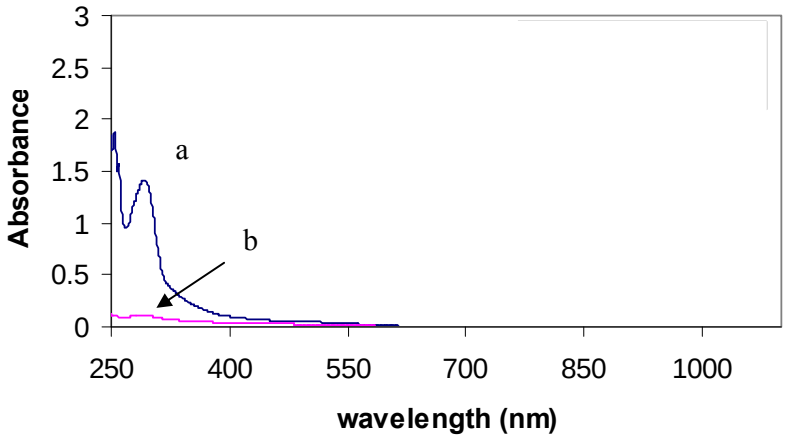

Figure 6.20. UV-vis spectra of (a) the first and (b) the forth supernatant of PAn/PMAS (exp3) after filtering by 0.45µm PTFE syringe filter.

The UV-vis spectra of the PAn/PMAS material is compared with PMAS and PAn/HCl in Figure 6.21. By increasing the concentration of PMAS, the band at 473 nm increased and was slightly shifted to higher wavelengths (478 nm). The new peaks at 360-370 nm and 445 nm were observed and the latter overlapped with the peak at 473 nm. The free carrier tail became more intense indicating the higher doping level and extended coil conformation. However no increase in the intensity of the free carrier tail was observed for concentrations above 1.00% w/v. Since the monomer conversion is about 70%, a PMAS concentration slightly below the stochiometrc ratio (PMAS/aniline 0.5:1) is also enough for doping of polyaniline. The peak ratio of 445/360 increases with PMAS concentration which is in agreement with the observed increase in conductivity [11].

The addition of aqueous NaOH solution to the dispersions described in Figure 6.21 caused a rapid color change from yellow/green to blue (Figure 6.22). As disussed earlier, the peaks at ca 320 and ca 600 nm are attributed to the EB of polyaniline and the overlapping bands between 330 and 390 nm and the strong peak at 750 nm are assigned to the compact coil conformation of PMAS. When the PAn/PMAS material with low concentration of PMAS (0.25% w/v) was treated by aqueous NaOH, two well-defined overlapping bands between 570 and 750 nm were observed indicating the presence of PMAS and polyaniline. As the concentration of PMAS was increased the second peak became more dominant.

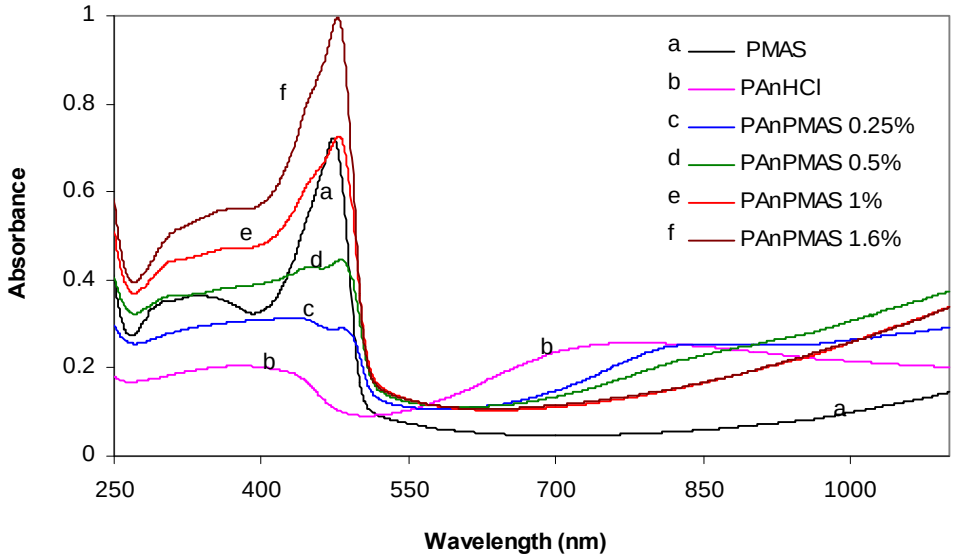

Figure 6.21. Solution UV-vis spectra of (a) PMAS, (b) PAn/HCl and (c-d) PAn/PMAS dispersions (~25 ppm) obtained using different concentration of PMAS (0.25-1.60% w/v) after purification .

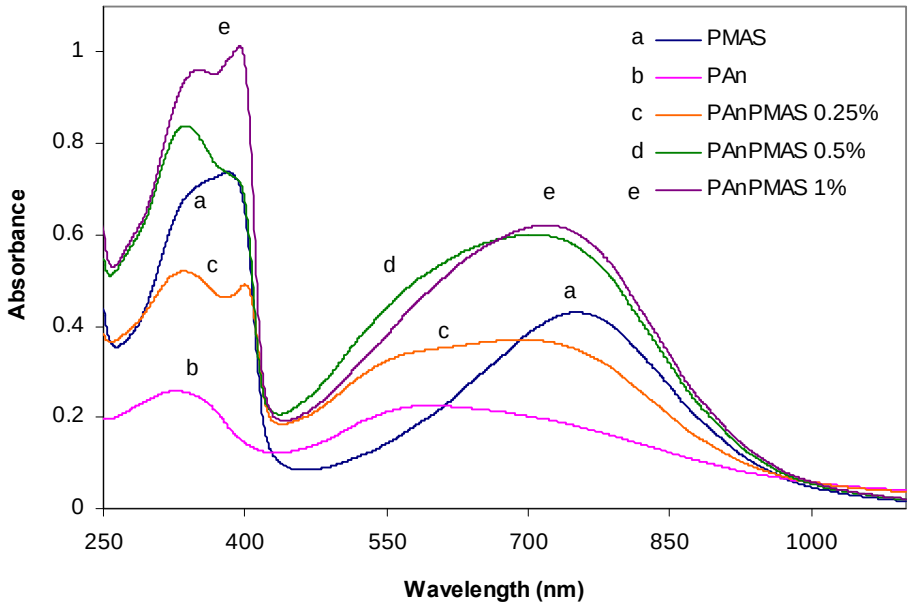

Figure 6.22. UV-vis spectra of (a) PMAS, (b) PAn/HCl and (c-d) PAn/PMAS dispersions (~25 ppm) from Figure 6.21 in 0.06 M NaOH.

It was found that the stability of the dispersions depended on the PMAS concentration used during polymerisation. Highly stable dispersions and small particles were found by using a large amount of PMAS 1.00% w/v (Figure 6.23). A dilute dispersion of polyaniline nanofibres was stable for about 3-5 hours. When the concentration of PMAS was below 1.00% w/v the PAn/PMAS dispersions were stable only for a few hours. However when 1.00% (w/v) or more PMAS was used no precipitation was observed even after standing for a few months. The dispersion synthesised from 1.60% (w/v) PMAS was even stable at very high concentrations (about 10 mg/mL), whilst some precipitate was observed for the 10 mg/mL dispersion prepared from 1.00% (w/v) PMAS overnight. Films formed from the PAn/PMAS dispersion were found to have good conductivity and mechanical properties. The films were cast from PAn/PMAS dispersions in water.

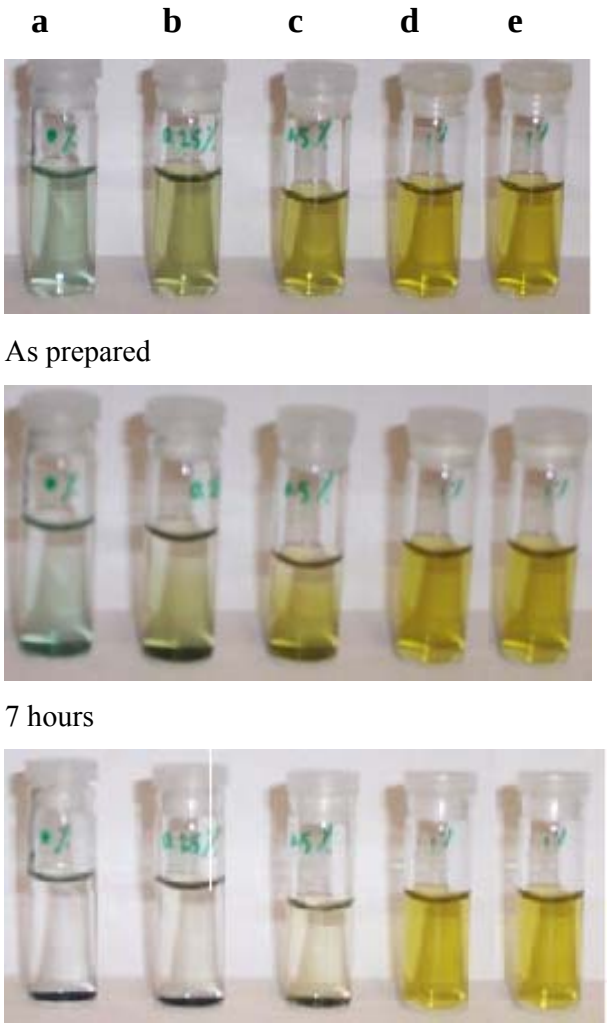

Figure 6.23. Stability of 0.05 mg/mL PAn/PMAS dispersion in water. Concentration of PMAS used was (a): 0%, (b): 0.25%, (c): 0.50%, (d): 1.00% and (e): 1.60% (w/v).

The conductivity of polyaniline was significantly increased by increasing the PMAS concentration used during synthesis (Figure 6.24). The highest conductivity obtained was about 3 S/cm which is about 2 orders of magnitude higher than films prepared from polyaniline in the presence of PSS [36] or phosphomannan [37]. When the PMAS concentration was low, the films were brittle and discontinuous, however higher

concentrations of PMAS improved the flexibility of the films. Both the yield and monomer conversion were also significantly increased by addition of PMAS (Table 6.3).

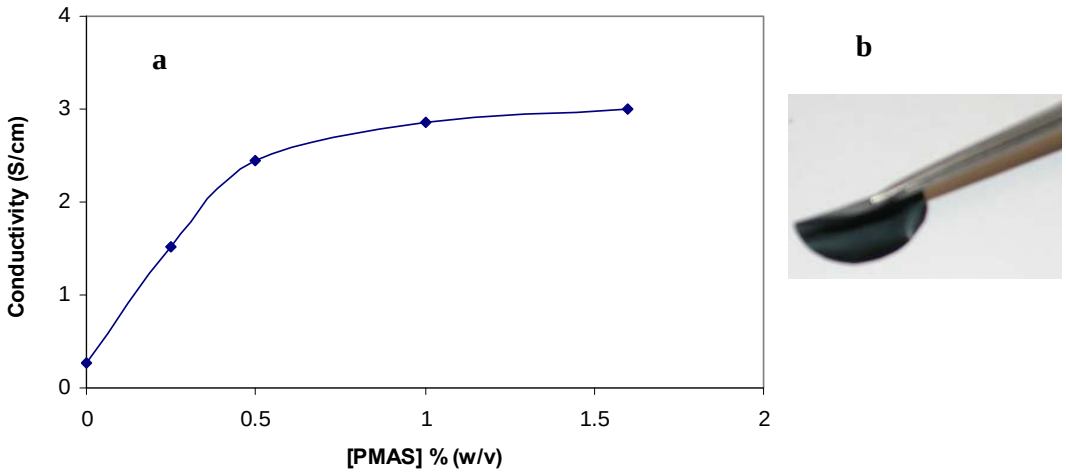

Figure 6.24. (a) Effect of PMAS concentration on the conductivity of PAn/PMAS (b) Flexibility of a PAn/PMAS free standing film at highest PMAS loading. The film was bended using a tweezer.

Table 6.3. Charactrisation of PAn/PMAS synthesised in 1.0 M HCl using different PMAS concentrations.

PAn/PMAS/HCl (1.0 M)	%PMAS (w/v)	Yeild %	Monomer conversion (%)	Conductivity (S/cm)
1	0.0	17.0	63.5 ± 0.9	0.27 ± 0.03
2	0.25	37.0	68.0 ± 0.3	1.52 ± 0.14
3	0.5	37.2	69.7 ± 0.7	2.45 ± 0.23
4	1.0	37.2	70.2 ± 0.8	2.85 ± 0.03
5	1.6	45.3	76.0 ± 1.2	3.0 ± 0.18

Effect of pH on the synthesis of PAn/PMAS (0.10M and 1.0 M HCl)

By polymerisation of aniline/PMAS in 1.0 M acid (initial pH 0.4) no significant difference was observed in the UV-Vis spectrum of the product when compared to that of the product synthesised in 0.10 M HCl (initial pH 2.5) (Figure 6.25). The

conductivity also did not change significantly (by comparing experiment 7 in Table 6.1 with experiment 3 in Table 6.3).

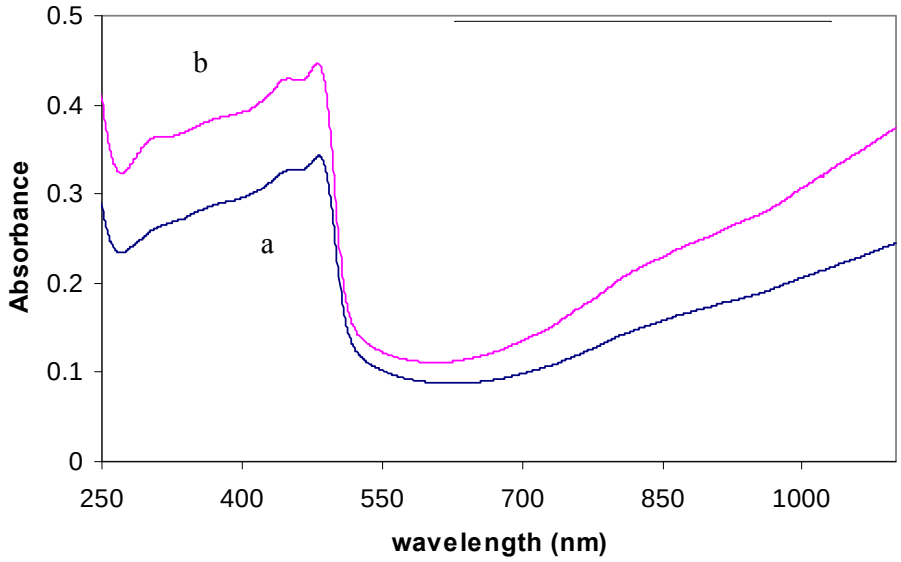

Figure 6.25. UV-vis spectra of PAn/PMAS, synthesised from 0.08 M aniline in 12 mM PMAS and aniline to oxidant ratio of 1:4 using different concentration of (a) 0.10 M HCl and (b) 1.0 M HCl .

IS PAn/PMAS material a mixture of PAn and PMAS?

Durning aniline polymerisation both HCl and PMAS are present and can compete to dope polyaniline. It can be postulated that the product is a mixture of PMAS and HCl doped polyaniline. In order to establish the roles of the HCl and PMAS as a dopant the UV-vis spectrum of the product was compared to the spectra of PMAS, PAn/HCl and their 1:1 mixture.

The UV-Vis spectrum of the product was not a simple additive spectrum and was different from a simple 1:1 mixture of a polyaniline dispersion and PMAS solution (Figure 6.26). The new band at 370 nm and an intense carrier tail at higher wavelengths are characteristic of the PMAS doped PAn. The spectrum of the PAn/PMAS has the characteristics of extended-coil conformation and provides further evidence that PMAS

acts as a template for aniline molecules and induces the extended coil conformation to the templated polyaniline.

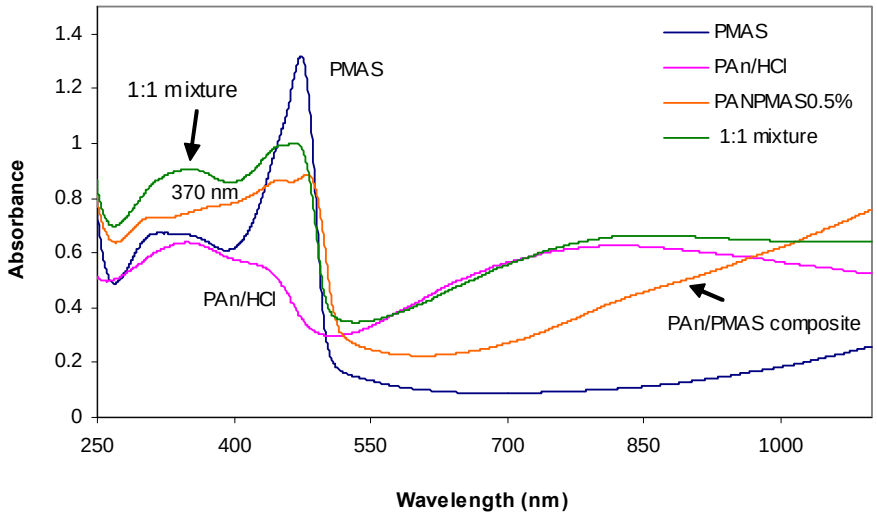

Figure 6.26. UV-vis spectra of PAn/PMAS (using 0.50% w/v PMAS), compared to PAn/HCl, PMAS and their 1:1 mixture (~50 ppm for all the samples).

6.3.3.1 Particle size measurements of PAn/PMAS dispersions

The particle size of a dilute dispersion of PAn/PMAS at different concentrations of PMAS was measured by dynamic light scattering. The results are illustrated in Table 6.4 . The size of the particles is largely affected by the concentration of PMAS. No particles smaller than 3 micron were observed for the PAn/HCl dispersion. At a PMAS concentration of 0.25% w/v, big particles (~2400 nm) were detected presumably due to agglomeration of particles, as seen in. Increasing the PMAS concentration to 0.50% w/v resulted in an extra peak with an average size of ~520 nm. Very small particles (~50 nm) were observed at PMAS concentration of 1.00% w/v, however, further addition of PMAS did not decrease the particle size. Particles of about 105 nm diameter were observed using 1.60% w/v PMAS. Nanoparticles with diameters about 100 nm or less were obtained using PMAS concentrations of 1.00% w/v and above.

Table 6.4. The particle size of a dilute dispersion of PAn/PMAS at different concentrations of PMAS

PAn/PMAS dispersions prepared from experiments listed in Table 6.2	Concentration of PMAS employed (w/v)	Particle size (nm)
1 (PAn/HCl)	0%	>3000
2	0.25%	2400 ± 220
3	0.50%	520 ± 62
4	1.00%	51 ± 4
5	1.60%	105 ± 9

6.3.3.2 Morphology of PAn/PMAS materials

Kaner *et al.* has reported the formation of nanofibers of polyaniline having diameters between 30 and 50 nm and with lengths varying from 500 nm to several micrometers using interfacial or rapidly mixed reactions [20-22]. Polyaniline nanofibers are formed using different inorganic or organic acid over a wide range of temperatures (0-100 ˚C), however the diameters of the resulting nanofiber are affected by the dopant used in the polymerisation [20, 21].

Transmission electron micrographs of PAn/PMAS cast onto TEM grids from dilute dispersions after purification were obtained. In the absence of PMAS, nanofibres with diameters of 50-80 nm were obtained for PAn/HCl (Figure 6.27), similar to those reported by Kaner *et al*. Polymerisation of aniline in the presence of PMAS resulted in different morphology depending on the concentration of PMAS. Using 0.25 and 0.50% w/v PMAS resulted in highly agglomerated fibres and irregular aggregation (Figure 6.28 and Figure 6.29). When the concentration of PMAS increased to 1.00% w/v, a mixture of well-defined distinct nanofibres and small spherical nonoparticles was obtained (Figure 6.30). Nanoparticles had diameters between 20 and 100 nm.

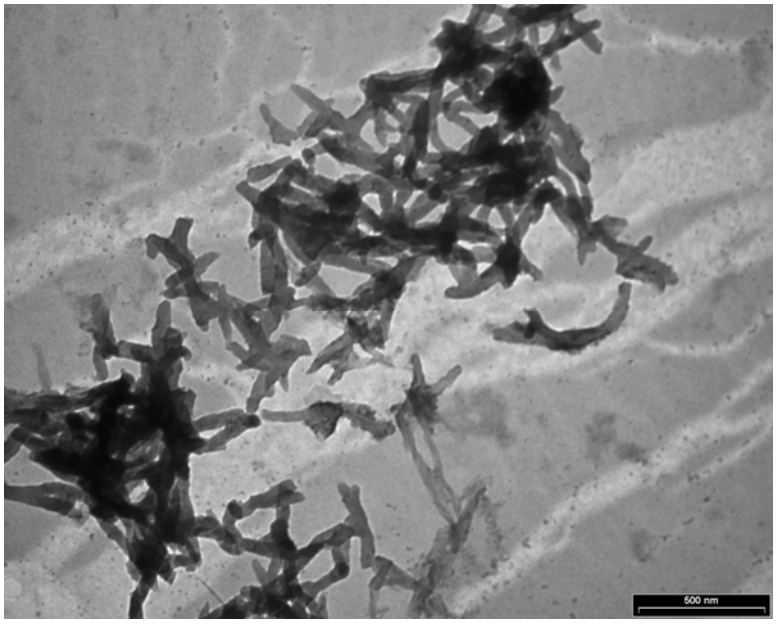

Figure 6.27. TEM image of PAn/HCl nanofibers cast from dispersion after purification.

Wan et al [38] have obtained microtubules of PAn by template-free polymerisation of aniline in the presence of naphtalenesulfonic acid as dopant. Nanotubes having diameters in the range 100-300 nm and up to 2 micrometer have been reported by Qiu et al [18] using a hydrogensulfated fullerenol with six -(O)SO3H groups ($C60\text{-}(OSO3H)_6$) or sulfonated dendrimer containing 24 terminal groups of 3,6-disulfonaphthylthiourea ($PAMAM4.0\text{-}[naphthyl(SO_3H)_2]_{24}$) as the protonic acid dopant under ultrasonic conditions. Self-assemble of these dopant molecules and/or their aniline salts into a microstructured intermediate that acts as both a supramolecular template and a self-doping reagent is believed to result in the formation of these micro or nanostructures. Polyaniline nanoparticles have also been formed by using stabilisers and templates such as surfactants and polyelectrolytes [11-19]. The shape and size of the particles depends on different factors such as the concentration of the stabiliser and template. It is proposed that a water soluble polymer or steric stabiliser in dispersion polymerisation provides a site for the adsorption of the oligomeric intermediates in which the polymerisation of aniline preferentially started [16]. The number of primary nucleation sites and thus the dispersed particles are determined by the concentration of stabiliser. The chemical interaction of polyaniline and stabiliser is also important provided there are suitable functional groups in the stabiliser molecule. Such an interaction is likely

between sulfonated groups of PMAS and aniline monomers or oligomers (in a wide pH range) providing a template and stabiliser for the polymerisation of aniline.

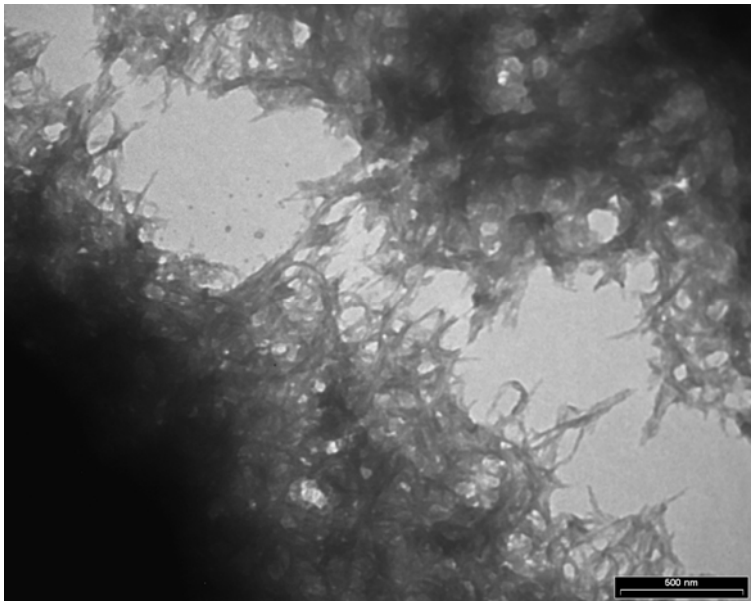

Figure 6.28. TEM images of PAn/PMAS cast from purified dispersion synthesised using 0.25% w/v PMAS.

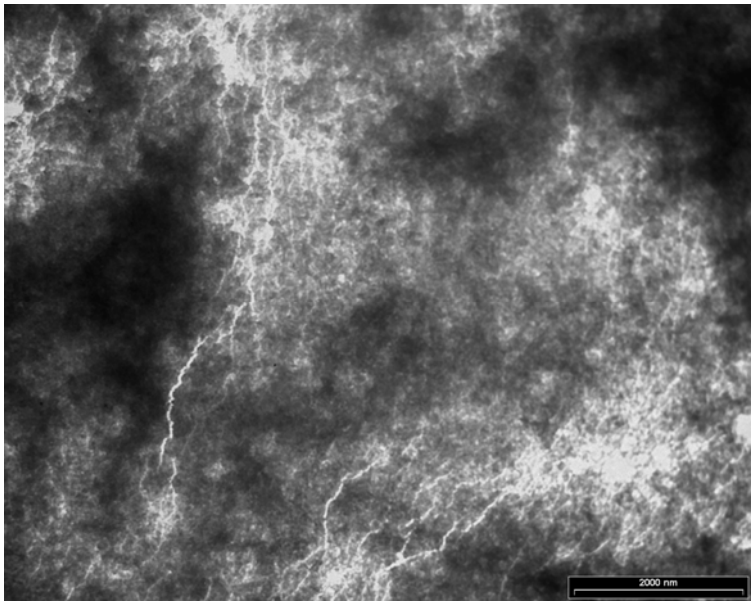

Figure 6.29. TEM image of PAn/PMAS cast from purified dispersion synthesised using 0.50% w/v PMAS.

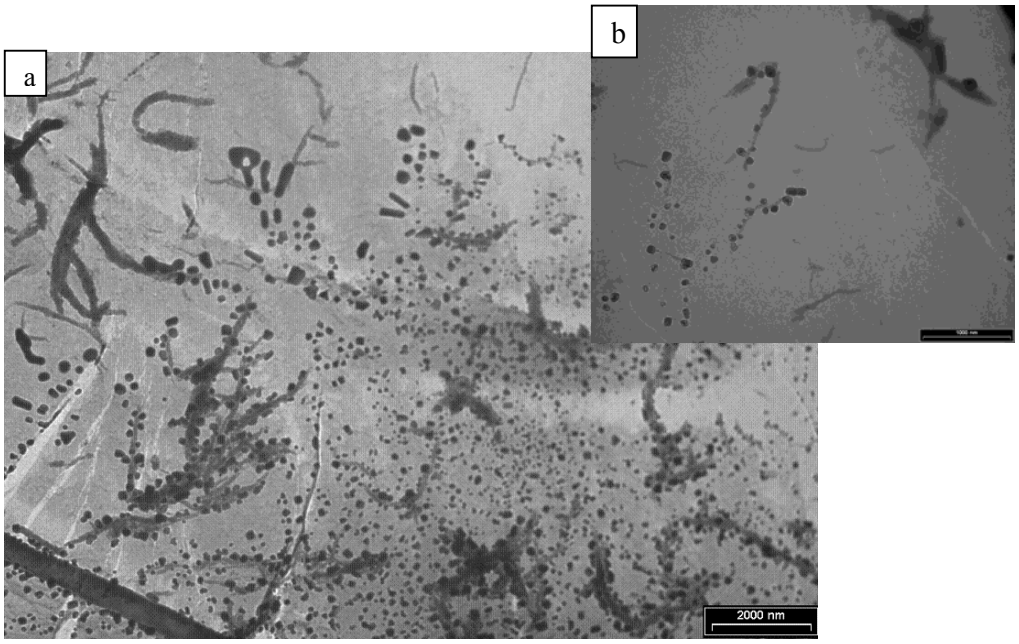

Figure 6.30. TEM images of PAn/PMAS cast from purified dispersion synthesised using 1.00% w/v PMAS (a: scale bar 2000 nm, b: scale bar 1000 nm).

When the concentration of PMAS is low, some areas are not supported by stabiliser and particles may adhere together resulting in the agglomeration of the particles observed in Figure 6.28 and Figure 6.29. At high PMAS concentrations the aggregation of the particles was reduced. Using a high concentration of PMAS (1.00% w/v or more) resulted in nanoparticles and nanofibers with diameters less than 100 nm (Figure 6.30). To investigate the relationship between the concentration and ionic conductivity of PMAS, the solution conductivity of PMAS was measured at different concentrations. Two linear curves crossing at 0.9% (w/v) PMAS were observed (Figure 6.31). This point is consistent with the concentration of PMAS at which the stable dispersion of nanoparticles was observed.

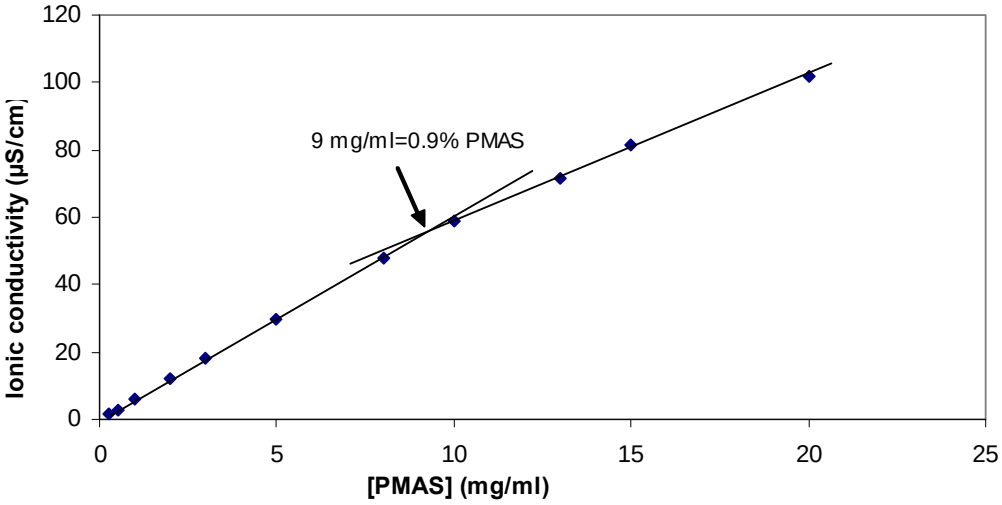

Figure 6.31. Ionic conductivity of PMAS solution at different concentration.

6.3.3.3 Electroactivity

The PAn/PMAS materials obtained using different concentrations of PMAS were characterised by cyclic voltammetry. The films were drop-cast onto separate glassy carbon electrodes by evaporative casting of 20 µL of dispersions in water (~ 5 mg/mL). Insoluble coatings were formed after air drying for a day. The voltammograms were recorded in 0.10 M HCl electrolyte. The second scans of the cyclic voltammograms are shown in Figure 6.32. Two redox peaks (the anodic peaks at 0.37 V and 0.86 V) were obtained for the PAn/HCl film. In the presence of PMAS, an additional redox peak (0.64 V) was observed and the above anodic peaks became more well-defined while shifting to lower potentials. For the PAn/PMAS (synthesised from 1.00% w/v PMAS), three redox couples with anodic peaks at 0.26, 0.64, and 0.76 V were observed. The first redox pair corresponded to the interconversion between leucoemeraldine and emeraldine states of both PAn and PMAS. The third redox pair is attributed to the transformation of emeraldine into pernigraniline of polyaniline. The second redox pair can be attributed to the interconversion between emeraldine and pernigraniline states of PMAS. Similar behavior has been reported for the PMAS – PLL complex films [39] and PMAS-PVP complex [40]. Tatsuma *et al.* have also observed similar responses for the PMAS-PLL complex film coated on SnO_2 electrodes in different buffer solutions [28]. Their results show that this second redox peak is pH-dependent and shifts to more

negative potentials with increasing pH. The second anodic peak has been reported at ca. 0.35 V in buffer solution pH 4.4. A second anodic peak at ca 0.64 V for the PAn/PMAS in Figure 6.32 obtained in 0.10 M HCl (pH=1) (shifted to more positive potentials at lower pH) is similar to what has been reported by Tatsuma et al. Similar redox waves (the oxidation potentials at ca. 0.34 V and 0.65 V) have also been reported for highly sulfonated polyaniline (SPAN) in pH 1 electrolyte [6].

Upon increasing the PMAS concentration used during synthesis, the third anodic peak shifted towards more negative potentials. Several studies have shown that sulfonation of polyaniline altered the electrochemical behavior of polyaniline and its derivatives. The shift towards negative potentials has been reported by electrochemical doping of reduced polyaniline with polyaniline-sulfonic acid [30]. The more negative second redox pair has also been reported for the self-doped copolymer of aniline and m-aminobenzenesulfonic acid (metanilic acid) [31]. Doping of polyaniline by potential cycling in some aromatic sulfonate anions such as naphthalene sulfonic acid has resulted in shifting of the second oxidation pair toward more and more negative direction with time [32].

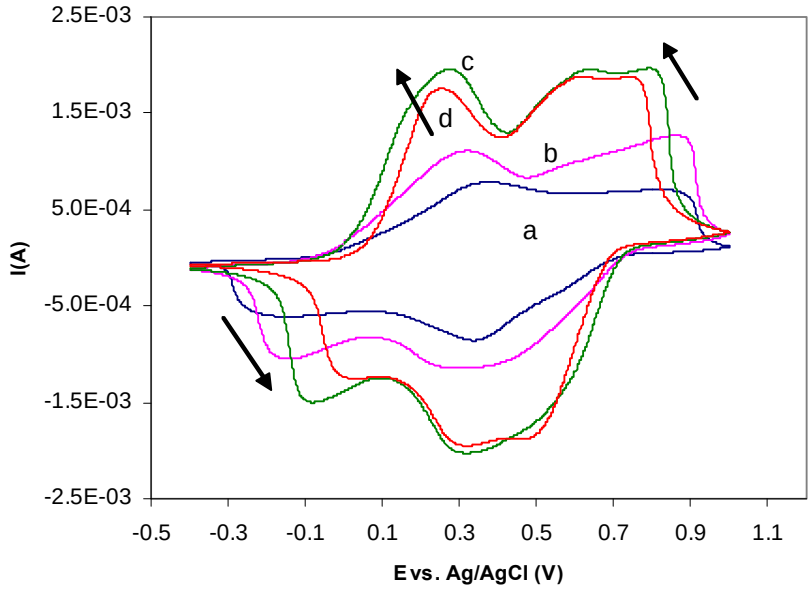

Figure 6.32. Cyclic voltammogram of PAn/PMAS synthesized using different concentration of (a) 0 (b) 0.25, (c) 0.50 and (d) 1.00% (w/v) PMAS drop cast on a glassy carbon electrode in 0.10 M HCl, scan rate 50 mV/sec.

In subsequent scans, significant changes were observed in the CV (Figure 6.33). Visual inspection of the electrode during cycling revealed that the film dissolved slightly in water.

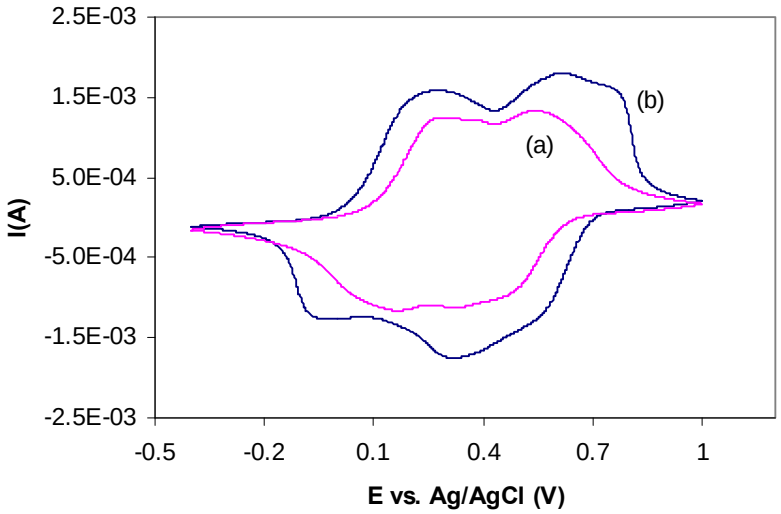

Figure 6.33. Cyclic voltammogram of PAn/PMAS, obtained using 0.50% (w/v) PMAS, drop cast on a glassy carbon electrode in 0.10 M HCl, scan rate 50 mV/sec, cycles (a) 3 and (b) 30.

6.3.3.4 Elemental analysis

The characterisation of the PAn/PMAS suggests that PMAS functions as a dopant and stabiliser in the templated product. This possibility was further investigated through elemental analysis. The ratio of PMAS to polyaniline and the Cl/S ratio were measured based on the C, N, S and Cl analysis. The amount of PMAS in the PAn/PMAS material was calculated using S, present in the sulfonated groups of PMAS. As a reference, since the APS oxidant concentration in the polymerisation solution was very low (0.02 M), this analysis assumed that there were negligible amounts of free SO_4^{2-} arising from the reduced APS in the purified material. Significant purification steps in the form of repeated and rigorous washing and UV-vis analysis of the supernatant washings were made to validate this assumption.

The ratio of PAn/PMAS was calculated from the N/S ratio which was considered as:

$$N/S = (N_{PMAS} + N_{PAn})/S = (S + N_{PAn})/S$$

Having the N_{PAn} from above, the ratio of PMAS to polyaniline was obtained as following:

$$PMAS/PAn = N_{PMAS} /N_{PAn} = S/ N_{PAn}$$

PMAS used during the polymerisation of aniline was the acid-form and was prepared by passing the PMAS through a proton exchange resin to effectively remove residual ammonium cations. The N component originating from ammonia salt of PMAS can therefore be ignored. The C/S ratio was also used to obtain the composition ratio and led to similar results. Table 6.4 summarises the elemental analysis of PAn/PMAS obtained under various conditions of pH and PMAS concentration.

For PAn/HCl (no PMAS, sample 1), based on the analysed N/Cl ratio (5.0), a low doping level of 0.2 was estimated for the PAn/HCl material. By increasing the PMAS concentration (samples 2-5), the ratio of PMAS to polyaniline was increased and reached the higher value of 1.65 at the stochiometric ratio (1 PMAS dimer unit per two aniline molecules). This strongly supports the idea that PMAS acts as a template for polymerisation of aniline. In the synthesis of PAn/PMAS at pH above 4.0 (in the absence of HCl, samples 6 and 7), this PMAS:PAn ratio also increased with PMAS concentration, however the values were lower than those observed for PAn/PMAS materials obtained in the presence of HCl. This indicates that the templatng effect of PMAS for aniline molecules is more effective in acidic environment due to a better interaction of anilinium ions with the sulfonate groups of PMAS.

The higher content of PMAS was as a consequence of the dual role of PMAS acting simultaneously to dope and stabilise the dispersion. The Cl/S ratio was 0.056, indicating traces of chloride dopant. This clearly indicated that Cl^- is in competition with the free sulfonate group of PMAS in doping polyaniline. Overall, doping by the free sulfonate groups of the PMAS was clearly the dominant process and directly relates to the proximity of the sulfonate groups to the nitrogen centres on the polyaniline backbone.

As discussed above, stable dispersions were obtanied at higher concentrations of PMAS. The ratio of PMAS to PAn for these stable dispersions was 1.5 and above, indicating that there is sufficient PMAS to dope the PAn in the emeraldine state, with excess sulfonate groups providing a stabilising agent in the resultant dispersion.

Table 6.5. Effect of PMAS concentration and pH (employed in the synthesis of PAn/PMAS) on the PMAS:PAn ratio of the material obtained.

PAn/PMAS Sample	**Aniline:PMAS (**dimer unit)	**PMAS : PAn ratio**	**Synthetic conditions**
1	-	-	0.08M An, 1.0 M HCl
2	2 : 0.15	0.62	0.08M An, 0.25%(w/v) PMAS, 1.0 M HCl
3	2 : 0.3	0.95	0.08M An, 0.50%(w/v) PMAS, 1.0 M HCl
4	2 : 0.6	1.25	0.08M An, 1.00%(w/v) PMAS, 1.0 M HCl
5	2 : 1.0	1.65	0.08M An, 1.60%(w/v) PMAS, 1.0 M HCl
6	2 : 0.15	0.37	0.16M An, 0.50%(w/v) PMAS
7	2 : 0.93	0.79	0.16M An, 3.00%(w/v) PMAS

1) PAn.HCl (0% w/v PMAS) (1.0 M HCl, 0.08 M aniline, 0.02 M APS, Aniline/APS 4:1)

Specifications	**(%)**	**Mole%**	**N/Cl ratio**
C	**58.37**	**4.86**	
H	**5.00**		**5.02**
N	**10.96**	**0.78**	
Cl	**5.54**	**0.16**	

2) 0.25% w/v PMAS (1.0 M HCl, 0.08 M aniline, 0.02 M APS, Aniline/APS 4:1, PMAS 0.25% w/v=6 mM)

Specifications	**(%)**	**Mole %**	**N/S ratio**	**N_{PAn}**	**N_{PMAS}**	**Cl/S**
C	**50.37**	**4.20**				
H	**4.41**		**2.63**	**0.39**	**0.24**	**0**
N	**8.89**	**0.64**				
S	**7.73**	**0.24**				
Cl	**0.00**	**0.00**				

3) 0.50% w/v PMAS (1.0 M HCl, 0.08 M aniline, 0.02 M APS, Aniline/APS 4:1, PMAS 0.50% w/v =12 mM)

Specifications	**(%)**	**Mole %**	**N/S ratio**	**N_{PAn}**	**N_{PMAS}**	**Cl/S**
C	**46.93**	**3.91**				
H	**4.39**		**2.05**	**0.30**	**0.28**	**0.00**
N	**8.17**	**0.58**				
S	**9.09**	**0.28**				
Cl	**0.00**	**0.00**				

4) 1.00% w/v PMAS (1.0 M HCl, 0.08 M aniline, 0.02 M APS, Aniline/APS 4:1, PMAS 1.00% w/v = 24 mM)

Specifications	**(%)**	**Mole %**	**N/S ratio**	**N_{PAn}**	**N_{PMAS}**	**Cl/S**
C	**44.65**	**3.72**				
H	**3.82**		**1.80**	**0.26**	**0.32**	**0.04**
N	**8.02**	**0.57**				
S	**10.16**	**0.32**				
Cl	**0.44**	**0.01**				

5) 1.60% w/v PMAS (1.0 M HCl, 0.08 M aniline, 0.02 M APS, Aniline/APS 4:1, PMAS 1.60% w/v= 40 mM)

Specifications	**(%)**	**Mole %**	**N/S ratio**	**N_{PAn}**	**N_{PMAS}**	**Cl/S**
C	**43.33**	**3.61**				
H	**4.50**		**1.61**	**0.21**	**0.32**	**0.06**
N	**7.59**	**0.54**				
S	**10.80**	**0.34**				
Cl	**0.67**	**0.02**				

6) PAn/PMAS 0.50% w/v (0.16 M aniline, 0.08 M APS, Aniline/APS 2:1, PMAS 0.50% w/v=12 mM)

Specifications	**(%)**	**Mole %**	**N/S ratio**	**N_{PAn}**	**N_{PMAS}**	**PAn/PMAS ratio**
C	**55.45**	**4.62**				
H	**4.47**		**3.67**	**0.53**	**0.20**	**2.67**
N	**10.16**	**0.73**				
S	**6.32**	**0.20**				

7) PAn/PMAS 3.00% w/v (0.16 M aniline, 0.08 M APS, Aniline/APS 2:1, PMAS 3.00% w/v = 74 mM)

Specifications	**(%)**	**Mole %**	**N/S ratio**	**N_{PAn}**	**N_{PMAS}**	**PAn/PMAS ratio**
C	**47.82**	**3.99**				
H	**4.22**		**2.27**	**0.35**	**0.28**	**1.27**
N	**8.79**	**0.63**				
S	**8.87**	**0.28**				

6.3.3.5 ESR spectroscopy

The ESR spectra were recorded for the PAn/PMAS samples at different PMAS concentrations and compared to pure PMAS (Figure 6.34 and Table 6.5). All the samples exhibited symmetric lines with the g value close to that of a free electron implying the same radical type. The ESR spectrum of PMAS was broad with a line width of 3.95 G. The polyaniline samples showed lower line width values. Increasing the concentration of PMAS used during synthesis lowered the line width due to an increase in doping level and spin delocalisation. A low linewidth of 1.11 G was obtained for PAn/PMAS polymerised using 1.00% (w/v) PMAS. The broad ESR line of PMAS suggest that PMAS has more localised spin than polyaniline [41, 42].

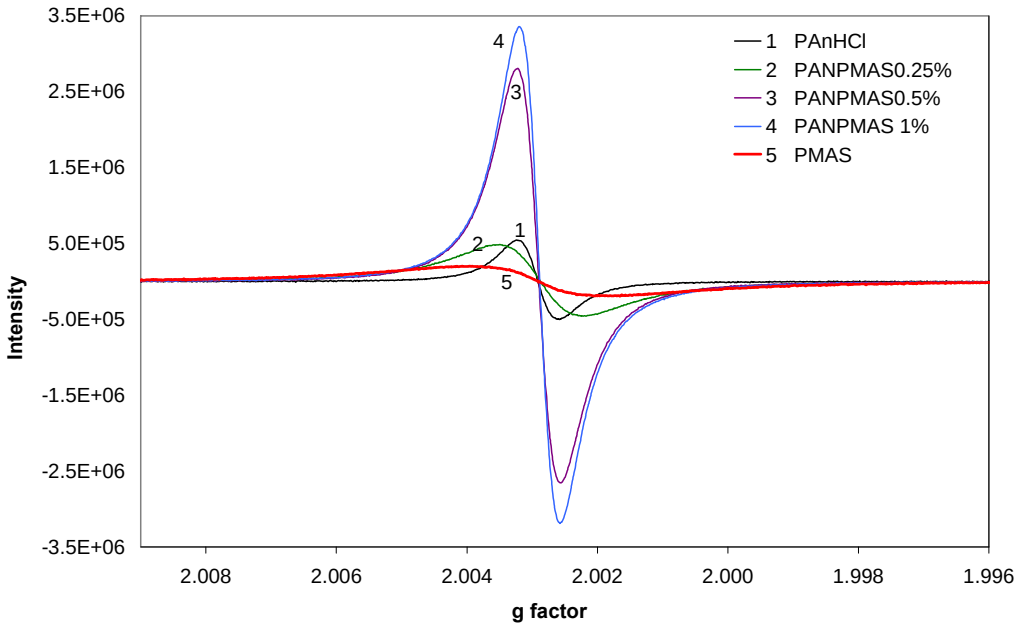

Figure 6.34. The ESR spectra of aqueous dispersion of PAn/PMAS (1.5 mg/mL for all samples) synthesised using various concentrations of PMAS. Numbers 1 to 5 refer to 0, 0.25, 0.50 and 1.60% w/v PMAS used for polymerization of PAn/PMAS.

Increasing the PMAS concentration used during polymerisation of aniline had a significant effect on the spin concentration of the PAn/PMS, increasing with the PMAS content (Table 6.5). This confirms a higher doping level of polyaniline with the increased amounts of PMAS. These are in close agreement with the conductivity of the

samples obtained. The most conducting sample showed the highest spin with lowest line width indicating a high number of delocalised charge carriers in the templated polyaniline/PMAS.

Table 6.6. EPR data for PAn/PMAS dispersions (1.5 mg/mL) synthesised using various concentrations of PMAS (0, 0.25, 0.50 and 1.00% w/v)

Polymer dispersion	**g value**	**ΔH(G)[linewidth]**	**Relative Spin concentration**	**Conductivity (S/cm)**
PAn/HCl	2.00293	1.15	0.33×10^{10}	0.27 ± 0.03
PAn/PMAS 0.25%	2.00288	2.32	1.26×10^{10}	1.52 ± 0.14
PAn/PMAS 0.50%	2.00296	1.17	2.04×10^{10}	2.45 ± 0.23
PAn/PMAS 1.00%	2.00297	1.11	2.32×10^{10}	2.85 ± 0.03
PMAS	2.00293	3.95	1.39×10^{10}	0.23 ± 0.02

6.3.3.6 Thermal analysis

In order to investigate the thermal stability of PAn/PMAS, thermogravimetric analysis was carried out under N_2 for the PAn/PMAS materials and the results were compared to the PMAS and PAn/HCl nanofibres (Figure 6.35).

The samples were preheated at 35˚C for 20 min under N_2 atmosphere. The first weight loss observed in the temperature range 50-110˚C for all the samples, is attributed to water evaporation as reported for polyaniline [43, 44]. Another two weight losses were obtained for PAn/HCl. The weight loss (~ %10) in the range 160-260˚C was due to the liberation of HCl [44] from PAn. The weight loss observed above 300˚C was a result of structural decomposition of PAn. The result was in agreement with the TGA of HCl doped chemically synthesised polyaniline [44]. A major weight loss of 32% was observed for PMAS in the temperature range 230-325˚C due to decomposition of PMAS. PAn/PMAS was thermally stable until about 220-240˚C followed by a major weight loss of 19-22% (depending on the PMAS/PAn ratio) due to the loss and decomposition of the dopant (PMAS). No weight loss was observed in the range 160-

230˚C indicating the absence of HCl as dopant in the PAn/PMAS materials. This was in good agreement with the elemental analysis of PAn/PMAS (Section 6.3.3.4). The weight loss due to de-doping of PAn/PMAS was much higher than PAn/HCl. This reflects the removal of a heavy macromolecular PMAS dopant. This result suggested that the thermal stability of polyaniline was improved in the presence of PMAS. As seen in Figure 6.35, the major weight loss observed for PAn/PMAS samples in the range 230-325˚C is lower than PMAS itself. This further confirms the formation of polyaniline with more stable polymeric backbone compared to PMAS.

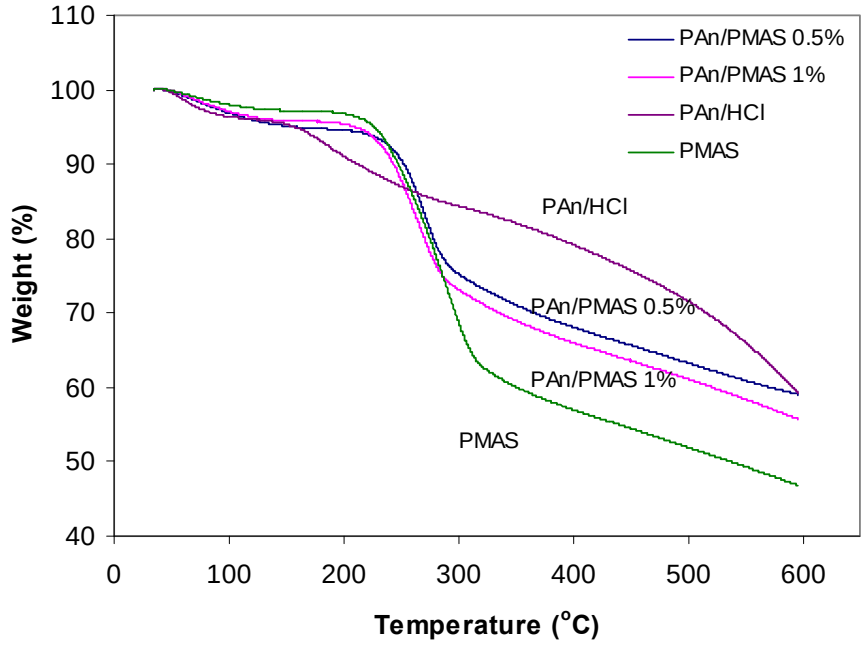

Figure 6.35. TGA themograms of PAn/PMAS (synthesized using 0.50 or 1.00% (w/v) PMAS) compared to PAn/HCl and PMAS under nitrogen atmosphere.

6.3.3.7 Contact angle measurements

The properties of the PAn/PMAS material were also explored using contact angle measurements. A 2 µL water droplet was placed on the surface of polymer films prepared by evaporative casting of PAn/HCl and PAn/PMAS dispersions onto glass substrates. The droplet spread over the polymer surface and reached a constant contact angle after about 15 sec (Figure 6.36 and Figure 6.37). The contact angle was measured

after this time. The hydrophilicity of the PAn/PMAS surface was compared to the polyaniline nanofibres. The contact angle was found to be 22.2º for PAn/PMAS (Table 6.6), indicating the enhanced hydrophilic properties of the PAn/PMAS surface (induced by PMAS) compared to the PAn/HCl nanofibres (contact angle = 54.3º).

Table 6.7. Contact angle measurements of polyaniline obtained by chemical polymerisation of aniline using different dopants.

Polyaniline samples	**Contact angle (º)**
PAn/HCl	54.3 ± 2.1
PAn/PMAS	22.2 ± 2.1

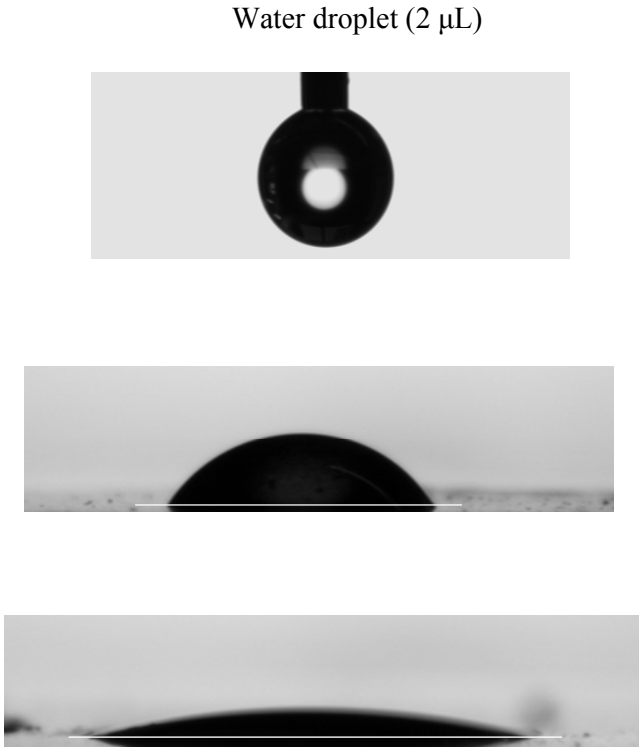

Figure 6.36. Contact angles for the films cast on glass substrate from polyaniline dispersions in water. 2 μL water was dropped on the polymer surface and the advanced contact angle was measured.

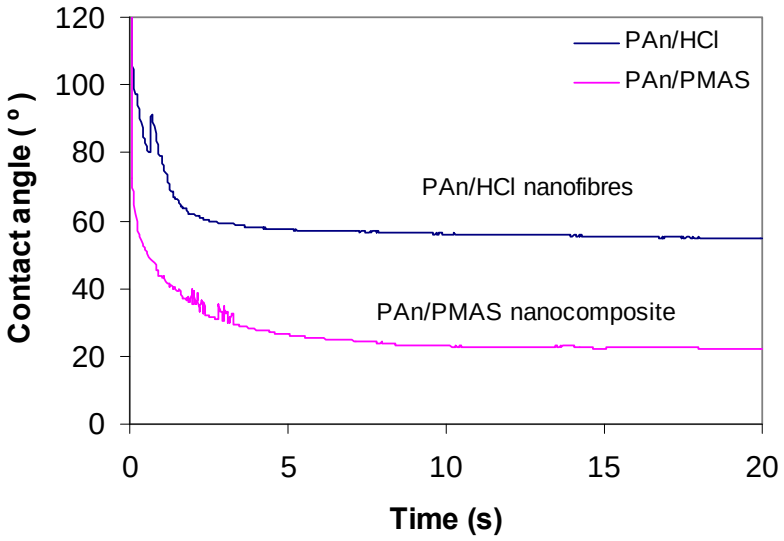

Figure 6.37. Contact angle measurements vs. time for polyaniline films (~10μm) cast on the glass substrates from polyaniline dispersion in water.

6.3.3.8 Conductivity of PAn/PMAS – Effect of pH

Sulfonated polyanilines have demonstrated an independence of conductivity over a wide pH range [45] while the emeraldine salt of PAn is conducting in acidic pH and shows a sharp drop in conductivity to an insulator at pH ~3. Here the effect of pH on conductivity of the PAn/PMAS material is compared to the PAn/HCl material.

Table 6.8 Conductivity of PAn/PMAS and PAn/HCl at different pH.

Solution pH	Conductivity (S/cm)	
	PAn/PMAS	**PAn/HCl**
3.0	**1.88 ± 0.03**	**0.333 ± 0.001**
5.0	**1.33 ± 0.04**	**0.128 ± 0.001**
7.0	**(2.12 ± 0.08) x 10^{-2}**	**(1.48 ± 0.19) x 10^{-4}**
9.0	**(1.00 ± 0.03) x 10^{-3}**	**-**

The electrical conductivity of the PAn/PMAS film evaporatively cast onto a glass substrate from the dispersion in water was measured after immersing in solutions

buffered at different pH and compared with the conductivity of a PAn/HCl film (Table 6.8). The PAn/PMAS was more conductive than PAn/HCl after treating with neutral or even moderately basic solutions. The conductivity of PAn/PMAS was approximately 6 times higher than PAn/HCl at pH 3.0 and 10-fold higher at pH 5.0. In contrast to PAn/HCl, the PAn/PMAS was found to be conducting (0.02 S/cm) at neutral pH. These nanostructured materials are promising in the area of biosensing when conducting materials are needed in a neutral environment.

6.4 Conclusion

Polyaniline nanoparticles with very high dispersion stability and high conductivity have been synthesised in the presence of conductive, electroactive PMAS polyelectrolyte. The PMAS concentration significantly affects the conductivity, morphology and spectral properties of the obtanied PAn/PMAS..

Novel PAn/PMAS materials can be synthesised over a wide pH range of 0.5-6.0 and various PMAS concentrations, with optimal conductivity and higher doping levels achieved by decreasing the pH and increasing the PMAS concentration.

The UV-vis spectra of the PAn/PMAS material in water and in alkaline media confirm the presence of both PAn and PMAS. The presence of an intense free carrier tail in the near infrared region and the absence of a 800 nm peak in the UV-vis spectra of the PAn/PMAS, indicates that polyaniline chains adopted an extended coil conformation in the presence of PMAS dopant.

A highly stable dispersions or water soluble PAn/PMAS can be obtained when the ratio of PMAS (based on dimer unit) to aniline is 0.6:2 and above.

TEM images illustrate how the use of low concentrations of PMAS will result in nanofibres agglomeration, however a mixture of well defined nanofibers (diameters between 20 and 100 nm) and nanoparticles with diameters less than 50 nm are also produced using PMAS: aniline ratios of 0.6:2 and above.

The novel PAn/PMAS materials have enhanced electrical conductivity and stability compared to PAn/HCl nanofibre based materials prepared under equivalent conditions. The conductivity of PAn/PMAS, synthesised using PMAS:aniline ratio of 1:2 and 1.0 M HCl, is 3.0 ± 0.18 S/cm, which is about two orders of magnitude higher than those reported for polyaniline in the presence nonconducting polyelectrolytes. In contrast to PAn/HCl, the PAn/PMAS is conducting (0.02 S/cm) at neutral pH. These nanostructured materials may be promising in the area of biosensing when conducting materials are needed in a neutral environment.

Electrochemical studies of PAn/PMAS show that both of the conducting polymer components are capable of undergoing oxidation and reduction, attributed to the interconversion between leucoemeraldine, emeraldine and pernigraniline oxidation states.

The high S/Cl molar ratio obtained from elemental analysis and the high conductivity of PAn/PMAS indicate that PMAS is the dominant dopant. By increasing the PMAS concentration, the ratio of PMAS to polyaniline increased and reached the value of 1.65 at the stochiometric ratio (1 PMAS dimer unit per two aniline molecules). This high PMAS:PAn ratio indicates that there is sufficient PMAS to dope the PAn in the emeraldine state, with excess sulfonate groups providing a stabilising function in the resultant dispersion. The spin concentration (directly related to doping levels) of PAn/PMAS is increased by higher PMAS loading. Accompanying this observation a decrease in ESR spin linewidth is observed, indicating an increase in delocalised charge carriers in the templated polyaniline/PMAS material.

Thermal analysis of the PAn/PMAS suggests that the thermal stability of polyaniline is improved in the presence of PMAS.

The novel PAn/PMAS material has enhanced conductivity and water solubility making it promising for different applications such as batteries, electronic textiles, electrochromics and chemical sensors. This stable nanoparticle dispersion is printable using ink jet printing.

6.5 References

1. Thiemann, C. and Brett, C.M.A., *Electropolymerisation and properties of conducting polymers derived from aminobenzenesulphonic acids and from mixtures with aniline.* Synthetic Metals, 2001. **125**(3): p. 445-451.
2. Chan, H.S.O., Ho, P.K.H., Ng, S.C., Tan, B.T.G., and Tan, K.L., *A New Water-Soluble, Self-Doping Conducting Polyaniline from Poly(o-aminobenzylphosphonic acid) and Its Sodium Salts: Synthesis and Characterization.* J. Am. Chem. Soc., 1995. **117**(33): p. 8517-8523.
3. Shimizu, S., Saitoh, T., Uzawa, M., Yuasa, M., Yano, K., Maruyama, T., and Watanabe, K., *Synthesis and applications of sulfonated polyaniline.* Synthetic Metals, 1997. **85**(1-3): p. 1337-1338.
4. Guo, R., Barisci, J.N., Innis, P.C., Too, C.O., Wallace, G.G., and Zhou, D., *Electrohydrodynamic polymerization of 2-methoxyaniline-5-sulfonic acid.* Synthetic Metals, 2000. **114**(3): p. 267-272.
5. Zhou, D., Innis, P.C., Wallace, G.G., Shimizu, S., and Maeda, S.-I., *Electrosynthesis and characterisation of poly(2-methoxyaniline-5-sulfonic acid)-effect of pH control.* Synthetic Metals, 2000. **114**(3): p. 287-293.
6. Wei, X.-L.W., Y. Z.; Long, S. M.; Bobeczko, C.; Epstein, A. J., *Synthesis and Physical Properties of Highly Sulfonated Polyaniline.* J. Am. Chem. Soc., 1996. **118**(11): p. 2545-2555.
7. Kitani, A., Satoguchi, K., Tang, H.-Q., Ito, S., and Sasaki, K., *Eletrosynthesis and properties of self-doped polyaniline.* Synthetic Metals, 1995. **69**(1-3): p. 129-130.
8. Yue, J. and Epstein, A.J., *Synthesis of self-doped conducting polyaniline.* J. Am. Chem. Soc., 1990. **112**(7): p. 2800-2801.
9. Wei, X. and Epstein, A.J., *Synthesis of highly sulfonated polyaniline.* Synthetic Metals, 1995. **74**(2): p. 123-125.
10. Malinauskas, A., *Self-doped polyanilines.* Journal of Power Sources, 2004. **126**(1-2): p. 214-220.
11. Han, M.G., Cho, S.K., Oh, S.G., and Im, S.S., *Preparation and characterization of polyaniline nanoparticles synthesized from DBSA micellar solution.* Synthetic Metals, 2002. **126**(1): p. 53-60.
12. Moulton, S.E., Innis, P.C., Kane-Maguire, L.A.P., Ngamna, O., and Wallace, G.G., *Polymerisation and characterisation of conducting polyaniline nanoparticle dispersions.* Current Applied Physics, 2004. **4**(2-4): p. 402-406.
13. Kinlen PJ, D.Y., Graham CR, Remsen EE, Macromolecules, 1998. **31**: p. 1735-44.
14. Kim, D., Choi, J., Kim, J.-Y., and Sohn, D., Macromolecules, 2002. **35**: p. 5314-6.
15. Barisci, J.N., Innis, P.C., Kane-Maguire, L.A.P., Norris, I.D., and Wallace, G.G., *Preparation of chiral conducting polymer colloids.* Synthetic Metals, 1997. **84**(1-3): p. 181-182.
16. Stejskal, J. and Sapurina, I., *On the origin of colloidal particles in the dispersion polymerization of aniline.* Journal of Colloid and Interface Science, 2004. **274**(2): p. 489-495.

17. Blinova, N.V., Sapurina, I., Klimovic, J., and Stejskal, J., *The chemical and colloidal stability of polyaniline dispersions.* Polymer Degradation and Stability, 2005. **88**(3): p. 428-434.
18. H. J. Qiu, M.X.W., b. Matthews, L. M. Dai, Macromolecules, 2001. **35**: p. 675.
19. Aboutanos, V., Barisci, J.N., Kane-Maguire, L.A.P., and Wallace, G.G., *Electrochemical preparation of chiral polyaniline nanocomposites.* Synthetic Metals, 1999. **106**(2): p. 89-95.
20. Huang, J.X. and Kaner, R.B., *A general chemical route to polyaniline nanofibers.* Journal of the American Chemical Society, 2004. **126**(3): p. 851-855.
21. Huang, J.X. and Kaner, R.B., *Nanofiber formation in the chemical polymerization of aniline: A mechanistic study.* Angewandte Chemie-International Edition, 2004. **43**(43): p. 5817-5821.
22. Li, D. and Kaner, R.B., *Processable stabilizer-free polyaniline nanofiber aqueous colloids.* Chemical Communications, 2005(26): p. 3286-3288.
23. Strounina, E.V., Kane-Maguire, L.A.P., and Wallace, G.G., *Optically active sulfonated polyanilines.* Synthetic Metals, 1999. **106**(2): p. 129-137.
24. Dominis, A.J., Spinks, G.M., Kane-Maguire, L.A.P., and Wallace, G.G., *A de-doping/re-doping study of organic soluble polyaniline.* Synthetic Metals, 2002. **129**(2): p. 165-172.
25. Zhao H., Wallace G.G., *Polypyrrole/poly(2-methoxy aniline, 5-sulfonic acid) polymer composite.* Polymer Gels nad Networks, 1998. **6**: p. 233-245.
26. Masdarolomoor, F., Innis, P.C., Ashraf, S., and Wallace, G.G., *Purification and characterisation of poly(2-methoxyaniline-5-sulfonic acid).* Synthetic Metals, 2005. **153**(1-3): p. 181-184.
27. Stejskal, J., Omastova, M., Fedorova, S., Prokes, J., and Trchova, M., *Polyaniline and polypyrrole prepared in the presence of surfactants: a comparative conductivity study.* Polymer, 2003. **44**(5): p. 1353-1358.
28. T. Tatsuma, T.O., R. Sato, and N. Oyama, J. Electroanal. Chem., 2001. **501**: p. 180-185.
29. Strounina, E.V., Shepherd, R., Kane-Maguire, L.A.P., and Wallace, G.G., *Conformational changes in sulfonated polyaniline caused by metal salts and OH.* Synthetic Metals, 2003. **135**(1-3): p. 289-290.
30. Kitani, A., Satoguchi, K., Iwai, K., and Ito, S., *Electrochemical Behaviors of Polyaniline / Polyaniline-sulfonic Acid Composites.* Synthetic Metals, 1999. **102**(1-3): p. 1171-1172.
31. Mazeikiene, R., Niaura, G., and Malinauskas, A., *Voltammetric study of the redox processes of self-doped sulfonated polyaniline.* Synthetic Metals, 2003. **139**(1): p. 89-94.
32. Tawde, S., Mukesh, D., and Yakhmi, J.V., *Redox behavior of polyaniline as influenced by aromatic sulphonate anions: cyclic voltammetry and molecular modeling.* Synthetic Metals, 2001. **125**(3): p. 401-413.
33. Beadle, P.M., Nicolau, Y.F., Banka, E., Rannou, P., and Djurado, D., *Controlled polymerization of aniline at sub-zero temperatures.* Synthetic Metals, 1998. **95**(1): p. 29-45.
34. Stejskal, J., Kratochvil, P., and Jenkins, A.D., *The formation of polyaniline and the nature of its structures.* Polymer, 1996. **37**(2): p. 367-369.

35. Sbaite, P., Huerta-Vilca, D., Barbero, C., Miras, M.C., and Motheo, A.J., *Effect of electrolyte on the chemical polymerization of aniline.* European Polymer Journal, 2004. **40**(7): p. 1445-1450.
36. Jayanty, S., Prasad, G.K., Sreedhar, B., and Radhakrishnan, T.P., *Polyelectrolyte templated polyaniline--film morphology and conductivity.* Polymer, 2003. **44**(24): p. 7265-7270.
37. Yuan, G.-L., Kuramoto, N., and Su, S.-J., *Template synthesis of polyaniline in the presence of phosphomannan.* Synthetic Metals, 2002. **129**(2): p. 173-178.
38. Wan, M.X.S., Y. Q.; Huang, J., Chinese Patent, No. 98109916.5.
39. Pornputtkul, Y., *Development of Chiral Conducting Polymers for Asymmetric Electrosynthesis*, in University of Wollongong, 2005.
40. Tallman, D.E. and Wallace, G.G., *Preparation and preliminary characterization of a poly (4-vinylpyridine) complex of a water-soluble polyaniline.* Synthetic Metals, 1997. **90**(1): p. 13-18.
41. Kahol, P.K., Perera, R.P., Satheesh Kumar, K.K., Geetha, S., and Trivedi, D.C., *Electron localization length in polyaniline.* Solid State Communications, 2003. **125**(7-8): p. 369-372.
42. Kahol, P.K., Satheesh Kumar, K.K., Geetha, S., and Trivedi, D.C., *Effect of dopants on electron localization length in polyaniline.* Synthetic Metals, 2003. **139**(2): p. 191-200.
43. S. Palaniappan, B.H.N., *Temperature effect on conducting polyaniline salts: Thermal and spectral studies.* Journal of Polymer Science Part A: Polymer Chemistry, 1994. **32**(13): p. 2431-2436.
44. Yen Wei, K.F.H., *Thermal analysis of chemically synthesized polyaniline and effects of thermal aging on conductivity.* Journal of Polymer Science Part A: Polymer Chemistry, 1989. **27**(13): p. 4351-4363.
45. Wei, X.-L., Wang, Y.Z., Long, S.M., Bobeczko, C., and Epstein, A.J., *Synthesis and Physical Properties of Highly Sulfonated Polyaniline.* J. Am. Chem. Soc., 1996. **118**(11): p. 2545-2555.

Chapter 7

Electrochemical synthesis of PAn/PMAS

7.1 Introduction

The dopant incorporated into inherently conducting polymers at the point of synthesis is known to have a profound effect on the physical and chemical properties of the resultant material [1]. With polyaniline emeraldine salts (Scheme 7.1 shown below) a range of anions, including polyelectrolytes and functional molecules can be incorporated as the dopant (A^-). However, the range of dopants that can be directly incorporated is limited due to the fact that an acidic environment must be used to induce aniline solubility in aqueous media and to maintain the polymer in the conductive emeraldine salts state during growth.

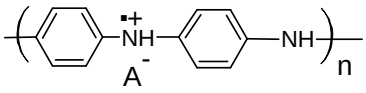

Scheme 7.1. Polyaniline emeraldine salt

However, even variations in the anion used in simple acids (Cl^-, NO_3^-, SO_4^{2-}) has been shown to have a profound effect on growth and the properties of the resultant materials [2-4]. Organic sulfonic acids [5, 6], chiral dopants [7] and redox active sulfonated ferrocene [8] have been incorporated as functional dopants.

A range of polyelectrolytes has also been incorporated as dopants [9-12]. Polyelectrolytes are incorporated even in the presence of smaller anions when acids are added to lower the pH [13]. The incorporation of polyelectrolytes introduces some unique properties to the resultant conducting polymer, such as high water content electroactive hydrogels [14, 15], biocompatibility [16, 17] , and improved mechanical properties [18]. A number of researchers have studied the application of

polyaniline/polyelectrolyte systems in areas such as sensors [9, 19, 20] batteries [21] and electrochromic devices [22-24].

Polyelectrolytes such as polystyrene sulfonic acid [25] are known to provide the counterions and a local low pH environment for producing the conducting form of polyaniline. The polyelectrolyte also provides a template for electrostatic alignment of aniline monomers which promotes head-to-tail coupling. This later function minimizes branching during polymerisation and promotes linear polyaniline chain growth. The mechanistic role of polyelectrolytes in template polymerisation of polyaniline has been studied by Samuelson et al. [25].

The use of the conducting fully-sulfonated polyaniline polyelectrolyte (PMAS) as a dopant was first reported for polypyrrole [26]. One year later in 1999, Kitani et al. [27] reported the synthesis of a polyaniline/polyaniline-sulfonic acid composite by electrochemical dopant exchange using poly(aniline-2-sulfonic acid). Sulfonated polyanilines are water soluble polyelectrolytes which are electroactive and conducting over a wide pH range [28].

A method was developed in Chapter 3 for the separation of high and low molecular weight PMAS. As explained in Chapter 5, these fractions exhibited different physical properties. The high molecular weight PMAS (HMWt PMAS) is conductive, electroactive and non-fluorescent. In contrast, the low molecular weight PMAS (LMWt PMAS) is not conductive or electroactive, but exhibits photoluminescence. Due to the presence of negatively charged sulfonate groups in their structure, these materials are capable of electrostatic interaction with positively charged groups such as anilinium ions, which may potentially act as templates in the polymerisation of aniline. It is also expected that this approach would result in production of a unique material containing a conducting backbone and a conducting dopant with multiple switching capabilities. This Chapter presents the electrochemical synthesis and characterisation of novel polyaniline material using PMAS as an electroactive and electrically conductive dopant polyelectrolyte (Scheme 7.2). The capability of LMWt PMAS for doping polyaniline is also examined.

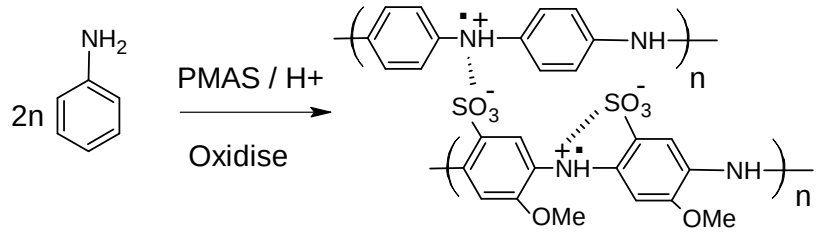

Scheme 7.2. Polymerisation of aniline in the presence of PMAS.

7.2 Experimental

7.2.1 Materials

Aniline purchased from Aldrich was distilled and then stored at -4 ºC (freezer) prior to use. PMAS (HMWt and LMWt) was synthesised and purified in house [29]. Ammonium persulfate, hydrazine hydrate and sodium hydroxide were purchased from Aldrich. Poly(styrenesulfonate) sodium salt (Mw 70,000 Da) was obtained from Aldrich. Hydrochloric acid 32% (w/v) was purchased from Ajax. Amberlite IR-120 ion exchange resin purchased from Ajax was used to acidify pure PMAS. All reagents used were of analytical grade and all solutions were prepared in Milli-Q water (18 MΩ cm).

7.2.2 Instrumentation

pH was measured using a TPS Instruments Model 900-P pH meter. UV-vis spectra were recorded with a Shimadzu UV-1601 spectrophotometer (300-1100 nm) ,or a Cary 500 spectrophotometer (Varian) (300-2500 nm). Cyclic voltammetry (CV) was carried out in a three electrode cell using a glassy carbon working electrode with a platinum mesh auxiliary electrode and Ag/AgCl (3M NaCl) reference electrode connected to an E-Corder 401 with an EDAQ Potentiostat. Spectroelectrochemical studies of the PAn/PMAS film were performed in a quartz cell, containing three electrodes in aqueous 0.10 M HCl, using a Shimadzu MultiSpec-1501 with Hyper UV 1.50 software and an EDAQ Potentiostat.

ITO-coated glass was sputter coated with platinum using a magnetron sputter coater SC100MS (Dynavac Engineering, AU), to assist with the adherence of uniform

polyaniline films on the surface. Typical Pt coatings were made by DC magnetron sputter coating at a pressure of 2 x 10^{-6} bar of argon by applying a current of 30-50 mA to the Pt target for 5 seconds.

The surface morphology of the polymer was investigated using scanning electron microscopy (SEM, Leica Model Stereoscan 440) with a secondary electron detector. SEM imaging was conducted using an accelerating voltage of 20 kV.

The resonance frequency of polyaniline coated quartz crystals was measured in-situ during electrochemical polymerisation of aniline using a Stanford Research System (QCM 200) Quartz Crystal Microbalance. The quartz crystals, having an unloaded resonant frequency of approximately 5 MHz, were obtained from Stanford Research Systems. The electrochemically available surface area of the crystal (1.37 cm^2) was much larger than the oscillation surface area (0.4 cm^2), thus the edge effects on the frequency measurement were disregarded. Mass change was directly calculated from the resonance frequency change using the Sauerbrey equation [30].

Elemental analyses were performed by the Australian National University Microanalytical laboratory. The samples (3 mg) were heated to 50°C in a vacuum oven for 5 hrs prior to microanalysis.

The ESR spectra of PAn/PMAS films deposited onto Pt wire were recorded using a Bruker EMX ESR spectrometer under identical conditions of microwave frequency (9.76 GHz), attenuator (30.0 dB), sweep width (15 G), modulation frequency (100 KHz), modulation amplitude (0.5 G), time constant (1.28 msec), conversion time (5.12 msec) resulting in a scan sweep time of 5.24 sec. The ESR sweep field conditions for PAn/PSS films were tuned at a microwave frequency (9.76 GHz), attenuator (10.0 dB), sweep width (40 G), modulation frequency (100 KHz), modulation amplitude (1.0 G), time constant (5.12 msec), conversion time (20.48 msec) yielding a scan sweep time of 10.49 sec.

Contact angles were measured using a DataPhysics OCAZO Goniometer (employing SCAZI software). A 2 μL drop of water was lowered onto the polymer surface and the

contact angle was recorded after the angle reached a relatively constant value (advanced contact angle).

7.2.3 Electrochemical synthesis of PAn/PMAS

Electrochemical polymerisation of aniline was carried out using a three-electrode electrochemical cell as mentioned above. The polymer was electrodeposited on a glassy carbon (GC) electrode for electrochemical characterisation of the polymer during or after growth; onto platinised ITO-coated glass for subsequent characterisation by UV-Vis spectroscopy, or onto Pt wire for Echem-ESR characterisation. A Pt plate (3 cm x 3 cm) was used as the substrate to prepare the polymer required for characterisation by elemental analysis. The aqueous solutions used for electrodeposition of PAn/PMAS emeraldine salt typically contained 0.01 M aniline monomer and 0.10-0.20% (w/v) PMAS (acid form), unless otherwise stated. The concentration of HCl used was varied between experiments, and was either 0.10 or 1.0 M. The solutions were purged with nitrogen gas for 5-10 min prior to use. Polymerisation was performed at room temperature. PAn/PMAS film was deposited by potentiodynamic polymerisation of aniline in the presence of the PMAS dopant by applying a potential sweep between -0.5 V and 1.1 V (vs. Ag/AgCl) for 10-30 cycles using a scan rate of 25 or 50 mV/s. The polymer films were washed by dipping in 40 ml of water to remove unwanted reactants and products. Potentiostatic polymerisation of aniline in the presence of PMAS or PSS was carried out by applying a constant potential in the range 0.5 to 1.0 V and passing 200 mC/cm^2 charge.

Electrodeposition of PAn/PSS **:**

PAn/PSS was synthesised electrochemically using 0.20% (w/v) polystyrene sulfonate (sodium salt) as dopant under conditions identical to those used to synthesise PAn/PMAS.

7.2.4 Echem-ESR of PAn/Polyelectrolyte

The polymer coated Pt wire was placed in an Echem-ESR flat quartz cell containing 0.10 M HCl. The potential was cycled between -0.3 and 1.0 V at 5 mV/sec and the ESR spectra were recorded every 5.24 sec for PAn/PMAS and every 10.49 sec for PAn/PSS

(as stated above in the ESR conditions). For Echem-ESR studies under steady state conditions, the polymer film was equilibrated stepwise at potentials in from -0.2 V to 0.8V for 3 min before the ESR measurements.

7.3 Results and Discussion

7.3.1 Doping PAn film with HMWt and LMWt PMAS solutions

The idea of using PMAS as dopant for polyaniline was initially explored by post-doping polyaniline films with aqueous HMWt PMAS and LMWt PMAS solutions and monitoring with UV-vis spectroscopy. PAn/HCl films electrodeposited onto Pt-ITO glass were de-doped with 0.30 M NaOH solution to give the emeraldine base (EB) form of polyaniline. The de-doped polyaniline films were successfully doped by immersing in the HMWt PMAS and LMWt PMAS aqueous solutions (5 mg/mL, pH 2.5) or 1.0 M HCl solution (pH = 0) for 10 min. After 10 min, the UV-vis spectra recorded the features of the doped polyaniline emeraldine salt, as shown in Figure 7.1. The broad band at 600 nm for the EB was replaced by a free carrier tail above 800 nm, indicative of the doped material.

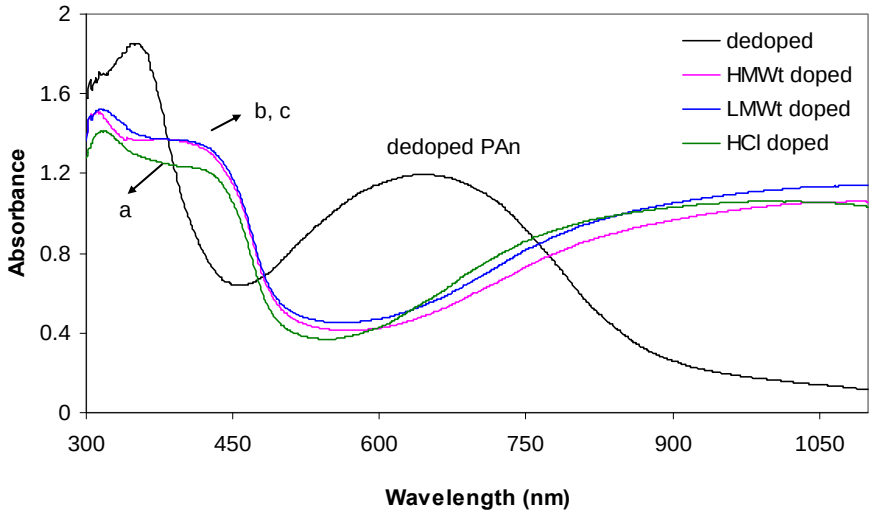

Figure 7.1. UV-vis spectra of PAn EB film (dedoped) on ITO glass, and after doping with (a) 1.0 M HCl, (b) 0.5% (w/v) HMWt PMAS, and (c) 0.5% (w/v) LMWt PMAS for 10 min.

7.3.2 Electrochemical polymerisation of aniline using PMAS as dopant.

Attempts to induce electropolymerisation of 0.10 M aniline in the presence of 0.5% (w/v) PMAS solution were not successful. The oxidation peak (a) observed on the first anodic sweep is attributed to the production of the radical monomer cation, however no increase in current density was observed on subsequent potential scans (Figure 7.2). It was found that after addition of aniline to a 0.5% (w/v) PMAS (acid form) the pH increased from 2.5 to approximately 6. The pH of this solution was not sufficiently acidic to sustain electropolymerisation of aniline. However, visual inspection of the electrode surface revealed a very thin film of polymer after 20 cycles. Cyclic voltammetry of the coated glassy carbon electrode in 0.10 M HCl showed weak redox peaks (a/a', and b/b') indicative of polyaniline. Two anodic peaks at 0.25 V and 0.50 V, with corresponding cathodic peaks at 0.34 V and 0.07 V, were observed (Figure 7.3).

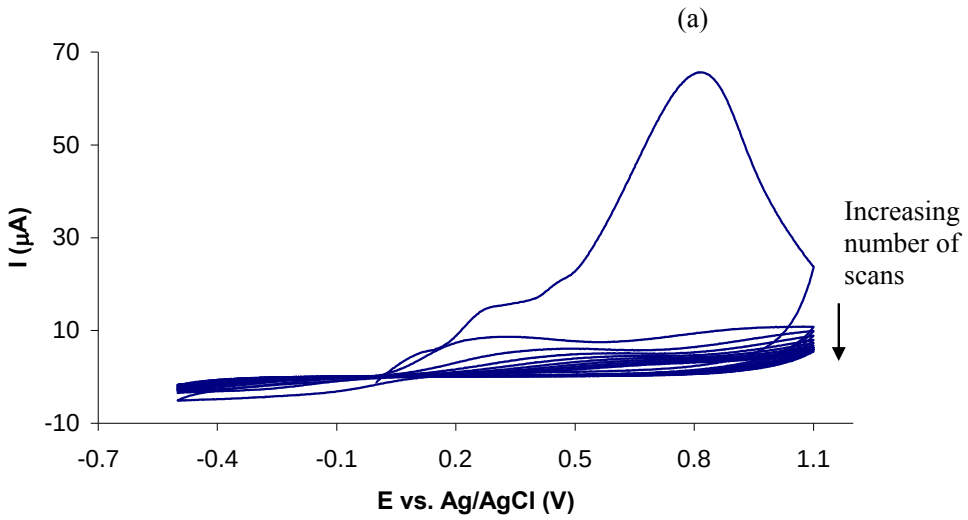

Figure 7.2. Cyclic voltammogram of 0.10 M aniline in 0.5% (w/v) PMAS at a glassy carbon electrode. Scan rate was 25 mV/sec.

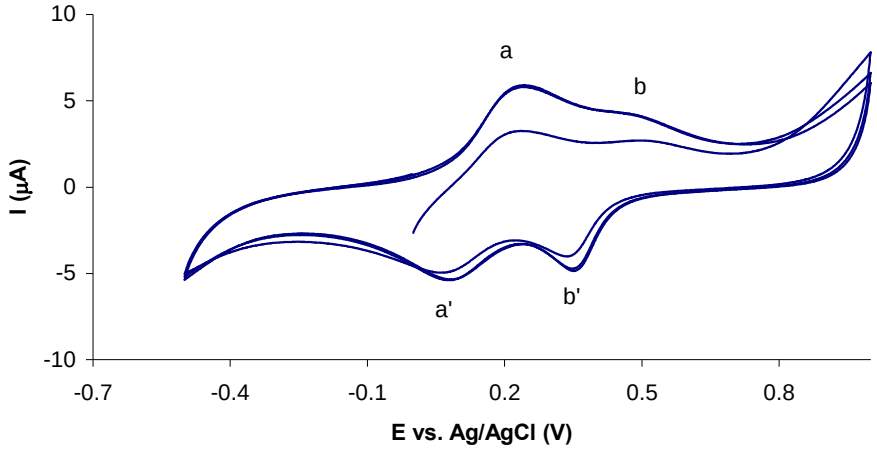

Figure 7.3. Cyclic voltammogram of PAn/PMAS coated glassy carbon electrode (prepared as in Figure 7.2 in 0.10 M HCl solution. Scan rate was 50 mV/sec.

An acidic media (pH <3) is required for polymerisation of aniline to form conducting PAn [31, 32]. Initial attempts to overcome this limitation involved reducing the aniline concentration. Using a solution containing 0.01 M aniline and 0.5% PMAS (pH 2.45) (An:PMAS molar ratio = 1:2.5), cyclic voltammograms were recorded (Figure 7.4). The current density increased slowly on subsequent scans, exhibiting peaks at 0.15 V and 0.45 V. Post-growth cyclic voltammetric characterisation of the polymer-coated electrode in 0.10 M HCl showed two redox pairs (a/a' and b/b') with well-defined anodic peaks at 0.28 V and 0.48 V, indicating that electroactive polyaniline was attained (Figure 7.5). The results show that at low pH (obtained using low concentration of aniline in PMAS) aniline can be polymerised with PMAS as dopant, even using a low concentration of 0.01 M aniline, which is typically insufficient to grow conducting polyaniline (see discussion below).

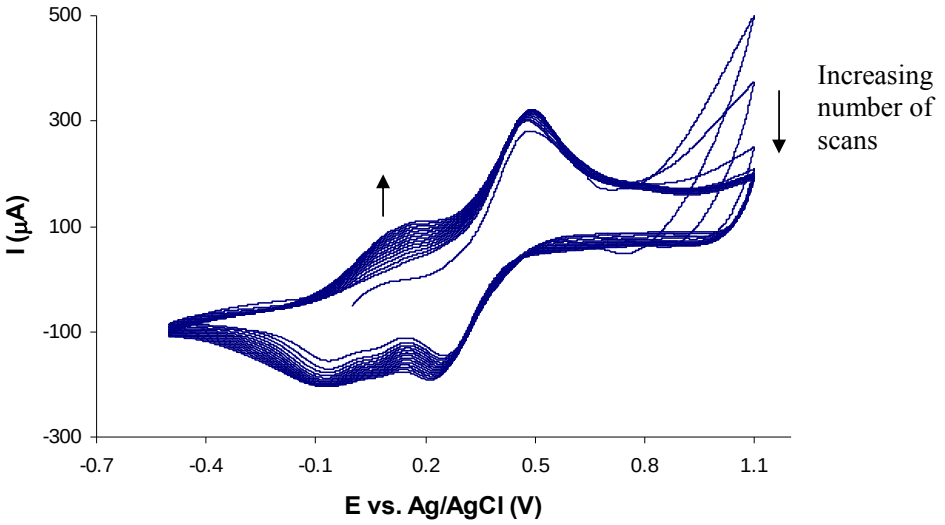

Figure 7.4. Cyclic voltammogram of 0.01 M aniline in 0.5% PMAS (pH 2.45) at a glassy carbon electrode. Scan rate was 25 mV/sec for 10 cycles..

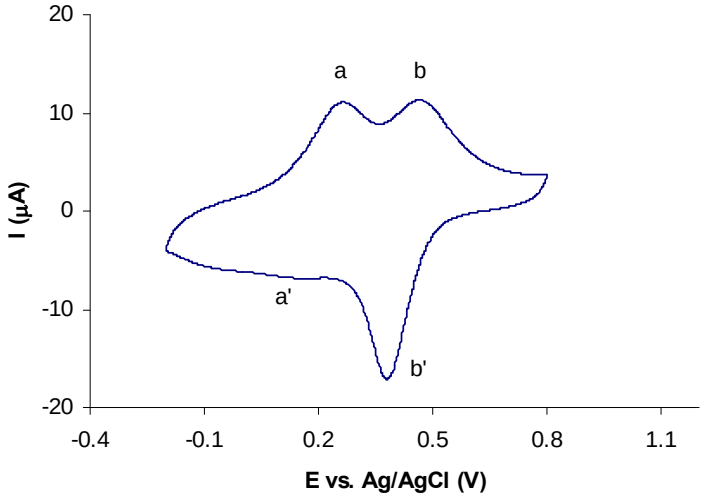

Figure 7.5. Cyclic voltammogram of PAn/PMAS-coated glassy carbon electrode in 0.10 M HCl solution, scan rate 50 mV/sec. The polymer was deposited from 0.01 M aniline and 0.5% PMAS solution at pH 2.45.

7.3.3 Electrochemical synthesis of PAn/PMAS in the presence of acid, effect of pH.

To further probe the influence of pH during polymerisation, aniline was dissolved in 0.10% (w/v) PMAS solution along with either 0.10 M HCl (pH 1.3) or 1.0 M HCl (pH 0.0). As a control, polymerisation of aniline was also carried in the absence of PMAS.

7.3.3.1 Polymerisation of 0.01 M aniline in 0.10 M HCl

Potentiodynamic polymerisation of 0.01 M aniline in 0.10 M HCl was attempted (Figure 7.6). No PAn growth was observed using these conditions. The oxidation peak observed on the first anodic sweep is attributed to the production of the radical monomer cation, and diminished in subsequent scans. The decrease in the current density of this anodic peak may be due to radical-radical coupling and production of non-electroactive oligomers that can not proceed to longer polymeric chains. This indicates that the concentration of monomer is not sufficient to initiate polymerisation under the polymerisation conditions used.

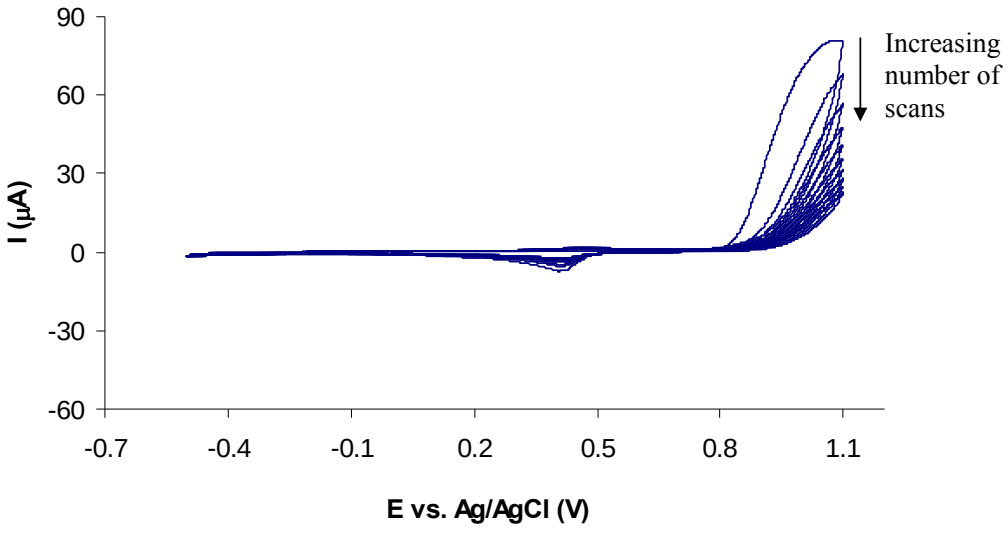

Figure 7.6. Cyclic voltammogram of 0.01 M aniline in 0.10 M HCl at a glassy carbon electrode. Scan rate 25 mV/sec for 10 cycles.

7.3.3.2 Polymerisation of 0.01 M aniline in 0.10 M HCl in the presence of PMAS

The polymerisation of aniline was performed after 0.10% (w/v) PMAS was added to the above solution. Cyclic voltammograms (Figure 7.7) clearly illustrated the rapid deposition of a conductive electroactive material. Since no polymer growth was observed in the absence of PMAS, the dramatic increase in peak current density in the presence of PMAS shows the deposition of polyaniline with PMAS as dopant. After 20 cycles, two main oxidation peaks were observed with anodic peaks at 0.25 V and 0.48 V, consistent with leucoemeraldine to emeraldine and emeraldine to pernigraniline redox transitions, respectively.

It is proposed that anilininum ions created in the acidic media interact with the free sulfonate groups of PMAS to form an aniline-PMAS complex. As a polyelectrolyte, PMAS facilitates charge transfer. Electropolymerisation of aniline in this medium involves the oxidation of aniline to a radical cation, coupling of the radical cations in the vicinity along the PMAS polymeric chain, and progressive chain propagation. The free sulfonate group of PMAS (one per dimer unit) also acts as the dopant for the polyaniline chain. The enhanced polymerisation observed is hypothesised to arise from strong electrostatic interaction between anilinium ions created in slightly acidic media and free sulfonate groups along the polymer chain of PMAS. Templating of the aniline monomer, as described previously using other (non-conducting) sulfonated polyelectrolytes [25], facilitates the chain propagation due to a supramolecular preordering of the PMAS polyelectrolyte template. The PMAS simultaneously acts as the molecular dopant to the electropolymerised material.

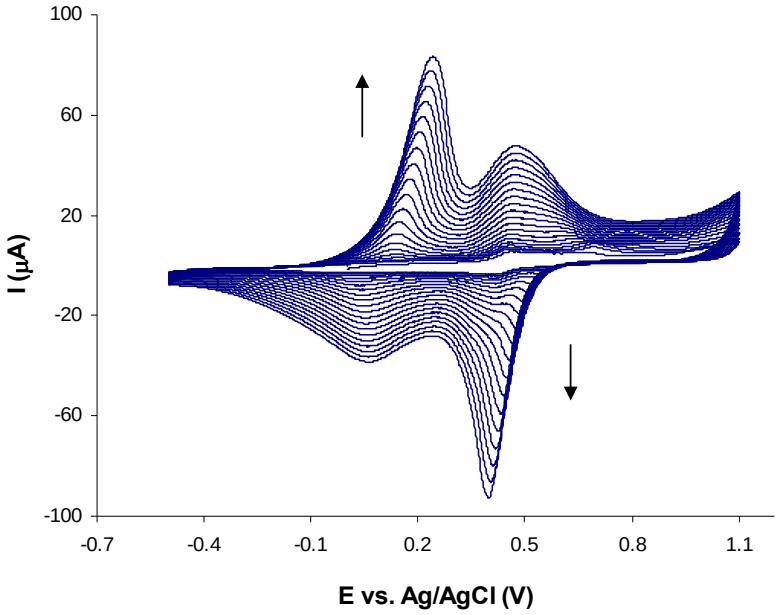

Figure 7.7. Potentiodynamic polymerisation of 0.01 M aniline in 0.10 M HCl after addition of 0.10% PMAS (pH 1.3) at a glassy carbon electrode. Scan rate was 25 mV/sec for 20 cycles. Arrows indicate growth direction.

CV characterisation of the PAn-coated electrode (Figure 7.8) demonstrated two well-defined redox waves (a/a', and b/b') with anodic potentials at 0.30 V and 0.51 V and corresponding cathodic peaks at 0.35 and 0.06 V, which are typical of PAn systems.

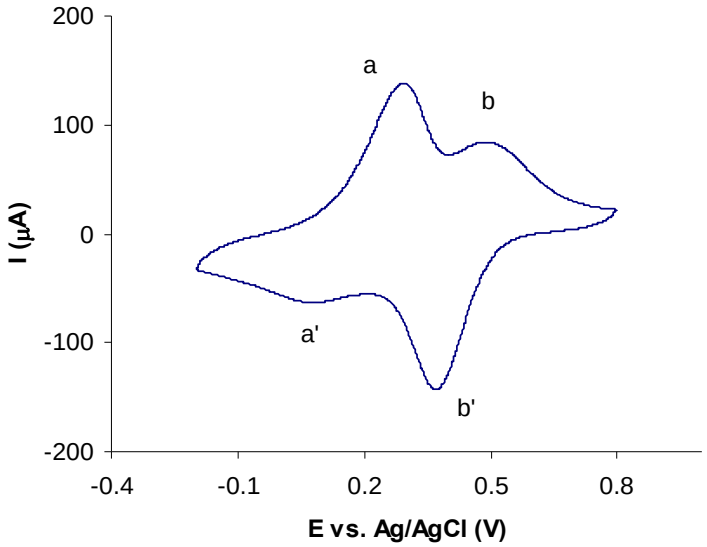

Figure 7.8. Cyclic voltammogram of PAn/PMAS coated glassy carbon electrode in 0.10 M HCl solution. Scan rate 50 mV/sec.

7.3.3.3 Effect of ionic strength on polymerisation of 0.01 M aniline.

Growth of polymer in the presence of PMAS may be due to increased ionic strength of electrolyte, and may be achieved by addition of other electrolytes. To investigate the effect of ionic strength of the electrolyte on the polymerisation of aniline, molar concentrations equivalent to 0.10% PMAS (5 mM based on dimer unit) of NaCl and HCl were added to polymerisation solutions and the polymer was grown by CV.

The results are illustrated in Figure 7.9. To compare the effect of the additives, the 10^{th} cycle of the polymerisation has been plotted in each case. No significant growth was observed when 5 mM of NaCl or HCl was added to the initial 0.01 M aniline / 0.10 M HCl solution. The slight increase in current density with the HCl additive can be attributed to the decrease in pH compared with the NaCl additive. However, the addition of 5 mM PMAS resulted in a dramatic increase in current density and polymerisation of aniline. Therefore, the role of PMAS is not limited to a simple increase in ionic strength but also to the fact that it acts as an effective template and dopant during the polymerisation of aniline.

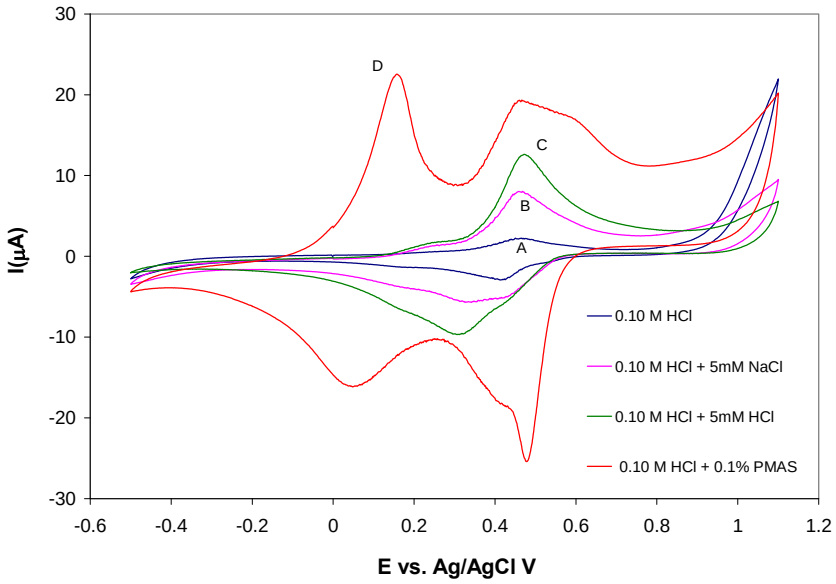

Figure 7.9. Polymerisation of 0.01 M aniline in 0.10 M HCl (A), and after addition of 5 mM of (B) NaCl, (C) HCl and (D) PMAS. The 10^{th} cycle is shown in each case for comparison.

Cyclic voltammograms of PAn-coated electrodes grown with these additives were also compared (Figure 7.10). Only the polymer obtained in the presence of PMAS showed two well-defined redox waves, as discussed earlier.

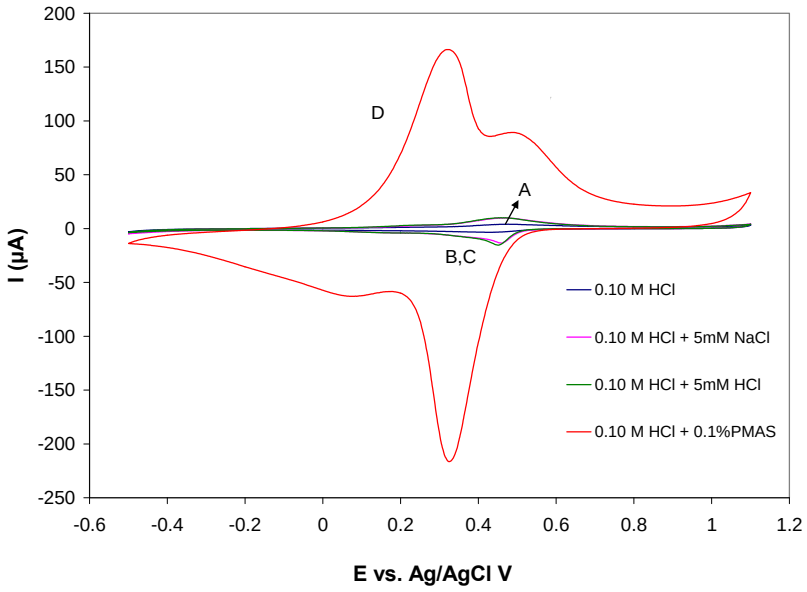

Figure 7.10. The post-growth cyclic voltammograms of the polyanilines, deposited on glassy carbon electrodes under conditions described in Figure 7.9, in 0.10 M HCl electrolyte. Scan rate was 50 mV/sec. The labels are as for Figure 7.9.

7.3.3.4 Stability in HCl, effect of acid concentration on the CV

The electroactivity of PAn/PMAS was examined in hydrochloric acid electrolyte over a range of different concentrations. As shown in Figure 7.11, two redox couples were observed in all cases, appearing at more positive potentials with increasing acid concentration. CVs obtained in 1.0 M HCl or 2.0 M HCl were not stable. This was evident by a noted decrease in the current density and a shift in the position of the observed redox peaks. The CVs of the PAn/PMAS were reasonably stable in 0.10 M HCl. Therefore, 0.10 M HCl was used for all subsequent CV characterisation of PAn/PMAS. The oxidative degradation of polyaniline in strong acidic conditions due to nucleophilic attack on bipolaronic sites by water may be responsible for the instability observed [33].

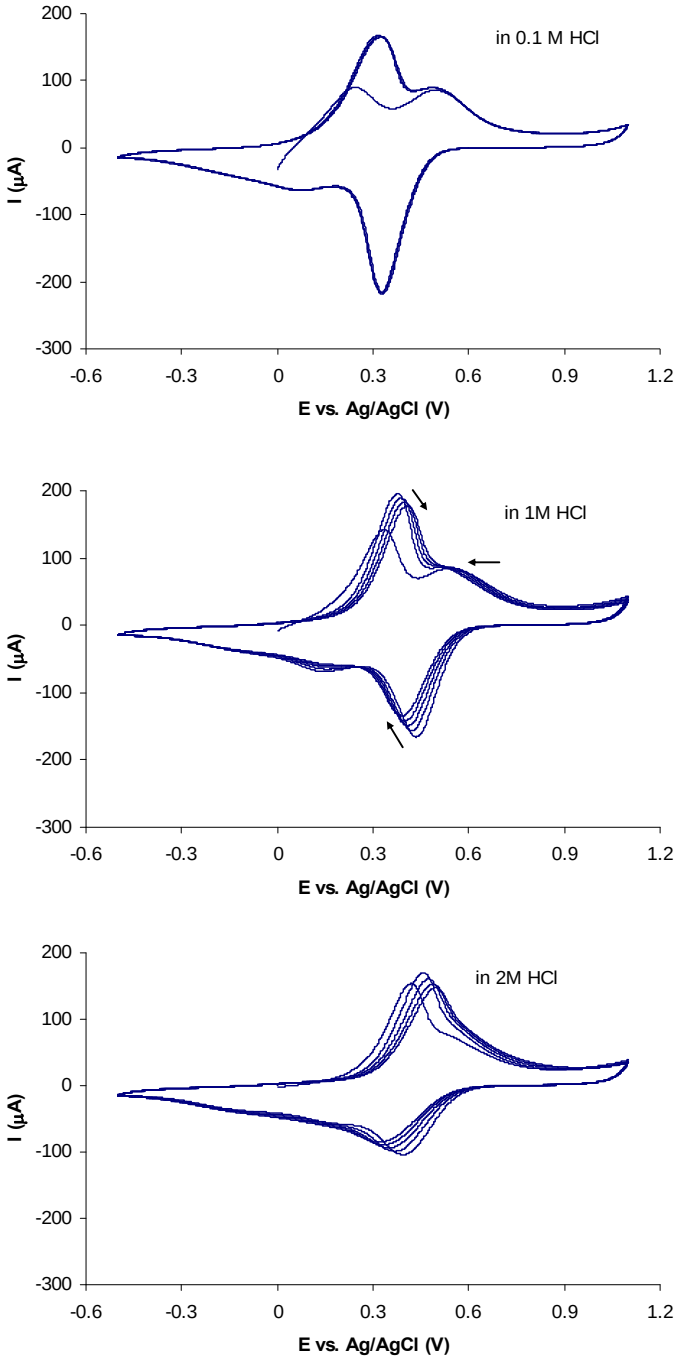

Figure 7.11. Cyclic voltammograms of PAn/PMAS coated glassy carbon electrodes in different concentrations of HCl. Scan rate was 50 mV/sec for 5 cycles. The arrows represent the shift observed in the peak potential and current with successive scans.

7.3.3.5 Electrochemical polymerisation of 0.01 M aniline using 1.0 M HCl as dopant.

Following the successful chemical polymerisation of aniline with PMAS as dopant in slightly acidic media, PAn/PMAS was electrochemically synthesised in 1.0 M HCl in order to investigate the effect of solution pH. The result was compared with the polymerisation of aniline in 1.0 M HCl alone.

7.3.3.5.1 Polymerisation of aniline in 1.0 M HCl

Polymerisation of aniline was initially carried out in the absence of PMAS (Figure 7.12). Increasing the concentration of HCl had no marked effect on the polymer growth compared to using 0.1 HCl and consequently polyaniline could not be deposited.

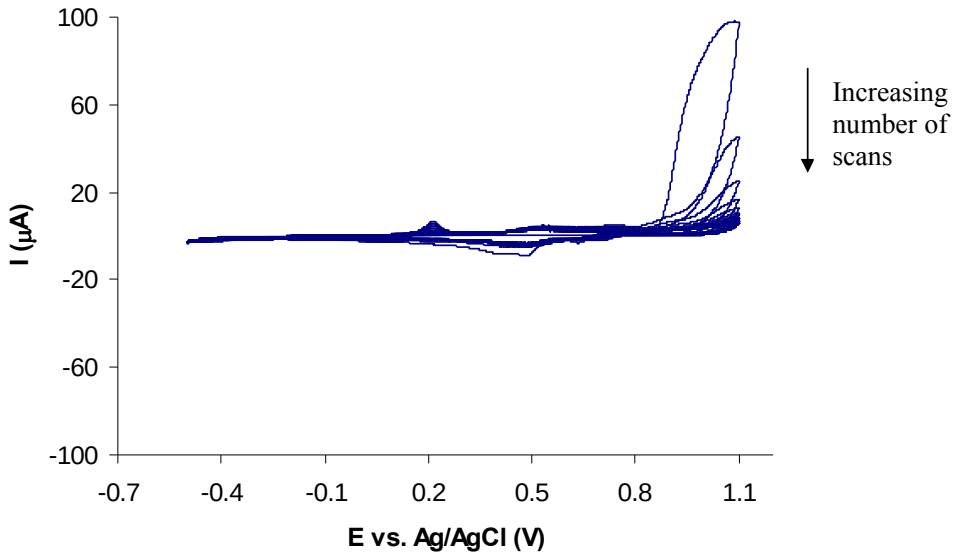

Figure 7.12. Polymerisation of 0.01 M aniline in 1.0 M HCl for 20 cycles, scan rate 25 mV/sec.

7.3.3.5.2 Polymerisation of aniline in 1.0 M HCl after addition of 0.10% PMAS

Polyaniline was then grown from an aqueous solution containing 0.01 M aniline in 1.0 M HCl and 0.10% (w/v) PMAS. Figure 7.13 illustrates how the polymer effectively grows in the presence of PMAS. As seen for polymerisation in 0.10 M HCl, three redox couples (with anodic peaks at 0.27 V, 0.55 V and 0.70 V) were observed, increasing in intensity with successive cycles (with the latter two peaks merging at higher cycle numbers). Once again the dramatic increase in current density (compare to Figure 7.12) clearly demonstrates the deposition of conducting polyaniline with PMAS as dopant.

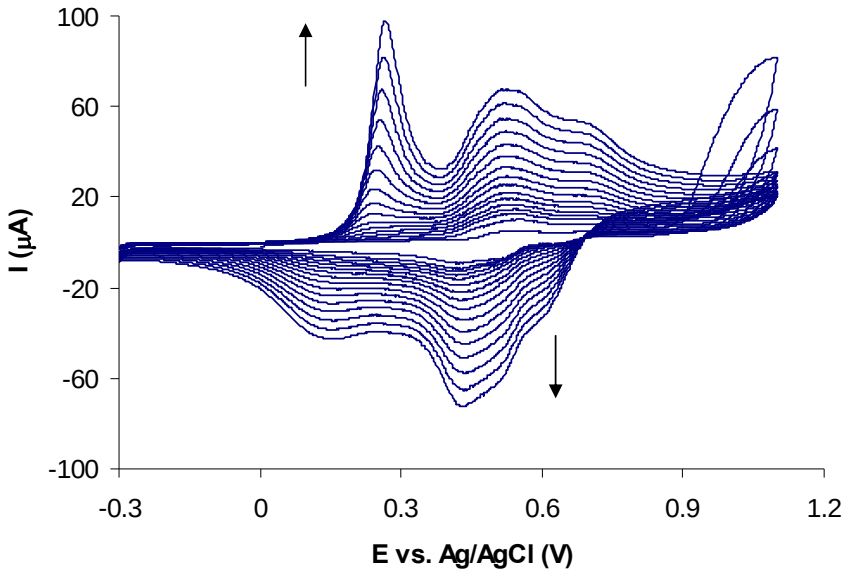

Figure 7.13. Cyclic voltammogram of 0.01 M aniline in 1.0 M HCl after addition of 0.1.0% PMAS (pH ~0) at a glassy carbon electrode. Scan rate was 25 mV/sec for 15 cycles. Arrows indicate growth direction.

For a comparison of the polymerisation of aniline with or without PMAS, the 10^{th} cycle of the potentiodynamic growth of polymer is illustrated in Figure 7.14.

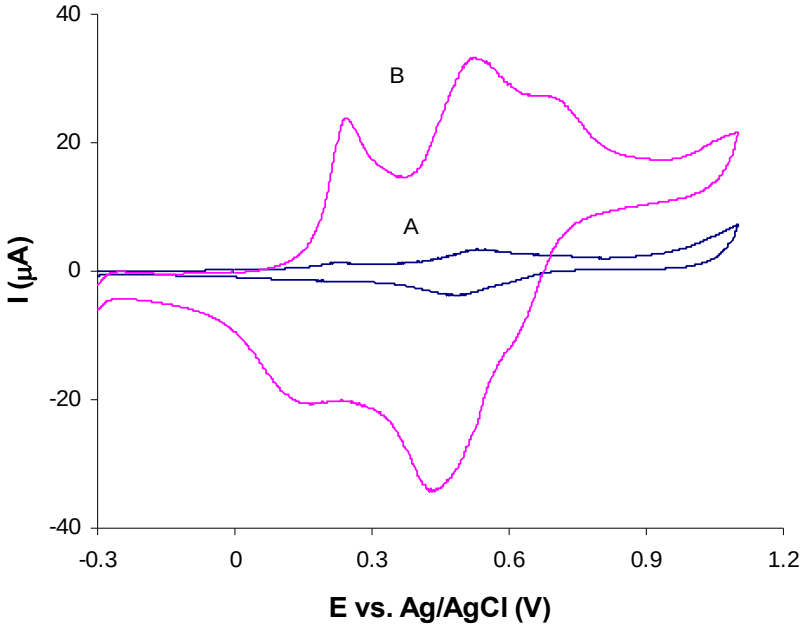

Figure 7.14. Polymerisation of 0.01 M aniline in 1.0 M HCl, (A) before, and (B) after addition of 0.10% (w/v) PMAS. The 10th cycle of each polymerisation is presented for comparison.

Post-growth cyclic voltammograms of the polymer-coated electrode with and without PMAS are also shown in Figure 7.15. The current density observed for PAn/PMAS is 10 fold higher than that for PAn/HCl and has been auto-scaled to allow comparison. The anodic peak at 0.64 V for PAn/HCl has been replaced by the anodic potential at 0.50 V. These observations correspond with the changes in the redox peaks observed during the potentiodynamic polymerisation of aniline in the presence of PMAS. For PAn/HCl the first redox pair (a-a') and the third redox peaks (c-c') correspond to the interconversions between leucoemeraldine/emeraldine and emeraldine/pernigraniline states of polyaniline, respectively. The second peak (b-b') has been reported as arissing from phenazine like defects formed during synthesis using high potential [34] or low monomer concentration [35]. In the case of PAn/PMAS, the first redox pair (A-A') can be attributed to swiching between the leucoemeraldine and emeraldine states of PAn and PMAS. The third redox pair (C-C'), which is apparently shifted to more negative potentials and merged with the second peak, can be attributed to the transformation of

the polyaniline moiety from the emeraldine into the pernigraniline oxidation state. The second redox peak (B-B') can be attributed to the interconversion of emeraldine and pernigraniline states of PMAS, similar to those that have been reported for the PMAS-poly(L-lysine) complex films [36, 37] and the PMAS-PVP complex [38, 39]. Similar redox waves (with oxidation potentials at ca. 0.34 V and 0.65 V) have also been reported for highly sulfonated polyaniline in pH 1 electrolyte [40].

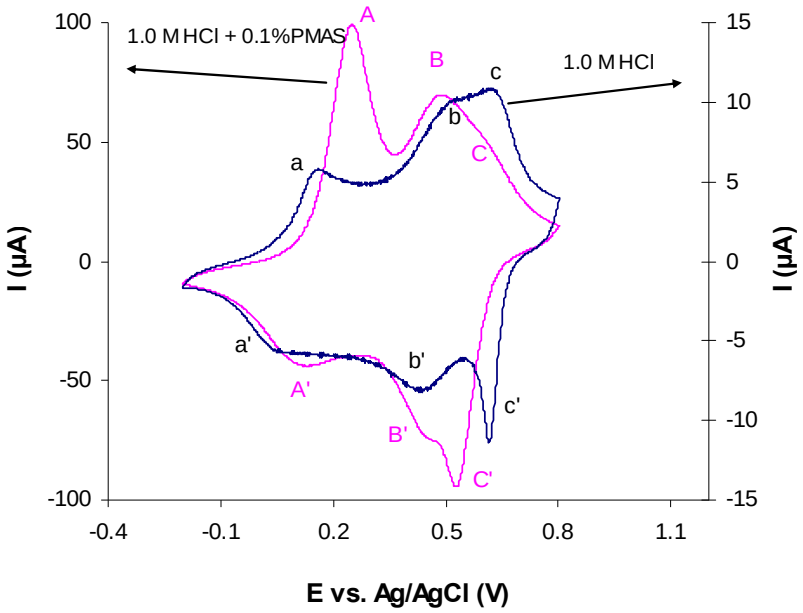

Figure 7.15. Post-growth cyclic voltammograms obtained using PAn/HCl and PAn/PMAS coated glassy carbon electrodes in 0.10 M HCl solution. Scan rate 50 mV/sec

During potentiodynamic growth of PAn/PMAS (Figure 7.7 and Figure 7.13), the third anodic peak shifts to more negative potentials. Similar behviour was also observed in the CV of obtained PAn/PMAS (Figure 7.8 and Figure 7.15). This effect may be due to doping of polyaniline with an aromatic sulfonate dopant (PMAS). Several studies have shown that sulfonation alters the electrochemical behavior of polyaniline and its derivatives. A shift towards negative potentials has also been reported for

electrochemical doping of un-doped polyaniline with polyaniline-sulfonic acid [27]. The more negative second redox pair has also been reported for the self-doped copolymer of aniline and *m*-aminobenzenesulfonic acid (metanilic acid) [41]. Doping of polyaniline by potential cycling in some aromatic sulfonate anions such as naphthalene sulfonic acid has also resulted in shifting of the second oxidation pair toward more negative potential with time [42].

7.3.3.6 Effect of acid concentration on the electrochemical synthesis of PAn/PMAS

PAn/PMAS can be synthesised by electrochemical polymerisation of 0.01 M aniline in the presence of PMAS using either 0.10 M or 1.0 M HCl. The 10^{th} cycle during potentiodynamic polymerisation of aniline in 0.10 M HCl is compared to that in 1.0 M HCl in Figure 7.16. As reported for polyaniline [43-45], the redox peaks were shifted to positive potentials by decreasing the pH of the polymerisation solution from 1.3 to about 0. However, no substantial difference was noted between acid concentrations (0.10 or 1.0 M) in terms of polymer growth (Figure 7.16) and electroactivity of the resultant polymer (Figure 7.8 and Figure 7.15). As seen earlier in Section 7.3.2, in the absence of HCl (pH 2.45), PAn/PMAS is not effectively deposited on the electrode. These results suggest that polymerisation of aniline in the presence of PMAS proceeds in mild acidic media (pH<2), and increasing the acid concentration (above 0.10 M) has no significant influence on the polymer growth and electroactivity of the resultant PAn/PMAS product. In contrast, large differences in polymer properties have been reported for electropolymerisation of aniline in the presence of different acid concentrations (0.20 – 2.0 M $HClO_4$) [36].

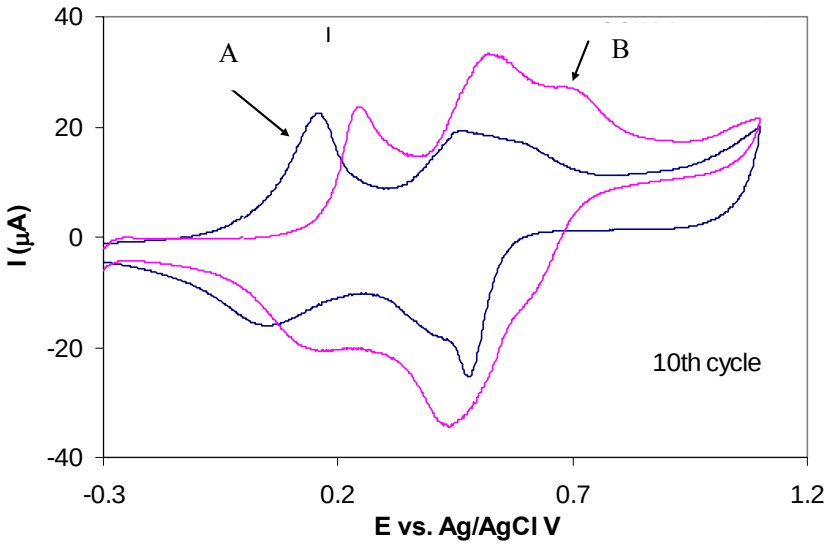

Figure 7.16. Polymerisation of 0.01 M aniline in 0.10% (w/v) PMAS at different acid concentrations, (A) 0.10 HCl, and (B) 1.0 M HCl. The 10th cycle using both 0.10 M and 1.0 M HCl is shown for comparison.

7.3.3.7 Influence of PMAS concentration on electrochemical synthesis of PAn/PMAS

PMAS serves several functions. It functions as a template to electrostatically align the aniline monomers and increase the local concentration of aniline, and as a polyacid to provide the necessary counterions and a local low pH for producing the conducting emeraldine salt form of polyaniline. The other unique feature of PMAS compared to non-conducting polyelectrolytes such as PSS [25] is to facilitate charge transfer, as a conducting template, along the growing polyaniline chains.

Polymerisation was carried out in the presence of 0.20% w/v PMAS. This corresponds to a 2:1 molar ratio of aniline to PMAS dimer unit. Fast polymer growth/deposition was observed upon potential scanning between -0.5 and 1.1 V for 20 cycles (Figure 7.17). A dramatic increase in current was observed when the PMAS concentration was increased from 0.10% to 0.20% w/v (Figure 7.18), indicating faster growth/deposition of PAn/PMAS on the electrode.

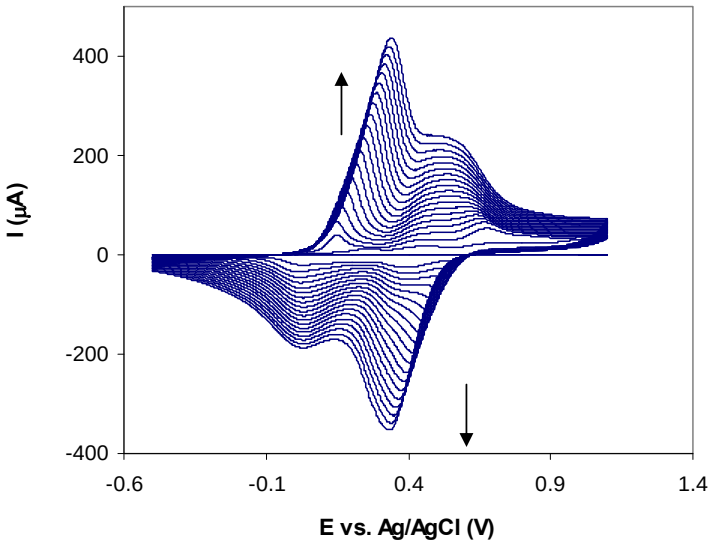

Figure 7.17. Potentiodynamic polymerisation of 0.01 M aniline in 0.10 M HCl at a glassy carbon electrode after addition of 0.20% (w/v) PMAS . Scan rate was 25 mV/sec for 20 cycles. Arrows indicate growth direction.

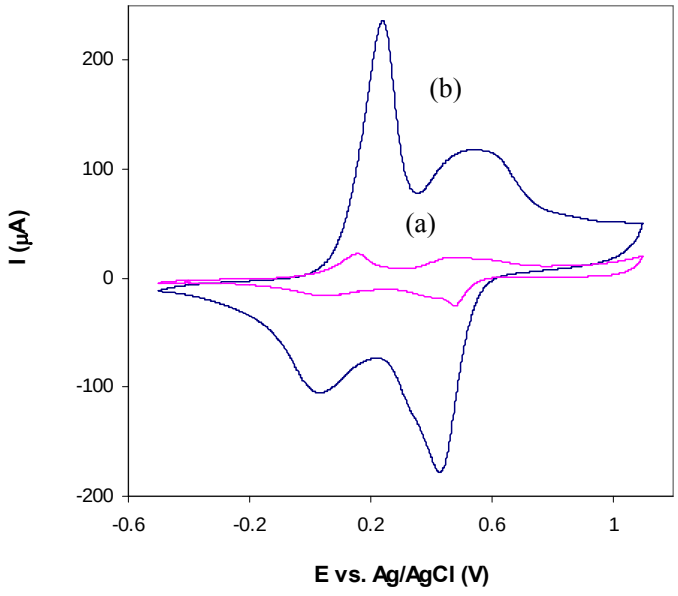

Figure 7.18. Potentiodynamic polymerisation of 0.01 M aniline in 0.10 M HCl using different concentrations of PMAS. The 10th cycle using either (a) 0.10% or (b) 0.20% (w/v) PMAS is shown for comparison.

Cyclic voltammetry of the polymer film deposited on a GC electrode in 0.10 M HCl exhibited two redox couples (a/a', and b/b') (Figure 7.19). The anodic peaks were observed at 0.23 V and 0.47 V, with the corresponding cathodic peaks appearing at 0.11 V and 0.41 V, respectively. The redox couples were similar to those observed for PAn/PMAS obtained using 0.10% (w/v) PMAS (Figure 7.8), indicating the interconversions between leucoemeraldine, emeraldine and pernigraniline states of PAn/PMAS.

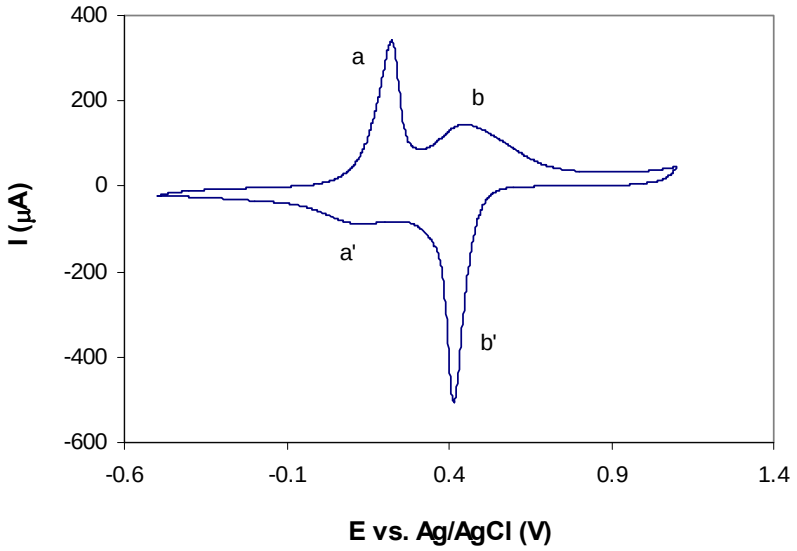

Figure 7.19. Cyclic voltammogram of PAn/PMAS coated glassy carbon electrode in 0.10 M HCl at a scan rate of 50 mV/sec. The polymer was grown from 0.01 M aniline in 0.10 M HCl and 0.20% (w/v) PMAS for 5 cycles.

7.3.4 UV-Vis spectroscopic characterisation of PAn/PMAS film

A typical spectrum of an electrodeposited PAn/HCl film exhibits a broad absorption peak in the 350-450 region attributed to the π-π* transition, a low wavelength polaron band, and a free carrier tail in the near infrared, sometimes with a small shoulder at *ca.* 750 nm attributed to a higher wavelength polaron band. These characteristics are believed to indicate a partially to largely extended coil conformation of polyaniline chains [46-48]. The UV-Vis spectrum of PMAS exhibits a characteristic band at 473 nm

which is assigned as a lower wavelength polaron band and a free carrier tail in the NIR indicative of an extended coil conformation [49].

The UV-Vis spectrum of PAn/PMAS film deposited potentiodynamically on ITO-Pt-coated glass was compared to PAn/HCl (Figure 7.20). The PAn/PMAS film was stable after washing with water in order to remove excess PMAS and unwanted materials on the polymer surface (Figure 7.21). The absorption peak at 473 nm and the free carrier tail at higher wavelengths, demonstrates the incorporation of PMAS as dopant and a fully extended coil conformation for polyanilne induced by PMAS. Similar spectra were obtained for the PAn/PMAS films electrodeposited from either 1.0 M HCl or 0.10 M HCl.

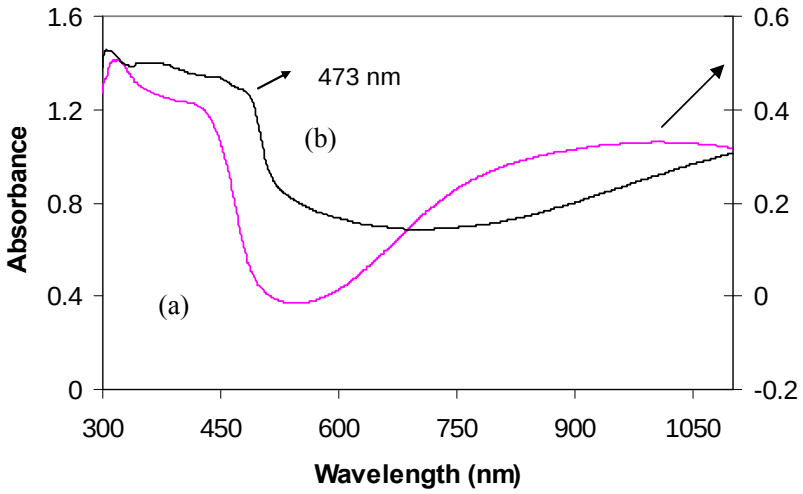

Figure 7.20. UV-vis spectra of (a) PAn/HCl and (b) PAn/PMAS films on platinised ITO-glass substrates. The PAn/PMAS film was obtained by potentiodynamic polymerisation of 0.01 M aniline in 1.0 M HCl and 0.10% (w/v) PMAS between -0.5 V and 1.1 V for 20 cycles at room temperature. The PAn/PMAS film was obtained by potentiodynamic polymerisation of 0.20 M aniline in 1.0 M HCl for 5 cycles.

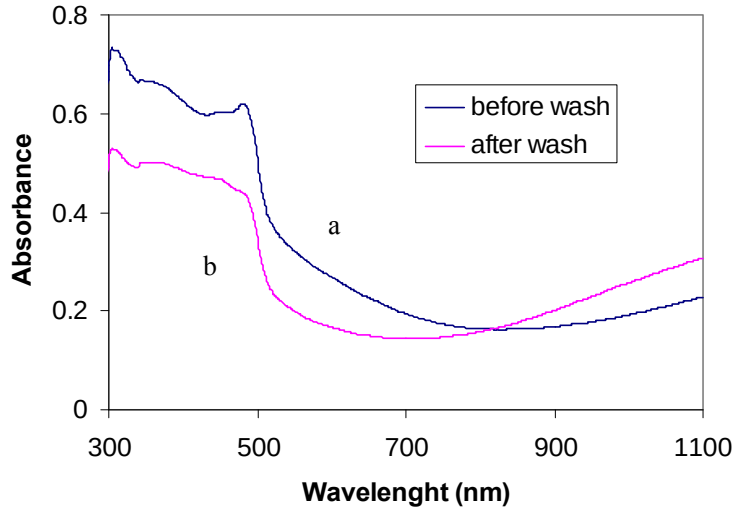

Figure 7.21. UV-vis spectra of PAn/PMAS film (polymerised from 0.01 M aniline, 1.0 M HCl and 0.10% (w/v) PMAS on Pt-ITO glass) (a) before and (b) after washing with water.

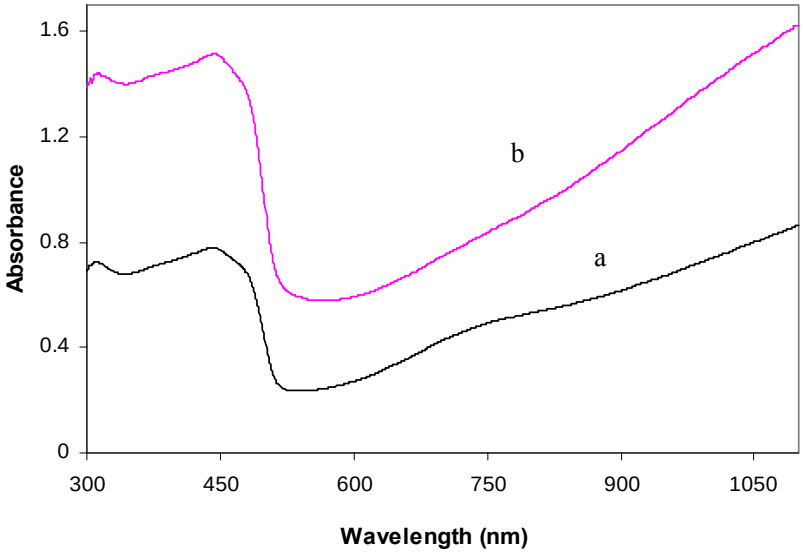

Figure 7.22. UV-vis spectra of PAn/PMAS film deposited onto Pt-ITO glass by potentiodynamic polymerisation of 0.01 M aniline in 1.0 M HCl and 0.20% (w/v) PMAS between -0.5 V and 1.1 V for (a) 10 cycles, and (b) 20 cycles.

When the concentration of PMAS during polymerisation of 0.01 M aniline was increased to 0.20% (w/v), the UV-vis spectrum of the resultant PAn/PMAS material after washing also showed the features discussed above. However, the intensity of the free carrier tail (attributed to a delocalised polaron band) was significantly increased (Figure 7.22). This indicated that PAn/PMAS with a higher doping level and higher conductivity was obtained [48]. It should be noted that a small hump about 750 nm was observed in some cases after washing the polymer film (Figure 7.22a) indicating a partial localised structure and compact coil conformation [48].

The spectral properties of the polyaniline films were further explored in the near infra red (NIR) region (300-2500 nm). The free carrier tail observed for PAn/PMAS in Figure 7.20 is the beginning of a broad absorption band in the NIR region attributed to a delocalised long wavelength polaron band. Comparison of a PMAS film evaporatively cast onto glass with the PAn/PMAS film reveals similar characteristic features induced by PMAS on the polyaniline backbone (Figure 7.23). Compared to PAn/HCl, the high wavelength polaron band is clearly red-shifted for the PMAS and the PAn/PMAS materials.

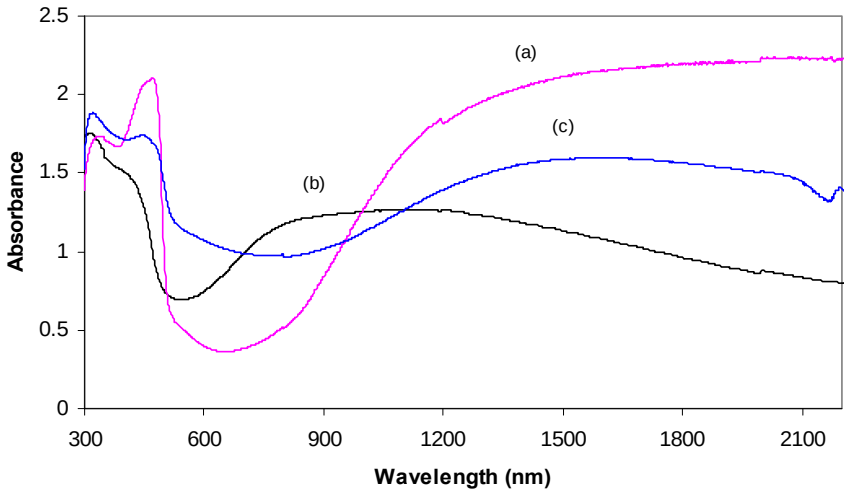

Figure 7.23. UV-vis-NIR spectra of (a) PMAS film evaporatively cast onto glass, (b) PAn/HCl and (c) PAn/PMAS (0.20% w/v) films electrodeposited onto Pt-ITO glass.

7.3.4.1 Acid-base treatment of PAn/PMAS films

In order to further investigate the incorporation of PMAS as dopant for the polyaniline, the PAn/PMAS film was treated with NaOH. In alkaline solutions, polyaniline emeraldine salts undergo de-doping. This causes shifting of the π-π∗ band to ca 320 nm and the characteristic exciton band of the EB form appears at ca 600 nm [12]. In contrast, treating PMAS with aqueous NaOH solution is reported to result in replacement of the initial bands by two bands at 350-390 nm and 750 nm, consistent with a compact coil conformation of PMAS emeraldine salt [49], i.e. a conformational change occurs rather than de-doping of the polymer .

The PAn/PMAS film electrodeposied on ITO-Pt-coated glass was washed slowly with 2 ml aqueous 0.30 M NaOH solution. The colour of the film turned from green to blue and the 0.30 M NaOH wash solution was also blue. The UV-Vis spectrum of the blue wash solution exhibited strong bands at 330 nm and 740 nm, which are characteristic of PMAS emeraldine salt in a compact coil conformation (Figure 7.24). Upon acid treatment of this solution with 3 drops of conc. HCl a yellow-green solution was obtained. The UV-Vis spectrum showed a peak at 473 nm and a free carrier tail in the infrared region which are characteristics of an extended coil conformation of PMAS (Figure 7.24), i.e. a reversible conformational change had occurred. Traces of polyaniline, dissolved through washing the PAn/PMAS film with NaOH solution, can also be observed in spectrum of this blue solution.

The blue film obtained after washing the PAn/PMAS film with aqueous 0.30 M NaOH exhibited a UV-Vis spectrum (Figure 7.25) with two strong bands at *ca*. 340 nm and 610 nm, characteristic of the the π-π∗ and exciton bands, respectively, of emeraldine base, i.e. de-doping of the polyaniline had occurred. When the film was dipped in 2.0 M HCl solution, it turned from blue to green. Its UV-Vis spectrum after drying (Figure 7.25), showed a free carrier tail in the near infrared region and red shifting of the π-π∗ band to 375 nm, consistent with polyaniline in emeraldine salt form.

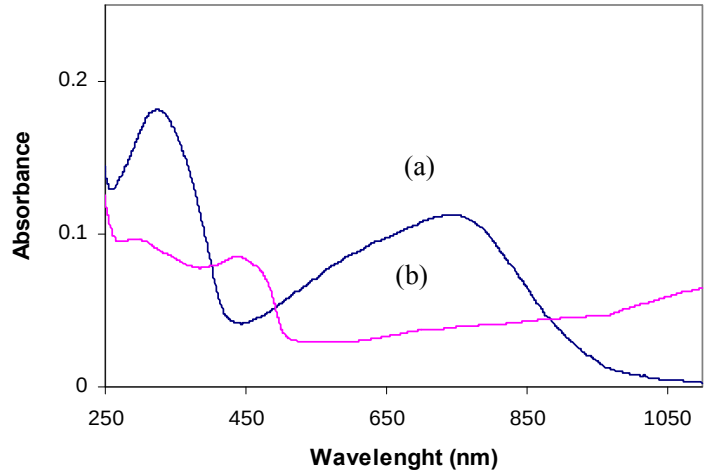

Figure 7.24. UV-vis spectra of (a) solution collected from washing PAn/PMAS film with aqueous NaOH 0.30 M (pH 12) and (b) the same solution after adding HCl (pH 3). The film was polymerised from 0.01 M aniline, 0.10 M HCl and 0.10% (w/v) PMAS.

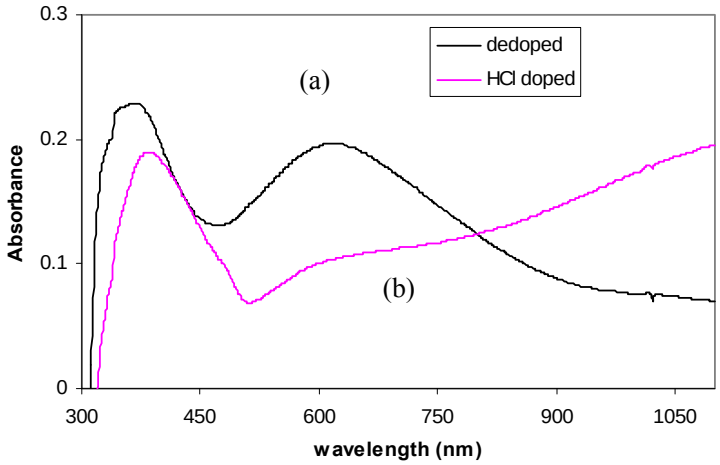

Figure 7.25. UV-vis spectra of PAn/PMAS film (a) after de-doping using aqueous 0.30 M NaOH and then (b) re-doping with 2.0 M HCl.

Therefore, acid base treatment of the PAn/PMAS film strongly supported that polyaniline had been electrochemically synthesised with PMAS as dopant.

7.3.5 Polymerisation of aniline in the presence of LMWt PMAS

Potentiodynamic polymerisation of aniline was carried out in the presence of LMWt PMAS. Using 0.10% (w/v) LMWt in the polymerisation solution (0.01 M aniline and 0.10 M HCl) was not sufficient for the formation of a polymer film on the electrode. However, a polyaniline/LMWt PMAS film was successfully deposited using a higher PMAS dopant concentration of 0.50% (w/v) (Figure 7.26).

The cyclic voltammogram of the polymer deposited on the glassy carbon electrode in 0.10 M HCl was similar to that obtained for the PAn/HMWt PMAS (Figure 7.27), exhibiting two redox pairs (a/a', and b/b') with anodic peaks at 0.28 V and 0.44 V and corresponding cathodic peaks at 0.10 V and 0.37 V. The second oxidation peak is shifted to negative potentials. This behaviour is similar to that observed earlier in this Chapter for the PAn/HMWt PMAS material, presumably caused by doping polyaniline with sulfonate groups as explained in detail in Section 7.3.3.5.2.

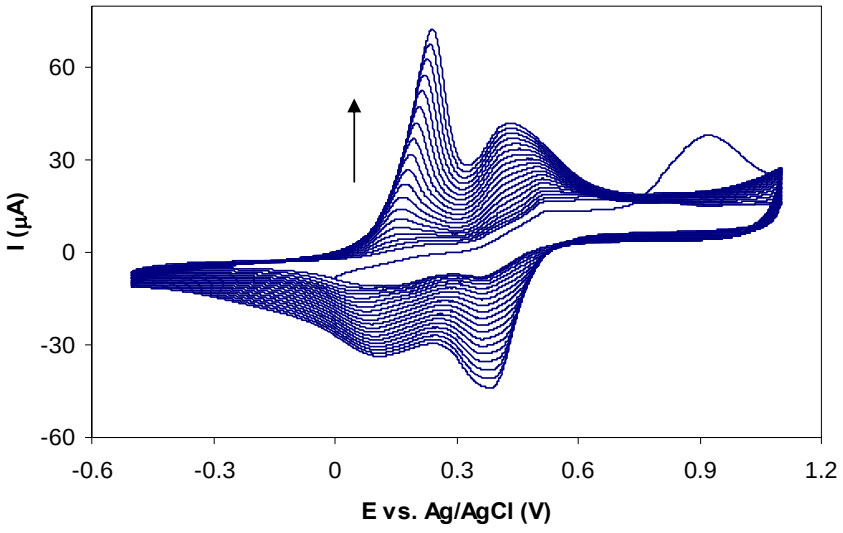

Figure 7.26. Potentiodynamic polymerisation of 0.01 M aniline in 0.10 M HCl in the presence of 0.50% (w/v) LMWt PMAS at a glassy carbon electrode. Scan rate was 25 mV/sec for 20 cycles.

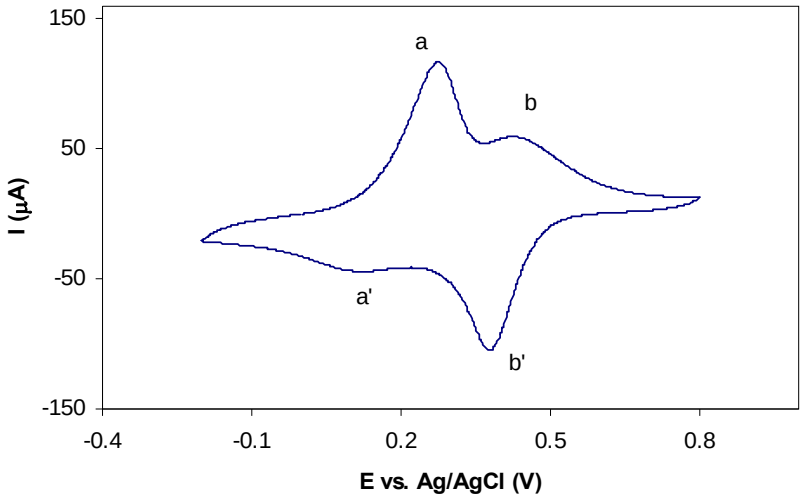

Figure 7.27. Post-growth cyclic voltammogram of PAn/LMWt PMAS coated glassy carbon electrode in 0.10 M HCl solution. Scan rate 50 mV/sec.

The UV-Vis spectrum of the PAn/LMWt PMAS film deposited onto a Pt-ITO glass (Figure 7.28) showed that doped polyaniline in the emeraldine salt state was produced. The broad absorption band at 350-430 nm was attributed to a π-π^* transition and a low wavelength polaron band, while the free carrier tail in the near infrared was assigned to a higher wavelength polaron band, indicating an extended coil conformation for the polyaniline. It should be noted that unlike HMWt PMAS, which has a characteristic band at 473 nm, LMWt PMAS has no absorption in this region and no peak was observed in the area for the PAn/LMWt PMAS material.

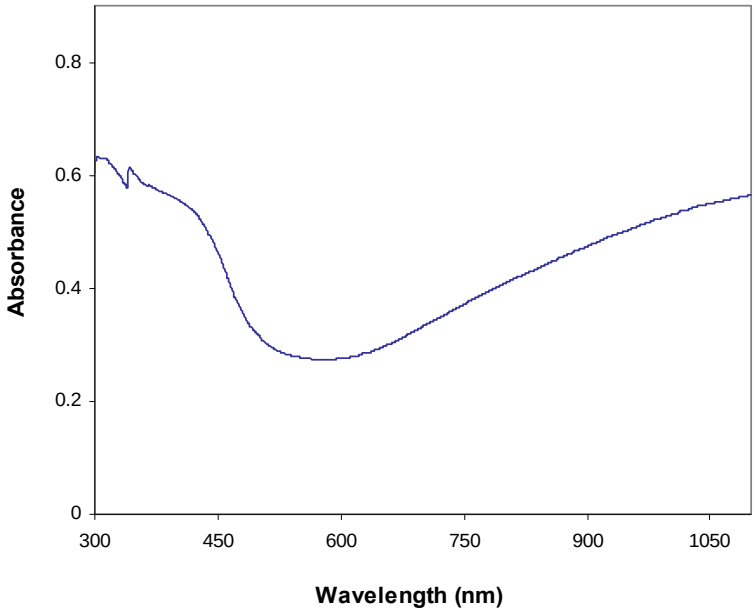

Figure 7.28. UV-vis spectrum of PAN/LMWt PMAS film electrodeposited onto Pt-ITO-glass by potentiodynamic polymerisation of 0.01 M aniline in 0.10 M HCl and 0.50% (w/v) LMWt PMAS.

7.3.6 QCM study of the potentiodynamic polymerisation of aniline in the presence of high and low molecular weight PMAS

Quartz crystal microbalance (QCM) studies were used to further explore the effect of HMWt PMAS and LMWt PMAS on the polymerisation of aniline, and the results were compared to the polymerisation of aniline under identical conditions but in the absence of PMAS. The frequency of the quartz crystal is changed by the deposition of polyaniline onto the QCM gold electrode and this change can be converted to mass changes at the gold electrode. Mass changes in the microgram range can therefore be detected by QCM at an electrode surface during electrochemical reactions .

The mass change with time during the potentiodynamic polymerisation of aniline in acidic media is illustrated in Figure 7.29. No significant deposition and mass change was observed in 0.10 M HCl during 20 cycles. The presence of PMAS (0.10% w/v) in the polymerisation solution resulted in a marked mass change, indicating extensive

polymer deposition on the QCM electrode. The results provide further evidence that polymerisation of aniline is facilitated by PMAS. This enhancement is attributed to strong electrostatic interactions occurring between anilinium ions created in slightly acidic media and the free sulfonate groups along the polymer chain of PMAS. This facilitates chain propagation due to a supramolecular pre-ordering by the PMAS polyelectrolyte template, which also simultaneously acts as the dopant for the electropolymerised material.

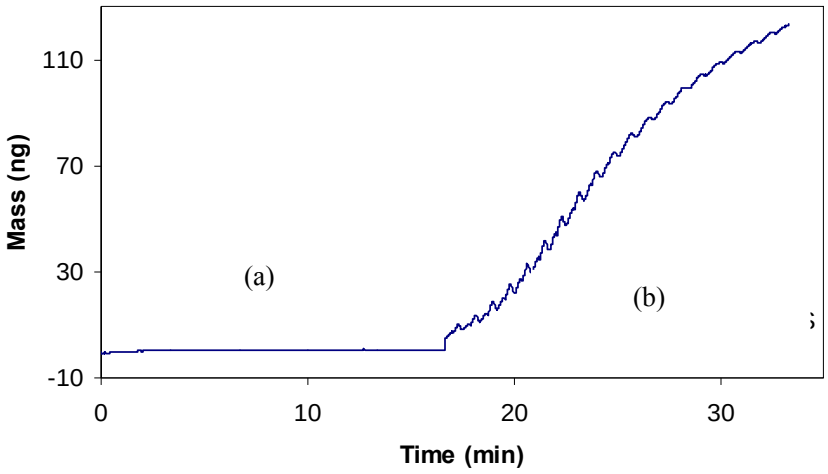

Figure 7.29. Mass changes versus time recorded during the potentiodynamic polymerisation of 0.01 M aniline in 0.10 M HCl (a) in the absence and (b) in the presence of 0.10% (w/v) HMWt PMAS. Polymerisation was performed by cyclic voltammetry between -0.5 and 1.1 V at 25 mV/sec for 20 cycles.

Polymerisation of aniline was also accelerated after addition of LMWt PMAS, however the mass changes were smaller than polymerisation of aniline in the presence of HMWt PMAS (Figure 7.30). The non-conducting nature of LMWt PMAS and the shorter polymer chain (~2 kDa) are presumably responsible for the difference observed. The high conductivity of HMWt PMAS as template and dopant accelerates the deposition of the polymer on the surface of electrode.

According to the QCM results, both HMWt and LMWt PMAS are capable of acting as effective dopants (to different extents) in the polymerisation of aniline producing different polymer materials.

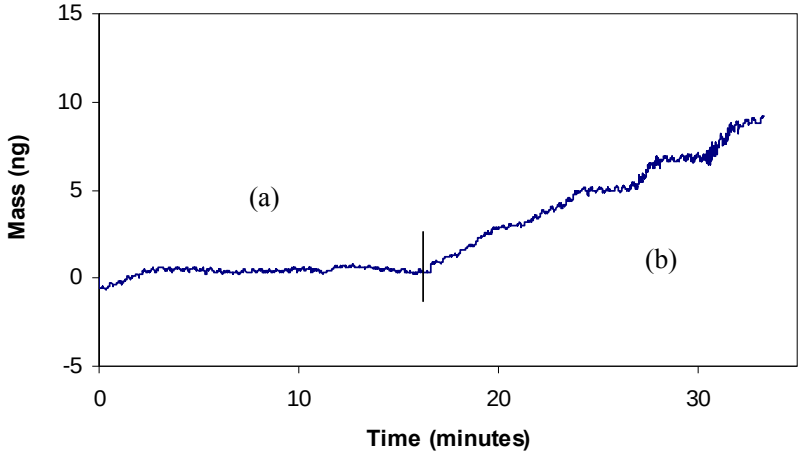

Figure 7.30. Mass changes versus time recorded during the potentiodynamic polymerisation of 0.01 M aniline in 0.10 M HCl (a) before and (b) after addition of 0.10% (w/v) LMWt PMAS. Polymerisation was performed by cyclic voltammetry between -0.5 and 1.1 V at 25 mV/sec for 20 cycles.

7.3.7 Effect of polyelectrolyte on polymerisation of aniline

Poly(styrenesulfonate) has been widely used as a dopant for polymerisation of aniline. However, using in-situ polymerisation of aniline in the presence of a conducting polyelectrolyte has not been reported yet. In the present study polymerisation of aniline in the presence of PMAS as a conducting polyelectrolyte is compared with polymerisation using non-conducting poly(styrenesulfonate) (PSS) as dopant. To make the comparison, the method developed here for polymerisation of PAn/PMAS is applied also for PAn/PSS. The polymerisation can be carried out either by potentiodynamic or potentiostatic methods.

7.3.7.1 Potentiodynamic polymerisation

Polymerisation of 0.01 M aniline in 0.005 M PSS and 0.10 M HCl resulted in deposition of a PAn/PSS film. The polymer was electroactive, showing two redox couples (a/a', and b/b') (Figure 7.31) very similar to those observed for PAn/PMAS (Figure 7.5 or Figure 7.19).

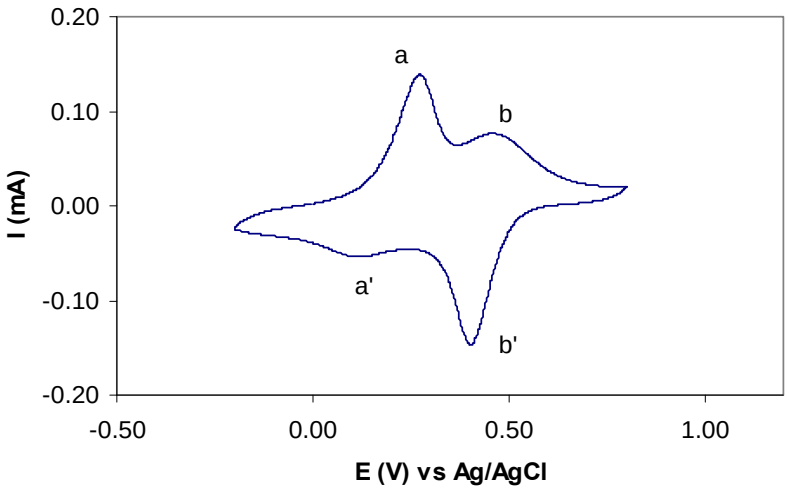

Figure 7.31. Cyclic voltammogram in 0.10 M HCl of a PAn/PSS film deposited onto a GC electrode by potentiodynamic polymerisation of 0.01 M aniline in 0.10 M HCl and 0.005 M PSS (based on dimer unit). Scan rate 50 mV/sec.

The 10^{th} cycle during potentiodynamic polymerisation of aniline using PMAS or PSS is compared in Figure 7.32. The current density during polymerisation was seen to be much higher for PAn/PMAS. The higher current density observed may be attributed to the conductive electroactive nature of PMAS in the Pan/PMAS film, facilitating the polymer growth.

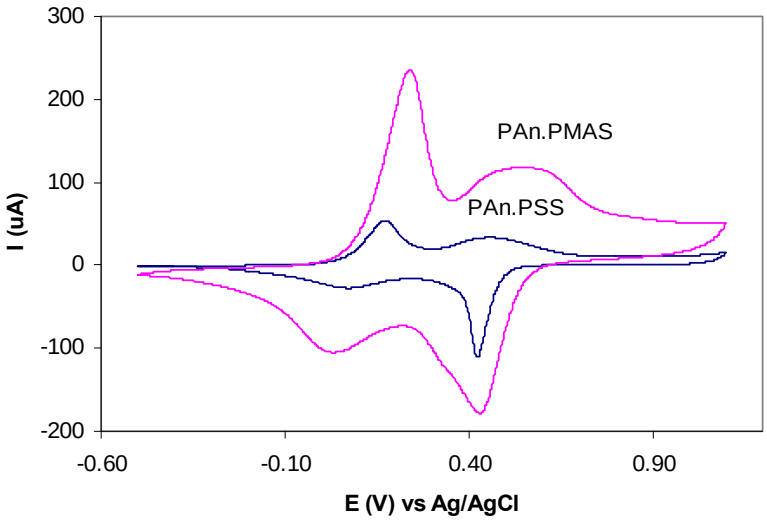

Figure 7.32. Polymerisation of 0.01 M aniline in aqueous 0.10 M HCl containing 0.005 M PSS or PMAS (based on dimer unit) as dopant by cycling the potential between -0.5 and 1.1 V at 25 mV/sec. The 10^{th} cycle is shown in both cases.

7.3.7.2 Polymerisation at constant potential

Polymerisation of aniline in the presence of PMAS using the potentiostatic technique was also successful (Figure 7.33). It was found that the polymer can be formed at potentials as low as 0.5 V. Increasing the applied potential, increased the rate of polymer deposition and polymers with similar electroactivity and spectral properties were obtained.

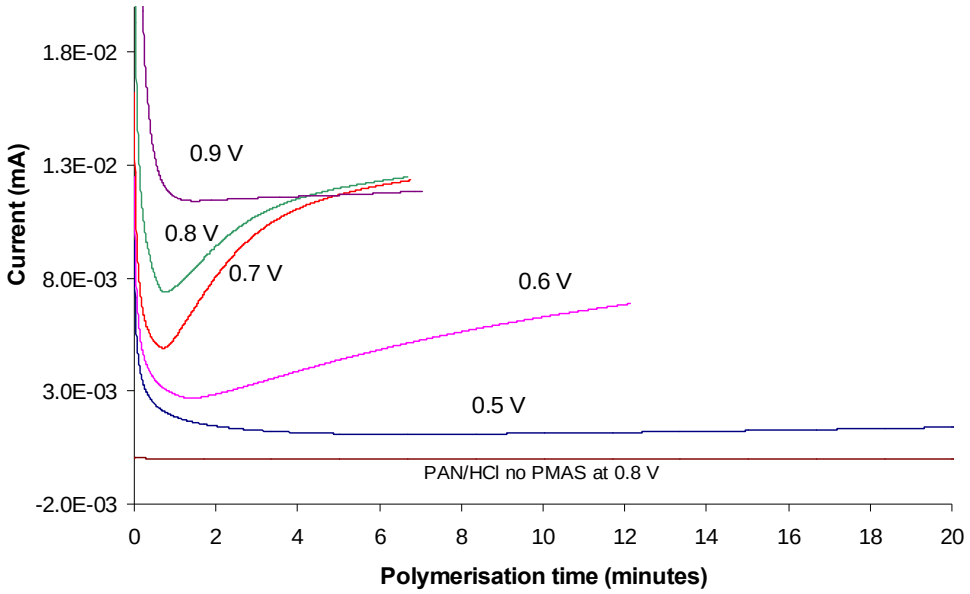

Figure 7.33. Chronoamperometric responses at different potentials during deposition of polyaniline onto a GC electrode (0.07 cm^2) using 70 mC/cm^2 charge passed and applied potential of 0.8 V. The first 20 min of polymerisation only is shown for clarity. Concentrations of aniline, HCl and PMAS were 0.01 M, 0.10 M and 0.20% (w/v), respectively.

Polymerisation of aniline in the presence of PMAS or PSS was then carried out by applying 0.8V and passing 200 mC/cm^2 of charge onto the Pt-ITO glass substrate (Figure 7.34). Chronoamperograms recorded during growth showed a rapid increase of current to 0.32 mA in 2.8 min for PAn/PMAS and a slow increase of the current to 0.27 mA in 12.5 min for PAn/PSS.

These results from potentiodynamic or potentiostatic polymerisation of aniline in the presence of different polyelectrolytes suggest that the rate and efficiency of polymer deposition is enhanced by employing the conductive polyelectrolyte, PMAS. Similar results were previously reported for polymerisation of pyrrole in the presence of PMAS [26].

The unique properties of this electronically conductive PMAS polyelectrolyte is probably responsible for the high current and the low deposition potential of the polymer. By applying a positive potential, the aniline monomer pre-mixed with PMAS is oxidised to form polyaniline incorporating PMAS as dopant. Electron transfer through the polymer deposited on the electrode can be achieved through the both polyaniline network and PMAS as a conducting counterion. By increasing the effective surface area during the deposition of PAn/PMAS, the rate of polymerisation is accelerated. Application of a positive potential above 0.6 V is also sufficient to oxidize PMAS (as an electroactive dopant) [26], creating potential electrocatalytic sites for subsequent polyaniline oxidation. The difference observed in the polymerisation rate of aniline using PMAS and PSS as dopant verifies the role of PMAS as a conductive polyelectrolyte and dopant compared to non-conducting PSS.

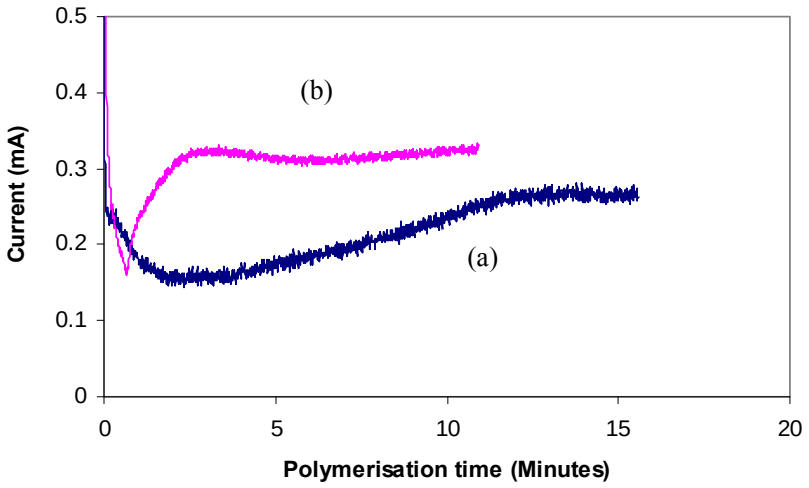

Figure 7.34. Chronoamperograms recorded during deposition of (a) PAn/PSS and (b) PAn/PMAS onto Pt-ITO coated glass using 200 mC/cm^2 charge passed and an applied potential of 0.8 V. Concentrations of aniline, HCl and polyelectrolyte are 0.01 M, 0.10 M and 0.005 M, respectively.

As seen in Figure 7.35, PAn/PMAS electrodeposited potentiostatically exhibits different electronic spectrum from PAn/PSS produced under similar conditions. Sakharov *et al.* [50] reported that a polyaniline-sulfonated polystyrene dispersion produced enzymatically showed the characteristic absorption bands for emeraldine salt of

polyaniline at 340-360 nm (π-π* transition whitin the benzenoid segments), and polaron bands at 400-415 nm and 800 nm. The absorption band at 800 nm was attributed to formation of a compact coil conformation of PAn chains in the polyaniline-sulfonated polystyrene complex. The band at 400-420 nm was sensitive to the doping level [50, 51].

The PAn/PSS film produced here exhibited a typical localised polaron absorption band at 820 nm, indicating a compact coil conformation [52-54] for the polyaniline. In contrast, the PAn/PMAS film showed a broad delocalised polaron band at 1400-1600 nm indicating that the polyaniline adopted an extended coil conformation [49] in the presence of PMAS. Moreover, the PAn/PMAS showed a more intense band at 420 nm, indicating a higher doping level in PAn/PMAS compared to PAn/PSS. This shows that the former provides better conditions for doping polyaniline due perhaps to similarity in structure and the extended coil conformation of PMAS.

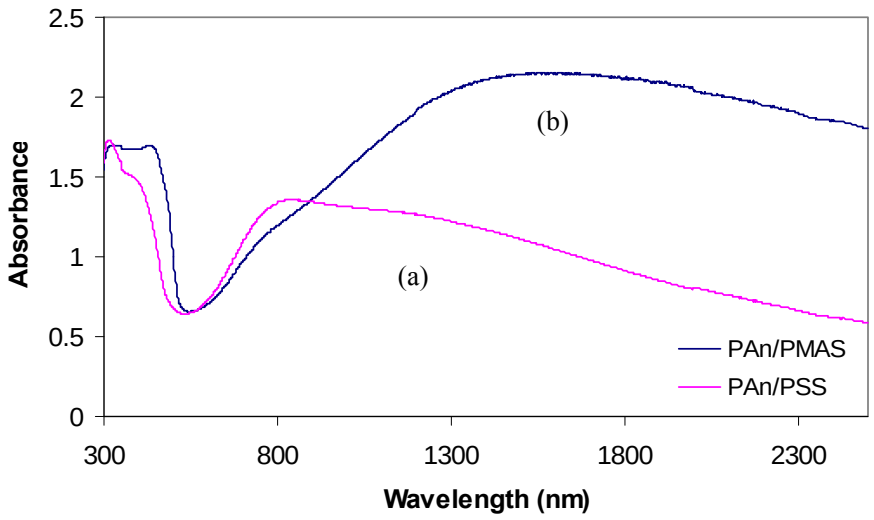

Figure 7.35. UV-vis spectra of (a) PAn/PSS and (b) PAn/PMAS films electropolymerised as stated in Figure 7.34.

7.3.8 Redox properties of electrodeposited PAn/PMAS film

7.3.8.1 Chemical oxidation and reduction

The electrochemically deposited PAn/PMAS film on ITO coated glass was dipped inside a quartz cuvette containing aqueous 0.20 M hydrazine reductant (pH 10.0) or 0.20 M APS oxidant (pH 2.8) and the UV-Vis spectra were recorded with time. The spectrum was also recorded in water for comparison. It should be noted that the colour of the film was stable after immersing in water and no colour change to blue was observed due to de-doping, in contrast to the behaviour reported for PAn films [55].

Treating a PAn/PMAS film with hydrazine resulted in rapid colour and spectral changes. The film turned from yellow-green to pale yellow. The reduced film exhibited a strong band at 336 nm and a sharp band at 405 nm (Figure 7.36). The peak at about 405 nm is attributed to the reduced leucoemeraldine form of PMAS [36], while the strong band at 336 nm is assigned as the leucoemeraldine form of polyaniline [55, 56]. In contrast to the leucoemeraldine form of pure HMWt PMAS (see Chapter 5, Section 5.3.3.1), the 336 nm peak is much more intense than the 405 nm peak. This clearly supports the co-existence of PAn and PMAS in the polymer. The absorbance intensity of the reduced film decreased with time. The UV-Vis spectrum of the hydrazine solution after removing the film exhibited the characteristic features of the reduced PAn/PMAS material, providing evidence that the decrease in the absorbance is caused by partial dissolving of the reduced PAn/PMAS into the solution (Figure 7.36, inset).

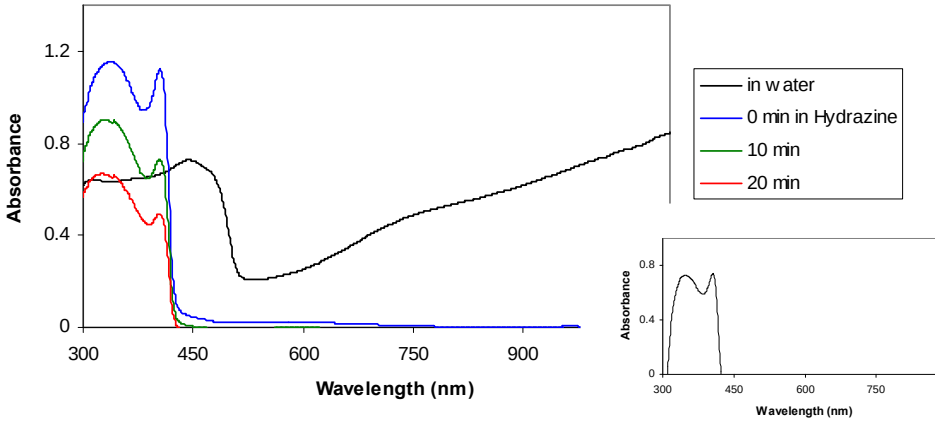

Figure 7.36. Spectral changes for a PAn/PMAS film deposited onto Pt-ITO glass in aqueous 0.20 M hydrazine with time. (Inset, UV-Vis spectrum of the 0.20 M hydrazine solution after removing the film).

When a PAn/PMAS film was dipped into aqueous 0.20 M APS (pH 2.75) the original polaron bands of PAn and PMAS at 440 and 473 nm gradually disappeared and new bands grew at about 310 nm and 600 nm (Figure 7.37). The free carrier tail of PMAS was also replaced with a broad band at *ca.* 990 nm. The appearance of the peaks at about 310 nm and 600 nm is consistent with formation of the pernigraniline base form of polyaniline [57] and PMAS [36]. The broad band above 900 nm has been reported for oxidised polyaniline films [22, 56-58], however no absorption band has been observed for PMAS in this region [36, 59]. The spectral changes in APS solution suggest that the pernigraniline base form of the PAn/PMAS material was produced. Three isosbestic points were observed at 330, 510 and 660 nm for the spectra recorded during the first 16 min of reaction, indicating a clean conversion to the oxidised form of the polymer.

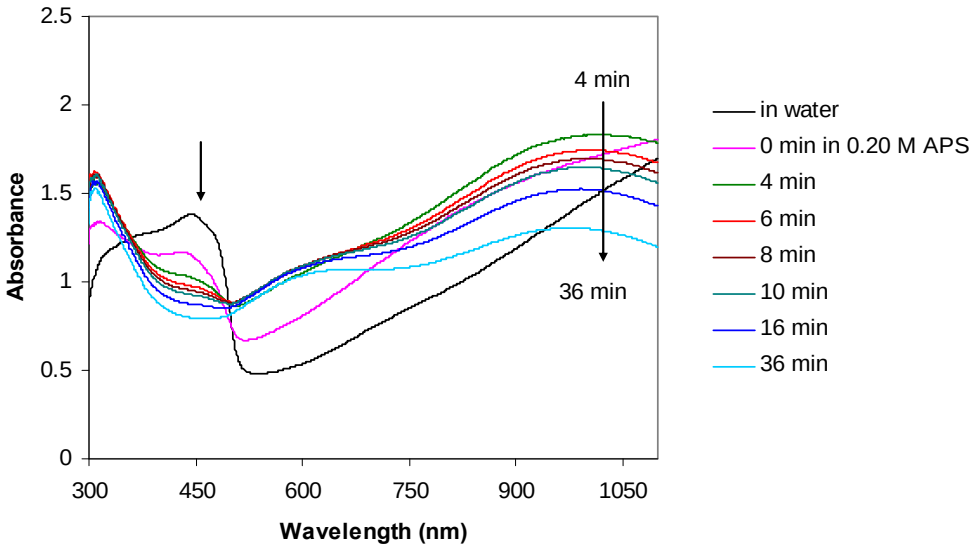

Figure 7.37. Spectral changes for a PAn/PMAS film in aqueous 0.20 M APS with time.

7.3.8.2 Spectroelectrochemistry of PAn/PMAS film

One of the attractive properties of conducting polymers is the reversible changes in their visible absorption spectra through electrochemical redox processes. For polyaniline the colour change ranges from pale yellow to green and dark blue when it is switched from the leuco to the emeraldine to the pernigraniline oxidation states. The electrochromic properties of polyaniline is varied to some extent by introduction of various substituents or by combining different electrochromic polymers as composites [60]. It has been reported that the incorporation of the polyelectrolyte PSS into PANI resulted in advantageous parameters for electrochromic applications [22, 23]. PMAS is a polyelectrolyte with electrical and electrochemical properties. The spectroelectrochemistry of a PMAS-poly(L-lysine) complex has been studied by Pornputtkul *et al.* revealing the spectral switching of PMAS with changes in potential [36]. The influence of PMAS as a conducting electroactive dopant for some conducting polymer systems such as polypyrrole and polythiophene has also recently been studied by Shanon Little in our laboratories [61]. Here the spectroelectrochemistry of the novel PAn/PMAS is investigated.

UV-vis spectral changes for a PAn/PMAS film electrodeposited onto Pt-ITO glass were recorded simultaneously during cyclic voltammetry between -0.2 and 1.0 V in 0.10 M HCl electrolyte (Figure 7.38 a). A 3-D plot showing the spectral changes of the PAn/PMAS film with time during three CV cycles is shown in Figure 7.38 b. Marked changes in the absorption spectrum were observed when the potential was changed between -0.2 and 1.0 V. For instance, the intensity of the free carrier tail at 800 nm was on its lowest level at negative potentials and reached a maximum at positive potentials.

The recorded spectra at time intervals could be transformed to spectra at specific potentials by considering the rate of the linear potential scan (Figure 7.38 c). The overall changes in the absorbance with potential were plotted at some specific wavelengths (Figure 7.38 d). Increasing the potential from -0.2 V to 1.0 V resulted in the development of the free carrier tail and a decrease in the 390 nm band, which is characteristic of the reduced form of PMAS as seen earlier in Figure 7.36. The polaron bands of PAn and PMAS at 440 and 473 nm gradually decreased in intensity at potentials above 0.0 V. An isosbestic point at 503 nm was observed, indicating a clean conversion between the oxidation states of PAn/PMAS with changes in potential. The characteristic polaron bands (440nm and 473 nm) showed maximum and a minimum absorbance at 0.0 V and 1.0 V, respectively. The UV-Vis spectrum at negative potential is, however, different from the expected spectrum for the reduced leucoemeraldine form of the PAn/PMAS with a sharp peak at about 400 nm and the absence of polaron bands.

The potential scanning mode has the advantage of providing a qualitative overview of the electrochromic switching properties as the potential is dynamically cycled. A drawback for this technique is that, in some instances, complete reduction or oxidation of the material being investigated may not occur within the timeframe of the measurement. The degree of switching will therefore be directly linked to the amount of material at the electrode surface, which may impede complete switching from one oxidation state to the next. As a consequence, a spectral lag may arise between the applied potential and the final redox state of the polymer coating.

(a)

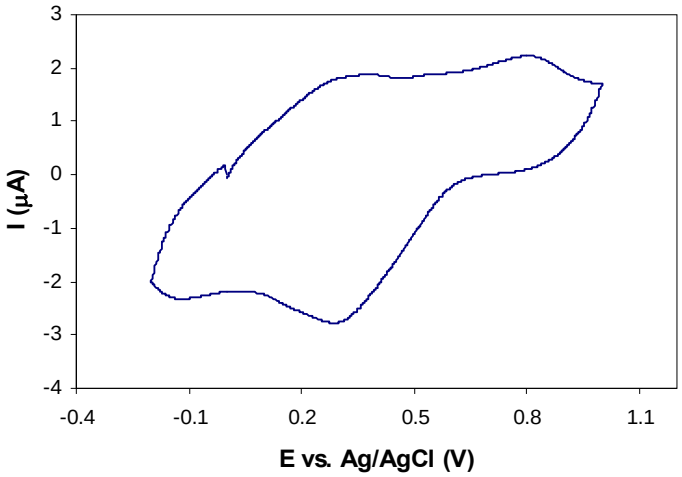

(b)

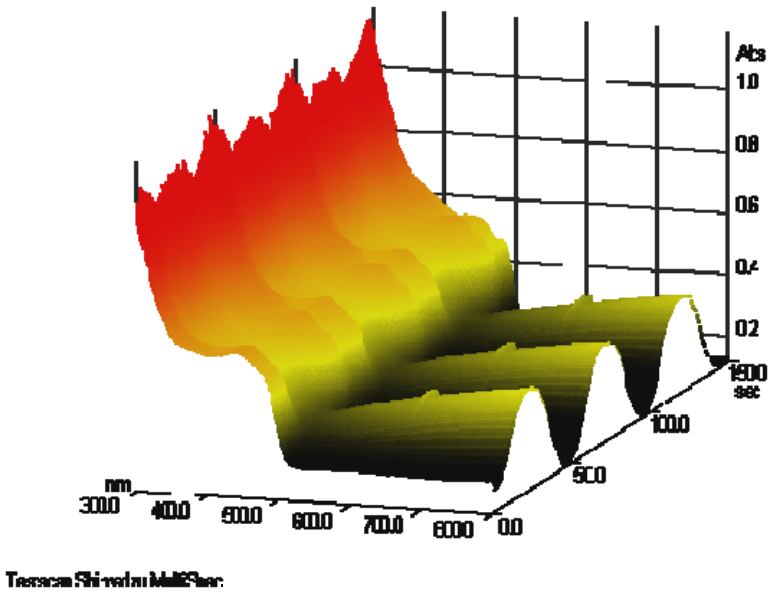

Figure 7.38. Spectroelectrochemistry of PAn/PMAS film deposited onto Pt-ITO glass: (a) CV in 0.10 M HCl, scan rate 50 mV/sec, (b) 3-D plot showing spectral changes with time (continued on the next page).

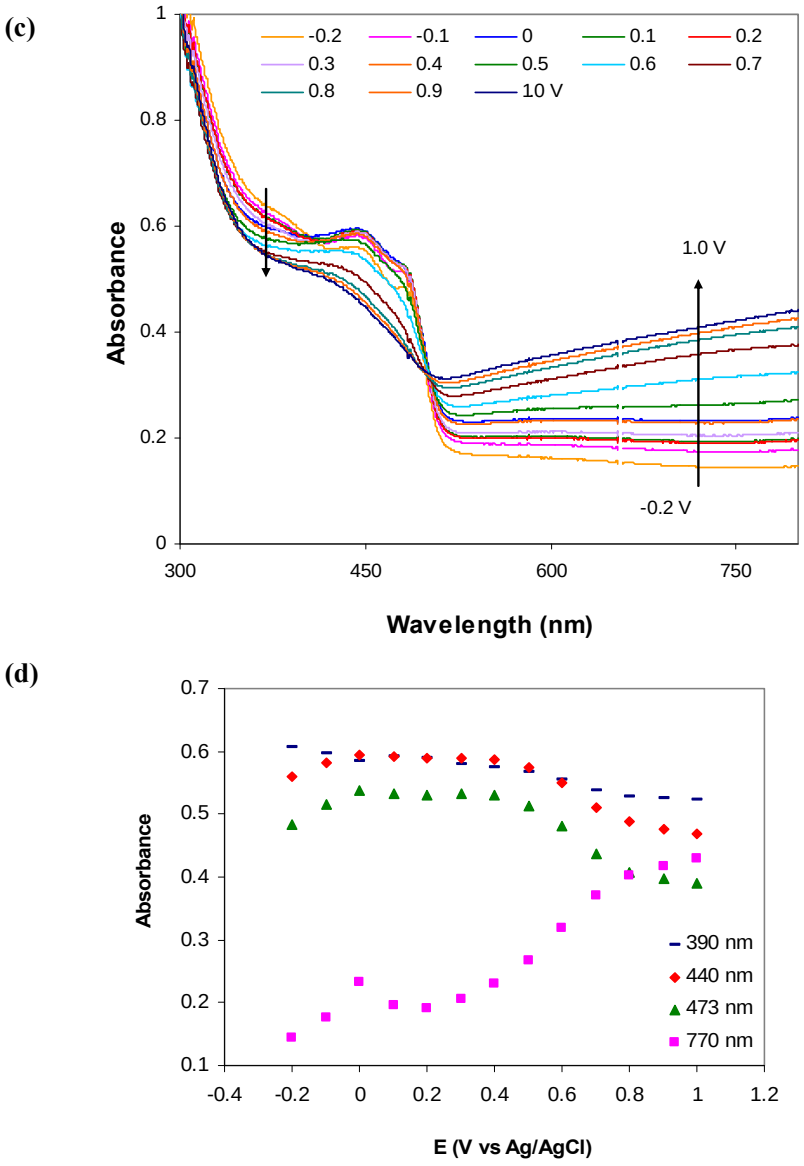

Figure 7.38. Spectroelectrochemistry of PAn/PMAS film deposited onto Pt-ITO glass: (c) spectral changes with potential by converting the time intervals to applied potential in the range -0.2 V to 1.0 V, and (d) changes in absorbance with potential at 390, 440, 473 and 770 nm {from (c)}.

In order to obtain more precise spectral changes with variation in potential, the spectroelectrochemistry of a PAn/PMAS film over the entire potential range was investigated under equilibrium conditions. In this case, the film was equilibrated for 1 min at each potential before recording the spectrum.

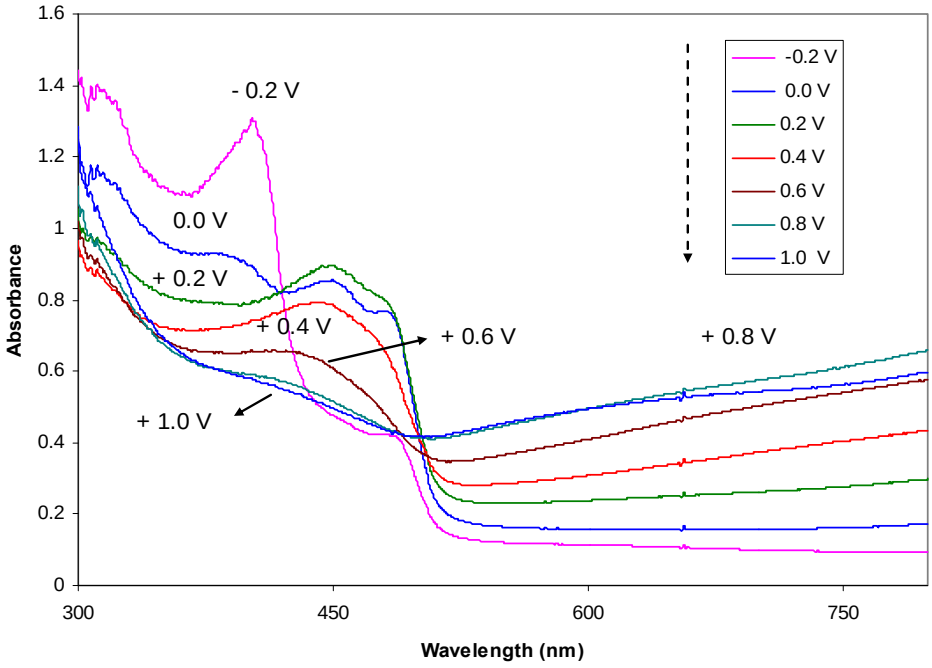

Figure 7.39. Spectral changes of a PAn/PMAS film in aqueous 0.10 M HCl with applied potential from -0.2 V to 1 V. The film was equilibrated at each potential for 1 min.

When the potential was held initially at -0.2 V, the PAn/PMAS was reduced to the leucomeraldine base form as evidenced by the spectral changes in Figure 7.39. The initial characteristic polaron bands at about 430-480 nm and the free carrier tail at 800 nm decreased significantly in intensity, while new peaks at 310 nm and 400 nm appeared. The latter two peaks are attributed to the PAn and PMAS reduced forms, respectively. By increasing the potential, the PAn/PMAS was gradually oxidised. The UV-Vis spectra of PAn/PMAS in the potential range 0.2-0.4 V showed the characteristic bands of the emeraldine salt form of PAn/PMAS, with the polaron

absorption bands at 440 and 473 nm and an absorbance tail above 700 nm. At potentials above 0.6 V, the polymer was oxidised further to the pernigraniline form and the polaron bands at 440 and 473 nm disappeared. At 1.0 V the observed spectrum was that of the fully oxidised pernigrnaline form of polyaniline.

These UV-Vis spectral changes were reversed when the potential was subsequently stepped down from 1.0 V to -0.2 V (Figure 7.40). When a negative potential of -0.4 V was applied, the characteristic polaron bands at 430-480 nm peak completely disappeared, consistent with the fully reduced leucoemeraldine base of PAn/PMAS being produced.

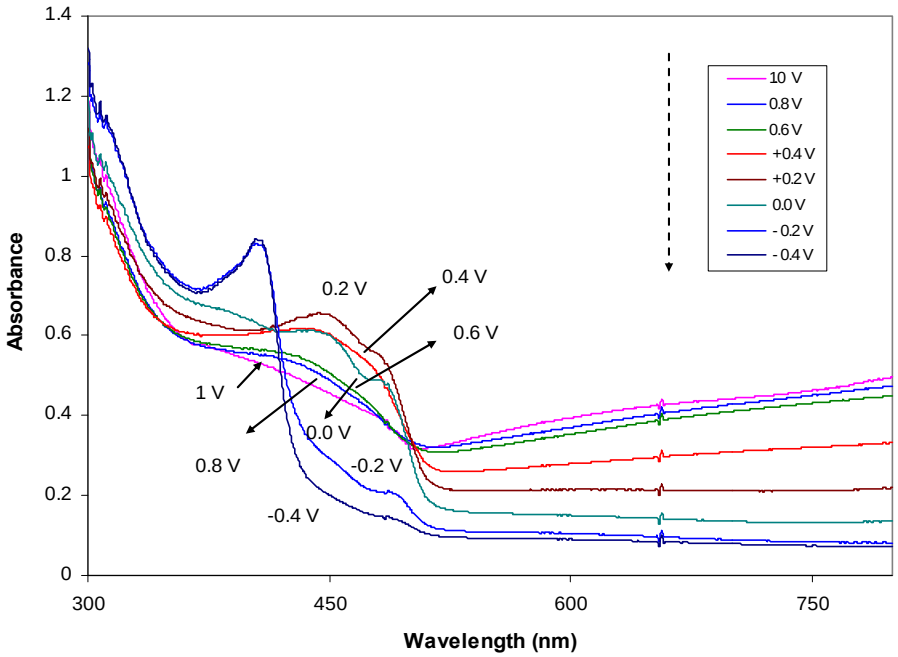

Figure 7.40. Spectral changes for a PAn/PMAS film in aqueous 0.10 M HCl with applied potential (reversed) from 1V to -0.4V. The film was equilibrated at each potential for 1 min before recording each spectrum.

Electrochromic properties of PAn/PMAS film

As seen in Figure 7.39, good absorbance changes were observed in the visible region of the spectrum (380-770 nm) for the PAn/PMAS film. A colour change from light yellow (at -0.2 V) to dark blue (at 1.0 V) was evident. At some selected wavelengths showing the most marked absorbance changes, the optical contrast were calculated. Electrochromic contrast (Δ%T) is defined as the percent change in transmittance at the wavelength where the electrochromic material has the highest optical difference [61]. The %T of the PAn/PMAS material was obtained considering the relationship between the absorbance (A) and the transmittance (T), which is given by A = 2 - log (%T).

As seen in Table 7.1, PAn/PMAS shows a high electrochromic contrast of 57% at 770 nm with a potential required of 1.0 V. This contrast is significantly higher than those reported for polyaniline [13, 62, 63]. An electrochromic contrast of 25% at 625 nm has been reported recently for polyamine deposited on a transparent carbon nanotube electrode [63]. Very recently, an electrochromic study of PMAS doped polypyrrole by Little [61] in our laboratories has shown that the incorporation of conducting electroactive PMAS improved the electrocromic contrast of PPy/PMAS by 31% over that of PPy/ClO_4. The electrochromic contrast of PPy/PMAS is 46% at 770 nm, with a potential required of 1.1 V.

Table 7.1. Table showing the transmittance contrast (Δ %T) achieved by a PAn/PMAS film at selected wavelengths, as well as the potential required to initiate the spectral change (from Figure 7.39).

Wavelength (nm)	Potential required (V)	Δ%T
450	0.8	20.2
480	0.4	20.4
770	1.0	57.0

The results indicate that conducting polymers doped with electroactive and electrically conducting PMAS are fascinating candidates for making spectroelectrochemical devices. The spectroelectrochemical features of PMAS improve the optical contrast, while the conducting behaviour of PMAS enhances the voltage distribution over the electrode

surface and consequently enhance the switching characteristics of the electrochromic device.

7.3.9 Echem-ESR of PAn/PMAS

Polyaniline containing the polyelectrolyte dopant PSS has been reported to exhibit an ESR signal with a g value and linewidth similar to simple PAn/HA emeraldine salts [50, 64]. In-situ electrochemical ESR studies of polyaniline have shown that the ESR properties of polyaniline change with potential and oxidation state of the polymer [65-68]. In most conducting polymers, the charged species on the chains are polarons or bipolarons. During the initial doping of polymer, polarons are dominant. Increasing the concentration of polarons results in recombination of polarons into bipolarons, which are energitically more favored than two polarons. Spinless conductivity in conducting polymers refers to transport by bipolarons as the dominant charged species. In-situ ESR-CV-conductivity studies of polyaniline have shown that in the potential range between two oxidation states, the conductivity is high but the ESR intensity is almost zero [65, 67, 69]. Simultaneous electrochemical-ESR is a powerful technique to study the models of charge transport in conducting polymers.

To explore the ESR properties of PAn/PMAS and the influence of oxidation state, electrochemical dependent ESR spectroscopy was studied and a comparison made to the PAn/PSS system.

Simultaneous electrochemical-ESR measurements were carried out during linear potential scan on a PAn/PMAS film deposited on a Pt wire in an Echem-ESR cell containing aqueous 0.10 M HCl electrolyte. The potential was cycled between -0.3 and 1 V at 5 mV/sec and the ESR spectra continuously recorded with a scan sweep time of 5.24 sec. The time could be converted to potential considering the rate of potential scan.

The second CV cycles are shown for PAn/PMAS and PAn/PSS in Figure 7.41, revealing two redox pairs in each case as described earlier in this Chapter. The current density observed for PAn/PMAS is notably higher than for PAn/PSS. This presumably is attributed to the electroactivity and low resistivity of the PMAS polyelectrolyte dopant.

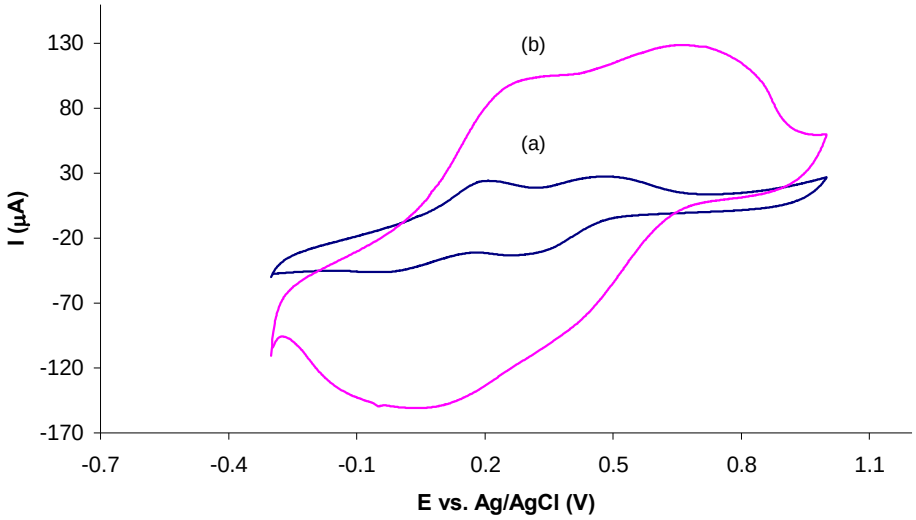

Figure 7.41. CV of (a) PAn/PSS and (b) PAn/PMAS potentiodynamically deposited on Pt wire in an Echem-ESR flat quartz cell containing aqueous 0.10 M HCl. Scan rate 5 mV/sec.

Figure 7.42 shows the changes in ESR response as a function of potential during CV. At -0.3 V initial potential, the PAn/PMAS film exhibited a weak ESR signal. However, no signal was observed for PAn/PSS at this potential. The ESR signal was developed by increasing the potential and reached a maximum at about 0.2 V. The ESR intensity then gradually decreased to about zero by further increase in potential to 1.0 V. In the reversed cathodic sweep, no ESR signal was observed in the range 1.0 to 0.4 V, and at more negative potentials the ESR signal was developed again with a maximum at about 0.0 V. The results obtained here are similar to those previously reported for polyaniline films [65, 67, 69, 70], which show a maximum at the first oxidation peak and another weaker peak or shoulder at the second oxidation peak correlating with the CV of polyaniline. However, no ESR signal was observed here for PAn/PMAS at potentials above 0.5 V.

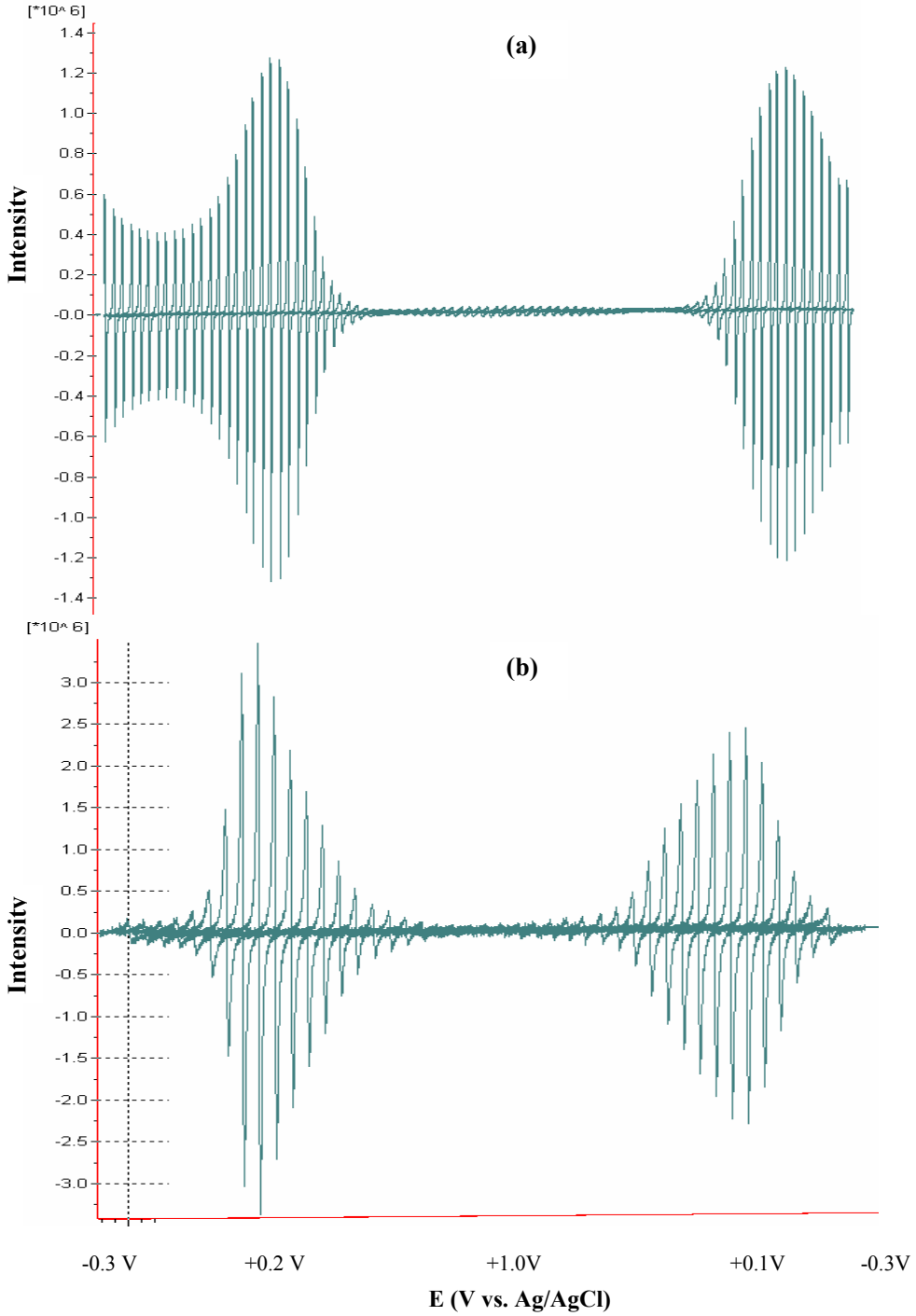

Figure 7.42. ESR response (intensity at 3480.72 G) following potential scan (second cycle) of (a) PAn/PMAS and (b) PAn/PSS electodeposited on Pt-wire in aqueous 0.10 M HCl.

In order to obtain a precise picture of the potential dependences of the ESR signal, Echem-ESR measurements were then carried out under steady state conditions. The polarisation time needed for the film to be held at was determined by recording sequential ESR spectra for the film when the potential applied was held at -0.3 V for 3 min. As seen in Figure 7.43. The ESR intensity declined from an initial value to about zero in 3 min. This time was then applied for study the Echem-ESR under equilibrium conditions over the potential range studied. The polymer was held at every potential for 3 min and the ESR spectrum recorded at the end of this period with a sweep time of 5.24 sec.

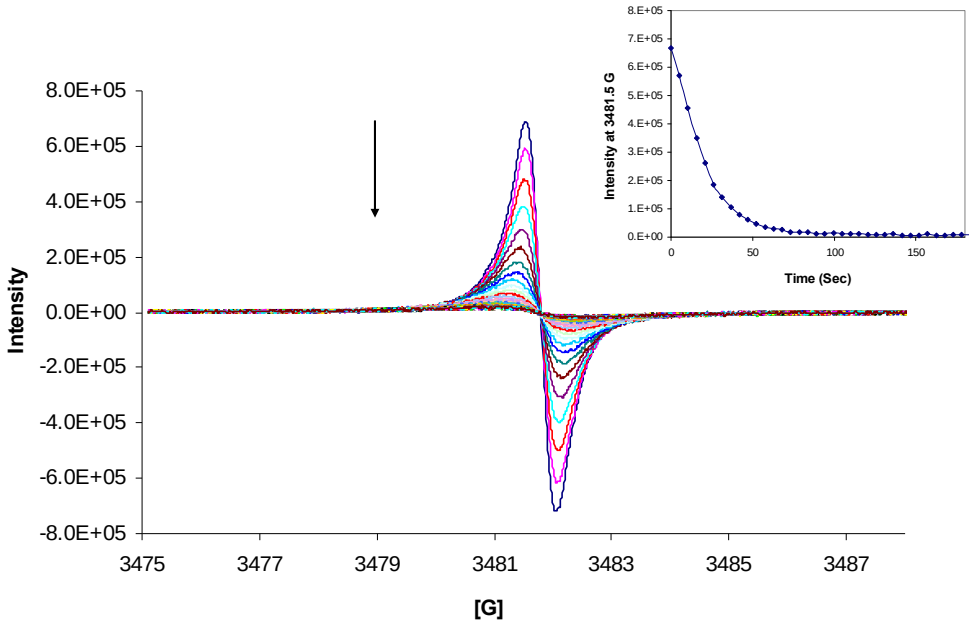

Figure 7.43. ESR spectra recorded for PAn/PMAS over 3 min at an applied potential of -0.3 V. Inset shows the intensity changes of the ESR signal at 3481.5 G with time.

Figure 7.44 shows the ESR spectra of PAn/PMAS and PAn/PSS films deposited onto Pt wire as a function of potential. The potential was stepped up from -0.3 V to 0.8 V and then stepped back to -0.3 V. The spin concentration was obtained from double integration of the ESR intensity [71], and then plotted against applied potential (Figure 7.45).

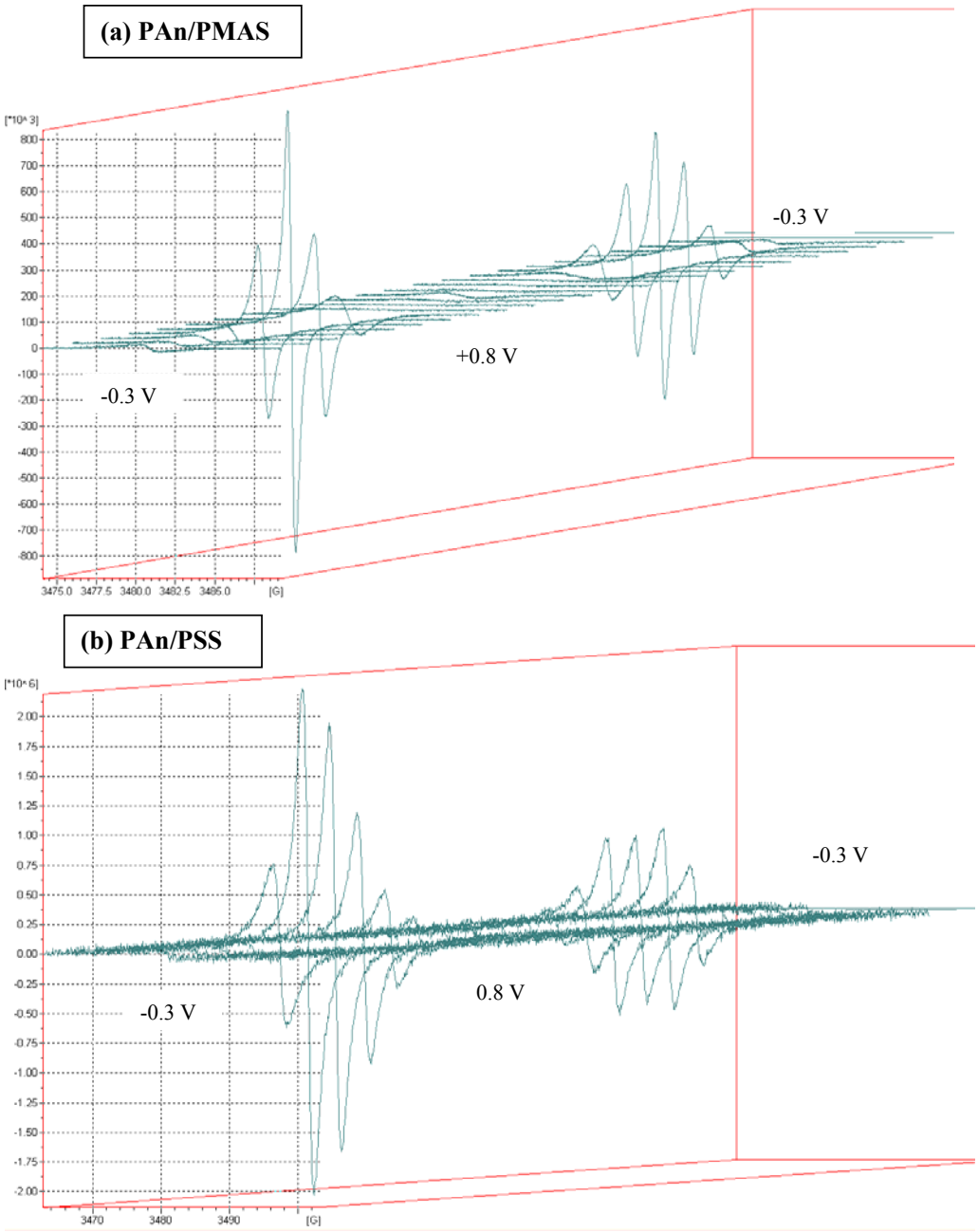

Figure 7.44. ESR spectral changes of (a) PAn/PMAS and (b) PAn/PSS electrodeposited onto Pt wires in aqueous 0.10 M HCl using applied potential from -0.3V to 0.8 V, and upon reversing the potentials. The film was equilibrated at each potential for 3 min.

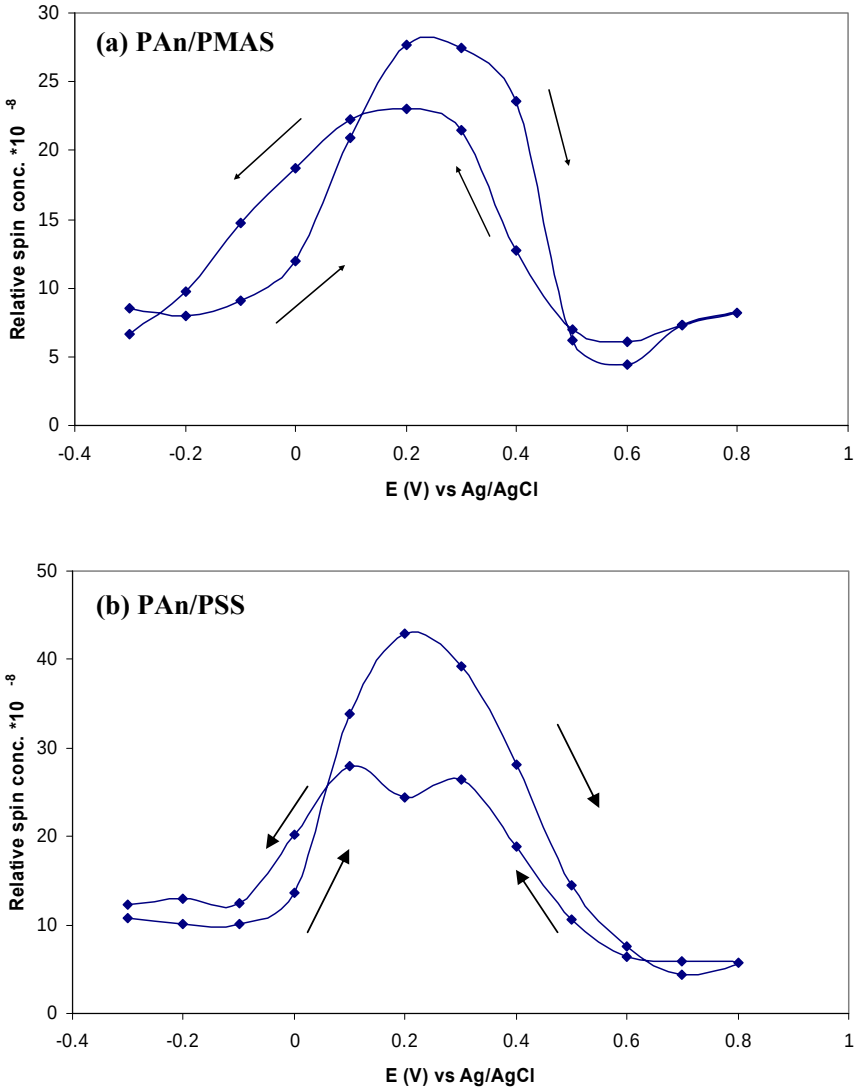

Figure 7.45. Relative spin concentration obtained under steady state conditions (from Figure 7.44) plotted against the pulsed to potential (-0.3 to 0.8V, and reversed), for (a) PAn/PMAS and (b) PAn/PSS.

When the potential was held at -0.3 V, the polyaniline film was reduced to the leucoemeraldine form and the ESR signal became very small. The polymer was then gradually oxidised by increasing the potential, causing an increase in ESR signal. A sharp increase with a maximum at 0.2 V was then observed indicating an increase in polaron concentration. In the potential region 0.2 to 0.5 V, the ESR intensity decayed

from the maximum to about zero. Polyaniline in this range is in the conducting emeraldine salt form. Simultaneous ESR-CV-conductivity studies of polyaniline by other researchers has shown that in this region polyaniline has the minimum resistance [65-67]. Decreasing ESR intensity in this region may be attributed to bipolaron formation and spinless conductivity. Mu *et al.* [72] reported that a transfer of polarons in polyaniline to bipolarons occurs from 0.26 to 0.95 V. A slight increase in spin concentration was observed at 0.7 to 0.8 V especially for PAn/PMAS. The small increase observed in this range may be caused by oxidation of aniline trapped inside the polyelectrolyte template during electrochemical polymerisation [72].

When the potential was subsequently stepped down, the spin concentration gradually increased reaching a maximum at about 0.1 to 0.2 V with the intensities slightly lower than in the anodic direction. This indicates that bipolarons in polyaniline are converted to polarons. The results suggest that the electrochemical dependence of the electron spin resonance properties of both the PAn/PMAS and PAn/PSS are reversible in the potential range studied. A background spin was observed which can be attributed to the polarons formed during polymerisation not being reduced completely due to electrically isolated regions in the more resistive state [67], or alternatively attributed to an equilibrium being established between polarons and bipolarons [72].

A comparison was made of the ESR properties of PAn with non-conducting PSS and conducting PMAS polyelectrolyte dopants at the potential with the highest observed ESR signal (0.2V). Both PAn/PMAS and PAn/PSS showed symmetric lines with a g value of 2.0033 close to that of the free electron implying the same type of radical. However, the linewidths were found to be markedly different, being 0.52 G and 1.71 G for PAn/PMAS and PAn/PSS, respectively. A similar linewidth of 1.626 G has been reported for PAn/PSS [73]. The lower linewidth observed for PAn/PMAS implies a higher degree of spin delocalisation and protonation using the conducting polyelectrolyte PMAS as dopant.

-Investigation into the source of spin observed for PAn/PMAS at negative potential

In the Echem-ESR studies of the PAn/PMAS films, some spin was observed in aqueous 0.10 M HCl at negative potentials. However, no significant ESR signal was observed for the PAn/PSS in this region (

Figure **7.42**). Since no ESR signal is expected for polyaniline at negative potentials (< -0.1 V) [65], the spin observed may originate from hydrogen radicals produced from reduction of H^+ present in the 0.10 M HCl electrolyte. The residual polarons formed during potential cycling used for polymerisations could also be a source of the spin in this region [67].

To further investigate the origin of this spin, the electroactivity of PAn/PMAS and PAn/PSS electrodeposited on the glassy carbon electrodes were studied in aqueous 1.0 M H_2SO_4 electrolyte and compared with that of a bare glassy carbon electrode (Figure 7.46). The reduction of H^+ to ½ H_2 was initiated at -0.45 V for the bare GC electrode. For the PAn/PMAS modified electrode, hydrogen generation was observed at -0.5 V, which is close to the potential (-0.45V) observed with the bare GC electrode and much less than that (-0.8V) of the PAn/PSS modified electrode. The reduction of hydrogen ions was initiated at less negative potentials at PAn/PMAS (-0.5 V) than at PAn/PSS (-0.8 V). The production of hydrogen radicals as a result of reduction of hydronium ions in the presence of PMAS can be a source for the spin observed at reduced potential with the PAn/PMAS film. PMAS is a conducting polymer and it has been shown in the previous Chapter that the incorporation of PMAS as dopant in polyaniline results in a better conductivity compared to the use of non-conducting polyelectrolytes such as PSS. This higher conductivity, together with the facile transferring of the hydrogen ions onto the electrode, could be the cause of the observed spin at reduced potentials. The results also showed that PMAS had similar catalytic influence on hydrogen generation when compared to the bare glassy carbon electrode.

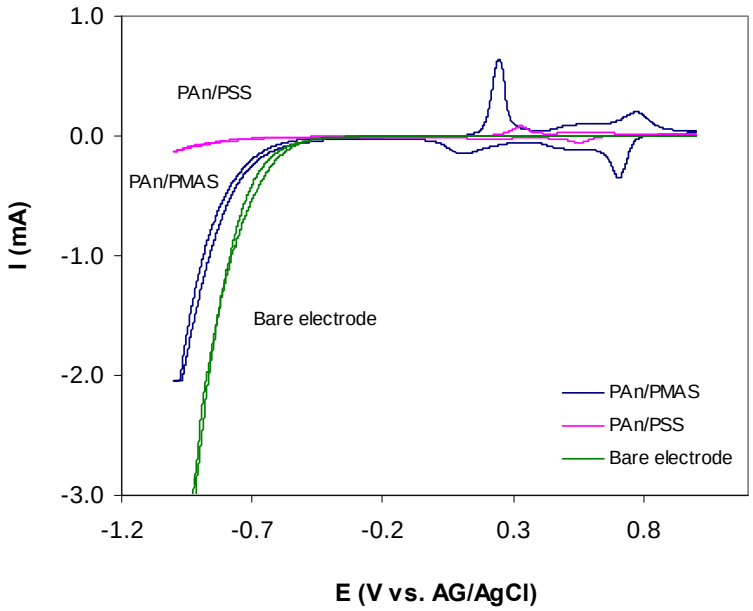

Figure 7.46. Cyclic voltammograms for catalytic hydrogen generation at different electrodes; (a) PAn/PMAS modified GC, (b) PAn/PSS modified GC, and (c) bare GC electrode in aqueous 1.0 M H_2SO_4. Scan rate 50 mV s^{-1}.

7.3.10 Elemental analysis of PAn/PMAS

Elemental analysis was carried out to determine the ratio of PMAS to PAn based on the C, N, S and Cl contents (Table 7.2).

Table 7.2. Elemental analysis of PAn/PMAS potentiodynamically polymerised from an aqueous solution of 0.01 M aniline in 0.10 M HCl and 0.2% w/v PMAS.

Specifications	%	Mole %	N/S ratio	C/S ratio	Cl/S ratio	PMAS/PAn ratio
C	**35.7**	**2.97**				
H	**3.59**		**2.29**	**15.02**	**0.1**	**0.88**
N	**6.34**	**0.45**				
S	**6.34**	**0.198**				
Cl	**0.8**	**0.022**				

The amount of PMAS in the PAn/PMAS material was calculated from the S that is the only source of sulfur in the electrochemical synthesis of PAn/PMAS. The PMAS:PAn ratio in the PAn/PMAS material was calculated from the N/S ratio, as stated in Chapter 6, Section 6.3.3.4. It was found to be 0.88, i.e. close to a 1:1 ratio. This PMAS:PAn ratio is much higher than the PMAS:PPy ratio reported for polypyrrole/PMAS by Zhao *et al.* [26].

The Cl/S ratio was 0.1, indicating only small amounts of chloride anionic dopant in the PAn/PMAS. This indicated that free sulfonate groups of PMAS are the predominant dopant in electropolymerisation of aniline in the presence of PMAS. This result is similar to that found for the chemical polymerisation of aniline in the presence of PMAS in Chapter 6.

7.3.11 Morphology of electrodeposited PAn/PMAS film

The SEM image of a thin PAn/PMAS film on Pt-ITO glass showed a smooth surface with a porous structure in some parts (Figure 7.47a). Further growth of the polymer resulted in filling the pores (not shown). However, a cross section image of the film showed a dense structure as shown in Figure 7.47b.

a **b**

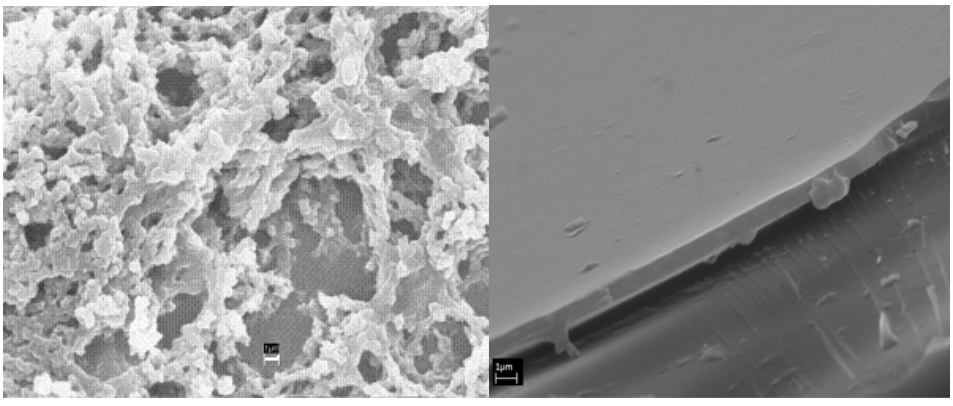

Figure 7.47. SEM image of thin film of PAn/PMAS deposited electrochemically onto Pt-ITO glass from an aqueous solution of 0.01 M aniline, 0.2% PMAS and 0.10 M HCl by cycling the potential between -0.5 V and 1.1 V for 10 cycles at 25 mV/s: (a) surface image, (b) cross section image. The scale bar is 1 micron in both cases.

7.3.12 Contact angle measurements

To investigate the hydrophilic properties of the PAn/PMAS, the contact angle of a water droplet on the polymer surface was measured. A 2 μL water droplet was placed on the polyaniline surface electrodeposited using different dopants of chloride, poly(styrenesulfonic acid) (PSS), and PMAS (Figure 7.48). The highest and the lowest contact angles were obtained for PAn/HCl and PAn/PSS, respectively. The contact angle was found to be 22º for PAn/PMAS independent of the method of deposition (Table 7.3). These results indicate that the hydrophilic properties of the polymer surface are manifestly affected by the dopant. Hydrophilicity of PAn/PMAS is higher than PAn/HCl (62.1º) but less than PAn/PSS (7º).

Table 7.3. Contact angles for polyanilines obtained by chemical and electrochemical polymerisation of aniline using different dopants. (a) refers to potentiodynamic polymerisation, and (b) to polymerisation at constant potential.

Polyaniline samples	Contact angle (º)
PAn/HCl [a]	62 ± 4
PAn/PMAS [a]	22 ± 2
PAn/PSS [a]	7 ± 1
PAn/PMAS [b]	22 ± 2
PAn/PSS [b]	7 ± 1

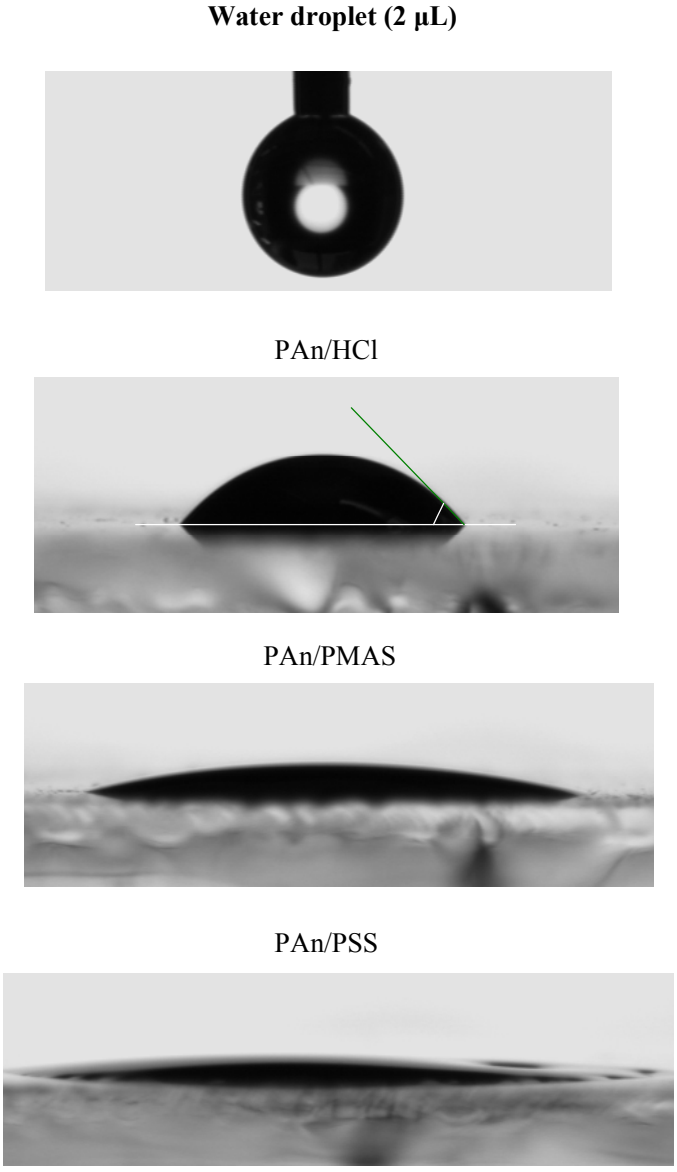

Figure 7.48. Contact angles for polyaniline emeraldine salt films electrodeposited potentiodynamically using different dopants. 2 µL water was lowered onto the polymer surface and the advanced contact angle measured.

7.4 Conclusions

PAn/PMAS can be successfully synthesised using either potentiodynamic or potentiostatic polymerisation of aniline in the presence of PMAS. PMAS as a conducting electroactine polyelectrolyte effectively dopes polyaniline and electrocatalytically facilitates the polymerisation of aniline at lower monomer concentration and applied potential. This will assist the subsequent incorporation of biomolecules where the moderate voltage is required. QCM studies during the polymerisation of 0.01 M aniline in the presence of HMWt and LMWt PMAS confirm the deposition of polyaniline with PMAS dopant.

The UV-vis spectra of the PAn/PMAS film and and after its alkaline treatment confirm that PAn and PMAS co-exist in the polymer. The polaron bands of PAn and PMAS and the intense absorbance in the infrared region show that PAn/PMAS is in the emeraldine salt form with an extended coil conformation for its polymer chains.

The CV of PAn/PMAS in aqueous 0.10 M HCl confirms electrochemical swiching between leucoemeraldine, emeraldine and pernigraniline states of PAn and PMAS. The redox switching of PAn/PMAS film is also confirmed by in-situ spectrochemical studies, revealing reversible spectral changes at different applied potentials consistent with different oxidation states of PAn and PMAS. Incorporation of PMAS as an electroactive dopant results in enhanced electrochromic contrast (57.0 %ΔT at 770 nm) in the visible region.

The ESR spectrum of PAn/PMAS shows a symmetric line with a g value of 2.0033, close to that of a free electron. The ESR of PAn/PMAS is similar to that of PAn/PSS, however the linewidth is significantly smaller. The lower linewidth observed for PAn/PMAS compared to PAn/PSS implies a higher degree of spin delocalisation and protonation using the conducting polyelectrolyte PMAS. An Echem-ESR study of PAn/PMAS reveals ESR spectral changes with potential in the range -0.3 to 0.8 V, with a maximum signal intensity observed at 0.2 V similar to the PAn/PSS system. The electrochemical dependence electron spin resonance properties of the PAn/PMAS and

PAn/PSS are reversible in the potential range studied, indicating that bipolarons in polyaniline reversibly convert to polarons.

Elemental analysis of the PAn/PMAS confirms that PMAS is a dominant dopant for polyaniline, with an estimated PMAS:PAn ratio of 0.88.

The PAn/PMAS film shows a smooth surface with hydrophilic properties. Its wettability is higher than that of PAn/HCl but lower than PAn/PSS.

The successful synthesis of PAn/PMAS with enhanced properties such as electroactivity, less resistivity and electrochromic contrast suggest that this novel material is a good candidate for use in applications such as sensing and electrochromic systems.

7.5 References

1. G.G. Wallace, G.M.S., P.R. Teasdale, *Conducting Electroactive Polymers: Intelligent Materials Systems*. 1997, P.1., Lancaster, USA: Technomic.
2. Borole, D.D., Kapadi, U.R., Kumbhar, P.P., and Hundiwale, D.G., *Effect of inorganic dopants (in presence of electrolyte) on the conductivity of polyaniline, poly(o-toluidine) and their copolymer thin films.* Materials Letters, 2002. **57**(4): p. 844-852.
3. Borole, D.D., Kapadi, U.R., Mahulikar, P.P., and Hundiwale, D.G., *Electrochemical behaviour of polyaniline, poly(o-toluidine) and their copolymer in organic sulphonic acids.* Materials Letters, 2004. **58**(29): p. 3816-3822.
4. Mohamoud, M.A. and Hillman, A.R., *The effect of anion identity on the viscoelastic properties of polyaniline films during electrochemical film deposition and redox cycling.* Electrochimica Acta. **In Press, Accepted Manuscript**: p. 183.
5. Dominis, A.J., Spinks, G.M., Kane-Maguire, L.A.P., and Wallace, G.G., *A de-doping/re-doping study of organic soluble polyaniline.* Synthetic Metals, 2002. **129**(2): p. 165-172.
6. Gazotti, J., W.A., Faez, R., and Paoli, M.-A.D., *Electrochemical, electrochromic and photoelectrochemical behavior of a highly soluble polyaniline derivative: poly(o-methoxyaniline) doped with functionalized organic acids.* Journal of Electroanalytical Chemistry, 1996. **415**(1-2): p. 107-113.
7. Aboutanos, V., Barisci, J.N., Kane-Maguire, L.A.P., and Wallace, G.G., *Electrochemical preparation of chiral polyaniline nanocomposites.* Synthetic Metals, 1999. **106**(2): p. 89-95.
8. Mu, S., *The electrocatalytic oxidation of gallic acid on polyaniline film synthesized in the presence of ferrocene phosphonic acid.* Synthetic Metals, 2003. **139**(2): p. 287-294.

9. Chen, Y.-H., Wu, J.-Y., and Chung, Y.-C., *Preparation of polyaniline-modified electrodes containing sulfonated polyelectrolytes using layer-by-layer techniques.* Biosensors and Bioelectronics Selected Papers from the 2nd International Meeting on Microsensors and Microsystems, 2006. **22**(4): p. 489-494.
10. Etchenique, R. and Brudny, V.L., *Characterization of porous polyaniline-polystyrenesulfonate composite films using EQCM.* Electrochemistry Communications, 1999. **1**(10): p. 441-444.
11. F., Judith, *Conducting polymers and polymer electrolytes : from biology to photovoltaics / Judith F. Rubinson, editor, Harry B. Mark, Jr., editor*. c2003, Washington, DC :: American Chemical Society : distributed by Oxford University Press,.
12. Ivanov, V.F., Gribkova, O.L., Cheberyako, K.V., Nekrasov, A.A., Tverskoi, V.A., and Vannikov, A.V., *Template Synthesis of Polyaniline in the Presence of Poly-(2-acrylamido-2-methyl-1-propanesulfonic Acid).* Russian Journal of Electrochemistry, 2004. **V40**(3): p. 299-304.
13. Hu, H., Hechavarria, L., and Campos, J., *Optical and electrical responses of polymeric electrochromic devices: effect of polyacid incorporation in polyaniline film.* Solid State Ionics, 2003. **161**(1-2): p. 165-172.
14. Tao, Y., Zhao, J.X., and Wu, C.X., *Polyacrylamide hydrogels with trapped sulfonated polyaniline.* European Polymer Journal, 2005. **41**(6): p. 1342-1349.
15. Siddhanta, S.K. and Gangopadhyay, R., *Conducting polymer gel: formation of a novel semi-IPN from polyaniline and crosslinked poly(2-acrylamido-2-methyl propanesulphonicacid).* Polymer, 2005. **46**(9): p. 2993-3000.
16. Yuan, G.-L., Kuramoto, N., and Su, S.-J., *Template synthesis of polyaniline in the presence of phosphomannan.* Synthetic Metals, 2002. **129**(2): p. 173-178.
17. Hodgson, A.J., Gilmore, K., Small, C., Wallace, G.G., Mackenzie, I.L., Aoki, T., and Ogata, N., *Reactive supramolecular assemblies of mucopolysaccharide, polypyrrole and protein as controllable biocomposites for a new generation of `intelligent biomaterials'.* Supramolecular Science, 1994. **1**(2): p. 77-83.
18. Wernet, W., *Thermoplastic and elastic conducting polypyrrole films.* Synthetic Metals, 1991. **41**(3): p. 843-848.
19. Li, D., Jiang, Y., Li, Y., Yang, X., Lu, L., and Wang, X., *Fabrication of a prototype humidity-sensitive capacitor via layer-by-layer self-assembling technique.* Materials Science and Engineering: C, 2000. **11**(2): p. 117-119.
20. Prasad, G.K., Radhakrishnan, T.P., Kumar, D.S., and Krishna, M.G., *Ammonia sensing characteristics of thin film based on polyelectrolyte templated polyaniline.* Sensors and Actuators B: Chemical, 2005. **106**(2): p. 626-631.
21. Devendrappa, H., Rao, U.V.S., and Prasad, M.V.N.A., *Study of dc conductivity and battery application of polyethylene oxide/polyaniline and its composites.* Journal of Power Sources, 2006. **155**(2): p. 368-374.
22. Huang, L.-M., Chen, C.-H., and Wen, T.-C., *Development and characterization of flexible electrochromic devices based on polyaniline and poly(3,4-ethylenedioxythiophene)-poly(styrene sulfonic acid).* Electrochimica Acta, 2006. **51**(26): p. 5858-5863.
23. Huang, L.-M., Chen, C.-H., Wen, T.-C., and Gopalan, A., *Effect of secondary dopants on electrochemical and spectroelectrochemical properties of polyaniline.* Electrochimica Acta, 2006. **51**(13): p. 2756-2764.

24. Kim, Y., Teshima, K., and Kobayashi, N., *Improvement of reversible photoelectrochromic reaction of polyaniline in polyelectrolyte composite film with the dichloroethane solution system.* Electrochimica Acta, 2000. **45**(8-9): p. 1549-1553.
25. Liu, W., Cholli, A.L., Nagarajan, R., Kumar, J., Tripathy, S., Bruno, F.F., and Samuelson, L., *The Role of Template in the Enzymatic Synthesis of Conducting Polyaniline.* J. Am. Chem. Soc., 1999. **121**(49): p. 11345-11355.
26. Zhao, H. and Wallace, G.G., *Polypyrrole/poly(2-methoxyaniline-5-sulfonic acid) polymer composite.* Polymer Gels and Networks, 1998. **6**(3-4): p. 233-245.
27. Kitani, A., Satoguchi, K., Iwai, K., and Ito, S., *Electrochemical Behaviors of Polyaniline / Polyaniline-sulfonic Acid Composites.* Synthetic Metals, 1999. **102**(1-3): p. 1171-1172.
28. Li, C. and Mu, S., *The electrochemical activity of sulfonic acid ring-substituted polyaniline in the wide pH range.* Synthetic Metals, 2005. **149**(2-3): p. 143-149.
29. Masdarolomoor, F., Innis, P.C., Ashraf, S., and Wallace, G.G., *Purification and characterisation of poly(2-methoxyaniline-5-sulfonic acid).* Synthetic Metals, 2005. **153**(1-3): p. 181-184.
30. G. Sauerbrey, Z., Phys., 1959. **155**: p. 206.
31. Cao, Y., Andreatta, A., Heeger, A.J., and Smith, P., *Influence of chemical polymerization conditions on the properties of polyaniline.* Polymer, 1989. **30**(12): p. 2305-2311.
32. Duic, L. and Mandic, Z., *Counter-ion and pH effect on the electrochemical synthesis of polyaniline.* Journal of Electroanalytical Chemistry, 1992. **335**(1-2): p. 207-221.
33. Fenelon, A.M. and Breslin, C.B., *An investigation into the degradation of polyaniline films grown on iron from oxalic acid.* Synthetic Metals, 2004. **144**(2): p. 125-131.
34. Genies, E.M., Lapkowski, M., and Penneau, J.F., *Cyclic voltammetry of polyaniline: interpretation of the middle peak.* Journal of Electroanalytical Chemistry, 1988. **249**(1-2): p. 97-107.
35. Viva, F.A., Andrade, E.M., Molina, F.V., and Florit, M.I., *Electropolymerization of 2-methoxy aniline. Electrochemical and spectroscopical product characterization.* J. Electroanal. Chem., 1999. **471**: p. 180-189.
36. Pornputtkul, Y., *Development of Chiral Conducting Polymers for Asymmetric Electrosynthesis*, in University of Wollongong, 2005.
37. T. Tatsuma, T.O., R. Sato, and N. Oyama, J. Electroanal. Chem., 2001. **501**: p. 180-185.
38. Tallman, D.E. and Wallace, G.G., *Preparation and preliminary characterization of a poly (4-vinylpyridine) complex of a water-soluble polyaniline.* Synthetic Metals, 1997. **90**(1): p. 13-18.
39. Strounina, E.V., Kane-Maguire, L.A.P., and Wallace, G.G., *Optically active sulfonated polyanilines.* Synthetic Metals, 1999. **106**(2): p. 129-137.
40. Wei, X.-L.W., Y. Z.; Long, S. M.; Bobeczko, C.; Epstein, A. J., *Synthesis and Physical Properties of Highly Sulfonated Polyaniline.* J. Am. Chem. Soc., 1996. **118**(11): p. 2545-2555.
41. Mazeikiene, R., Niaura, G., and Malinauskas, A., *Voltammetric study of the redox processes of self-doped sulfonated polyaniline.* Synthetic Metals, 2003. **139**(1): p. 89-94.

42. Tawde, S., Mukesh, D., and Yakhmi, J.V., *Redox behavior of polyaniline as influenced by aromatic sulphonate anions: cyclic voltammetry and molecular modeling.* Synthetic Metals, 2001. **125**(3): p. 401-413.
43. Batich, C.D., Laitinen, H.A., and Zhou, H.C., *Chromatic Changes in Polyaniline Films.* Journal of The Electrochemical Society, 1990. **137**(3): p. 883-885.
44. Kitani, A., Kaya, M., Yano, J., Yoshikawa, K., and Sasaki, K., *"Polyaniline": Formation reaction and structure.* Synthetic Metals, 1987. **18**(1-3): p. 341-346.
45. Okamoto, H. and Kotaka, T., *Structure and properties of polyaniline films prepared via electrochemical polymerization. I: Effect of pH in electrochemical polymerization media on the primary structure and acid dissociation constant of product polyaniline films.* Polymer, 1998. **39**(18): p. 4349-4358.
46. Avlyanov, J.K., Min, Y., MacDiarmid, A.G., and Epstein, A.J., *Polyaniline: conformational changes induced in solution by variation of solvent and doping level.* Synthetic Metals, 1995. **72**(1): p. 65-71.
47. MacDiarmid, A.G. and Epstein, A.J., *Secondary doping in polyaniline.* Synthetic Metals, 1995. **69**(1-3): p. 85-92.
48. Xia, Y., Wiesinger, J.M., MacDiarmid, A.G., and Epstein, A.J., *Camphorsulfonic Acid Fully Doped Polyaniline Emeraldine Salt: Conformations in Different Solvents Studied by an Ultraviolet/Visible/Near-Infrared Spectroscopic Method.* Chem. Mater., 1995. **7**(3): p. 443-445.
49. Strounina, E.V., Shepherd, R., Kane-Maguire, L.A.P., and Wallace, G.G., *Conformational Changes in Sulfonated Polyaniline Caused By Metal Salts and OH-.* Synthetic Metals, 2003. **135-136**: p. 289-290.
50. Sakharov, I.Y., Ouporov, I.V., Vorobiev, A.K., Roig, M.G., and Pletjushkina, O.Y., *Modeling and characterization of polyelectrolyte complex of polyaniline and sulfonated polystyrene produced by palm tree peroxidase.* Synthetic Metals, 2004. **142**(1-3): p. 127-135.
51. Kim, B.-J., Oh, S.-G., Han, M.-G., and Im, S.-S., *Synthesis and characterization of polyaniline nanoparticles in SDS micellar solutions.* Synthetic Metals, 2001. **122**(2): p. 297-304.
52. Norris, I.D., Kane-Maguire, L.A.P., and Wallace, G.G., *Electrochemical Synthesis and Chiroptical Properties of Optically Active Poly(o-methoxyaniline).* Macromolecules, 2000. **33**(9): p. 3237-3243.
53. Yuan, G.-L. and Kuramoto, N., *Water-Processable Chiral Polyaniline Derivatives Doped and Intertwined with Dextran Sulfate: Synthesis and Chiroptical Properties.* Macromolecules, 2002. **35**(26): p. 9773-9779.
54. Han, C.-C. and Hong, S.-P., *A Novel Electrochemical Method for Enhancing the Conductivity of Polyaniline Solid Matrices in Preformed Films.* Macromolecules, 2001. **34**(14): p. 4937-4941.
55. Huang, W.S. and MacDiarmid, A.G., *Optical properties of polyaniline.* Polymer, 1993. **34**(9): p. 1833-1845.
56. Lin, T.-H. and Ho, K.-C., *A complementary electrochromic device based on polyaniline and poly(3,4-ethylenedioxythiophene).* Solar Energy Materials and Solar Cells, Selected Papers from the Sixth International Meeting on Electrochromism, 2006. **90**(4): p. 506-520.
57. Palys, B. and Celuch, P., *Redox transformations of polyaniline nanotubes: Cyclic voltammetry, infrared and optical absorption studies.* Electrochimica Acta, 2006. **51**(20): p. 4115-4124.

58. Abd-Elwahed, A. and Holze, R., *Ion size and size memory effects with electropolymerized polyaniline.* Synthetic Metals, 2002. **131**(1-3): p. 61-70.
59. Strounina, E.V., *Synthesis and Characterisation of Chiral Substituted Polyanilines*, in University of Wollongong, 2001.
60. Mitsuyuki Morita, *Multicolor electrochromic behavior of polyaniline composite films combined with polythiophene and poly(3-methylthiophene) films.* Die Makromolekulare Chemie, 1993. **194**(8): p. 2361-2374.
61. Little, S., *Preparation, Characterisation and Application of Novel Redox-Functionalised Polymers*, in *Chemistry Department*. 2006, University of Wollongong.
62. Bessiere, A., Duhamel, C., Badot, J.-C., Lucas, V., and Certiat, M.-C., *Study and optimization of a flexible electrochromic device based on polyaniline.* Electrochimica Acta, 2004. **49**(12): p. 2051-2055.
63. Hu, L., Gruner, G., Li, D., Kaner, R.B., and Cech, J., *Patternable transparent carbon nanotube films for electrochromic devices.* Journal of Applied Physics, 2007. **101**(1): p. 016102-3.
64. Yang, S.M., Chen, W.M., and You, K.S., *The properties of polyaniline-polyelectrolyte complexes.* Synthetic Metals International Conference on Science and Technology of Synthetic Metals, 1997. **84**(1-3): p. 77-78.
65. Wei, X.-L. and Epstein, A.J., *Simulations of the In situ cyclic voltammetry dependent EPR spectra and DC conductivity.* Synthetic Metals International Conference on Science and Technology of Synthetic Metals, 1997. **84**(1-3): p. 791-792.
66. Lippe, J. and Holze, R., *Electrochemical in-situ conductivity and polaron concentration measurements at selected conducting polymers.* Synthetic Metals, 1991. **43**(1-2): p. 2927-2930.
67. Zhuang, L., Zhou, Q., and Lu, J., *Simultaneous electrochemical-ESR-conductivity measurements of polyaniline.* Journal of Electroanalytical Chemistry, 2000. **493**(1-2): p. 135-140.
68. Monkman, A.P., Bloor, D., Stevens, G.C., Stevens, J.C.H., and Wilson, P., *Electronic structure and charge transport mechanisms in polyaniline.* Synthetic Metals, 1989. **29**(1): p. 277-284.
69. Tang, J., Allendoerfer, R.D., and Osteryoung, R.A., *Simultaneous EPR and electrochemical measurements on polyaniline in ambient temperature molten salts.* J. Phys. Chem., 1992. **96**(8): p. 3531-3536.
70. Glarum, S.H. and Marshall, J.H., *Electron delocalization in poly(aniline).* J. Phys. Chem., 1988. **92**(14): p. 4210-4217.
71. Kang, Y.S., Lee, H.J., Namgoong, J., Jung, B., and Lee, H., *Decrease in electrical conductivity upon oxygen exposure in polyanilines doped with HCl.* Polymer, 1999. **40**(9): p. 2209-2213.
72. Mu, S., Kan, J., Lu, J., and Zhuang, L., *Interconversion of polarons and bipolarons of polyaniline during the electrochemical polymerization of aniline.* Journal of Electroanalytical Chemistry, 1998. **446**(1-2): p. 107-112.
73. Lin, D.-S. and Yang, S.-M., *Syntheses of ethyl and ethoxy-substituted polyaniline complexes.* Synthetic Metals, 2001. **119**(1-3): p. 111-112.

Chapter 8

Conclusions

The current study presents the synthesis and characterisation of novel nanostructured conducting polymer systems based on the fully sulfonated polyaniline, poly(2-methoxyaniline-5-sulfonic acid) (PMAS). The research conducted in this thesis includes (a) the enhancement of the properties and further characterisation of the previously prepared PMAS, and (b) the incorporation of the highly purified PMAS material as dopant into the conducting polymer polyaniline. The major findings are summarised in this Chapter.

(a) PMAS: purification, synthesis optimisation, and characterisation

A new method for purification of PMAS has been developed using a tangential cross flow filtration system. This procedure provides a simple, rapid and scalable method to isolate high molecular weight HMWt PMAS and low molecular weight LMWt PMAS of high purity, which possess different colours and redox properties, are obtainable via this method. Tangential cross flow filtration is a faster and more effective method of gram-scale purification and fractionation than the time-consuming traditional tube dialysis that produces an impure PMAS/oligomer mixture. The new purification system using a range of different MWCO membranes also provides a facile route for isolation and study of the pure products that are produced at different stages of polymerisation of MAS monomer. Most significantly, it has made it possible to systematically study the influence of a range of polymerisation conditions on the characteristics of poly(2-methoxyaniline-5-sulfonic acid) (PMAS) obtained, to achieve optimal conductivity and redox activity. Synthesis conditions such as temperature, pH, monomer and oxidant concentration, and the rate of addition of oxidant are found to greatly affect the properties of the resultant PMAS.

The use of synthesis temperatures above 10°C is detrimental to the conductivity and molecular weight of PMAS. However, monomer conversion and polymer yield are negligibly affected by temperature. Both conductivity and yield are significantly influenced by monomer concentration. A minimum concentration of 0.20 M MAS is required for chemical polymerisation to form conducting PMAS. The rate of synthesis is strongly dependent on monomer concentration, with a typical reaction time (to > 90% completion) of 8 hours required in a [MAS] range of 0.33-0.47 M. The optimum oxidant/monomer to produce maximum conductivity is 1.00. Increasing the ratio to 1.25 is detrimental to the conductivity, however an increase in the polymer yield is observed. Over-oxidation and degradation of PMAS will occur at higher oxidant/monomer ratios, leading to a dramatic drop in both conductivity and yield. The conductivity of PMAS is also sensitive to the rate of addition of oxidant. The optimum conductivity can be obtained when the oxidant solution is rapidly mixed with monomer solution.

The optimum initial pH for the polymerisation reaction is 4.0. This pH is required for complete solubilisation of the MAS monomer. As the reaction proceeds, a pH drop is observed resulting in the formation of conducting HMWt PMAS. Using a constant pH of either 3 or 4, oligomeric and low molecular weight materials are the major products. These results suggest that, as for polyaniline, C-N *para*-coupling and chain propagation in polymerisation of MAS only occur at sufficiently low pH values.

The optimal PMAS synthesis conditions are 0.47 M MAS, temperatures below 10°C, and equimolar oxidant/monomer ratio with rapid mixing initiated at pH 4. This procedure results in HMWt PMAS with conductivity of 1.74 ± 0.09 S/cm, M_p 16,900 and recovered yield (after tangential cross flow filtration) of 49.5% w/w. The conductivity of PMAS using these optimal conditions is close to two orders of magnitude higher than previously reported for PMAS (0.01-0.04 S/cm).

The separation via tangential cross flow filtration of the dominant high molecular weight HMWt and low molecular weight LMWt PMAS fractions from the as-synthesised PMAS has permitted detailed characterisation of these pure fractions. The HMWt PMAS fraction has M_n of 13,400 kDa, M_w of 33,600 kDa, M_p of 16,900 kDa

and PDI of 2.5, while the LMWt PMAS fraction is an oligomer with M_n of 2,400 kDa, M_w of 2,700 kDa, M_p of 2,800 kDa and PDI of 1.1.

The UV-visible spectrum of LMWt PMAS is unaffected by changes in pH or treatment with oxidising or reducing agents, confirming its chemical inertness. In contrast, UV-vis spectroscopy and cyclic voltammetry studies on the HMWt PMAS fraction confirms that this material behaves in a similar fashion to un-substituted electroactive polyaniline emeraldine salts. Reversible redox interconversions are observed between the leucoemeraldine, emeraldine and pernigraniline states of the HMWt PMAS.

In contrast to HMWt PMAS (with a conductivity of 0.02-1.74 S/cm depending on the synthetic conditions), the LMWt PMAS is non-conducting and has no ESR signal, indicating the absence of polaron charge carriers typically found in polyaniline emeraldine salts. The ESR spectrum of aqueous PMAS shows a symmetrical line similar to un-substituted polyaniline emeraldine salt, with a g value of 2.00295 and a line width of ~2.55 G. Dialysed PMAS (containing *ca.* 20% LMWt PMAS) has a significantly lower electrical conductivity (typically 4 to 5 times less) than the purified HMWt PMAS fraction. The observed loss of electrical conductivity is presumably caused by interaction of the LMWt fraction with the charge carriers in the HMWt PMAS, inhibiting interchain charge transfer.

The photoluminescence characterisation of the PMAS fractions reveals that the LMWt PMAS is the source of the unexpected photoemission recently reported for aqueous PMAS. The fluorescence lifetime of LMWt PMAS is less than 10 ns. Pure HMWt PMAS does not photoluminesce, and is shown to statically quench the photoluminescence of LMWt PMAS. Fully reduced HMWt PMAS leucoemeraldine base (LB) strongly photoluminesces, in common with the LB form of unsubstituted polyaniline.

PMAS is soluble in water (>100 mg/mL) and DMSO (~20 mg/mL), which are highly polar protic and aprotic solvents, respectively. It is insoluble in other common protic and aprotic solvents.

Elemental analysis reveals that the HMWt PMAS is an ammonium salt with *ca*. 80% of the free sulfonate groups along the chain are associated with ammonium ions. The ammonium ions are completely exchanged by hydrogen ions (H^+) using a proton exchange resin.

The morphology of HMWt PMAS is affected by synthetic conditions, varying from rod-like (diameters about 100 nm) to spherical nanoparticles (with diameters less than 50 nm). A TEM micrograph of the LMWt PMAS shows a mixture of nanoparticles and needles with diameters less than 100 nm.

Characterisation of LMWt PMAS thus shows that this material is distinctly different from the conducting emeraldine salt form of PMAS, exhibiting different optical and electrical properties. The non-conducting behaviour of LMWt PMAS and some similarities of this fraction with the phenazine-like oligomeric products of polyaniline suggest the possible existence of phenazine-like structures in the LMWt PMAS fraction as a result of *ortho*-coupling of MAS monomer units during polymerisation at pH ~ 4.

(b) Novel PAn/PMAS materials

HMWt PMAS can be successfully incorporated as a conducting polyelectrolyte dopant during chemical and electrochemical polymerisation of polyaniline (PAn) to prepare a new class of PAn/PMAS material. PMAS is a self-doped and highly water soluble sulfonated polyaniline with free negatively charged sulfonic groups. This conductive and electroactive polymer also behaves like a polyelectrolyte and is subsequently able to function as a dopant in polyaniline. These unique properties result in PAn/PMAS material with interesting properties such as high conductivity, enhanced switching properties, water dispersability and nanodimensional morphology not seen in either the PAn or PMAS individually.

In this work, PMAS is shown to be capable of functioning as an effective dopant during the synthesis of polyaniline to the extent that polyaniline can be electropolymerised from an acidic solution of 0.01 M aniline. However, no significant PAn growth is observed in the absence of HMWt PMAS using this concentration of aniline monomer

in 1.0 M HCl. Chemical polymerisation of aniline is also facilitated in the presence of PMAS. This enhanced polymerisation arises from strong electrostatic interaction between anilinium ions formed in slightly acidic media and free sulfonate groups along the polymer chain of PMAS, facilitating chain propagation via supramolecular preordering of the anilinium cation onto the PMAS polyelectrolyte template, which simultaneously acts as the dopant for the resultant polymer.

PAn/PMAS can be prepared as water-insoluble films using electrochemical polymerisation, as well as highly dispersable nanomaterials via chemical polymerisation of aniline in the presence of PMAS.

UV-vis spectroscopy and CV studies of the PAn/PMAS material in water and alkaline media confirm the presence of both PAn and PMAS in their emeradine salt forms. The presence of an intense free carrier tail in the near-infrared region and the absence of a 800 nm peak in the UV-vis spectrum of the PAn/PMAS, indicates that the polyaniline chains adopt an extended coil conformation in the presence of PMAS dopant.

Elemental analysis of the PAn/PMAS prepared by either chemical or electrochemical methods shows that PMAS is the dominant dopant in the PAn/PMAS product. The mole ratio of PMAS:PAn in the highly dispersable PAn/PMAS material is estimated to be 1.65. To effectively dope PAn to the idealised emeraldine salt state, one sulfonate per aniline dimmer is required. The above composition mole ratio indicates that there is sufficient PMAS to dope the PAn to the emeraldine state, with excess PMAS sulfonate groups providing a stabilising function in the resultant dispersion.

These novel PAn/PMAS materials have enhanced electrical conductivity and dispersion stability compared to PAn/HCl nanofibre based materials prepared under equivalent conditions. The conductivity of PAn/PMAS, synthesised using a PMAS:aniline ratio of 1:2 in 1.0 M HCl, is 3.0 ± 0.18 S/cm, which is approximately two orders of magnitude higher than those reported for polyaniline in the presence of non-conducting polyelectrolytes. In contrast to PAn/HCl, the PAn/PMAS remains conducting (0.02

S/cm) at neutral pH. These nanostructured materials may be promising in the area of biosensing when conducting materials are needed in a neutral environment.

ESR studies of PAn/PMAS materials prepared by either chemical or electrochemical methods show that PAn has a higher level of spin concentration and spin localisation in the presence of PMAS. The ESR results are consistent with the higher conductivity of PAn with the PMAS dopant compared to the use of other dopants such as Cl^- and the Poly(styrenesulfonate) polyelectrolyte.

Redox switching of PAn/PMAS film electrodeposited onto PT-ITO glass is also confirmed by in-situ spectroelectrochemical studies which reveal reversible spectral changes at different applied potentials consistent with different oxidation states of PAn and PMAS. As an electrochromic coating, the incorporation of PMAS as an electroactive dopant for polyaniline results in an enhanced electrochromic contrast (57.0%ΔT at 770 nm) in the visible region.

Thermal analysis of the PAn/PMAS suggests that the thermal stability of polyaniline is improved in the presence of PMAS.

The PAn/PMAS film has enhanced hydrophilic properties with its wettability being higher than that of PAn/HCl, presumably due to the presence of excess sulfonate groups not involve in doping of the PAn.

Future work

From the studies presented in this thesis we can now prepare highly pure PMAS materials at large (gram) scales with definable electronic properties as required. The ability to prepare these materials in larger quantities opens many application opportunities that, to date, have been challenging due to unknown purity levels and limited availability of well characterised product.

Enhanced electrical and spectroelectrochemical properties as well as the water based stability of dispersions also enhances the likelihood of application in areas such as

electronic textiles, electrochromics, chemical sensors, and batteries. A PAn/PMAS nanoparticle dispersion is also amenable to printing using ink jet printing.

Another area of future work would be incorporation of PMAS into other conducting polymer systems such as polypyrroles and polythiophenes. This would result in new water dispersible conducting polymers based on the fully sulfonated polyaniline, PMAS.